



UNIVERSITY OF
BIRMINGHAM

Applications of Ultrasound for the Functional Modification of Proteins and Submicron Emulsion Fabrication

by

Jonathan James O'Sullivan

A thesis submitted to
The University of Birmingham
for the degree of
DOCTOR OF ENGINEERING

School of Chemical Engineering
College of Physical and Engineering Sciences
The University of Birmingham

February 2015

UNIVERSITY OF
BIRMINGHAM

University of Birmingham Research Archive

e-theses repository

This unpublished thesis/dissertation is copyright of the author and/or third parties. The intellectual property rights of the author or third parties in respect of this work are as defined by The Copyright Designs and Patents Act 1988 or as modified by any successor legislation.

Any use made of information contained in this thesis/dissertation must be in accordance with that legislation and must be properly acknowledged. Further distribution or reproduction in any format is prohibited without the permission of the copyright holder.

Abstract

This thesis aims to advance the understanding of ultrasonic processing for the alteration of food microstructures. The motivation of this work was based on recent research highlighting the significance of low frequency, high power ultrasound for the functional modification of food ingredients, and furthermore, the fabrication of submicron emulsion droplets. Be that as it may, a fundamental understanding of the factors associated with ultrasonic processing are yet to be fully elucidated. This thesis considers the impact of ultrasonic processing in terms of how physicochemical alterations of proteins are determined by untreated protein structure and processing conditions, and additionally, the significance of the relationship between emulsion formulation and ultrasonic process parameters on the formation of submicron emulsion droplets.

To achieve these aims food proteins from a range of sources (*i.e.* dairy, animal and vegetable) were irradiated with ultrasound, after which, physicochemical differences were probed in the terms of molecular structure and hydrodynamic properties, and compared to their untreated counterparts. From this, the influence of ultrasound treatment upon protein structure was investigated and related to functional differences for the formation and long-term stability of submicron emulsion droplets.

It was shown that ultrasound treatment of proteins altered the conformational structure of proteins in aqueous solution due to disruption of associative non-covalent interactions maintaining untreated protein aggregates, reducing the hydrodynamic volume of protein aggregates by ultrasonic cavitations. However, insufficient acoustic energy was provided to achieve scission of peptide bonds. Emulsions prepared with ultrasound treated milk protein isolate, pea protein isolate and bovine gelatin performed better as emulsifiers

than their untreated counterparts, as smaller emulsion droplets were achieved exhibiting a static droplet size for the duration of stability studies. This behaviour is ascribed to a combination of more rapid adsorption of protein molecules to the oil-water interface, reduced times for the conformational denaturation required for surface stabilisation and improved interfacial packing, all owing to reduction in size of protein associates.

Furthermore, to assess the efficacy of ultrasound for the fabrication of submicron emulsion droplets, a microstructural engineering approach was conducted whereby the effect of emulsion formulation, emulsifier type and concentration, and processing conditions, residence time within the acoustic field, acoustic energy transmitted, effective processed volume and processing methodology (*i.e.* batch or continuous), upon resultant emulsion droplet size were investigated.

Emulsification from ultrasound occurs due to the implosion of ultrasonic cavitations, yielding regions of high hydrodynamic shear, allowing for emulsion droplet breakup. For emulsions whereby sufficient emulsifier is present (> 0.5 wt. %) it was shown that emulsion droplet size can be predicted from a mathematical relation, regardless of the process configuration implemented or process conditions employed, from the derived relationship between the emulsion droplet size ($d_{3,2}$) and energy density (E_v), an amalgamation of the process parameters, an inverse power law. Droplet size predictions were unattainable at low emulsifier concentrations (≤ 0.5 wt. %) due to the exhibited re-coalescence behaviour attributed to insufficiency of emulsifier and droplet collisions within the acoustic field. Furthermore, this work highlighted the efficient utilisation of acoustic energy of continuous processing methodologies in comparison to batch configurations due to the intense transmission of acoustic energy within the smaller processing volumes.

Acknowledgements

I would like to express my gratitude to my academic supervisor Prof. Ian Norton for affording me unique opportunities, and instilling me with an appreciation of the merits of pure research. Additionally, I would also like to thank Dr. Roman Pichot, the research fellow who assisted me throughout the start of this project.

Within the University of Birmingham, I would like to thank Dr. Richard Greenwood for his continued support and reviewing my work throughout the EngD programme, and also the support staff, in particular Kathleen Hynes, John Hooper and Lynn Draper. I would also like to thank Paul Stanley and Theresa Morris for assistance with cryo-SEM equipment, and the EPSRC for their sponsorship of this work.

Within Kerry, I would like to thank Cal Flynn, John O'Connell (formerly of Kerry), Brian Murray and Maurice O'Sullivan, all for their continued assistance and support throughout the project, and highlighting the industrial relevance of this work. I would also like to thank Kevin Lyons and John Maguire (formerly of Kerry) for useful discussions, and the technicians of the R,D&A laboratories for their support during the time I spent in Kerry.

I thank my friends at the University of Birmingham for all the great memories and lasting friendships, and in Ireland for always being there. I thank my parents, Michael and Shayron, for their continued love and support through the highs and lows, and my brothers, Peter and Michael, and sisters, Kate and Jennifer. Lastly, Olga, thank you for making my EngD possible and enjoyable, due to your continued encouragement and love, and for making our time in Birmingham so memorable.

Dedicated to my parents, Michael and Shayron

“Ideas are like rabbits. You get a couple and learn how to handle them, and pretty soon you have a dozen.”

- John Steinbeck (1902 – 1968)

Table of Contents

Abstract.....	i
Acknowledgements.....	iii
Table of Contents.....	v
List of Figures.....	viii
List of Tables.....	xii
Nomenclature.....	xiii
Chapter 1. Introduction.....	1
1.1. Background.....	2
1.2. Aims of the research.....	5
1.3. Relevance to Kerry Group.....	5
1.4. Thesis layout.....	7
1.5. Publications and conferences.....	8
1.6. References.....	9
Chapter 2. State of the Art.....	11
2.1. Background literature survey: proteins and emulsions.....	12
2.1.1. Proteins.....	13
2.1.2. Emulsions.....	25
2.1.3. References.....	41
2.2. Literature review: ultrasound.....	49
2.2.1. Abstract.....	50
2.2.2. Introduction.....	51
2.2.3. Fundamentals of ultrasound.....	53
2.2.4. Physicochemical alteration of food proteins via ultrasonic processing.....	61
2.2.5. Nanoemulsion fabrication from ultrasound and the associated parameters.....	67
2.2.6. Conclusions and future trends.....	72
2.2.7. References.....	73
Chapter 3. The Effect of Ultrasound Treatment on the Structural, Physical and Emulsifying Properties of Dairy Proteins.....	81
3.1. Abstract.....	82
3.2. Introduction.....	83
3.3. Materials and methodology.....	86
3.3.1. Materials.....	86

3.3.2.	Methods.....	87
3.3.3.	Statistical analysis.....	92
3.4.	Results and discussions.....	92
3.4.1.	Effect of ultrasound treatment on the structural and physical properties of NaCas, WPI and MPI.....	92
3.4.2.	Comparison of the emulsifying properties of untreated and ultrasound treated NaCas, WPI and MPI.....	102
3.5.	Conclusions.....	109
3.6.	References.....	110
Chapter 4.	The effect of ultrasound treatment on the structural, physical and emulsifying properties of animal and vegetable proteins.....	114
4.1.	Abstract.....	115
4.2.	Introduction.....	116
4.3.	Materials and methodology.....	120
4.3.1.	Materials.....	120
4.3.2.	Methods.....	121
4.3.3.	Statistical analysis.....	127
4.4.	Results and discussions.....	128
4.4.1.	Effect of ultrasound treatment on the structural and physical properties of animal and vegetable proteins.....	128
4.4.2.	Comparison of the emulsifying properties of untreated and ultrasound treated animal and vegetable proteins.....	139
4.5.	Conclusions.....	149
4.6.	References.....	150
Chapter 5.	Comparison of batch and continuous ultrasonic emulsification processes.....	157
5.1.	Abstract.....	158
5.2.	Introduction.....	159
5.3.	Materials and methodology.....	161
5.3.1.	Materials.....	161
5.3.2.	Methods.....	161
5.3.3.	Statistical analysis.....	167
5.4.	Results and discussions.....	167
5.4.1.	Comparison of lab scale batch and continuous configurations for effect of processing time and ultrasonic power.....	167
5.4.2.	Effect of emulsifier concentration and type on emulsion formation.....	174

5.4.3. Effect of energy density on pilot scale continuous ultrasonic emulsification .	181
5.5. Conclusions	183
5.6. References	184
Chapter 6. Conclusions and future recommendations	187
6.1. Understanding the ultrasonic effect upon the physicochemical properties of proteins	189
6.2. Understanding the ultrasonic effect of the emulsifying performance of proteins...	190
6.3. Understanding acoustic emulsification	192
6.4. Future recommendations	193
6.5. References	197
Appendix A. Mathematical models for acoustic streaming.....	198
A.1. Rayleigh, Nyborg and Westervelt (RNW) streaming theory	199
A.2. Stuart streaming theory	201
A.3. References	205
Appendix B. Selected droplet size distribution data from results presented in chapters 3, 4 and 5.....	206
Appendix C. Selected rheology flow profile data from results presented in chapters 3 and 4	216

List of Figures

- Fig. 2.1. Depiction of alpha helices and beta sheets secondary protein structures. Image adapted from Berg et al., (2012)..... 14
- Fig. 2.2. Graphical representation of the relationship between viscosity and polymer concentration, showing the dilute regime, the critical coil overlap concentration and the concentrated regime. Image adapted from Morris *et al.* (1981).24
- Fig. 2.3. Depiction of a longitudinal wave showing compressions, rarefactions and wavelength.53
- Fig. 2.4. Cryo-SEM micrographs of (a) 1% untreated bovine gelatin solution, (b) 1% ultrasound treated bovine gelatin solution, (c) 1% untreated bovine gelatin stabilised emulsion and (d) 1% ultrasound treated bovine gelatin stabilised emulsion. Scale bars are 2 μm and 10 μm for solutions and emulsions, respectively. Image adapted from O’Sullivan et al., (2015b).66
- Fig. 3.1. Cryo-SEM micrographs of protein solutions: (a) 1 wt. % Untreated NaCas solution, (b) 1 wt. % Ultrasound treated NaCas solution, (c) 1 wt. % Untreated WPI solution, (d) 1 wt. % Ultrasound treated WPI, (e) 1 wt. % Untreated MPI solution and (f) 1 wt. % Ultrasound treated MPI. Scale bar is 2 μm in all cases.96
- Fig. 3.2. SDS-PAGE electrophoretic profiles of protein solutions: (a) Molecular weight standard (10 kDa – 250 kDa), (b) Untreated NaCas, (c) Ultrasound treated NaCas, (d) Untreated MPI, (e) Ultrasound treated MPI, (f) Untreated WPI and (g) Ultrasound treated WPI.97
- Fig. 3.3. Fitting of the Huggins (●) and Kraemer (○) equations to the viscosity data of the studied protein solutions: (a) Untreated NaCas, (b) Ultrasound treated NaCas, (c) Untreated WPI, (d) Ultrasound treated WPI, (e) Untreated MPI and (f) Ultrasound treated MPI. Average $[\eta]$ values displayed on each plot.....99
- Fig. 3.4. Emulsion droplet size ($d_{3,2}$) as a function of concentrations of: (a) Untreated NaCas, sonicated NaCas and Tween 80, (b) Untreated WPI, sonicated WPI and Tween 80, and (c) Untreated MPI, sonicated MPI and Tween 80..... 104
- Fig. 3.5. Interfacial tension between water and pure vegetable oil as a function of emulsifier type: (a) Untreated NaCas, sonicated NaCas and Tween 80, (b) Untreated WPI, sonicated WPI and Tween 80 and (c) Untreated MPI, sonicated MPI and Tween 80. The concentration for all emulsifiers was 0.1 wt. %..... 106
- Fig. 3.6. Effect of emulsifier type on droplet size as a function of time for O/W emulsions stabilised by: (a) Untreated NaCas, sonicated NaCas and Tween 80, (b) Untreated WPI,

sonicated WPI and Tween 80 and (c) Untreated MPI, sonicated MPI and Tween 80. The concentration for all emulsifiers was 1 wt. %..... 108

Fig. 4.1. Effect of sonication time on the D_z (nm) of (a) BG, (b) EWP, (c) PPI and (d) RPI. 129

Fig. 4.2. Cryo-SEM micrographs of protein solutions: (a) 1% Untreated BG, (b) 1% Ultrasound treated BG, (c) 1% Untreated SPI and (d) 1% Ultrasound treated SPI. Scale bar is 2 μm in all cases..... 133

Fig. 4.3. SDS-PAGE electrophoretic profiles of protein solutions: (a) Molecular weight standard (10 kDa – 250 kDa), (b) Untreated BG, (c) Ultrasound treated BG, (d) Untreated FG, (e) Ultrasound treated FG, (f) Untreated EWP, (g) Ultrasound treated EWP, (h) Untreated PPI, (i) Ultrasound treated PPI, (j) Untreated SPI, (k) Ultrasound treated SPI, (l) Untreated RPI and (m) Ultrasound treated RPI. 134

Fig. 4.4. Fitting of the Huggins (\bullet) and Kraemer (\circ) equations to the viscosity data of the studied protein solutions: (a) Untreated EWP, (b) Ultrasound treated EWP, (c) Untreated PPI and (d) Ultrasound treated PPI..... 136

Fig. 4.5. Average droplet size as a function of concentrations of: (a) Untreated BG, sonicated BG and Brij 97, (b) Untreated FG, sonicated FG and Brij 97, (c) Untreated EWP, sonicated EWP and Brij 97 and (d) Untreated PPI, sonicated PPI and Brij 97. 140

Fig. 4.6. Interfacial tension between water and pure vegetable oil as a function of emulsifier type: (a) Untreated BG, ultrasound treated BG and Brij 97, (b) Untreated FG, ultrasound treated FG and Brij 97, (c) Untreated PPI, ultrasound treated PPI and Brij 97 and (d) Untreated SPI, ultrasound treated SPI and Brij 97. 144

Fig. 4.7. Cryo-SEM micrographs of protein stabilised O/W pre-emulsions: (a) 1% Untreated BG stabilised emulsion, (b) 1% Ultrasound treated BG stabilised emulsion and (c) 1% Untreated SPI stabilised emulsion, (d) 1% Ultrasound treated SPI stabilised emulsion. Scale bar is 10 μm in all cases..... 146

Fig. 4.8. Effect of emulsifier type on droplet size as a function of time for O/W emulsions stabilised by: (a) Untreated BG, ultrasound treated BG and Brij 97, (b) Untreated FG, ultrasound treated FG and Brij 97, (c) Untreated PPI, ultrasound treated PPI and Brij 97, and (d) Untreated SPI, ultrasound treated SPI and Brij 97..... 147

Fig. 5.1. Schematic of continuous ultrasonic emulsification setups for (a) lab scale and (b) pilot scale trials. 164

Fig. 5.2. Effect of batch size and ultrasonic processing time on droplet size ($d_{3,2}$) of emulsions stabilised with 1.5 wt. % Tween 80 prepared employing lab scale batch ultrasonic homogenisation..... 168

Fig. 5.3. Effect of acoustic processing time on droplet size ($d_{3,2}$) of emulsions stabilised with 1.5 wt. % Tween 80 prepared employing continuous lab scale ultrasonic processor (40% amplitude).	169
Fig. 5.4. Effect of ultrasonic amplitude and processing time (t) with the acoustic field upon droplet size ($d_{3,2}$) of emulsions fabricated with 1.5 wt. % Tween 80 prepared utilising (a) lab scale batch (50 g) and (b) lab scale continuous configurations.	171
Fig. 5.5. Effect of energy density (E_v) upon emulsion droplet size ($d_{3,2}$) utilising (a) lab scale batch ultrasonic processing (20 - 40% amplitudes) and (b) lab scale continuous ultrasonic processing (20 - 40% amplitudes) for 1.5 wt. % Tween 80 stabilised emulsions.	173
Fig. 5.6. Effect of emulsifier type and concentration (0.1 – 3 wt. %) upon emulsion droplet size ($d_{3,2}$) of: (a) Tween 80 for batch ultrasonic processing, (b) Tween 80 for continuous ultrasonic processing, (c) MPI for batch ultrasonic processing, (d) MPI for continuous ultrasonic processing, (e) PPI for batch ultrasonic processing and (f) PPI for continuous ultrasonic processing. All data is for lab scale methodologies (ultrasonic amplitude of 40%) and the batch size is 50 g.	175
Fig. 5.7. Comparison of interfacial tension between distilled water (●), Tween 80 (○), MPI (▼) and PPI (Δ) with rapeseed oil. The concentration for all emulsifiers was 0.1 wt. %.....	178
Fig. 5.8. Effect of energy density (E_v) upon emulsion droplet size ($d_{3,2}$) for emulsions prepared with (a) Tween 80 for batch ultrasonic processing, (b) Tween 80 for continuous ultrasonic processing, (c) MPI for batch ultrasonic processing, (d) MPI for continuous ultrasonic processing, (e) PPI for batch ultrasonic processing and (f) PPI for continuous ultrasonic processing, at emulsifier concentrations ranging from 0.75 – 3 wt. % (40% amplitude and 50 g for batch processing).	180
Fig. 5.9. Effect of energy density (E_v) upon emulsion droplet size ($d_{3,2}$) utilising pilot scale continuous ultrasonic processing (ultrasonic amplitudes of 50% and 90%) for (a) 1.5 wt. % Tween 80 , (b) 1.5 wt. % MPI and (c) 1.5 wt. % PPI stabilised emulsions.	182
Fig. B.1. Comparison of DSD of untreated NaCas, UST NaCas and Tween 80, all at an emulsifier concentration of 0.1 wt. %.....	207
Fig. B.2. Comparison of DSD of untreated WPI, UST WPI and Tween 80, all at an emulsifier concentration of 0.1 wt. %.....	208
Fig. B.3. Comparison of DSD of untreated BG, UST BG and Brij 97, all at an emulsifier concentration of 0.1 wt. %.....	209
Fig. B.4. Comparison of DSD of untreated FG, UST FG and Brij 97, all at an emulsifier concentration of 0.1 wt. %.....	210

Fig. B.5. Comparison of DSD of untreated EWP, UST EWP and Brij 97, all at an emulsifier concentration of 0.1 wt. %	211
Fig. B.6. Comparison of DSD of untreated SPI, UST SPI and Brij 97, all at an emulsifier concentration of 0.1 wt. %	212
Fig. B.7. Comparison of processing times (0, 30, 60 and 300 s) for the fabrication of emulsions via batch ultrasonic emulsification with an acoustic amplitude of 40% and a batch size of 150 g	213
Fig. B.8. Comparison of processing times (0, 30, 60 and 300 s) for the fabrication of emulsions via batch ultrasonic emulsification with an acoustic amplitude of 40% and a batch size of 50 g	214
Fig. B.9. Comparison of processing times (0, 1, 3 and 10 s) for the fabrication of emulsions via batch ultrasonic emulsification with an acoustic amplitude of 40% and a batch size of 3 g	214
Fig. B.10. Comparison of ultrasonic amplitude (20, 30 and 40 %) for the fabrication of emulsions via batch ultrasonic emulsification with a processing time of 60 s and a batch size of 50 g	215
Fig. C.1. Comparison of the flow curves of untreated sodium caseinate (NaCas) solutions as a function of concentration (0.15 – 0.35 wt . %), used for the determination of intrinsic viscosity	217
Fig. C.2. Comparison of the flow curves of UST NaCas solutions as a function of concentration (0.15 – 0.35 wt . %), used for the determination of intrinsic viscosity	218
Fig. C.3. Comparison of the flow curves of untreated milk protein isolate (MPI) solutions as a function of concentration (0.5 – 2 wt . %), used for the determination of intrinsic viscosity	218
Fig. C.4. Comparison of the flow curves of UST MPI solutions as a function of concentration (0.5 – 2 wt . %), used for the determination of intrinsic viscosity	219
Fig. C.5. Comparison of the flow curves of untreated egg white protein (EWP) solutions as a function of concentration (1.5 – 3 wt . %), used for the determination of intrinsic viscosity	219
Fig. C.6. Comparison of the flow curves of UST EWP solutions as a function of concentration (1.5 – 3 wt . %), used for the determination of intrinsic viscosity	220
Fig. C.7. Comparison of the flow curves of untreated soy protein isolate (SPI) solutions as a function of concentration (1.5 – 3 wt . %), used for the determination of intrinsic viscosity	220
Fig. C.8. Comparison of the flow curves of UST SPI solutions as a function of concentration (1.5 – 3 wt . %), used for the determination of intrinsic viscosity	221

List of Tables

Table 2.1. Examples of studies examining the effect of ultrasonic treatment related to dairy, animal, cereal, legume and fruit protein sources, in relation to solubilisation, aggregate size, molecular structure, rheology and interfacial behaviour.	62
Table 2.2. Bond energy (kJ mol ⁻¹) associated with intra- and intermolecular bonds present in proteins (McMurry, 2011).	65
Table 3.1. Composition of acid casein, whey protein isolate (WPI) and milk protein isolate (MPI).	86
Table 3.2. Effect of sonication time on pH and protein size (D_z) of NaCas, WPI and MPI solutions at a concentration of 0.1 wt. %. The standard deviation for all pH measurements was < 0.04 in all cases.	93
Table 3.3. Average protein size (D_z) and span of untreated and ultrasound treated NaCas, MPI and WPI at a concentration of 0.1 wt. %.	94
Table 3.4. Intrinsic viscosity ($[\eta]$), Huggins (k_H) and Kraemer (k_K) constants obtained for untreated and ultrasound treated NaCas, WPI and MPI solutions.	100
Table 4.1. Composition and pH (measured at a concentration of 1 wt. % and a temperature of 25 °C) of bovine gelatin (BG), fish gelatin (FG), egg white protein (EWP), pea protein isolate (PPI), soy protein isolate (SPI) and rice protein isolate (RPI).	121
Table 4.2. Effect of sonication time on pH of BG, FG, EWP, PPI, SPI and RPI solutions at a concentration of 0.1 wt. %. The standard deviation for all pH measurements was < 0.04 in all cases.	130
Table 4.3. Average protein size (D_z) and span of untreated and ultrasound treated animal and vegetable proteins at a concentration of 0.1 wt. %.	131
Table 4.4. Intrinsic viscosity ($[\eta]$), Huggins (k_H) and Kraemer (k_K) constants obtained for untreated and ultrasound treated animal and vegetable protein solutions.	135
Table 5.1. Composition and pH of milk protein isolate (MPI) and pea protein isolate (PPI)	161
Table 5.2. Acoustic power (P_a) and acoustic intensity (I_a) for lab (Viber Cell 750) and pilot (UIP1000hd) scale ultrasonic processors.	163
Table 5.3. Residence times (t) of pre-emulsion within acoustic field for lab (Viber Cell 750) and pilot (UIP1000hd) scale ultrasonic processors with respect to volumetric flowrate (Q).	166

Nomenclature

Ultrasound

$(\vec{v} \cdot \nabla \vec{v})$	Convective acceleration or inertia term associated with acoustic streaming
\vec{F}	Force per unit volume inducing acoustic streaming
\bar{p}	Time average variation of pressure
\vec{v}	Velocity of acoustic waves
\bar{v}	Time average variation of velocity
C	Speed of sound in a given medium
c_p	Specific heat capacity of medium
dT/dt	Rate of change of temperature with respect to time
$e^{-\beta x}$	Damping term accounting for spatial attenuation of acoustic beam
F_a	Acoustic momentum
F_h	Hydrodynamic momentum
F_L	Spatial rate of decay of hydrodynamic momentum flow rate
I_0	Acoustic power intensity at the tip of the sonotrode
I_a	Acoustic power intensity
K	Bulk modulus for solids and liquids and modulus of elasticity for gases
K_m	Mechanical momentum

M	Mass of ultrasound treated medium
P	Pressure amplitude
P_0	Acoustic power at the tip of the sonotrode
P_a	Acoustic power
R	Radius of the acoustic beam
S	Width of the acoustic jet as a function of distance from the sonotrode tip
S_A	Surface area of ultrasound emitting surface
U	Voltage of the transducer
x	Distance from source emanating the sound beam
α	Absorption coefficient
β	Attenuation coefficient
μ	Viscosity
μ_t	Eddy viscosity
ρ	Density of a given medium
ρc	Acoustic resistance
ω	Frequency of acoustic wave

Rheology

$[\eta]$	Intrinsic viscosity
c^*	Critical overlap concentration
K	Mark-Houwink constant
k_H	Huggins' constant
k_K	Kraemer constant
A	Mark-Houwink exponent
η	Apparent viscosity
η_0	Zero shear viscosity
η_{rel}	Relative viscosity
η_s	Viscosity of solvent
η_{sp}	Specific viscosity

Emulsions

α	Characteristic length scale for the LSW theory
ΔG	Free energy differential
ΔP_L	Laplace pressure
D	Diffusion coefficient of dispersed phase through the continuous phase

$d_{3,2}$	Sauter mean diameter
G	Velocity gradient
R	Emulsion droplet radius
$S(\infty)$	Solubility of dispersed phase within continuous phase for an emulsion droplet with a planar interface
u'	RMS average difference between u and the overall flow velocity
v_s	Separation velocity
V_m	Molar volume of the dispersed phase
We	Weber number
We_{cr}	Critical Weber number
X	Average eddy size
x_0	Smallest eddy size
γ	Interfacial tension
Γ	Surface loading at emulsion droplet interface
η_c	Viscosity of the continuous phase
η_D	Viscosity of the dispersed phase
ρ_c	Density of the continuous phase
ρ_d	Density of the dispersed phase

τ_{def} | Duration of drop deformation

τ_{dis} | Duration of disruptive forces

Other

g | Local gravitational acceleration

M_w | Molecular weight

R_h | Hydrodynamic radius

R | Ideal gas constant

S | Svedberg sedimentation unit

T | Temperature

t | Time

Abbreviations

BG | Bovine gelatin

CAC | Critical association concentration

CFC | Critical flocculation concentration

CMC | Critical micelle concentration

DLS | Dynamic light scattering

DSD	Droplet size distribution
EWP	Egg white protein
FG	Cold water fish gelatin
IEP	Isoelectric point
L-wave	Longitudinal wave
MPI	Milk protein isolate
NaCas	Sodium caseinate
O/W	Oil-in-water (emulsion)
O/W/O	Oil-in-water-in-oil (emulsion)
PPI	Pea protein isolate
RMS	Root mean square
RPI	Rice protein isolate
SDS-PAGE	Sodium dodecyl sulphate polyacrylamide gel electrophoresis
SEM	Scanning electron microscopy
SLS	Static light scattering
SMD	Sauter mean diameter
SPI	Soy protein isolate
T-wave	Transverse wave

W/O	Water-in-oil (emulsion)
W/O/W	Water-in-oil-in-water (emulsion)
WPI	Whey protein isolate
wt. %	Weight percentage

Chapter 1. Introduction

1.1. Background

From the 17th century population growth accelerated exponentially due to increases in agricultural production as well as increasing medical knowledge and technological innovation, linked to the industrial revolution (Boserup, 1981). According to Thomas Malthus, a prominent 18th century English cleric and scholar, populations tend to increase faster than the supply of food available for its needs. Overtime population will exceed the increase in agricultural production and population will decrease due to food shortages, known as a Malthusian crisis. Malthus concluded that “the power of population is indefinitely greater than the power in the earth to produce subsistence for man.” However, Malthus recognised that technological development and better agricultural techniques could raise the ceiling of population and delay the point of crisis. However, inevitably, population growth will outstrip technological driven food production and crash (Malthus, 1798).

Since the time of Malthus, human population has grown sevenfold to 7.2 billion people (US Census Bureau, 2014) and to date the growth of food production has outstripped the rate of population growth, however there are indications that the rate of food production is slowing (FAO, 2014). In the first decade of the 21st century food prices increased rapidly (World Bank, 2014a), and in particular, between 2005 and the summer of 2008 the prices of wheat and corn tripled, and the price of rice increased fivefold, leading to food riots in over two dozen countries primarily in the developing world (World Bank, 2014b). However, unlike previous price fluctuations, driven by short term local regional food shortages, this peak in grain price occurred in a year where the world’s farmers achieved a record grain crop. The high food prices were a symptom of a greater problem within the global food web. For most of the first decade of the 21st century the world has been consuming more food than has been produced. After years of drawing down stockpiles, in 2007 the world saw global grain reserves fall to 60 days of global consumption, the second lowest on record at that time

(USDA, 2014). Given the decreasing rate of agricultural production, at present 1-2% per annum, and expected to decline further in coming decades, suggesting that it could become too low to meet population growth and increasing demand.

Of the components necessary for human nutrition, including proteins, carbohydrates, fats, vitamins and minerals, proteins are essential for the formation of body proteins such as structural proteins (*i.e.* keratin and collagen), for the building and repair of tissue, and enzymes for carrying out metabolic processes (Smil, 2002). In addition they can be utilised as an energy source containing 4 kcal per gram, similar to carbohydrates, unlike lipids though possessing approximately 9 kcal per gram (Damodaran, 1997a). Nonetheless, from a nutritional standpoint the defining characteristics of proteins are their amino acid sequence. During human digestion proteins are broken down to polypeptides and peptides by the action of hydrochloric acid and proteases, whereby this action allows for the synthesis of essential amino acids, which cannot be biosynthesised by the body. There are nine essential amino acids, phenylalanine, valine, tryptophan, threonine, methionine, leucine, isoleucine, lysine and histidine, which are necessary in order to prevent protein malnutrition (Friedman, 1996).

In the middle of the 20th century one of the issues regarding protein in nutrition was not one of quantity, but rather of quality, a source of protein that would provide a balance of the essential amino acids. In areas where wheat is the major part of the caloric intake the main deficiency is that of lysine, in addition corn is lacking lysine and tryptophan, and rice is lacking lysine and threonine (Jansen & Howe, 1964). Currently, there are major concerns associated with disparities in protein intake between the richer countries, where protein intake is excessive and at inadequate levels of protein consumption, from both a quality and quantity perspective, for hundreds of millions living in Asia, Africa and Latin America (Smil, 2002). To overcome these issues of protein deficiency a number of methodologies are being

implemented, namely the adoption of alternative protein sources, and novel processing technologies for the development of functional ingredients and food products.

Traditional proteins commonly utilised within food applications are either dairy based (skimmed milk powders, milk protein concentrates/isolates, whey protein concentrates/isolates, caseinates, etc) or animal derived proteins (bovine/porcine gelatin, egg white/yolk proteins, etc), whilst proteins can be sourced from other areas, namely vegetable sources, such as cereals (*e.g.* rice, wheat and barley) or legumes (*e.g.* pea, soy and lentil). Recently these protein sources have gained much interest due to their abundant availability and improved public perception, by comparison to the traditional dairy and animal proteins, yet the fundamentals of how these proteins behave within food systems are yet to be fully understood. Moreover, the protein component of these sources was often discarded to waste, after extraction of the more ample component, for example in the case of rice, where the protein component (~ 8 %) was discarded, as the starch component (~ 80 %) yields greater commercial value (Cao *et al.*, 2009; Gonzalez-Perez & Arellano, 2009).

A relatively new application within the food industry is power ultrasound for the modification of food microstructures. Ultrasound treatment (low frequency, high power) of foodstuffs generates regions of high hydrodynamic shear, elevated temperatures and the potential for chemical reactions from free radical generation (O'Brien, 2007). Ultrasound processing of proteins has the potential to improve the functionality (emulsifying, foaming, gelation, viscosity enhancement, etc.) and in addition replace current emulsification technologies, as it has displayed potential for the efficient fabrication of submicron emulsions. This will rely on a detailed understanding of the fundamentals of low frequency, high power ultrasound and how it impacts upon food ingredients, namely proteins, for functional modification, and lipids, for emulsification. Whilst significant progress has been made in this subject matter, there is still much to be gained.

1.2. Aims of the research

Given the preceding gaps in knowledge required for the utilisation of new protein sources and the novel technologies for the development of these sources, the aim of this thesis is to advance the understanding of novel technologies for both the improvement of the functional properties of proteins, emulsion formation in the presence of proteins and fabrication of emulsions using ultrasound. Specifically, the effect of ultrasound treatment upon the physicochemical properties of a range of proteins derived from different sources and ultrasonic emulsification, are investigated.

To achieve these objectives, solutions of proteins, derived from dairy, animal and vegetable sources, were treated with low frequency, high power ultrasound and their physicochemical properties were thoroughly analysed using a wide range of techniques. The analysis of these results will be discussed in relation to submicron emulsion formation, investigated by comparing the effect of ultrasound treatment of proteins, protein type and emulsifier concentration, on the formation and stability of submicron emulsions.

Low frequency, high power ultrasound has shown the capacity for emulsion formation, yet the fundamentals involved are yet to be fully understood. In this work, emulsions are prepared via batch and continuous configurations varying the process parameters and compared between them to discern factors involved in emulsification and the energy required to yield submicron droplets in the presence of proteins.

1.3. Relevance to Kerry Group

Kerry Group PLC., the industrial collaborator of this study, is a public multinational company which primarily trades, develops and markets food ingredient and flavours. Kerry Group was founded in Listowel, Ireland in 1972 and was initially a privately owned dairy co-operative prior to becoming a public company in 1986 (Kennelly, 2000). They are now world

leaders in the ingredients and flavours markets employing 24,000 people in 43 countries with an annual revenue of ~ €5.93 billion (Kerry, 2014a). Kerry Group's business can be identified into three primary segments: ingredients and flavours (operating globally), foods (operating within UK and Irish markets) and agribusiness (operating solely within Ireland). Within the ingredients and flavour sector, Kerry Ingredients and Flavour is the business unit that markets, develops and distributes ingredients and flavours to the global food, beverage, nutrition (infant and clinical) and pharmaceutical industries.

Increasing global population is adding strains on the current food resources, producing circumstances whereby vast numbers of people are unable to secure balanced sources of nutrition, sufficient carbohydrate, protein, both quantity and quality, vitamins and minerals. Consequently, there has been a shift within industry to develop infant and clinical nutrition bases and beverages which have the capacity of fulfilling the dietary requirements of infants and the elderly effectively. This industrial shift has arisen due to concerns regarding the standards of nutrition globally, in particular in the field of infant nutrition and the development of high protein concentration clinical nutrition beverages. This is particularly problematic as high protein clinical nutrition beverages tend to have high viscosities as a consequence of the elevated proteins, making their consumption difficult.

As discussed previously, proteins are vital for human nutrition and as functional ingredients within a wide range of sectors. Additionally, the implementation of novel technologies, such as ultrasound, has the capability to improve protein functionality, either from emulsifying or rheological perspectives. Therefore, since Kerry manufactures and distributes a wide range of proteins ingredients and protein based infant formulae, the results of this thesis are to their benefit as they are in a prime position to improve the understanding of proteins as emulsifiers and implement novel technologies (ultrasound) for the development of functional protein ingredients. Kerry Group's mission statement states that they aim "to be

the world leaders in food ingredients and flavours serving the food and beverage industry” (Kerry, 2014b). Thus, Kerry Group has an interest in implementing novel technology for the development of proteins with improved functionality. More specifically, the results and discussion contained within this thesis allow Kerry Group to develop novel ingredients with improved emulsifying and rheological properties, and efficient emulsification processes.

1.4. Thesis layout

This manuscript is composed of six chapters, an introduction, a literature survey, three results chapters, and a conclusions and future work chapter.

- Chapter 1 is an introduction outlining background information, the rationale for the work and the industrial relevance.
- Chapter 2 details the state of the art for proteins, emulsion science, the fundamentals of ultrasonic processing and applications of ultrasound for the alteration and generation of microstructures.
- Chapter 3 is the first results chapter, detailing the effect of ultrasound treatment upon the structural and emulsifying properties of three dairy proteins.
- Chapter 4 is the second results chapter investigating the effect of ultrasound treatment of three animal derived proteins and three vegetable proteins, upon their physical and emulsifying properties.
- Chapter 5, the final results chapter, investigates sonication for the fabrication of submicron emulsions in the presence of proteins, comparing batch and continuous processing methodologies.
- Chapter 6 summarises the conclusions of this study and provides recommendations for future work.

1.5. Publications and conferences

Results and discussions obtained throughout this study have been published and presented at conferences as follows.

Publications:

O'Sullivan, J.J. and Norton, I.T. 2016. Novel ultrasonic emulsification technologies, *Gums and stabilisers for the food industry*, 18. (Submitted)

O'Sullivan, J.J., Greenwood, R.W. and Norton, I.T. 2015. Applications of ultrasound for the functional modification of proteins and nanoemulsion formation: A review. *Trends in Food Science and Technology*. (Submitted)

O'Sullivan, J.J., Murray, B., Flynn, C. and Norton, I.T. 2015. Comparison of batch and continuous ultrasonic emulsification processes. *Journal of Food Engineering*. (In press)

O'Sullivan, J.J., Murray, B., Flynn, C. and Norton, I.T. 2015. The effect of ultrasound treatment on the structural, physical and emulsifying properties of animal and vegetable proteins. *Food Hydrocolloids*. (In press)

O'Sullivan, J.J., Arellano, M., Pichot, R. and Norton, I.T. 2014. The effect of ultrasound treatment on the structural, physical and emulsifying properties of dairy proteins. *Food Hydrocolloids*, **42(3)**, 386-396.

O'Sullivan, J.J., Pichot, R. and Norton, I.T. 2014. Protein stabilised submicron emulsions, *Gums and stabilisers for the food industry*, 17, 223 – 229.

Poster presentation:

O'Sullivan, J.J., Pichot, R. and Norton, I.T. Effect of protein structure and molecular weight on the formation of O/W emulsions. *1st UK Hydrocolloids Symposium*, Huddersfield, 2013.

O'Sullivan, J.J. and Norton, I.T. Ultrasonic effect on the rheology of protein solutions. *1st Congress on Food Structure Design*, Porto, 2014.

O'Sullivan, J.J. and Norton, I.T. Comparison of batch and continuous acoustic emulsification processes. *28th EFFoST International Conference*, Uppsala, 2014.

Oral presentation (speaker underlined):

O'Sullivan, J.J., Pichot, R. and Norton, I.T. Protein stabilised submicron emulsions, *17th Gums and Stabilisers for the Food Industry*, Wrexham, 2013.

O'Sullivan, J.J., Arellano, M. and Norton, I.T. The ultrasonic effect on the physicochemical properties of animal and vegetable proteins as emulsifiers, *12th International Hydrocolloids Conference*, Taipei, 2014.

O'Sullivan, J.J. and Norton, I.T. Ultrasonic effect on the rheology of protein solutions. *28th EFFoST International Conference*, Uppsala, 2014.

1.6. References

Boserup, E. (1981). *Population and technological change: a study of long-term trends*.

Chicago: University of Chicago Press Chicago Ill. United States 1981. Retrieved from <http://www.popline.org/node/389788>

Cao, X., Wen, H., Li, C., & Gu, Z. (2009). Differences in functional properties and biochemical characteristics of congenetic rice proteins. *Journal of Cereal Science*, 50(2), 184–189.

Damodaran, S. (1997). Food Proteins: An Overview. In S. Damodaran & A. Paraf (Eds.), *Food Proteins and Their Applications* (1st ed., pp. 1–24). New York: Marcel Dekker.

FAO. (2014). Food Situation. Retrieved October 03, 2014, from <http://www.fao.org/worldfoodsituation/en/>

Friedman, M. (1996). Nutritional Value of Proteins from Different Food Sources. A Review. *Journal of Agricultural and Food Chemistry*, 44(1), 6–29.

Gonzalez-Perez, S., & Arellano, J. B. (2009). Vegetable protein isolates. In G. O. Philips & P. A. Williams (Eds.), *Handbook of Hydrocolloids* (2nd ed., pp. 383 – 419). Woodhead Publishing Limited.

Jansen, G. R., & Howe, E. E. (1964). World Problems in Protein Nutrition. *Am J Clin Nutr*, 15(5), 262–274. Retrieved from <http://ajcn.nutrition.org/content/15/5/262.abstract>

Kennelly, J. (2000). *The Kerry Way: From Dairy Co-operative to Multinational Corporation, Kerry Group PLC, 1972-1999*. Cork: Oak Tree Press.

Kerry. (2014a). *Kerry Group - An Introduction*. Retrieved October 03, 2014, from http://www.kerrygroup.com/docs/Kerry_Group_Business_Description.pdf

Kerry. (2014b). Our Mission. Retrieved October 03, 2014, from <http://www.kerrygroup.com/our-company/our-mission>

Malthus, T. R. (1798). *An Essay on the Principle of Population*. London: J. Johnson.

O'Brien, W. D. (2007). Ultrasound-biophysics mechanisms. *Progress in Biophysics and Molecular Biology*, 93(1-3), 212–55.

Smil, V. (2002). Nitrogen and Food Production: Proteins for Human Diets. *AMBIO: A Journal of the Human Environment*, 31(2), 126–131.

US Census Bureau. (2014). U.S. and World Population Clock. Retrieved October 03, 2014, from <http://www.census.gov/popclock/>

USDA. (2014). *World Agricultural Supply and Demand Estimates*. Retrieved October 03, 2014, from <http://www.usda.gov/oce/commodity/wasde/latest.pdf>

World Bank. (2014a). Food Price Watch, May 2014: First Quarterly Increase Since August 2012; The Role of Food Prices in Food Riots. Retrieved October 03, 2014, from <http://www.worldbank.org/en/topic/poverty/publication/food-price-watch-may-2014>

World Bank. (2014b). Food Security. Retrieved October 03, 2014, from <http://www.worldbank.org/en/topic/foodsecurity>

Chapter 2. State of the Art

Discussions contained within this chapter have been submitted for publication within:

O’Sullivan, J.J., Greenwood, R.W. and Norton, I.T. 2015. Applications of ultrasound for the functional modification of proteins and the nanoemulsion formation: A review. *Trends in Food Science and Technology*.

2.1. Background literature survey: proteins and emulsions

The aim of this section of this chapter is to present a comprehensive survey of relevant literature, including an overview of general protein structure, and association behaviour of proteins in aqueous solutions. Then, the functional properties, emulsifying, foaming, gelation and viscosity enhancement, of proteins is discussed. Emulsion theory is then examined in terms of basic terminology, emulsion formation, in terms of droplet breakup mechanism and the role of the emulsifier, and emulsion destabilisation mechanisms (gravitational separation, flocculation, phase separation and Ostwald ripening).

2.1.1. Proteins

Proteins serve a variety of functions in both biological settings and food systems owing to the complex chemical make-up of these biopolymers. Some of the roles which proteins perform in these systems include biocatalysis (*i.e.* enzymes; *e.g.* amylase, lactase, lipase, maltase, etc.), hormones (*e.g.* insulin, oxytocin, growth hormone, etc.), antibodies (*i.e.* immunoglobulins), chelation of metal ions (*e.g.* phosvitin, phytochelatin, etc.), protective proteins (*i.e.* toxins and allergens), transport proteins (*e.g.* haemoglobin, serum albumin, etc.), structural components within organisms (*e.g.* collagen, keratin, lamin, elastin, etc.), contractile proteins (*e.g.* actin, tubulin, etc.) and as storage proteins (*e.g.* micellar casein, egg and legume albumens, etc.) as sources of energy and nitrogen for developing embryos (Berg *et al.*, 2012; Boye *et al.*, 1997; Damodaran, 1997; DeMan, 1999).

Proteins are biological polymers constituted of monomer units known as amino acids, of which 19 are true amino acids and 1 is an imino acid, proline, however, they are all commonly referred to as amino acids (Damodaran, 1997a). These 20 amino acids can be categorised by their characteristics: aliphatic (alanine, glycine, leucine, isoleucine, proline and valine), aromatic (phenylalanine, tryptophan and tyrosine), acidic (aspartic acid and glutamic acid), alkaline (arginine, histidine and lysine), hydroxylic (serine and threonine), thiolic (cysteine and methionine) and amidic (asparagines and glutamine) (DeMan, 1999). Protein structure has four levels of complexity: primary, secondary, tertiary and quaternary (Berg *et al.*, 2012).

The *primary structure* of a protein refers to the linear amino acid sequence of a given polypeptide chain. The amino acid subunits of the primary structure are held together by covalent bonds called peptide bonds. The peptide bond possesses a partial double bond character due to its resonance structure, restricting rotation of this bond to a maximum of 6°.

This sequence of amino acids gives the protein its three dimensional conformation and its functionality (Berg *et al.*, 2012; Damodaran, 1997a). The *secondary structure* of proteins refers to the highly regular local sub-structures. The two main structures that occur are alpha-helices and beta-sheets or -strands (*cf.* Fig. 2.1; Pauling *et al.*, 1951). These secondary structures are defined by patterns of hydrogen bonds between the primary chain peptide groups, the C=O and N-H groups (Damodaran, 1997a).

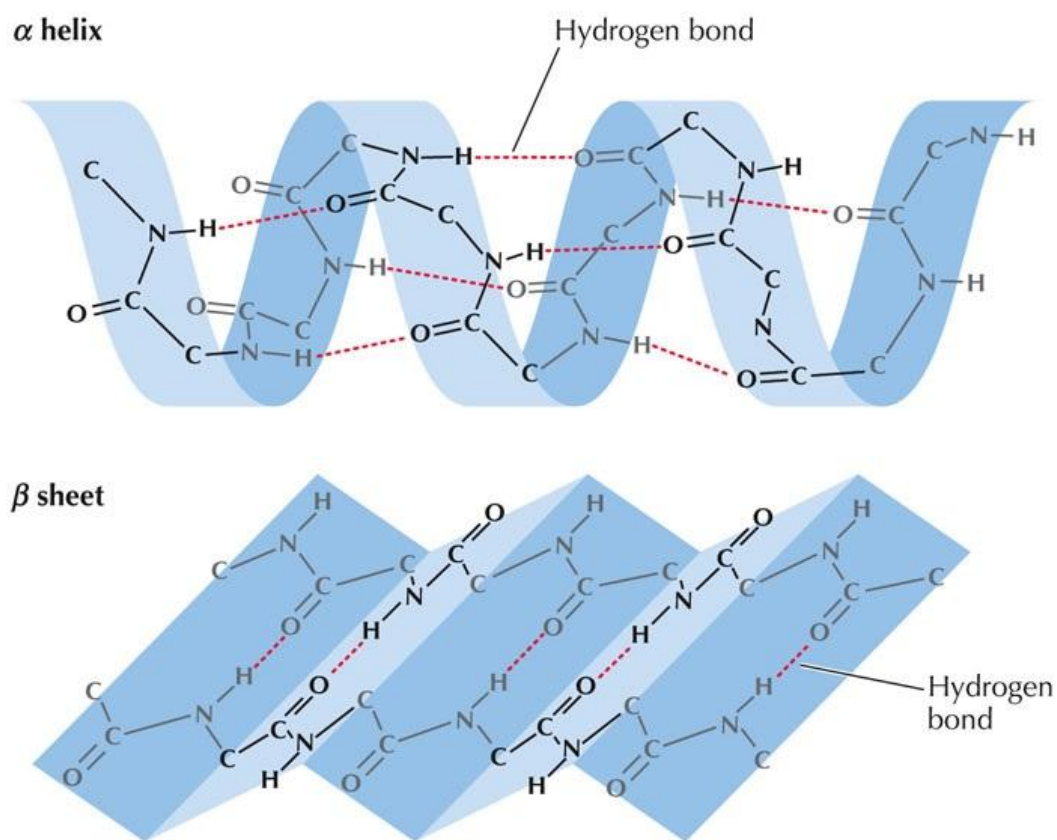


Fig. 2.1. Depiction of alpha helices and beta sheets secondary protein structures. Image adapted from Berg *et al.*, (2012)

The *tertiary structure* of proteins refers to the three-dimensional structure of a single protein molecule. The alpha-helices and beta-sheets are folded into a compact globule. This folding is driven thermodynamically by hydrophobic interactions to minimise the free energy of the molecule, which are locked in place by specific tertiary interactions, such as salt

bridges, hydrogen bonds, tight packing of side chains and disulphide bonds (DeMan, 1999). The most important rearrangement associated with the tertiary structure of proteins is the geometric displacement of hydrophobic residues to the interior of the globule and expulsion of hydrophilic residues to the exterior of the globule (Damodaran, 1997a). The *quaternary structure* of proteins is the three-dimensional structure composed of a number of polypeptide chains, whereby these polypeptide chains are known as sub units, and the quaternary complex comprising of these sub units is referred to as oligomeric structures. The quaternary structure is stabilised by the same non-covalent interactions and disulphide bonding, as in the tertiary structure. Proteins molecules containing greater than 28% hydrophobic residues (*i.e.* valine, leucine, isoleucine, phenylalanine and proline) possess a tendency to associate into oligomeric structures, as with this percentage of hydrophobic residues in the primary structure it is physically impossible to conceal all of the hydrophobic residues within the interior of the globule, yielding non-polar regions on the exterior of the globule. These non-polar regions interact with one another to form oligomeric structures (Damodaran, 1997a; DeMan, 1999). Complex oligomeric structures are commonly exhibited in vegetable proteins where the percentage of hydrophobic residues is typically greater than 35 %, and the association and disassociation behaviour of these oligomeric structures has been shown to be highly dependent on the serum conditions, such as pH and ionic strength (Gonzalez-Perez & Arellano, 2009).

In aqueous solutions proteins either manifest in a monomeric state, as discrete protein molecules, or as associates, a cluster of protein molecules. Micellisation of protein molecules arises, either due to decreases in solvent quality which induces the formation of protein associates, or owing to an increase in protein concentration allowing for interactions between protein molecules, similar to molecular associations exhibited by low molecular weight surfactants (micelles), referred to as the critical micelle concentration (CMC), driven

entropically by reducing the Gibbs free energy of the system. In the case of proteins the concentration dependent association is known as the critical association concentration (CAC) (O'Connell *et al.*, 2003). In particular, proteins which exhibit an amphiphatic character are susceptible to these association mechanisms, whereby they arise due to hydrophobic associative forces between protein molecules, while electrostatic and steric repulsive forces are responsible for associate integrity (Damodaran, 1997a). Removal of the steric repulsive forces present within protein associates through reduction of the molecular weight profile of proteins by proteolysis leads to a plastein type reaction, whereby insoluble particulates, plasteins, are formed (Clemente, 2000). Proteolysis of proteins involves the breakdown of the protein molecules into smaller protein fractions, yielding a mixture of hydrophobic, hydrophilic or amphiphatic peptides. These peptides rearrange themselves to form plasteins, insoluble polypeptides formed by the action of proteolytic enzymes on the hydrolysis of proteins. Plasteins have a core of hydrophobic and hydrophobic sections of amphiphilic peptides and a shell of hydrophilic and hydrophilic sections of amphiphilic peptides. The plastein reaction is driven by hydrophobic forces and is a purely entropy-driven physical phenomenon. Gel electrophoresis (reducing SDS-PAGE) has shown that these aggregates were not held together by covalent bonds, indicating that the aggregates were maintained by hydrophobic associative forces (Mozaffar & Haque, 1992; Yamashita *et al.*, 1976).

2.1.1.1. Protein functionality

The term 'functionality' as applied to food ingredients describes any property other than nutritional attributes that contribute to an ingredient's beneficial aspects within a formulation. Proteins are highly functional molecules within food systems capable of the stabilisation of oil droplets and air bubbles, formations of gel structures and the enhancement of viscosity. This functionality is due to the complex chemical makeup of these molecules

owing to their unique amino acid sequences (O'Connell & Flynn, 2007; Walstra & van Vliet, 2003).

2.1.1.1.1. Emulsions and foams

Emulsions and foams are colloidal dispersions of two immiscible liquids (*i.e.* oil and water), and a liquid and a gas, respectively (Foegeding & Davis, 2011; Walstra, 1993). Proteins are capable of stabilising both oil-water and air-water interfaces owing to their surface active nature and amphiphilic characteristics. Proteins are surface active due to their unique amino acid sequence which produces hydrophobic and hydrophilic regions throughout the polypeptide chain. At the interface proteins adapt to the most entropically stable state, where the hydrophilic and hydrophobic amino acid side chains associate with the continuous and dispersed phases respectively with the state of least energy (O'Connell & Flynn, 2007). The continuous phase for both protein stabilised foams and emulsions is an aqueous protein solution, whilst the dispersed phase is either oil droplets or air bubbles for emulsions and foams, respectively.

Proteins in solution are capable of forming emulsions and foams by reducing the free energy at the interface between the apolar (*i.e.* oil or air) and polar (*i.e.* aqueous) phases, by reducing the interfacial tension, known as surface tension for air-water systems (Caetano da Silva Lannes & Natali Miquelim, 2013). There are two main stages in the reduction of interfacial tension by proteins of the air-water and oil-water interfaces. The first stage is adsorption of proteins from the bulk to the interface, and is primarily dictated by the molecular weight of the proteins. Proteins possessing lower molecular weights have greater molecular mobility through the bulk allowing for more rapid adsorption to the interface. The second stage is conformational denaturation or re-alignment of proteins upon adsorption at interfaces, whereby the protein rearranges itself to the most entropically stable state,

positioning the hydrophobic residues at the interface and the hydrophilic residues extend into the bulk (Beverung *et al.*, 1999). Proteins possessing lower molecular weights exhibit greater rheomorphic properties allowing for more rapid conformational changes at interfaces (O'Connell & Flynn, 2007).

In addition to lowering the interfacial tension, proteins are capable of forming strong viscoelastic films around oil droplets and air cells (McClements, 2004). These viscoelastic films form via a combination of non-covalent intermolecular associative interaction (*i.e.* hydrogen bonding and van der Waals forces) and covalent mechanisms, notably disulphide cross-linking between cysteine residues (Lam & Nickerson, 2013). The formation of these films at interfaces prevents coalescence of oil droplets and air bubbles prolonging the stability of multiphase systems. The efficacy of a protein to develop a strong viscoelastic film at an interface is highly dependent on the surface activity of the protein, where the surface activity of a protein includes conformational stability at interfaces, rapid transformations of conformation to environmental changes, the availability and the distribution of hydrophobic and hydrophilic regions throughout both the primary amino acid sequence and on the surface of the protein globule (Foegeding & Davis, 2011).

Proteins are amphiphatic molecules, yielding an overall electrical charge on the surface of the protein associate, characterised by the ζ -potential (DeMan, 1999). Adsorbed proteins at interfaces confer electrostatic repulsive stability to emulsion droplets and air bubbles, enhancing stability by reducing the likelihood of droplet contact and maintaining bubble separation (Given, 2009). Furthermore, as a consequence of the proteins molecular weight and adsorption patterns at interfaces (*i.e.* hydrophilic residue extension into the bulk) steric stabilisation of emulsion droplets occurs and this interaction has two components (O'Connell & Flynn, 2007). The first is the osmotic repulsion between the overlapping segments, favouring the stretching of chains, and the second is associated with the elastic

energy of the chains, which opposes stretching. The osmotic repulsive force is the dominant of the two interactions allowing for droplet stabilisation (Damodaran, 1997b).

Be that as it may, many food formulations use high concentrations (> 10 wt. %) of protein for nutrition purposes, such as in clinical or parenteral nutrition beverages (Waitzberg, 2014). In these circumstances a large proportion of the protein in the formulation remains in the bulk, in the form of protein associates (Hunt & Dalgleish, 1994). These colloidal protein associates can contribute to depletion flocculation mechanisms, increasing the associative osmotic forces between droplets by the exclusion of these associates from a narrow region between adjacent droplets. This destabilisation mechanism can be minimised by reduction of the emulsion droplet size, reducing the van der Waals forces between droplets (Dickinson, 2010; Radford & Dickinson, 2004).

2.1.1.1.2. Gelation

Gelation is the mechanism by which aqueous solutions of high molecular weight carbohydrates or proteins are cross-linked to form an intermolecular network distributed through the volume of the liquid medium (Ziegler & Foegeding, 1990). A colloquial definition for a gel is defined as a “system of a solid character, in which colloidal particles somehow constitute a coherent structure,” (Bungenberg de Jong, 1949) whilst the most useful definitions for gels are derived from rheology, the study of the deformation and flow of matter. A gelatinous material is a semi-solid, known as a viscoelastic material, having rigidity yet deforms under applied stresses, possessing both solid-like and liquid-like rheological aspects (Oakenfull *et al.*, 1997).

The structure of proteins, owing to their unique amino acid sequences, allows a range of practical applications unrivalled by other polymers. In biology, the majority of natural gels are constituted of proteins or proteins attached to carbohydrates. Collagen appears to be the

gel-forming protein in jellyfish (Kimura *et al.*, 1983) and blood clots are formed by the action of thrombin, a serine protease, on fibrinogen, a plasma glycoprotein (340 kDa), resulting in end-to-end aggregation and the formation of a gel network structure (Davie & Ratnoff, 1964). Proteins display two mechanisms of gelation, irreversible and reversible gelation (Oakenfull *et al.*, 1997). Irreversible gelation is the mechanism whereby proteins possessing globular structures unfold in the presence of changes in temperature, pH or ionic conditions and aggregation occurs (Boye *et al.*, 1997). Reversible gelation is uncommon for proteins, with the notable exception of gelatin, whereby heating a gel fabricated with gelatin liquefies the gel (Haug *et al.*, 2004).

2.1.1.1.2.1. Irreversible gelation – thermal denaturation and coagulation of proteins

Irreversible gelation of proteins occurs through a sequence of events, starting with protein denaturation, followed by aggregation of denatured protein molecules and lastly cross-linking of protein strands (Boye *et al.*, 1997). Denaturation of proteins is defined as any modification in the conformational structure of a protein (secondary, tertiary or quaternary structure) without scission of peptide linkages between amino acids involved in the primary structure (Cheftel *et al.*, 1985). One of the most common methods for achieving protein denaturation is to heat them in solution. Heat treatment of globular proteins in solution increases the molecular motion due to increasing thermal energy, leading to disruption of inter- and intramolecular associative bonds which maintain the structure of native proteins. This results in rearrangements of the secondary and tertiary structures where previously internally and concealed hydrophobic amino acid sequences become exposed to the solvent, yielding the formation of new intermediary conformations (Sakurai *et al.*, 2009).

Denatured protein chains associate through intermolecular interactions to form aggregates of irreversibly denatured entities, leading to precipitation, coagulation or gelation

(Mine, 2002). Protein aggregation involves the formation of higher molecular weight species from denatured protein, which then cross-link by specific bonding at specific sites along protein chains or by non-specific bonding which occurs throughout the peptide backbone. Cross-linking of protein aggregates, after denaturation, involves one or more of the following mechanisms; (1) oxidative chemical reactions of protein molecules resulting from the covalent linkage of amino acid residues, (2) cross-linking of proteins by agents dissolved within the solvent (*i.e.* metal ions), (3) physiochemical changes leading to reduced solubility (*i.e.* pH near the isoelectric point, IEP, or changes in ionic conditions), and (4) chemical modifications of proteins leading to decreases in protein solubility (*i.e.* the Maillard reaction). Disulphide and hydrogen bonding, as well as ionic interactions, are involved in cross-linking mechanisms of aggregates from denatured proteins (Alvarez *et al.*, 2008; Foegeding *et al.*, 2002; Sun & Arntfield, 2012; Ziegler & Foegeding, 1990).

Irreversible gelation of food proteins is exhibited by the globular proteins present within milk, whey proteins (Fox, 2008). Gelation of whey protein occurs by heating a whey protein solution, at a concentration above the critical point, to a temperature in excess of the denaturation temperature. The critical point is the minimum concentration required to achieve protein gelation, 8% for whey protein concentrate (WPC). The denaturation temperature of WPC is within the range of 85 – 100 °C, and is dependent on the concentration of WPC in solution (Oakenfull *et al.*, 1997). Initial denaturation of protein structure is followed by intermolecular interactions that form the cross-linked matrix of the gel. Environmental factors, such as pH and ionic strength, influence the intermolecular interactions, thus affecting the viscoelastic properties of the resultant gel (Fitzsimons *et al.*, 2007).

2.1.1.1.2.2. Reversible gelation – gelatin and collagen

In contrast to gels prepared using polysaccharides, whereby typically gels revert to a liquid state upon heating, yet there are examples of chemical gelation induced by addition of ions and changes in solvent quality, protein gels are invariably thermally irreversible, with the evident exception of gelatin (Garrec & Norton, 2012; Veis, 1964). Gelatin is the hydrolysed form of collagen, prepared by heat treatment in the presence of acid or alkali, yielding segments of the parent collagen molecule (Schrieber & Gareis, 2007). The mechanism of gelation of gelatin is different to that of other proteins, where gelation occurs upon cooling of solutions below the helix-coil transition temperature and the protein chains cross-link by forming small regions of the collagen triple helix structure. Increasing the temperature of a gel prepared with gelatin above the gelation temperature liquefies the gel and the helical structure reverts to a random coil configuration (Haug & Draget, 2009).

2.1.1.1.3. Viscosity enhancement

The development of viscosity within food systems is typically achieved by the addition of high molecular weight biopolymers, carbohydrates or proteins, at elevated concentrations. The contribution of a polymeric solute to the viscosity of a solution is dictated by its intrinsic viscosity, $[\eta]$, which is determined for the most part by polymer geometry ('shape') and hydrodynamic volume ('size') (Harding, 1997; Lefebvre, 1982). This relationship is described by the Mark-Houwink equation (Eq. 2.1) where M_w is the molecular weight of the polymer, K is the Mark-Houwink constant and α is the Mark-Houwink exponent, related to the polymer geometry in solution. Values of α range between 0 and 1.8, where 0 represents a theoretical spherical shape, 0.5 – 0.8 gives the range for polymers exhibiting random coil (equivalent sphere) behaviour, and greater values indicate increasing stiffness of the polymer up to values of 1.8 for rigid rod like structures (Sousa *et al.*, 1995).

$$[\eta] = KM_w^\alpha \quad (2.1)$$

The viscosity of protein solutions is determined by the intrinsic factors associated with proteins such as intrinsic viscosity, protein concentration and the intermolecular interaction mechanisms (*i.e.* associative interactions, globule conformation, oligomeric structures, etc.) (Curvale *et al.*, 2008; Lefebvre, 1982). Protein solution viscosity follows a power-law dependence with concentration until the critical overlap concentration (c^*), above which a marked increase in the dependence of concentration occurs (Morris *et al.*, 1981). At concentrations less than c^* , the dilute region, the polymer molecules (colloidal associates for the case of proteins) behave as discrete entities sufficiently distanced with respect to one another, whilst at concentrations greater than c^* , the concentrated region, the combined hydrodynamic radii of the chains exceeds that of the solvent volume and physical chain interpenetration and network development arises (*cf.* Fig. 2.2).

In addition to the intrinsic protein factors which dictate bulk viscosity, extrinsic variations in the serum quality influence the bulk viscosity of protein solutions via modifications to a protein's intrinsic viscosity (*i.e.* hydrodynamic volume) and intermolecular interaction mechanisms. Extrinsic factors include changes to the pH, ionic strength and type of ion (Harding, 1997). The isoelectric point (IEP) of a protein is the pH at which the overall electrical charge (*i.e.* ζ -potential) of a globule surface is 0, and at pH values close to the IEP (± 0.5) reduced electrical surface charges are observed by comparison to pH values further from the IEP (> 1.5), whereby surface electrical charges are sufficient to prevent contact of protein associates (Damodaran, 1997a). As the overall surface electrical charge of protein globules is reduced by approaching the IEP, protein globules come into contact with one another, increasing the hydrodynamic volume of protein globules (Curvale *et al.*, 2008). Increasing the ionic strength of the serum by addition of salts yields a comparable effect upon the hydrodynamic volume of protein globules as approaching the IEP. Increasing the

concentration of ions in serum increases the shielding effect upon the surface electrical charge of globules allowing for contact of discrete protein associates with one another increasing the overall hydrodynamic volume of the protein in solution (Dickinson & Ritzoulis, 2000). These increases in hydrodynamic volume associated with approaching the IEP and increasing ionic strength of the serum environment increase the contribution of protein globule size to the bulk viscosity of the solution (Sousa *et al.*, 1995; Tanner & Rha, 1980).

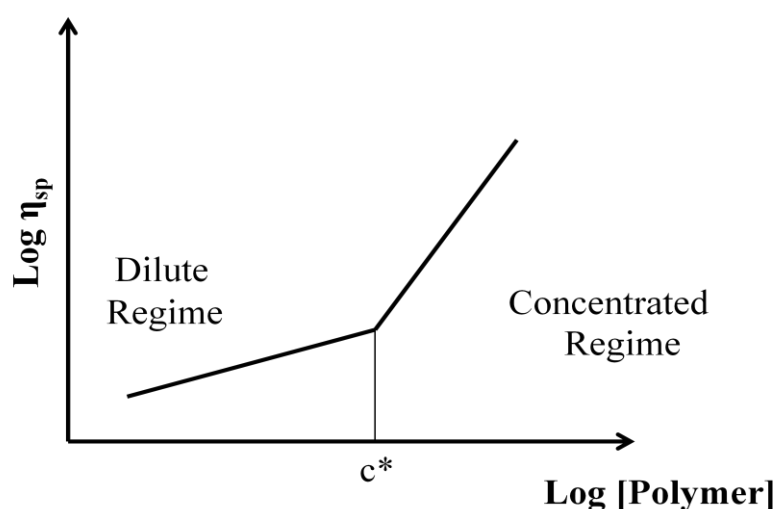


Fig. 2.2. Graphical representation of the relationship between viscosity and polymer concentration, showing the dilute regime, the critical coil overlap concentration and the concentrated regime. Image adapted from Morris *et al.* (1981).

2.1.2. Emulsions

An emulsion is defined as a ‘fluid system in which liquid droplets are dispersed in a liquid’ (IUPAC, 1997). The two liquids in emulsions are immiscible with one another, typically oil and water (McClements, 2005). The process of dispersing one fluid in the form of droplets within another is known as emulsification. Emulsification requires four components, oil, water, an emulsifier and energy (Walstra, 1993). An emulsifier is a material which is often necessary to stabilise emulsion droplets, as oil or water droplets tend to merge together in a process known as coalescence (McClements, 2005; Walstra, 1993). Energy is required for emulsification so as to disrupt and breakup the dispersed phase into droplets within the continuous phase and this is opposed by the Laplace pressure, the pressure differential between the convex and concave side of a curved interface (Walstra, 1993).

Emulsions were first categorised by Ostwald, (1910) in terms of the material of dispersed phase with respect to the continuous phase. More specifically, an emulsion is classified as an oil-in-water (O/W; ‘Oel in Wasser’) emulsion for which the dispersed phase is oil and the continuous phase is water, and conversely as a water-in-oil (W/O; ‘Wasser in Oel’) emulsion whereby the dispersed phase is water and the continuous phase is oil (McClements, 2009; Ostwald, 1910). The primary methods for classifying these types of emulsions are the size of the emulsion droplets. The Sauter mean diameter (SMD), $d_{3,2}$, is commonly used to characterise emulsion droplets, and is defined as the ratio of the third to the second moment of the probability density function (Pacek *et al.*, 1998). The droplet size of an emulsion can be used to classify emulsions either as macroemulsions, nanoemulsions or microemulsions.

Macroemulsions are kinetically stabilised mixtures of two immiscible fluids, for which the dispersed phase has a $d_{3,2}$ approximately of 1 μm to 100 μm . Macroemulsions

scatter light effectively yielding a milky appearance as the droplets are larger than that of the wavelength of light. The scattering of light is due to the difference in refractive indices of the oil and aqueous phases (McClements, 2005).

Nanoemulsions, also referred to as miniemulsions, nano-emulsions, ultrafine emulsions and submicron emulsions (Solans *et al.*, 2005), typically have a $d_{3,2}$ range of 50 nm to 200 nm (Tadros *et al.*, 2004). Unlike microemulsions, nanoemulsions are only kinetically stable, while microemulsions are in addition thermodynamically stable (Eastoe, 2002; Tadros *et al.*, 2004). Nanoemulsions are kinetically stable from considerations of their steric stabilisation and the ratio of the adsorbed layer thickness to the dispersed phase radius (Tadros *et al.*, 2004).

Due to their droplet size, nanoemulsions are translucent in appearance, as the wavelength of light is larger than that of emulsion droplets. The uniformity of droplet size distribution (DSD) and degree of Ostwald ripening (*cf.* section 2.1.2.2.4) of nanoemulsions with respect to time are factors leading to growth in emulsion droplet size and loss of optical transparency (Solans *et al.*, 2005; Tadros *et al.*, 2004). The rate of Ostwald ripening is a strong function of emulsion droplet size and solubility of the dispersed phase in the continuous phase (Henry, 2007).

Nanoemulsions offer several benefits over macroemulsions, including improved stability against creaming/sedimentation (*cf.* section 2.1.2.2.2), flocculation and coalescence due to small emulsion droplet size (*cf.* section 2.1.2.2.3), large surface area for controlled release and optically transparent (McClements, 2011; Solans *et al.*, 2005; Tadros *et al.*, 2004). Despite these benefits, nanoemulsions have only attracted limited interest in recent years due to the specialised equipment necessary for their formation (such as microfluidics or ultrasonics), the perception that these emulsions are expensive to produce, lack of both,

understanding of production mechanisms and demonstration of benefits to list just a few (Tadros *et al.*, 2004).

A microemulsion can be defined as a ‘dispersion made of water, oil and surfactant(s) that is an isotropic and thermodynamically stable system with dispersed domain diameter varying approximately from 1 to 100 nm, usually 10 to 50 nm’ (Slomkowski *et al.*, 2011). Due to the size of the droplets, microemulsions are optically translucent and are thermodynamically stable due to their droplet size (Eastoe, 2002). Microemulsions have many important commercial applications in fields such as personal care, agrichemicals and pharmaceuticals (Eastoe, 2002; Gibaud & Attivi, 2012).

In contrast to macro- and nanoemulsions, requiring high shear for their formation, microemulsions only require simple mixing of their components for their formation, and can form spontaneously under the right conditions (Ansari *et al.*, 2008; Eastoe, 2002). These conditions include a low dispersed phase volume fraction and a high surfactant concentration. Other components may be required in the formulation for the formation of microemulsions, such as co-surfactants and/or salts (Eastoe, 2002). For example, in a microemulsion where SDS is the surfactant, an aliphatic alcohol as a co-surfactant and an electrolyte, such as NaCl, are necessary for the formation of a microemulsion (Eastoe, 2002).

Due to overlap of the droplet size range there are misunderstandings between microemulsions and nanoemulsions. The IUPAC definition of an emulsion excludes microemulsions if the word ‘dispersed’ is interpreted as non-equilibrium and opposite to ‘solubilised’, a term that is applied to both microemulsions and micellar systems, which are thermodynamically stable (Gutiérrez *et al.*, 2008). Nanoemulsions are non-equilibrium systems which, due to the interfacial tension between the two phases (*cf.* section 2.1.2.1.3), will spontaneously phase separate into constituent phases (Gutiérrez *et al.*, 2008).

Nevertheless, the droplet size of nanoemulsions confers kinetic stability to these emulsions, even for several years (Tadros *et al.*, 2004).

Multiple emulsions, also known as double emulsions, are ternary systems having either water-in-oil-in-water (W/O/W) or an oil-in-water-in-oil structure (O/W/O), whereby the dispersed phase contains smaller droplets of a different phase (Jiao & Burgess, 2008; McClements, 2005). Multiple emulsions have a wide range of potential application food, pharmaceutical and cosmetic sciences. In the food sector they could potentially be used for the controlled release of flavour and in the pharmaceutical sector have applications such as prolonged drug release and vaccine adjuvants (Grossiord & Stambouli, 2008; Jiao & Burgess, 2008; Khopade & Jain, 2008; McClements, 2005).

Multiple emulsions, like both macro- and nanoemulsions, are thermodynamically unstable due to the excess of free surface energy between the liquids due the interfacial tension. In simple emulsions, Laplace pressure works against the stability of these systems. In multiple emulsions it is necessary to balance both the Laplace pressure and osmotic pressure from the internal dispersed phase to ensure long term stability of multiple emulsion systems (Jiao & Burgess, 2008).

2.1.2.1. Droplet breakup

Emulsions are fabricated by a combination of a dispersed phase, a continuous phase, an emulsifier and the input of energy, in a process known as emulsification (Walstra, 1993). During emulsification the dispersed phase is disrupted into smaller volumes, in the form of droplets due to Laplace pressure forces (McClements, 2005). The disruption of oil into smaller volumes is known as droplet breakup, and is achieved by a process known as homogenisation. Due to differences in the hydrophobicity and hydrophilicity between the respective dispersed and continuous phases there is a tendency for phase separation to occur

in order to minimise the interfacial surface area between the two phases, an entropy driven mechanism, leading to droplet coalescence (*cf.* section 2.1.2.3.2) (McClements, 2009; O'Connell & Flynn, 2007).

Emulsification is a dynamic process by which two mechanisms occur, a forward reaction for the creation of dispersed phase droplets, droplet breakup, and a back reaction, whereby newly formed emulsion droplets come in contact with one another and re-coalesce. The balance between these processes is of great importance to predict whether emulsion droplets form and the size of the newly formed droplets. The size of the formed emulsion droplets is dependent on the type of the emulsifier, the concentration of the emulsifier and the energy density provided for emulsification (Lee *et al.*, 2013; Niknafs *et al.*, 2011).

The interfacial forces which maintain the spherical character of the dispersed phase within the continuous phase are described by the Laplace pressure (ΔP_L ; Pa), the pressure differential between the inside and the outside of an emulsion droplet. It is described by the following (Walstra, 1993):

$$\Delta P_L = \frac{2\gamma}{r} \quad (2.2)$$

Where, γ is the interfacial tension between the dispersed and continuous phases (N m^{-1}) and r is the emulsion droplet radius (m). The Laplace equation indicates that a system with higher interfacial tension between the two phases will have larger emulsion droplets, highlighting the importance of emulsifier for the reduction of interfacial tension for formation of smaller emulsion droplets (*cf.* section 2.1.2.1.3). Furthermore, it can be observed (*Eq.* 2.2) that a significant homogenisation pressure is required for the emulsification process in order to overcome the interfacial tension, and form emulsion droplets. In addition, when a balance between the interfacial tension and the Laplace pressure is achieved, droplet disruption does not occur, but solely drop deformation (Binks, 2000; Walstra & Smulders, 2000).

The feasibility of the formation of emulsion droplets from the bulk dispersed phase is quantified using the Weber number (We), the ratio of disruptive to interfacial forces (Eq. 2.3):

$$We = \frac{\text{Disruptive forces}}{\text{Interfacial forces}} = \frac{\eta_c Gr}{\gamma} \quad (2.3)$$

Where, η_c is the viscosity of the continuous phase (Pa.s) and G is the velocity gradient, similar to shear rate (s^{-1}). Generally, droplets are disrupted if $We > 1$, known as the critical Weber number, We_{cr} . Additionally, the time of the disruptive force (τ_{dis}) affecting the droplet must be greater than the deformation time (τ_{def}), for droplet breakup, for which the ratio of these terms must be greater than 1 for droplet disruption (Lee *et al.*, 2013; Walstra, 1993). Emulsion droplet breakup depends on the hydrodynamic conditions (*i.e.* the flow regime), and can be categorised as either laminar, whereby shear stresses dominate (*cf.* section 2.2.1.1), or turbulent regime, for which inertial effects (pressure differentials) are the ascribed mechanism for droplet breakup (*cf.* section 2.2.1.2) (Walstra & Smulders, 2000).

2.1.2.1.1. Laminar regime

The force exerted upon an emulsion droplet in laminar flow conditions is equivalent to the disruptive forces of the Weber equation (Eq. 2.3), $\eta_c G$. Droplet breakup occurs in the laminar regime if the critical Weber number, We_{cr} , is exceeded (Walstra, 1993). Additionally, Grace, (1982) demonstrated the influence of viscosity ratio of the dispersed phase (η_D) with respect to the continuous phase (η_c) for droplet breakup, whereby no droplet disruption occurs for $\eta_D/\eta_c > 4$.

2.1.2.1.2. Turbulent regime

Droplet breakup of emulsions whereby the continuous phase has a low viscosity (*i.e.* water continuous emulsion) occurs predominately in turbulent flow regimes, for which the droplet disruption mechanism is achieved through turbulent eddies (Walstra, 1993). Flow within the turbulent regime will have a spectrum of eddy sizes depending on the Reynolds number of the system, and this flow can be characterised using the Kolmogorov theory. Smaller turbulent eddies have larger velocity gradients, G (Eq. 2.4):

$$G = \frac{u'}{x} \quad (2.4)$$

Where, u' is the root-mean-square (RMS) average difference between u and the overall flow velocity (m s^{-1}), and x is the average eddy size (m). The smallest size of an eddy is known as the Kolmogorov scale, x_0 , and droplets smaller than this length scale are usually not formed due to the lack of droplet deformation achieved. Droplet disruption is attributed to larger eddies, known as energy-bearing eddies. Given the chaotic nature of the turbulent flow regime and range of length scales of energy bearing eddies depending on the flow behaviour, emulsions prepared in the turbulent regime tend to have a spread of emulsion droplet sizes, known as a droplet size distribution (DSD) (Lee *et al.*, 2013; Walstra & Smulders, 2000).

2.1.2.1.3. Interfacial tension

The common boundary between two phases is known as the interface. This boundary layer between the two phases is quite thin and often considered to be two-dimensional, where the thickness is assumed to be negligible, and thus neglected. The third dimension however plays a more significant role because of the interactions between the molecules of the two phases. The energy required to change the shape of a given interface is known as the interfacial tension, the units for which are J m^{-2} , however N m^{-1} is more commonly employed

(McClements, 2005; O'Connell & Flynn, 2007). The phrase interfacial tension refers to liquid-liquid interfaces, whilst surface tension refers to gas-liquid interfaces. The term interfacial tension, γ , will be used hereafter as emulsions are the consideration of this research.

Temperature and the presence of a solute (*e.g.* salt, sugar, surface active agent, etc.) within the continuous or dispersed phase are the two dominant factors which influence the interfacial tension. When interfacial tension values are quoted the corresponding temperature at which the measurement was conducted is often given, due to the strong dependence of temperature upon interfacial tension. There are conflicting reports in the literature as to the trend of increasing temperature upon interfacial tension. Lutton *et al.*, (1969) and Gaonkar, (1992) showed that elevated temperatures increased the interfacial tension between the dispersed and continuous phases, whilst conversely, Jennings, (1967) and Cabrerizo-Vílchez *et al.*, (1995) described how interfacial tension decreased as a function of temperature, ascribing the observed reduction to density differentials at the interface as a function of temperature.

The predominant factor contributing to differences in the interfacial tension of a system is that of solutes, the major of which are surface active components, such as surfactants or proteins, collectively known as emulsifiers. Other components play lesser roles in the influence of interfacial tension, such as sugars and salts. Sugar is thought to have very little to no effect upon interfacial tension, whilst salt is known to slightly increase it (Gaonkar, 1992). The effect of surface active components upon interfacial tension is under continual investigation, and is known that they significantly reduce the interfacial tension between the continuous and dispersed phases. Emulsifier molecules adsorb to the oil-water interface, extending hydrophilic moieties into the aqueous component (*i.e.* polar) and hydrophobic moieties into the oil component (*i.e.* apolar). This adsorption and rearrangement

of emulsifier molecules at the oil-water interface reduces the direct contact of these molecules with one another diminishing the surface free energy of the system, the main factor contributing to the phase separation of oil-water systems (Beverung *et al.*, 1999; McClements, 2009; O'Connell & Flynn, 2007),

2.1.2.1.4. Role of the emulsifier

The emulsifier has two primary roles in the emulsion formation, the reduction of interfacial tension, which facilitates droplet breakup, and the formation of a barrier between the two phases to prevent the re-coalescence of the two phases (*cf.* section 2.2.2.3.2; McClements, 2005; Walstra, 1993). The concentration of emulsifier affects the interfacial tension between the two phases, the higher the concentration, the lower the interfacial tension and consequently enhanced facilitation of droplet breakup (*cf.* section 2.2.1.3; Walstra, 1993). The degree of prevention of re-coalescence is dependent on both the concentration of the emulsifier, where the Gibbs-Marangoni effect can aid in the stabilisation of emulsions, and the type of emulsifier, whereby some emulsifiers (*i.e.* proteins) form thicker interfacial layers than others. There are a range of different emulsifiers which can be used to aid emulsion formation, such as surfactants (McClements, 2005), proteins (Dickinson, 1999) and solid particles, commonly referred to as Pickering particles (Pichot, 2010; Pickering, 1907; Ramsden, 1903).

The Gibbs-Marangoni effect provides coalescence stability to newly formed droplets due to interactions of emulsifier at the interface and in the continuous phase (Walstra, 1993). During emulsification, if two newly formed emulsion droplets with insufficient coverage of emulsifier move into close proximity with one another, they appropriate more surfactant during their approach. However, the amount of surfactant available for adsorption will be lowest at the point where the liquid film between two emulsion droplets is thinnest. The

interfacial differential in this region is greatest due to the lower concentration of adsorbed emulsifier (*i.e.* surface loading; Γ), inducing the Marangoni effect, whereby surface flowing in the direction of the region of higher interfacial tension occurs. More specifically, surfactant is redistributed to regions of low surface loading. The movement of emulsifier at the surface of the interface due to the interfacial differentials causes a streaming effect, moving the emulsions droplets from one another (*i.e.* a self stabilising mechanism). This effect is typically observed for low molecular weight surfactants, rather than proteins, owing to the significant molecular weight differences between these emulsifier types, inhibiting interfacial flowing in the case of proteins (Binks, 2000; Walstra & Smulders, 2000).

2.1.2.2. Emulsion stability

Emulsion stability is of great importance as many emulsion based products require prolonged storage which necessitates long term stability, often in excess of a year. Emulsion stability is characterised by a stable droplet size and droplet size distribution which does not change over the life time of the product, static rheological properties and no microbial activity. There are two factors which affect emulsions, stabilising effects and destabilisation effects, and will both be discussed hereafter. Emulsion stabilisation can either be kinetic or thermodynamic, which is dependent on the droplet size. Destabilisation mechanisms which can affect emulsions include phase separation, either creaming or sedimentation, depending on the type of emulsion (O/W or W/O), droplet aggregation mechanisms, such as flocculation or coalescence and Ostwald ripening.

2.1.2.2.1. Thermodynamic and kinetic stability

When considering emulsion systems it is necessary to distinguish between its thermodynamic and kinetic stability. Thermodynamics explains whether a process will occur, whilst kinetics determines the rate of the process if it occurs. Due to the interfacial tension

between the continuous and dispersed phases, emulsions are inherently thermodynamically unstable systems and tend to minimise the surface area between the two phases by phase separation (*cf.* section 2.1.2.2.2), with the exception of microemulsions which are thermodynamically stable (Eastoe, 2002; McClements, 2005).

The free energy differential (ΔG ; the interfacial tension between the continuous and dispersed phases) associated with emulsion formation indicates the thermodynamic stability of the system, yet provides no information as to the kinetic stability of emulsion systems. The kinetic stability of emulsions involves the rate of emulsion destabilisation with respect to the time, the nature of the changes occurring, and/or the fundamentals for these mechanisms. Regardless of thermodynamic instabilities associated with emulsions, prolonged stability can be achieved through kinetic stabilisation yielding a metastable system (Binks, 2000; Dickinson, 1998; McClements, 2005).

Kinetic stability of emulsions is understood in terms of the resultant emulsion droplet size (smaller emulsion droplets possess greater kinetic stability), the dynamics of the system and the type of surface stabilisation mechanism utilised for the formation of the emulsion. The dynamic stability of emulsions refers to the continual motion of emulsion droplets due to Brownian motion or gravity under quiescent conditions, and additional motion of droplets occurs when external forces are applied to the system. The surface stabilisation mechanisms determine the nature of the interactions between emulsion droplets which come into close proximity with one another, either moving apart, associating together (*i.e.* flocculation; *cf.* section 2.1.2.2.3.1) or merging together (*i.e.* coalescence; *cf.* section 2.1.2.2.3.2) (Chanamai & McClements, 2000; Singh, 2011).

In addition to surface stabilisation mechanisms for the improvement of kinetic stability, the rheology of the continuous phase can be altered with texture modifiers for

example to either increase the bulk viscosity or form a gel network, reducing the mobility of emulsion droplets within bulk reducing the likelihood of droplet collisions (McClements, 2009; Surh *et al.*, 2006).

2.1.2.2.2. Phase separation

As emulsions are dispersions of two immiscible fluids there is a thermodynamic tendency for the phases to separate due to the interfacial tension between the two phases and that the system aims from a thermodynamic perspective to achieve the lowest possible entropy. This may be achieved by reducing the interfacial area between the two phases (*i.e.* coalescence; *cf.* section 2.1.2.2.3.2). In emulsion systems with sufficient emulsifier to prevent phase separation due coalescence of the two phases, emulsions can be destabilised by the difference in density of the two phases. The two phases in emulsions often have different densities, and this leads to gravitational separation, called creaming in O/W emulsions where oil droplets rise to the surface, or sedimentation in W/O emulsions where water droplets go tend to the bottom of an emulsion (Chanamai & McClements, 2000; Dickinson & Ritzoulis, 2000).

Gravitational separation of emulsions is described by Stokes' law, which predicts the rate of gravitational separation of a given droplet size:

$$v_s = \frac{(\rho_d - \rho_c) \cdot g \cdot d_{3,2}^2}{18\eta_c} \quad (2.5)$$

Where, v_s is the separation velocity (m s^{-1}), ρ_d is the density of the dispersed phase (kg m^{-3}), ρ_c is the density of the continuous phase (kg m^{-3}), g is the local gravitational acceleration (m s^{-2}), $d_{3,2}$ is the emulsion droplet size ($\mu\text{m}/\text{nm}$) and η_c is the continuous phase viscosity ($\text{Pa}\cdot\text{s}$).

The primary methods for minimising gravitational separation of emulsions include reduction of the emulsion droplet size ($d_{3,2}$), increasing the viscosity of the continuous phase (η_c) and modification of the density differential between the continuous and dispersed phases to make them more comparable. Stokes' law shows that the rate of gravitational separation (v_s) has a quadratic relationship with emulsion droplet size, thus minimising emulsion droplet size reduces the rate at which emulsion droplets cream/sediment. In addition, increasing the viscosity of the continuous phase reduces the mobility of emulsion droplets within the bulk, reducing the rate of gravitational separation (McClements, 2005; Radford *et al.*, 2004).

2.1.2.2.3. Droplet aggregation

Emulsion systems have the potential to undergo a number of types of droplet aggregation, including flocculation (bridging or completion) or coalescence (partial or complete), due to the thermodynamic instabilities between the dispersed and continuous phases. Emulsions are dynamic systems, whereby droplets are in a state of motion due to gravitational forces and Brownian motion. This droplet motion inevitably leads to droplet collisions, which may lead to either flocculation or coalescence depending on the nature of the interfacial layer of the droplet (McClements, 2005).

2.1.2.2.3.1. Flocculation

Flocculation is the process whereby two or more emulsion droplets associate with one another, whilst maintaining their discrete integrity. These associations of droplets are referred to as flocs. The association of emulsion droplets as flocs increases the effective volume of the associates, increasing the rate of gravitational separation as described by Stokes' law (*cf.* section 2.1.2.2.2). Additionally, the development of flocculated emulsions yields a pronounced increase in the viscosity, due to the increase in the effective hydrodynamic volume of the floc, similar to the enhancement of viscosity as per protein solutions (*cf.*

section 2.1.1.1.3). There are two main mechanisms by which flocculation of emulsion systems occurs, including bridging or depletion flocculation (Chanamai & McClements, 2000; Dickinson *et al.*, 1997; McClements, 2005).

Bridging flocculation commonly occurs in emulsions stabilised with biopolymers (e.g. proteins), whereby the associative non-covalent interactions between the hydrophobic moieties adsorbed to one droplet interface interact with either the hydrophobic moieties of another or the hydrophobic dispersed phase, yielding the development of flocs. This type of flocculation tends to occur in systems containing insufficient emulsifier where regions of the emulsion droplet surface are not covered completely by emulsifier. Additionally, bridging flocculation may occur if an oppositely charged biopolymer is present within the continuous phase, linking emulsion droplets. These types of bridging flocculation can be mitigated against by sufficiency of emulsifier and ensuring that emulsifier and added biopolymer have similar charges, respectively (Dickinson & Golding, 1997; McClements, 2005; Tan & McGrath, 2012).

Depletion flocculation occurs due to the presence of unadsorbed or nonadsorbing colloidal entities within the continuous phase. These nonadsorbing entities may be an excess of emulsifier in the form of surfactant micelles or protein associates (*cf.* section 2.1.1). These nonadsorbing colloidal entities cause an attractive interaction between emulsion droplets due to the osmotic effect arising from the exclusion of these colloids from the confined volume between two adjacent emulsion droplets. This attractive force, due to osmotic pressure, increases as a function of concentration of free colloids in the continuous phase, eventually causing emulsion droplets to associate with one another in the form of flocs. The concentration of free biopolymer which initiates depletion flocculation is referred to as the critical flocculation concentration (CFC). The CFC decreases as a function of increasing emulsion droplet size, whereby the effective volume of colloidal entities increases. Therefore,

reduction of emulsion droplet size reduces the CFC, and the potential for depletion flocculation (Chanamai & McClements, 2000; Jenkins & Snowden, 1996; Radford & Dickinson, 2004).

2.1.2.2.3.2. Coalescence

Coalescence is an emulsion destabilisation mechanism by which emulsion droplets merge together yielding a larger emulsion droplet. This is a thermodynamically driven process, whereby the system is minimising the surface area, and thus the free surface energy. This growth in emulsion droplet size causes an increase in the rate of gravitational separation, often leading to an increased rate of coalescence due to greater contact of emulsion droplet surfaces. In water continuous emulsions the coalescence of emulsions results in the formation of an oil layer on the surface, known as oiling off, and in oil continuous emulsions, coalescence leads to the collecting of free water at the base of the material (McClements, 2005; Tcholakova *et al.*, 2006).

There are two primary methods for controlling and minimising coalescence within emulsions, through the prevention of droplet contact or development of a thicker interfacial layer. The prevention of droplet contact can be achieved by through the increase of viscosity of the continuous phase or the development of a gelled network reducing the mobility of emulsion droplets through the bulk. The development of a thicker interfacial layer is achieved through the use of sufficient emulsifier, or alternatively a layer-by-layer build up on the emulsion droplet surface, using oppositely charged biopolymers, such as positively charged chitosan and negatively charged proteins (*e.g.* sodium caseinate, gelatin, etc.) (Dalgleish, 1997; Dickinson, 1997; Guzey & McClements, 2006; McClements, 2009).

2.1.2.2.4. Ostwald ripening

Ostwald ripening is an emulsion destabilisation mechanism whereby emulsion droplet size increases at the expense of smaller droplets, due to mass transfer of dispersed phase through the bulk from one droplet to another. However, for standard food emulsions the effect of Ostwald ripening is minimal due to the limited solubility of food lipids (*e.g.* triglycerides) in water (McClements, 2005; Wooster *et al.*, 2008). Ostwald ripening plays a prominent role in emulsion stability where the lipids are more water soluble, such as the case for flavour oils (*e.g.* limonene, eugenol, etc.), or when the continuous phase contains alcohol, such as cream liqueurs (Heffernan *et al.*, 2011; Williams & Pierce, 1998).

The physical basis for Ostwald ripening is described by the Lifshitz-Slezov-Wagner (LSW) theory as follows (Lifshitz & Slyozov, 1961; Wagner, 1961):

$$\frac{d(R)^3}{dt} = \frac{4}{9} \alpha S(\infty) D \quad (2.6)$$

Where R is the radius of the emulsion droplet (m), t is time (s), $S(\infty)$ is the solubility of the dispersed within the continuous phase for an emulsion droplet with a planar interface (g L^{-1}), D is the diffusion coefficient of dispersed phase through the continuous phase ($\text{m}^2 \text{s}^{-1}$) and α is the characteristic length scale, determined from *Eq. 2.7* as follows:

$$\alpha = \frac{2\gamma V_m}{RT} \quad (2.7)$$

Where γ is the interfacial tension between the continuous and dispersed phases (N m^{-1}), V_m is the molar volume of the dispersed phase ($\text{m}^3 \text{mol}^{-1}$), R is the ideal gas constant ($8.314 \text{ J mol}^{-1} \text{ K}^{-1}$) and T is temperature (K).

The main factor of Ostwald ripening in emulsion systems is the degree of solubility of the dispersed phase within the aqueous phase, as well as the use of certain ingredients which

decrease solvent quality (e.g. ethanol), yielding systems demonstrating greater solubility of dispersed phase within the continuous phase. Utilisation of a dispersed phase with limited solubility in the continuous phase and omission of ingredients which decrease solvent quality minimises the mechanism of Ostwald ripening.

Improved packing of emulsifier at the interface yields a lower interfacial tension between the dispersed and continuous phases, which consequently reduces the rate of Ostwald ripening in emulsion systems (Taylor, 1998; Wooster *et al.*, 2008). Development of a structured interface either through fat sintering or protein gelation yields a more rigid interface inhibiting the diffusion of partially solubility dispersed phase within the continuous phase, minimising the effects of Ostwald ripening (Frasch-Melnik *et al.*, 2010).

2.1.3. References

- Alvarez, P. A., Ramaswamy, H. S., & Ismail, A. A. (2008). High pressure gelation of soy proteins: Effect of concentration, pH and additives. *Journal of Food Engineering*, 88(3), 331–340.
- Ansari, M. J., Kohli, K., & Dixit, N. (2008). Microemulsions as potential drug delivery systems: a review. *PDA Journal of Pharmaceutical Science and Technology / PDA*, 62(1), 66–79.
- Berg, J. M., Tymoczko, J. L., & Stryer, L. (2012). *Biochemistry* (7th ed.). New York: W.H. Freeman and Company.
- Beverung, C. J., Radke, C. J., & Blanch, H. W. (1999). Protein adsorption at the oil/water interface: characterization of adsorption kinetics by dynamic interfacial tension measurements. *Biophysical Chemistry*, 81(1), 59–80.
- Binks, B. . (2000). Emulsions - Recent Advances in Understanding. In B. P. Binks (Ed.), *Modern Aspects of Emulsion Science* (1st ed., pp. 1–55). Cambridge, UK: The Royal Society of Chemistry.
- Boye, J. I., Ma, C.-Y., & Harwalkar, V. R. (1997). Thermal Denaturation and Coagulation of Proteins. In S. Damodaran & A. Paraf (Eds.), *Food Proteins and Their Applications* (1st ed., pp. 25–56). New York: Marcel Dekker.
- Bungenberg de Jong, H. G. (1949). Gels. In H. R. Kruyt (Ed.), *Colloid Science II* (p. 2). Amsterdam: Elsevier.

- Cabrerizo-Vílchez, M. A., Policova, Z., Kwok, D. Y., Chen, P., & Neumann, A. W. (1995). The temperature dependence of the interfacial tension of aqueous human albumin solution/decane. *Colloids and Surfaces B: Biointerfaces*, 5(1-2), 1–9.
- Caetano da Silva Lannes, S., & Natali Miquelim, J. (2013). Interfacial Behavior of Food Proteins. *Current Nutrition & Food Science*, 9(1), 10–14.
- Chanamai, R., & McClements, D. (2000). Creaming Stability of Flocculated Monodisperse Oil-in-Water Emulsions. *Journal of Colloid and Interface Science*, 225(1), 214–218.
- Cheftel, J. C., Cuq, J.-L., & Lorient, D. (1985). Amino acids, peptides and proteins. In O. R. Fennema (Ed.), *Food Chemistry* (p. 45). New York: Marcel Dekker.
- Clemente, A. (2000). Enzymatic protein hydrolysates in human nutrition. *Trends in Food Science & Technology*, 11(7), 254–262.
- Curvale, R., Masuelli, M., & Padilla, A. P. (2008). Intrinsic viscosity of bovine serum albumin conformers. *International Journal of Biological Macromolecules*, 42(2), 133–7.
- Dalgleish, D. G. (1997). Adsorption of protein and the stability of emulsions. *Trends in Food Science & Technology*, 8(1), 1–6.
- Damodaran, S. (1997a). Food Proteins: An Overview. In S. Damodaran & A. Paraf (Eds.), *Food Proteins and Their Applications* (1st ed., pp. 1–24). New York: Marcel Dekker.
- Damodaran, S. (1997b). Protein-stabilized foams and emulsions. In S. Damodaran & A. Paraf (Eds.), *Food Proteins and Their Applications* (1st ed., pp. 57–110). New York: Marcel Dekker.
- Davie, E. W., & Ratnoff, O. D. (1964). Waterfall Sequence for Intrinsic Blood Clotting. *Science*, 145(3638), 1310–1312.
- DeMan, J. M. (1999). Proteins. In *Principles of Food Chemistry* (3rd ed., pp. 111–162). Maryland, USA: Aspen Publishers, Inc.
- Dickinson, E. (1997). Properties of Emulsions Stabilized with Milk Proteins: Overview of Some Recent Developments. *Journal of Dairy Science*, 80(10), 2607–2619.
- Dickinson, E. (1998). Proteins at interfaces and in emulsions Stability, rheology and interactions. *Journal of the Chemical Society, Faraday Transactions*, 94(12), 1657–1669.
- Dickinson, E. (1999). Caseins in emulsions: interfacial properties and interactions. *International Dairy Journal*, 9(3-6), 305–312.
- Dickinson, E. (2010). Flocculation of protein-stabilized oil-in-water emulsions. *Colloids and Surfaces. B, Biointerfaces*, 81(1), 130–40.
- Dickinson, E., & Golding, M. (1997). Rheology of Sodium Caseinate Stabilized Oil-in-Water Emulsions. *Journal of Colloid and Interface Science*, 191(1), 166–76.

- Dickinson, E., Golding, M., & Povey, M. (1997). Creaming and Flocculation of Oil-in-Water Emulsions Containing Sodium Caseinate. *Journal of Colloid and Interface Science*, 185(2), 515–29.
- Dickinson, E., & Ritzoulis, C. (2000). Creaming and Rheology of Oil-in-Water Emulsions Containing Sodium Dodecyl Sulfate and Sodium Caseinate. *Journal of Colloid and Interface Science*, 224(1), 148–154.
- Eastoe, J. (2002). Microemulsions. In *Surfactant Chemistry* (1st ed., pp. 59–95). Bristol: RIDCI.
- Fitzsimons, S. M., Mulvihill, D. M., & Morris, E. R. (2007). Denaturation and aggregation processes in thermal gelation of whey proteins resolved by differential scanning calorimetry. *Food Hydrocolloids*, 21(4), 638–644.
- Foegeding, E. A., & Davis, J. P. (2011). Food protein functionality: A comprehensive approach. *Food Hydrocolloids*, 25(8), 1853–1864.
- Foegeding, E. A., Davis, J. P., Doucet, D., & McGuffey, M. K. (2002). Advances in modifying and understanding whey protein functionality. *Trends in Food Science & Technology*, 13(5), 151–159.
- Fox, P. F. (2008). Chapter 1 - Milk: an overview. In A. Thompson, M. B. Mike Boland and Harjinder SinghA2 - Abby Thompson, & H. S. B. T.-M. Proteins (Eds.), (pp. 1–54). San Diego: Academic Press.
- Frasch-Melnik, S., Norton, I. T., & Spyropoulos, F. (2010). Fat-crystal stabilised w/o emulsions for controlled salt release. *Journal of Food Engineering*, 98(4), 437–442.
- Gaonkar, A. G. (1992). Effects of salt, temperature, and surfactants on the interfacial tension behavior of a vegetable oil/water system. *Journal of Colloid and Interface Science*, 149(1), 256–260.
- Garrec, D. A., & Norton, I. T. (2012). The influence of hydrocolloid hydrodynamics on lubrication. *Food Hydrocolloids*, 26(2), 389–397.
- Gibaud, S., & Attivi, D. (2012). Microemulsions for oral administration and their therapeutic applications. *Expert Opinion on Drug Delivery*, 9(8), 937–51.
- Given, P. S. (2009). Encapsulation of Flavors in Emulsions for Beverages. *Current Opinion in Colloid & Interface Science*, 14(1), 43–47.
- Gonzalez-Perez, S., & Arellano, J. B. (2009). Vegetable protein isolates. In G. O. Philips & P. A. Williams (Eds.), *Handbook of Hydrocolloids* (2nd ed., pp. 383 – 419). Woodhead Publishing Limited.
- Grace, H. P. (1982). Dispersion phenomena in high viscosity immiscible fluid systems and application of static mixers as dispersion devices in such systems. *Chemical Engineering Communications*, 14(3-6), 225–277.

- Grossiord, J.-L., & Stambouli, M. (2008). Potentialities of W/O/W Multiple Emulsions in Drug Delivery and Detoxification. In A. Aserin (Ed.), *Multiple Emulsions Technology and Applications* (1st ed., pp. 209–235). New Jersey: Wiley and Sons.
- Gutiérrez, J. M., González, C., Maestro, A., Solè, I., Pey, C. M., & Nolla, J. (2008). Nano-emulsions: New applications and optimization of their preparation. *Current Opinion in Colloid & Interface Science*, *13*(4), 245–251.
- Guzey, D., & McClements, D. J. (2006). Characterization of β -lactoglobulin–chitosan interactions in aqueous solutions: A calorimetry, light scattering, electrophoretic mobility and solubility study. *Food Hydrocolloids*, *20*(1), 124–131.
- Harding, S. E. (1997). The intrinsic viscosity of biological macromolecules. Progress in measurement, interpretation and application to structure in dilute solution. *Progress in Biophysics and Molecular Biology*, *68*(2–3), 207–262.
- Haug, I. J., & Draget, K. I. (2009). Gelatin. In G. O. Philips & P. A. Williams (Eds.), *Handbook of Hydrocolloids* (2nd ed., pp. 142 – 163). Woodhead Publishing Limited.
- Haug, I. J., Draget, K. I., & Smidsrød, O. (2004). Physical and rheological properties of fish gelatin compared to mammalian gelatin. *Food Hydrocolloids*, *18*(2), 203–213.
- Heffernan, S. P., Kelly, A. L., Mulvihill, D. M., Lambrich, U., & Schuchmann, H. P. (2011). Efficiency of a range of homogenisation technologies in the emulsification and stabilization of cream liqueurs. *Innovative Food Science & Emerging Technologies*, *12*(4), 628–634.
- Henry, J. (2007). The Formulation and Characterisation of Edible Nanoemulsions. *EngD Thesis*. The University of Birmingham.
- Hunt, J. a., & Dalgleish, D. G. (1994). Adsorption behaviour of whey protein isolate and caseinate in soya oil-in-water emulsions. *Food Hydrocolloids*, *8*(2), 175–187.
- IUPAC. (1997). *Compendium of Chemical Terminology*. Oxford: Blackwell Scientific Publications.
- Jenkins, P., & Snowden, M. (1996). Depletion flocculation in colloidal dispersions. *Advances in Colloid and Interface Science*, *68*, 57–96.
- Jennings, H. Y. (1967). The effect of temperature and pressure on the interfacial tension of benzene-water and normal decane-water. *Journal of Colloid and Interface Science*, *24*(3), 323–329.
- Jiao, J., & Burgess, D. J. (2008). Multiple Emulsion Stability: Pressure Balance and Interfacial Film Strength. In A. Aserin (Ed.), *Multiple Emulsions Technology and Applications* (1st ed., pp. 1–29). Wiley and Sons.
- Khopade, A. J., & Jain, N. H. (2008). Surface-Modified Fine Multiple Emulsions for Anticancer Drug Delivery. In A. Aserin (Ed.), *Multiple Emulsions Technology and Applications* (1st ed., pp. 235–256). New Jersey.

- Kimura, S., Miura, S., & Park, Y.-H. (1983). Collagen as the Major Edible Component of Jellyfish (*Stomolophus nomural*). *Journal of Food Science*, 48(6), 1758–1760.
- Lam, R. S. H., & Nickerson, M. T. (2013). Food proteins: A review on their emulsifying properties using a structure–function approach. *Food Chemistry*, 141(2), 975–984.
- Lee, L. L., Niknafs, N., Hancocks, R. D., & Norton, I. T. (2013). Emulsification: Mechanistic understanding. *Trends in Food Science & Technology*, 31(1), 72–78.
- Lefebvre, J. (1982). Viscosity of concentrated protein solutions. *Rheologica Acta*, 21(4-5), 620–625.
- Lifshitz, I. M., & Slyozov, V. V. (1961). The kinetics of precipitation from supersaturated solid solutions. *Journal of Physics and Chemistry of Solids*, 19(1–2), 35–50.
- Lutton, E. ., Stauffer, C. ., Martin, J. ., & Fehl, A. . (1969). Solid and liquid monomolecular film at interfaces. *Journal of Colloid and Interface Science*, 30(3), 283–290.
- McClements, D. J. (2004). Protein-stabilized emulsions. *Current Opinion in Colloid & Interface Science*, 9(5), 305–313.
- McClements, D. J. (2005). *Food Emulsions: Principles, Practices, and Techniques* (2nd ed.). CRC Press.
- McClements, D. J. (2009). *Biopolymers in Food Emulsions. Modern Biopolymer Science* (First Edit., pp. 129–166). Elsevier Inc.
- McClements, D. J. (2011). Edible nanoemulsions: fabrication, properties, and functional performance. *Soft Matter*, 7(6), 2297.
- Mine, Y. (2002). Recent advances in egg protein functionality in the food system, *World's Poultry Science Journal*, 58(1), 31-39.
- Morris, E. R., Cutler, A. N., Ross-Murphy, S. B., Rees, D. A., & Price, J. (1981). Concentration and shear rate dependence of viscosity in random coil polysaccharide solutions. *Carbohydrate Polymers*, 1, 5–21.
- Mozaffar, Z., & Haque, Z. U. (1992). Casein hydrolysate. III: Some functional properties of hydrophobic peptides synthesized from hydrolysate. *Food Hydrocolloids*, 5(6), 573–579.
- Niknafs, N., Spyropoulos, F., & Norton, I. T. (2011). Development of a new reflectance technique to investigate the mechanism of emulsification. *Journal of Food Engineering*, 104(4), 603–611.
- O'Connell, J. E., & Flynn, C. (2007). The Manufacture and Application of Casein-Derived Ingredients. In Y. H. Hui (Ed.), *Handbook of Food Products Manufacturing* (1st ed., pp. 557 – 593). New Jersey: John Wiley & Sons.

- O'Connell, J. E., Grinberg, V. Y., & de Kruif, C. G. (2003). Association behavior of β -casein. *Journal of Colloid and Interface Science*, 258(1), 33–39.
- Oakenfull, D., Pearce, J., & Burley, R. (1997). Protein Gelation. In S. Damodaran & A. Paraf (Eds.), *Food Proteins and Their Applications* (1st ed., pp. 111–142). New York: Marcel Dekker.
- Ostwald, W. (1910). Beiträge zur Kenntnis der Emulsionen. *Zeitschrift Für Chemie Und Industrie Der Kolloide*, 6(2), 103–109.
- Pacek, A. W., Man, C. C., & Nienow, A. W. (1998). On the Sauter mean diameter and size distributions in turbulent liquid/liquid dispersions in a stirred vessel. *Chemical Engineering Science*, 53(11), 2005–2011.
- Pauling, L., Corey, R. B., & Branson, H. R. (1951). The structure of proteins: Two hydrogen-bonded helical configurations of the polypeptide chain. *Proceedings of the National Academy of Sciences*, 37(4), 205–211.
- Pichot, R. (2010). Stability and Characterisation of Emulsions in the presence of Colloidal Particles and Surfactants. *PhD Thesis*. The University of Birmingham.
- Pickering, S. U. (1907). CXCVI. Emulsions. *Journal of the Chemical Society, Transactions*, 91, 2001.
- Radford, S. J., & Dickinson, E. (2004). Depletion flocculation of caseinate-stabilised emulsions: what is the optimum size of the non-adsorbed protein nano-particles? *Colloids and Surfaces A: Physicochemical and Engineering Aspects*, 238(1-3), 71–81.
- Radford, S. J., Dickinson, E., & Golding, M. (2004). Stability and rheology of emulsions containing sodium caseinate: combined effects of ionic calcium and alcohol. *Journal of Colloid and Interface Science*, 274(2), 673–86.
- Ramsden, W. (1903). Separation of solids in the surface-layers of solutions and suspensions. *Proceedings of the Royal Society of London*, 72, 156–164.
- Sakurai, K., Konuma, T., Yagi, M., & Goto, Y. (2009). Structural dynamics and folding of beta-lactoglobulin probed by heteronuclear NMR. *Biochimica et Biophysica Acta*, 1790(6), 527–37.
- Schrieber, R., & Gareis, H. (2007). *Gelatine Handbook - Theory and Industrial Practice* (1st ed., pp. 1 – 348). Wiley-Blackwell.
- Singh, H. (2011). Aspects of milk-protein-stabilised emulsions. *Food Hydrocolloids*, 25(8), 1938–1944.
- Slomkowski, S., Alemán, J. V., Gilbert, R. G., Hess, M., Horie, K., Jones, R. G., Stepto, R. F. T. (2011). Terminology of polymers and polymerization processes in dispersed systems (IUPAC Recommendations 2011). *Pure and Applied Chemistry*, 83(12), 2229–2259.

- Solans, C., Izquierdo, P., Nolla, J., Azemar, N., & Garcia-Celma, M. J. (2005). Nano-emulsions. *Current Opinion in Colloid & Interface Science*, 10(3–4), 102–110.
- Sousa, I. M. N., Mitchell, J. R., Hill, S. E., & Harding, S. E. (1995). Intrinsic Viscosity and Mark-Houwink Parameters of Lupin Proteins in Aqueous Solutions. *Les Cahiers de Rhéologie*, 14, 139–148.
- Sun, X. D., & Arntfield, S. D. (2012). Molecular forces involved in heat-induced pea protein gelation: Effects of various reagents on the rheological properties of salt-extracted pea protein gels. *Food Hydrocolloids*, 28(2), 325–332.
- Surh, J., Decker, E., & McClements, D. (2006). Properties and stability of oil-in-water emulsions stabilized by fish gelatin. *Food Hydrocolloids*, 20(5), 596–606.
- Tadros, T., Izquierdo, P., Esquena, J., & Solans, C. (2004). Formation and stability of nano-emulsions. *Advances in Colloid and Interface Science*, 108–109(0), 303–318.
- Tan, H. L., & McGrath, K. M. (2012). Na-caseinate/oil/water systems: Emulsion morphology diagrams. *Journal of Colloid and Interface Science*, 381(1), 48–58.
- Tanner, R., & Rha, C. (1980). Hydrophobic Effect on the Intrinsic Viscosity of Globular Proteins. In G. Astarita, G. Marrucci, & L. Nicolais (Eds.), *In Rheology, Volume 2: Fluids* (pp. 277–283). Boston, MA: Springer US.
- Taylor, P. (1998). Ostwald ripening in emulsions. *Advances in Colloid and Interface Science*, 75(2), 107–163.
- Tcholakova, S., Denkov, N. D., Ivanov, I. B., & Campbell, B. (2006). Coalescence stability of emulsions containing globular milk proteins. *Advances in Colloid and Interface Science*, 123–126(0), 259–293.
- Weis, A. (1964). *Macromolecular Chemistry of Gelatin* (1st ed.). New York: Academic Press.
- Wagner, C. (1961). Theorie der Alterung von Niederschlägen durch Umlösen (Ostwald-Reifung). *Zeitschrift Für Elektrochemie, Berichte Der Bunsengesellschaft Für Physikalische Chemie*, 65(7-8), 581–591.
- Waitzberg, D. L. (2014). Evolution of parenteral lipid emulsions. *Clinical Nutrition Supplements*, 1(3), 5–7.
- Walstra, P. (1993). Principles of emulsion formation. *Chemical Engineering Science*, 48(2), 333–349.
- Walstra, P., & Smulders, P. (2000). Emulsion Formation. In B. . Binks (Ed.), *Modern Aspects of Emulsion Science* (1st ed., pp. 56–99). Cambridge, UK: The Royal Society of Chemistry.
- Walstra, P., & van Vliet, T. (2003). Chapter II Functional properties. In R. J. H. W.Y. Aalbersberg P. Jasperse, H.H.J. de Jongh, C.G. de Kruif, P. Walstra and F.A. de Wolf

BT - Progress in Biotechnology (Ed.), *Industrial Proteins in Perspective* (Vol. Volume 23, pp. 9–30). Elsevier.

Williams, K. R., & Pierce, R. E. (1998). The Analysis of Orange Oil and the Aqueous Solubility of d-Limonene. Two Complementary Gas Chromatography Experiments. *Journal of Chemical Education*, 75(2), 223.

Wooster, T. J., Golding, M., & Sanguansri, P. (2008). Impact of oil type on nanoemulsion formation and Ostwald ripening stability. *Langmuir : The ACS Journal of Surfaces and Colloids*, 24(22), 12758–65.

Yamashita, M., Arai, S., & Fujimaki, M. (1976). Plastein reaction for food protein improvement. *Journal of Agricultural and Food Chemistry*, 24(6), 1100–1104.

Ziegler, G. R., & Foegeding, E. A. (1990). The Gelation Of Proteins. *Advances in Food and Nutrition Research*, 34, 203–298.

2.2. Literature review: ultrasound

This section critically assesses the fundamental theories of ultrasound, in particular low frequency high power ultrasound, are reviewed, with a specific focus on the functional modification of food proteins and nanoemulsion fabrication using power ultrasound. This section examines how ultrasound propagation in a liquid media exhibits cavitations, and how these phenomena yield regions of hydrodynamic shear, localised temperature increases and pressure differentials.

The discussion within this section has been submitted for publication within: O'Sullivan, J.J., Greenwood, R.W. and Norton, I.T. 2015. Applications of ultrasound for the functional modification of proteins and the nanoemulsion formation: A review. *Trends in Food Science and Technology*.

2.2.1. Abstract

This review surveys the most recent developments in low frequency, high power ultrasound for the functional modification of proteins derived from a number of food sources (*e.g.* dairy, animal, cereal, legume and fruit), and subsequently for the fabrication of nano-sized emulsion droplets. Aside from a overview of the fundamentals of ultrasound, including a cursory outline of the mathematical models for acoustic streaming phenomena, ultrasonic cavitation, heat generation and acoustic energy determination via calorimetry, examples of ultrasound treatment for improvements in the solubilisation, hydration, hydrophobicity, emulsifying and rheological performance of proteins are described.

Ultrasound possesses the industrial capability to improve the functional properties of proteins, and this review emphasises the improvement to the surface active properties of proteins, which is attributed to decreases in protein aggregate size and increases in hydrophobicity, demonstrating increased molecular mobility.

Finally, the utilisation of ultrasound for the fabrication of nanoemulsions is assessed with a particular focus on the intrinsic relationship between process configuration (*i.e.* batch or continuous), processing parameters (*i.e.* acoustic power and residence time) and emulsion formulation (*i.e.* emulsifier type and concentration). A better understanding of the effect of industrially relevant high molecular weight biopolymers (*i.e.* proteins) within ultrasonic emulsification processes would increase the utilisation of ultrasound as a fabrication technique for nano-sized emulsion droplets.

2.2.2. Introduction

Low frequency, high power ultrasound, commonly referred to as power ultrasound, has gained significant interest over the past decade as it possesses a wide range of uses within a myriad of sectors making it a versatile processing technology, for the alteration, generation and modification of microstructures. As a consequence, due to ultrasonic cavitation, it is capable of mechanically altering the structure of proteins in solution without the use of additives (chemical or biological) or excess heat, and disrupting volumes of dispersed phase in emulsion systems for the generation nano-sized emulsion droplets (McClements, 1995; O'Brien, 2007).

Proteins are ingredients utilised within a wide range of formulations due to both their nutritional value and functionality. The term 'functionality' as applied to food ingredients describes any property other than nutritional attributes that contribute to an ingredient's beneficial aspects within a formulation (Damodaran, 1997a). Proteins are highly functional molecules within food systems capable of the stabilisation of oil droplets and air bubbles, formations of gel structures and the enhancement of viscosity (O'Connell & Flynn, 2007; P Walstra & van Vliet, 2003). This functionality is due to the complex chemical makeup of these molecules owing to their unique amino acid sequences (Beverung *et al.*, 1999). Improvement to the functional properties of proteins is of great interest so as to increase their commercial value and improve utilisation of these high value ingredients, and is conventionally achieved through either increasing or reducing their molecular weight, or conjugation with other biopolymers (Kato *et al.*, 1993; Nik *et al.*, 2010).

As for emulsion formation, traditionally it is achieved industrially through the implementation of homogenisers, usually two stages, operating at pressures up to 25 MPa (McClements, 2005). Numerous technologies have shown the capacity for the fabrication of

nano-sized emulsion droplets, such as microfluidics, high and ultrahigh pressure valve homogenisers, and membrane emulsification (crossflow and rotary) (Lee & Norton, 2013; Lloyd *et al.*, 2014). However, industry is reluctant to readily adopt these technologies due to the associated capital expenditure and scalability issues.

Amongst the forthcoming technologies for the functional modification of proteins and generation of nano-sized emulsion droplets, power ultrasound has garnered particular interest due in part to the mechanical nature of this process (*i.e.* ultrasonic cavitations). Traditionally, the functionality of proteins is altered by aggregation (*i.e.* increasing molecular weight), proteolysis (*i.e.* reducing molecular weight) or conjugation with other entities (*e.g.* Maillard reaction with reducing sugars). Power ultrasound offers the possibility of altering protein structures without the use of additives or excessive thermal treatments, simplifying the processing of these ingredients and generating a ‘cleaner’ packaging label for consumers. Moreover, the main drawbacks limiting emergent technologies under investigation for the fabrication of nanoemulsions are that of scalability and the associated capital expenditure. With adequate sonoreactor design (*i.e.* chamber volume and volumetric flow rate selection), and high throughput cost effective generation of nano-sized emulsion droplets is readily achievable (Gogate *et al.*, 2011).

The aim of this review is to outline the fundamentals of ultrasound and critically assess applications of ultrasound treatment for the functional modification of proteins in aqueous solution (*e.g.* solubility, hydrophobicity, rheological behaviour, emulsifying performance, etc.) and the generation of nano-sized emulsion droplets. A particular focus has been placed on the industrial relevance of ultrasonic processing within the food industry, as a cost effective, mechanical method for the generation, alteration and modification of food microstructures.

2.2.3. Fundamentals of ultrasound

Ultrasound is an acoustic wave above the threshold of human auditory perception (> 16 kHz). Acoustic waves are the propagation of mechanical (*i.e.* acoustic) waves of pressure and displacement through a medium, as longitudinal waves, exhibiting compressions (high pressure regions) and rarefactions (low pressure regions). Longitudinal waves are waves whereby the displacement of the medium is in the same direction as the wave (Mansfield & O'Sullivan, 1998) (*cf.* Fig. 2.3).

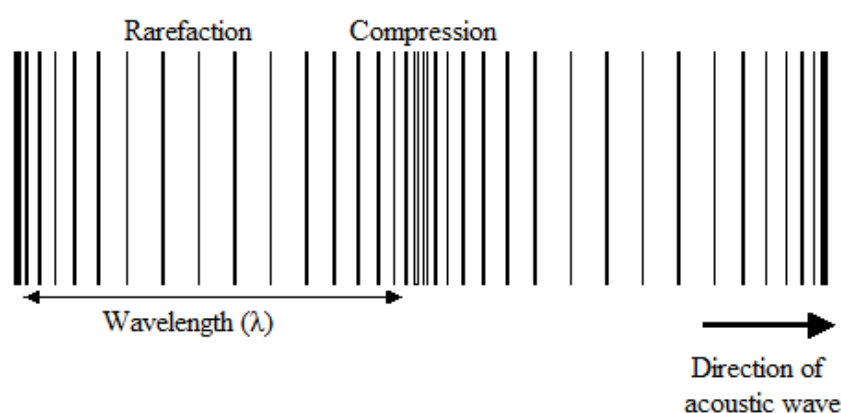


Fig. 2.3. Depiction of a longitudinal wave showing compressions, rarefactions and wavelength.

Ultrasound can be further classified in two distinct categories based on the frequency range, high frequency (100 kHz – 1 MHz) low power intensity ($< 1 \text{ W cm}^{-2}$) ultrasound, utilised most commonly for the analytical evaluation of the physicochemical properties of food (Chemat *et al.*, 2011; Demirdöven & Baysal, 2008), and low frequency (20 – 100 kHz) high power intensity ($10 - 1000 \text{ W cm}^{-2}$) ultrasound recently employed for the alteration, generation and modification of foods, either physically or chemically (McClements, 1995; Soria & Villamiel, 2010). The acoustic power intensity (I_a ; W cm^{-2}) is defined as the acoustic power (P_a ; W) per unit area of ultrasound emitting surface (S_A ; cm^{-2}). This review will focus solely upon low frequency, high power ultrasound, and hereafter will refer to it as simply power ultrasound.

The effects of power ultrasound on food structures are attributed to ultrasonic cavitation, the rapid formation and collapse of gas bubbles, generated by localised pressure differentials (~ 50 MPa) occurring over short periods of times (a few microseconds). These ultrasonic cavitations cause localised regions of intense hydrodynamic shear forces and a rise in temperature at the site of bubble collapse (up to 5000 °C), contributing to the observed effects of power ultrasound (Güzey *et al.*, 2006; O'Brien, 2007; O'Donnell *et al.*, 2010).

Acoustic waves are generated from the conversion of electrical energy into mechanical energy. A transducer, a device which converts energy from one form to another, is employed to produce acoustic waves. In acoustics, transducers are commonly referred to as tips. More specifically, the tip, a part of the sonotrode, is the point from which the acoustic waves emanate. The piezoelectric material (*e.g.* quartz or lithium sulphate zirconate titanates) within the transducer oscillates in response to electrical energy, leading to mechanical vibrations in the tip. When the tip is submerged in liquids, the mechanical energy at the tip is delivered to the medium as the tip vibrates generating acoustic waves (Martini, 2013; Soria & Villamiel, 2010; Trujillo & Knoerzer, 2011a).

2.2.3.1. Acoustic streaming

Ultrasonic emanation from the tip of the sonotrode is referred to as acoustic streaming (Nyborg, 1953; Tjøtta, 1999). There are two main acoustic streaming theories which describe this phenomena mathematically, those developed by Rayleigh (Rayleigh, 1896), Nyborg (Nyborg, 1953) and Westervelt (Westervelt, 1953), referred to as the RNW theory, and that proposed by Lighthill, the Stuart streaming theory (Lighthill, 1978). The RNW theory is applied to systems where the Reynolds number (*i.e.* the ratio of inertial to viscous forces) is very low, and the Stuart streaming theory is applicable to systems whereby the acoustic jets

take the form of an inertially dominated turbulent jet (*i.e.* high Reynolds number) with powers in excess of 4×10^{-4} W (Trujillo & Knoerzer, 2011a).

Even though solutions have been derived to describe acoustic streaming based on the RNW theory (Nowicki *et al.*, 1997; Nowicki *et al.*, 1998), it was demonstrated that it is applicable to systems with very low flows exhibiting low Reynolds numbers ($Re < 1$) and low sources of acoustic power (Lighthill, 1978; Zarembo, 1971). Therefore, the RNW theory is not applicable to the jet streaming exhibited by low frequency high power transducers (Trujillo & Knoerzer, 2011a) (*cf.* Appendix A).

The term ‘Stuart streaming’ was introduced to describe the acoustic streaming at higher Reynolds numbers resulting from high power acoustic beams from transducers (Lighthill, 1978; Stuart, 1963). This type of acoustic streaming is the most commonly exhibited within the food industry for the functional modification of ingredients and the development of microstructures. Lighthill, (1978) states that “it is hardly an exaggeration to say that all really noticeable acoustic streaming motions are Stuart streaming,” and furthermore proved that acoustic streaming takes the form of an inertially dominated turbulent jet upon exceeding an acoustic power threshold of 4×10^{-4} W.

High power acoustic streaming manifests in the form of a jet showing a narrower beam of sound emanating from the source with an acoustic power expressed as follows:

$$P_0 = I_0 S_A \tag{2.8}$$

Where P_0 is the acoustic power at the tip of the sonotrode (W), I_0 is the acoustic power intensity at the tip of the sonotrode ($W \text{ cm}^{-2}$) and S_A is the cross sectional area of the sonotrode tip (cm^2) (Lighthill, 1978; Margulis & Margulis, 2003). In the absence of attenuation the principles of conservation of energy are applicable, whereby the energy

entering the beam from the transducer tip is equal to that leaving the beam (Tjøtta, 1999).

Thus this conservation of energy can be expressed as follows:

$$IA = \text{constant} \quad (2.9)$$

Attenuation of the sound beam reduces the power of the sound beam according to:

$$P = P_0 e^{-\beta x} \quad (2.10)$$

Where x is the distance from the source emanating the sound beam (m) and $e^{-\beta x}$ is the damping term which accounts for spatial attenuation of the acoustic beam, primarily due to ultrasonic cavitations. β is the attenuation coefficient proposed by Lighthill defined as the proportional loss of ultrasonic energy per unit displacement travelled by a acoustic wave (Lighthill, 1978).

Lighthill proposed that the sonotrode emanates the ultrasonic power as a sound beam where the net force at a given distance, x , is determined by applying the law of conservation of momentum, yielding the acoustic momentum flow rate after attenuation (Lighthill, 1978). Application of the law of conservation of momentum allows for the conclusion that a reduction in the acoustic momentum, increases the hydrodynamic momentum in the path of the sound beam, also referred to as streaming (Trujillo & Knoerzer, 2011a, 2011b).

The spatial rate of decay of the hydrodynamic momentum flow rate acts as a net force per unit displacement in a given direction, x , generating motion of the medium. If there was no impedance present within the path of the sound beam as a consequence of cavitations, the attenuation coefficient, β , would have a value of zero, and the net force would thus become neglected. Therefore, streaming is a result of acoustic attenuation caused by ultrasonic cavitations in the locus of the sound beam (Tjøtta, 1999; Zarembo, 1971).

For high values of the attenuation coefficient, β , the streaming motion of the acoustic beam is comparable to that of a turbulent jet, whereby the damping term, $e^{-\beta x}$, approaches zero at short distances by which over short distances within the locus of the sonotrode tip the momentum delivered to the medium is equal to P_0/c (Trujillo & Knoerzer, 2011a).

Ultrasonic processing utilised within the food industry for the development of microstructures and functional modification of food ingredients is usually power ultrasound processing which is most adequately modelled and explained by the Stuart streaming theory (McClements, 1995; Trujillo & Knoerzer, 2011a).

2.2.3.2. Ultrasonic cavitations

High power ultrasonic waves generate several different types of cavitation bubbles due to pressure changes during wave propagation (Servant *et al.*, 2001). Cavitation bubbles are formed at acoustic intensities greater than that of the cavitation threshold. The cavitation threshold pressure required to initiate cavitations is a strong function of stream width and acoustic power, and once triggered bubble generation increases with increasing acoustic power (Leighton, 1995; Neppiras, 1980). Cavitation bubbles disperse (*i.e.* reflect or scatter) and attenuate (*i.e.* gradual reduction of ultrasonic intensity) ultrasonic waves due to the acoustic impedance differential between the liquid and gaseous phases. When an acoustic wave moves from one medium to another (*i.e.* from liquid to gaseous bubbles) differences in the speed of sound and compressibility between the two phases induces an impedance mismatch (McClements, 1995; O'Brien, 2007).

As a consequence, the acoustic wave is either partially or completely scattered by the bubble. Systems containing many bubbles exhibit multiple scatterings as bubbles behave like mirrors dispersing acoustic waves, yielding redirection of the acoustic wave, causing an effective increase in the absorption of acoustic waves (O'Brien, 2007). The cavitation locus is

situated in an area close to the tip of the sonotrode, whereby this region yields the highest levels of acoustic intensity, and thus an area of increased formation of cavitations. Therefore, the attenuation in this region is quite high and dominated by acoustic scattering (Martini, 2013). The acoustic intensity decays exponentially with respect to distance from sonotrode tip, almost completely dissipated at distances as low as 1 cm (Chivate & Pandit, 1995; Kumar *et al.*, 2006; Kumaresan *et al.*, 2006), highlighting the importance of adequate sonotrode positioning for effective processing of liquid medium (Gogate *et al.*, 2011; Gogate *et al.*, 2003).

Modelling the ultrasonic cavitation process in real, non-ideal conditions is difficult given the numerous multi-physics elements involved in the development and behaviour of bubbles in an acoustic field, such as the oscillating pressure field, formation and collapse of bubbles, and acoustic dispersion and attenuation. A model predicting cavitation should account for bubble formation due to acoustic pressure differentials, coalescence of adjacent bubbles, bubble breakup, lifespan of bubbles, and interactions between bubbles and the acoustic field emitted from the sonotrode tip (Lauterborn *et al.*, 2007; Leighton, 1995).

The presence and formation of bubbles within the acoustic field influences the transmission of ultrasound due to the impedance differential between liquids and gases, and the dispersion of ultrasonic waves upon contact with bubble surfaces (*i.e.* attenuation). Be that as it may, the acoustic field also influences bubbles within the medium through the Bjerknes force, a translational force exerted upon a bubble due to pressure gradients resulting in bubble oscillations, and acoustic streaming resulting from sound absorption (Metin *et al.*, 1997). Both of these mechanisms contribute to the migration of bubbles in the presence of an acoustic field (Lauterborn *et al.*, 2007; Metin *et al.*, 1997; Trujillo & Knoerzer, 2011b).

The modelling of single bubble mechanics under exertion of an acoustic field is well established (Crum, 1975; Doinikov & Dayton, 2006), yet the fundamentals underpinning the influence of acoustic fields upon multi-bubble systems has yet to be fully understood due to the greatly more complex nature of the system in comparison to the single bubble system.

2.2.3.3. Heat generation

Ultrasonic processing of fluid systems yields heat generation due to a number of factors which occur as a consequence of the transmission of an acoustic wave through the medium, including molecular absorption, dissipation of turbulence, dispersion of acoustic waves by gaseous bubbles and viscous losses. The acoustic energy transmitted to the medium manifests as both kinetic energy (*i.e.* bulk motion) and thermal energy (*i.e.* heat). The kinetic energy transmitted to the medium is dissipated as heat due to viscous losses (Tjøtta, 1999; Zisu *et al.*, 2010).

In ultrasonic processes where the attenuation coefficient, β , is high (*i.e.* a high number of ultrasonic cavitations) it can be assumed that the acoustic energy is rapidly converted to thermal energy in the locus of the sonotrode tip, from which the acoustic waves emanate (Lighthill, 1978). The validity of this assumption is true for systems exhibiting high attenuation coefficients where dissipation of acoustic energy occurs at the transducer, and additionally where the kinetic energy disperses at the sonotrode tip. Chivate & Pandit, (1995) confirmed that acoustic energy dissipates completely within close proximity of the sonotrode tip, approximately 1 cm, and it was found that the majority of kinetic energy (> 80 %) is dissipated in the form of thermal energy in a small volume (< 2 %) in the locus of the transducer (Kumar *et al.*, 2006; Kumaresan *et al.*, 2006).

2.2.3.4. Acoustic energy determination

The determination of the acoustic energy input into a volume of liquid is a topic under investigation, however a satisfactory description of the solution has thus far to be elucidated, even though the fields of sonochemistry and ultrasonic cavitation have been under investigation for several decades. The electrical consumption of the ultrasonic process and the acoustic power under non-cavitation conditions are attainable, however acoustic power measurements within the cavitation regime are lacking (Margulis & Margulis, 2003).

As acoustic energy is transmitted to a liquid medium via the sonotrode tip, this acoustic energy is dissipated as absorbed acoustic energy, manifesting as thermal energy, and unadsorbed energy. The absorbed acoustic energy is the active component of total acoustic energy involved in the processing. Acoustic power intensity, I_a , can be estimated from the following:

$$I_a = \frac{kf^2U}{\rho c} \quad (2.11)$$

Where f is the frequency of sound (Hz), U is the voltage of the transducer (V), k is a conversion coefficient dependent on the transducer type, ρ is the density of the liquid medium (kg m^{-3}) and c is the speed of the acoustic wave in a given medium (m s^{-1}). The product of density and speed of sound (*i.e.* ρc) is known as the acoustic resistance (Margulis & Margulis, 2003). Under non-cavitation conditions the acoustic energy can be estimated accurately using Eq. 2.11, whilst in the cavitation regime the acoustic resistance is significantly reduced. The reduction of both the speed of sound and bulk density of the medium by the presence of cavitation bubbles within the medium depresses the accuracy of the acoustic intensity determination from Eq. 2.11. The underlying principles involved in the formation of and interactions between cavitation bubbles are not fully understood, hence the

reliability of the acoustic resistance term and consequently Eq. 2.11 as an effective method for the estimation of the acoustic intensity within the cavitation regime is dubious (Leighton, 1995; Margulis & Margulis, 2003; O'Brien, 2007).

The drawbacks associated with Eq. 2.11 are mitigated against by the usage of a calorimetric method for the determination of absorbed energy (*cf.* Eq. 2.12), whereby the acoustic resistance term is neglected. The main assumption for the determination of acoustic energy via calorimetry is that all absorbed acoustic energy is converted to thermal energy.

$$I_a = \frac{P_a}{S_A} = \frac{m c_p \left(\frac{dT}{dt}\right)}{S_A} \quad (2.12)$$

Where P_a is the absorbed acoustic power (W), S_A is the surface area of the tip of the transducer (cm^2 ; *i.e.* ultrasound emitting surface), m is the mass of ultrasound treated medium (g), c_p is the specific heat capacity of the medium (J/gK) and dT/dt is the rate of change of temperature with respect to time, starting at $t = 0$ ($^{\circ}\text{C s}^{-1}$). As energy emitted from the sonotrode tip, it is absorbed within close proximity to the tip due to cavitation attenuation, the energy is dissipated as heat, allowing for estimation of the acoustic energy absorbed without the necessity to account for cavitation bubbles (*i.e.* the acoustic resistance term) (Jambrak *et al.*, 2008; Margulis & Margulis, 2003).

2.2.4. Physicochemical alteration of food proteins via ultrasonic processing

From the literature, the application of ultrasonic treatment has been related to proteins derived from dairy, animal, cereal, legume and fruit sources, see Table 2.1.

Table 2.1. Examples of studies examining the effect of ultrasonic treatment related to dairy, animal, cereal, legume and fruit protein sources, in relation to solubilisation, aggregate size, molecular structure, rheology and interfacial behaviour.

Protein source		Reference
Dairy	Micellar casein	Madadlou <i>et al.</i> , (2009)
	Sodium caseinate	O'Sullivan <i>et al.</i> , (2014), O'Sullivan <i>et al.</i> , (2014)
	Calcium caseinate	Zisu <i>et al.</i> , (2010)
	Milk protein concentrates/ isolates (including retentates and skim powders)	Chandrapala <i>et al.</i> , (2014), McCarthy <i>et al.</i> , (2014), O'Sullivan, <i>et al.</i> , (2014), Shanmugam <i>et al.</i> , (2012), Uluko <i>et al.</i> , (2013), Yanjun <i>et al.</i> , (2014), Zisu <i>et al.</i> , (2010)
	Whey protein concentrates/ isolates (including retentates, BSA and α -lactalbumin)	Arzeni <i>et al.</i> , (2012), Barukčić <i>et al.</i> , (2014), Chandrapala <i>et al.</i> , (2011), Gülseren <i>et al.</i> , (2007), Güzey <i>et al.</i> , (2006), Guzey & Weiss, (2001), Jambrak <i>et al.</i> , (2008), Jambrak <i>et al.</i> , (2010), Jambrak <i>et al.</i> , (2014), Martini <i>et al.</i> , (2010), O'Sullivan, <i>et al.</i> , (2014), Zisu <i>et al.</i> , (2010)
Animal	Egg white proteins	Arzeni <i>et al.</i> , (2012), Arzeni <i>et al.</i> , (2012), Krise, (2011), O'Sullivan <i>et al.</i> , (2015b)
	Gelatin (bovine and piscine)	O'Sullivan <i>et al.</i> , (2015b)
Cereal	Rice protein isolate	O'Sullivan <i>et al.</i> , (2015b)
	Wheat gluten	Zhang <i>et al.</i> , (2011)
Legume	Soy protein concentrates/ isolates (including flakes)	Arzeni <i>et al.</i> , (2012), Chen <i>et al.</i> , (2012), Hu <i>et al.</i> , (2013), Jambrak <i>et al.</i> , (2009), Karki <i>et al.</i> , (2010), O'Sullivan <i>et al.</i> , (2015b)
	Pea protein isolate	O'Sullivan <i>et al.</i> , (2015b)
	Black bean protein isolate	Jiang <i>et al.</i> , (2014)
	Mung bean protein isolate	Charoensuk <i>et al.</i> , (2014)
Fruit	Walnut protein	Jincai <i>et al.</i> , (2013)

Ultrasound treatment offers improved rates of dissolution and solubilisation of protein powders in comparison to conventional dissolution methodologies (*i.e.* high shear mixing)

(Chandrapala *et al.*, 2014; McCarthy *et al.*, 2014). The high levels of hydrodynamic shear associated with the high number ultrasonic cavitations disrupt agglomerates of powder imparting greatly increased rates of solubilisation in comparison to conventional rotor-stator mixing or high pressure homogenisation solubilisation methodologies for dairy powders with a high degree of micellar casein (Chandrapala *et al.*, 2014).

Moreover, ultrasound treatment reduced the size of aggregated caseins in aqueous solution (phosphocasein, calcium caseinate, milk protein concentrate from retentate and milk protein concentrate reconstituted from powder), and this size reduction is attributed to the high shear forces associated with ultrasonic cavitations in liquid mediums (Madadlou *et al.*, 2009; McCarthy *et al.*, 2014; Shanmugam *et al.*, 2012; Yanjun *et al.*, 2014; Zisu *et al.*, 2010). Be that as it may, prolonged ultrasound treatment led to growth in aggregate size, related to whey-whey or casein-whey protein interactions as a consequence of elevated temperatures from ultrasound treatment (McCarthy *et al.*, 2014; Shanmugam *et al.*, 2012). Sonication of whey protein (suspensions, concentrates, isolates, and from retentate) similarly reduced the size of protein aggregates due to disruption of non-covalent interactions (*i.e.* hydrogen bonding, hydrophobic and electrostatic interactions) (Arzeni *et al.*, 2012; Chandrapala *et al.*, 2011; Jambrak *et al.*, 2014; Martini *et al.*, 2010; Zisu *et al.*, 2010), yet similarly displayed growth of particle size attributed to increases in temperature (Gülseren *et al.*, 2007).

Furthermore, the ultrasound treatment of proteins derived from legume sources (pea protein, soy protein, black bean protein and mung bean protein) and wheat gluten displayed reduction in aggregate size (Charoensuk *et al.*, 2014; Jiang *et al.*, 2014; O'Sullivan, Murray, *et al.*, 2015b; Zhang *et al.*, 2011), whilst ultrasound treatment of egg white proteins (Arzeni *et al.*, 2012; Krise, 2011) exhibited growth in aggregate size attributed to thermal denaturation of protein due to increases in temperature from prolonged ultrasonic treatment. Sonication of rice protein isolate demonstrated no significant differences in size, associated with

insufficient provided acoustic energy to disrupt disulphide bonding maintaining the denatured aggregate structure (O'Sullivan, Murray, et al., 2015b). Size reduction of protein aggregates in aqueous solution from ultrasound treatment is associated with the disruption of associative non-covalent interactions which maintain protein aggregate structure in aqueous solutions.

Nonetheless, ultrasound treatment does not appear to cause scission of the primary structure for a large number of proteins, including milk protein concentrate (YanJun *et al.*, 2014), whey protein suspensions (Martini *et al.*, 2010), soy protein isolate (Hu *et al.*, 2013), pea protein isolate (O'Sullivan, Murray, et al., 2015b), wheat gluten (Zhang *et al.*, 2011), black bean protein isolate (Jiang *et al.*, 2014), gelatin (O'Sullivan, Murray, et al., 2015b) and egg white protein (Krise, 2011), as ultrasound treatment provides insufficient energy to cause scission of the primary acid sequence. Krise, (2011) observed a minor shift in the molecular weight distribution of egg white protein and attributed this to scission of disulphide bonds between cysteine residues present in egg white protein (Mine, 2002). The bond energy associated with the disulphide bond is less than that of the peptide bond maintaining the primary structure of proteins (*cf.* Table 2.2), nevertheless, the majority of ultrasonic energy is utilised in the disruption of the associative non-covalent interactions maintaining the protein associate structure, rather than disruption of covalent linkages. However, a significant reduction in the molecular weight of α -lactalbumin (Jambrak *et al.*, 2010) and whey protein concentrate/isolate (Jambrak *et al.*, 2014) has been observed which is contradictory to other results present in the literature.

Table 2.2. Bond energy (kJ mol⁻¹) associated with intra- and intermolecular bonds present in proteins (McMurry, 2011).

	Typical bonds present in proteins	Bond energy (kJ mol ⁻¹)
	C-N (peptide bond)	285
	C=N	615
Intramolecular bonds present within peptide chains	C-C	348
	N-H	391
	C-H	413
	C=O	799
Intermolecular bonds occurring between amino acids	Hydrogen bonding	4 – 13
	S-S	226

Sonication of protein solutions has been shown to either reduce the bulk viscosity, in the cases of calcium caseinate (Zisu *et al.*, 2010), milk protein concentrate (Yanjun *et al.*, 2014; Zisu *et al.*, 2010), whey protein from retentate (Zisu *et al.*, 2010), soy protein isolate (Hu *et al.*, 2013) and egg white protein (Arzeni *et al.*, 2012), or to yield no difference in bulk viscosity, as for skimmed milk powder (Shanmugam *et al.*, 2012) and α -lactalbumin (Jambrak *et al.*, 2010). The reduction in bulk viscosity is attributed to the reduction in aggregate size as a consequence of ultrasonic cavitations. The spatial distance between adjacent protein aggregates is increased upon size reduction via ultrasound treatment, increasing the critical overlap concentration, c^* , for a given protein solution, and thus, decreasing the bulk viscosity with respect to increasing protein concentration (Lefebvre, 1982; Morris *et al.*, 1981).

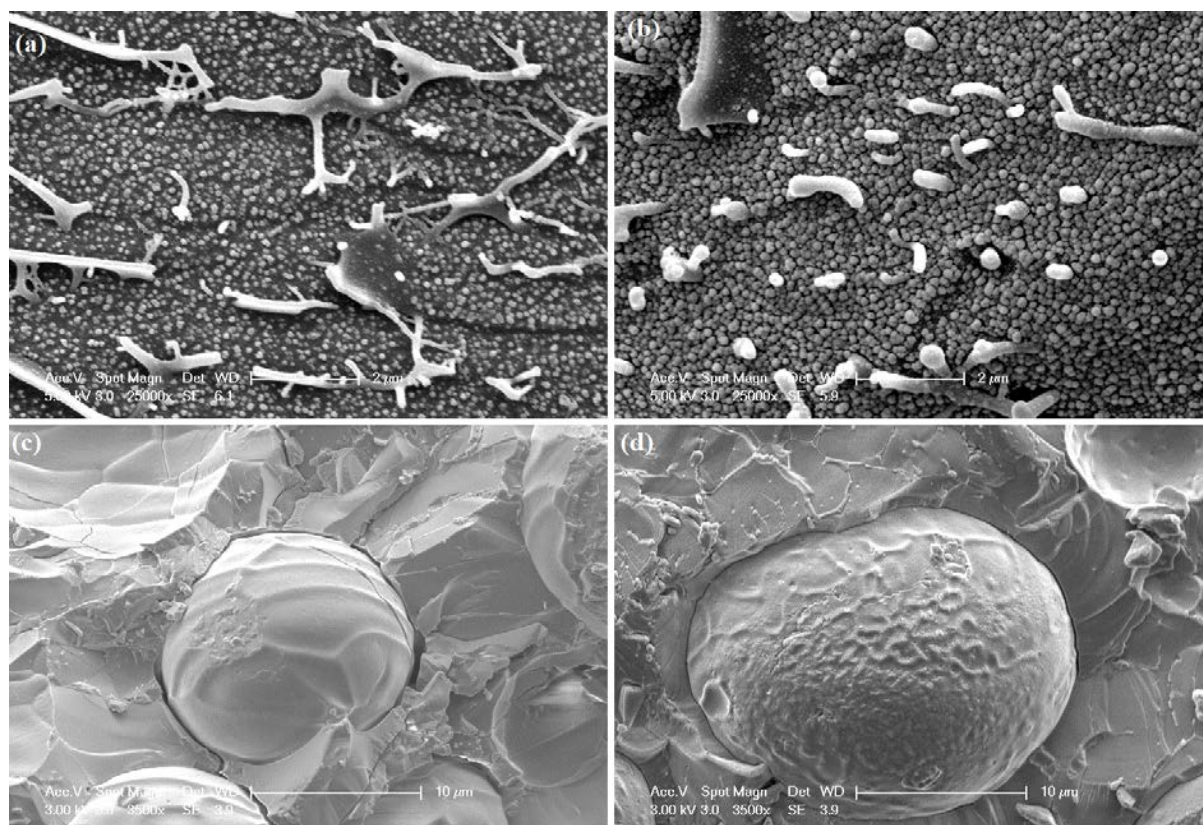


Fig. 2.4. Cryo-SEM micrographs of (a) 1% untreated bovine gelatin solution, (b) 1% ultrasound treated bovine gelatin solution, (c) 1% untreated bovine gelatin stabilised emulsion and (d) 1% ultrasound treated bovine gelatin stabilised emulsion. Scale bars are 2 μm and 10 μm for solutions and emulsions, respectively. Image adapted from O'Sullivan *et al.*, (2015b).

Proteins which have been treated with power ultrasound have shown improvements in both emulsion formation and stability, for milk protein concentrate (Yanjun *et al.*, 2014), milk protein isolate (O'Sullivan, *et al.*, 2014), egg white protein (O'Sullivan, Murray, *et al.*, 2015b), bovine gelatin (O'Sullivan, Murray, *et al.*, 2015b), soy protein isolate (Chen *et al.*, 2012), pea protein isolate (O'Sullivan, Murray, *et al.*, 2015b), wheat gluten (Zhang *et al.*, 2011) and walnut protein (Jincai *et al.*, 2013). These improvements in emulsion formation and stability were associated with increases in hydrophobicity, which occurred as hydrophobic protein residues within the interior of the untreated aggregate became revealed upon treatment with ultrasound, and improved interfacial packing at the emulsion droplet interface. In addition, ultrasound treatment of whey protein (Arzeni *et al.*, 2012; Gülseren *et*

al., 2007), soy protein (Arzeni *et al.*, 2012; Hu *et al.*, 2013), black bean protein (Jiang *et al.*, 2014) and egg white protein (Arzeni *et al.*, 2012) increased the hydrophobicity, and the rate of protein adsorption to and interfacial packing at the oil-water interface, as measured by interfacial tension. These differences were measured for the cases of milk protein isolate (O'Sullivan, *et al.*, 2014), bovine gelatin (O'Sullivan, Murray, *et al.*, 2015b), pea protein isolate (O'Sullivan, Murray, *et al.*, 2015b) and soy protein isolate (Chen *et al.*, 2012), further accounting for improvements in emulsion formation and stability. O'Sullivan *et al.*, (2015b) visualised the improved interfacial packing using cryo-SEM for ultrasound treated bovine gelatin in comparison to untreated bovine gelatin, whereby the reduction in fibre size of bovine gelatin after sonication allowed for improved packing at the oil-water interface (*cf.* Fig. 2.4).

Ultrasound treatment of a range of dairy proteins (whey protein concentrate, milk protein from retentate and calcium caseinate) utilising large scale sonoreactors demonstrated the capacity for ultrasound to modify the rheological behaviour of these proteins at pilot scale and was attributed to a reduction in protein aggregate size (Zisu *et al.*, 2010). This work highlights the potential applicability of ultrasound for the functional modification of proteins at larger scales, whilst more work is required to fully implement this technology industrially.

2.2.5. Nanoemulsion fabrication from ultrasound and the associated parameters

Power ultrasound is a well established technique for the formation of emulsions from either coarse pre-emulsions (*i.e.* $d_{3,2} > 50 \mu\text{m}$) or discrete continuous and dispersed phases, consistently yielding nano-sized emulsion droplets (Bondy & Söllner, 1935; Leong *et al.*, 2009). The resultant microstructure of emulsions is dependent upon formulation and the emulsification processing conditions. Processing configurations (*i.e.* batch or continuous processing methodologies) and associated parameters (*i.e.* acoustic power, residence time, etc.) have been extensively investigated, yet the fundamental influence of emulsion

formulation with industrial relevant emulsifiers (*i.e.* high molecular weight biopolymers), geometric configuration to optimise contact time and the intrinsic interactions between processing and formulations have yet to be fully explored.

Increasing the contact time of a coarse pre-emulsion within the acoustic field can decrease the emulsion droplet size to a minimum size, provided the residence time of the emulsion within the acoustic field is sufficient and there is sufficient emulsifier present for droplet coverage (Maa & Hsu, 1999). For batch processing methodologies increasing the processing time decreases the emulsion droplet size (Abisma I *et al.*, 1999; Cucheval & Chow, 2008; Delmas *et al.*, 2011; Jafari *et al.*, 2007; Jena & Das, 2006; Kaltsa *et al.*, 2013; Kentish *et al.*, 2008; Kiani & Mousavi, 2013; Leong *et al.*, 2009; O'Sullivan *et al.*, 2015a; Ouzineb *et al.*, 2006; Ramisetty & Shyamsunder, 2011; Shanmugam *et al.*, 2012; Tang *et al.*, 2013). Similarly increasing the residence time of emulsions for continuous processing, by decreasing the flow rate, decreases emulsion droplet size (Behrend *et al.*, 2000; Behrend & Schubert, 2001; Freitas *et al.*, 2006; Kentish *et al.*, 2008; O'Sullivan *et al.*, 2015a; Tang *et al.*, 2013). Nevertheless, prolonged residence time within the acoustic field can lead to growth in droplet size due to re-coalescence of emulsion droplets (*i.e.* over processing) in systems possessing insufficient emulsifier (Jafari *et al.*, 2008; O'Sullivan *et al.*, 2015a).

The acoustic energy transmitted from the tip of the sonotrode to the medium is highly localised (as low as 1 cm from the sonotrode; Chivate & Pandit, 1995) due to attenuation (*i.e.* dispersion of acoustic waves from cavitation bubbles). Ultrasonic cavitation bubbles are highly unstable entities yielding implosions creating highly localised regions of hydrodynamic shear within close proximity of the tip (Kumar *et al.*, 2006; Kumaresan *et al.*, 2006). These ultrasonically induced implosions from cavitations result in the disruption of micron sized oil droplets and facilitate the formation of nano-sized emulsion droplets. Batch processing of emulsions utilising ultrasound is often inefficient due to the nature of the

emulsification process, whereby less than 2 % of the medium of a given volume experiences acoustic energy due to acoustic attenuation (Kumar *et al.*, 2006; Kumaresan *et al.*, 2006), and the turbulent forces generated by the acoustic streaming transfer the coarse emulsion from the bulk to within the vicinity of the tip, whereby emulsification occurs. Depending on the volume of coarse emulsion being processed and the surface area of the tip via batch configuration this can be a time consuming process, in comparison to continuous processing methodologies, which typically demonstrate smaller chamber volumes relative to tip surface area.

Continuous processing configurations operate at lower residence times in comparison to batch processing (< 1 s), yet are capable of achieving comparable droplet sizes due to minimisation of chamber volume to maximise the volume of coarse emulsion within the acoustic field. By optimisation of the geometry, whereby the course of emulsion is pumped directly into the tip of the sonotrode, maximum droplet breakup can be achieved. The residence time for continuous processing is dictated by the flow rate of emulsion, whereby reduction of flow rate increases the contact time, allowing for a greater reduction in the droplet size (Freitas *et al.*, 2006; Kentish *et al.*, 2008; O’Sullivan, Murray, *et al.*, 2015a; S. Y. Tang *et al.*, 2013).

The rate of droplet breakup can be improved by increasing the acoustic power transmitted to the coarse emulsion for both batch processing (Abisma I *et al.*, 1999; Cucheval & Chow, 2008; Delmas *et al.*, 2011; Higgins & Skauen, 1972; Kaltsa *et al.*, 2013; O’Sullivan, Murray, *et al.*, 2015a) and continuous processing configurations (Freitas *et al.*, 2006; O’Sullivan, Murray, *et al.*, 2015a), decreasing the time required to achieve a minimum droplet size, as dictated by the emulsion formulation (Maa & Hsu, 1999). However the minimum achievable droplet is dictated by the formulation of the emulsion (Maa & Hsu,

1999). Thus, increasing the acoustic power minimises the processing time required to achieve the minimum droplet size dictated by emulsion formulation.

The resultant droplet size of emulsions fabricated via ultrasonic processes is dictated by the formulation of the emulsion (*i.e.* emulsifier type and concentration, dispersed phase type and volume fraction, presence of stabilisers, etc.), whilst the processing parameters determine the rate at which the resultant droplet is formed (Jafari *et al.*, 2007). The majority of studies conducted utilise model emulsifier systems (*i.e.* low molecular weight surfactants), whereby a high degree of purity can be guaranteed. These surfactants include Tween 40 (Kentish *et al.*, 2008), Tween 60 (Abisma l *et al.*, 1999), Tween 80 (O’Sullivan, Murray, et al., 2015a) and Span 80 (Leong *et al.*, 2009). Increasing the emulsifier concentration decreases the droplet size to a minimum size given optimal processing conditions to achieve the minimal droplet size, such as adequate processing power and time. Few studies have been conducted whereby industrial applicable ingredients are utilised, such as multi-component protein sources as the emulsifying agent. Kaltsa *et al.*, (2013), Heffernan *et al.*, (2011) and O’Sullivan *et al.*, (2015a) employed whey protein concentrate, sodium caseinate and milk protein isolate, respectively, as the emulsifying agent in oil-in-water emulsions. Submicron emulsion droplets have been prepared from these dairy proteins, whereby Kaltsa *et al.*, (2013) and Heffernan *et al.*, (2011) solely utilised batch processing, whilst O’Sullivan *et al.*, (2015a) comparatively assessed both batch and continuous configurations, highlighting the efficiency of continuous processing, as acoustic energy is utilised more efficiently in lower processing volumes associated with the chamber of the continuous configuration.

From an industrial perspective, the most practical method for the implementation of ultrasound within a production environment is the continuous processing configuration, due to a combination of higher throughputs and more effective utilisation of acoustic energy. Irrespective of configuration, the implementation of ultrasound within the food industry has

been limited for a number of reasons: including pitting of the sonotrode tip (*i.e.* the gradual erosion of the tip material due to mechanical vibrations), deposition of tip debris within the processed medium and poor performance of current ultrasound geometric configurations (*i.e.* dead zones). Freitas *et al.*, (2006) developed a configuration for continuous processing of emulsions, whereby the ultrasonic probe was welded to the steel jacket. Additionally the space in between the jacket and the glass tube, through which the medium passed, contained pressurised water which behaved as an acoustic conductor. This methodology prevents direct contact of the sonotrode with the medium being processed, hence removing the potential for contamination from ultrasonic pitting. O'Sullivan *et al.*, (2015a) compared the effect of continuous processing at both lab and pilot scale, through means of energy density (E_v ; MJ m^{-3}) and variation of both the residence time and acoustic power, demonstrating that the pilot scale continuous configuration is dependent upon the ultrasonic amplitude (*i.e.* acoustic power), unlike the lab scale, due to bypassing of elements of pre-emulsion from the acoustic field at lower ultrasonic amplitudes, highlighting the necessity for optimisation of processing conditions at larger scales to efficiently achieve nanoemulsions.

The design of conventional continuous configurations is under investigation and continual development (Gogate *et al.*, 2011, 2003). The primary design criteria for the development of continuous ultrasonic processes are the operating conditions (*i.e.* acoustic power and processing time) and geometric parameters (sonotrode location, chamber volume, tip location within the chamber, etc.). Be that as it may, several other factors must be taken into consideration during the development and design of continuous ultrasonic systems: such as the hydrodynamic conditions within the acoustic field, variance due to the presence of discrete entities within the liquid medium (*i.e.* gaseous bubbles, immiscible liquid droplets, solid particles or high molecular weight biopolymers), the degree of acoustic attenuation chiefly due to the non-homogeneous nature of food systems, and ratio of frequency

irradiation to power dissipation within the locus of the tip of the sonotrode (Gogate *et al.*, 2011, 2003).

2.2.6. Conclusions and future trends

Even though low frequency, high power ultrasonic processing is a well established technology within the food industry, numerous advances have been achieved in understanding the fundamental mechanisms for the functional modification of the physicochemical properties of proteins for specific applications and the factors associated with the efficient generation of nano-sized emulsion droplets in recent years. Ultrasound offers the potential for the functional modification of proteins through mechanical means, without the use of chemical or biological (*i.e.* enzymes) additives.

Ultrasonic treatment of proteins is related to physicochemical changes in structure, manifesting as: modifications to the functional attributes of proteins, reduction of bulk viscosity, increases of hydrophobicity and improvements in emulsion formation and stability. Ultrasound treatment of proteins in solutions affects the associative behaviour of proteins, disrupting the non-covalent forces which maintain protein aggregate structure, and reducing aggregate size. However there is debate within the literature as to whether sufficient energy is provided from low frequency, high power ultrasound to achieve scission of the peptide bond, the primary structure of proteins.

Power ultrasound has shown to be an effective emulsification methodology, either utilising batch or continuous configurations, for the formation of nano-sized droplets. The development of nano-sized droplets is related to a combination of process parameters (*i.e.* acoustic power and contact time), geometric considerations (*i.e.* sonotrode location within the chamber, chamber geometry, etc.) and emulsion formulation (*i.e.* emulsifier type and concentrations, dispersed phase volume fraction, etc.). Emulsion formation within the

acoustic field is attributed to the high levels of hydrodynamic shear generated by ultrasonic cavitations within close proximity to the tip of the sonotrode. Increasing the residence time of the coarse pre-emulsion within the acoustic field decreases the emulsion droplet size, to a minimum droplet size as determined by the emulsion formulation. In addition, increasing the acoustic power increases the rate by which this minimal droplet size is achieved. Nevertheless, further investigations of emulsification implementing ultrasound are required to develop optimised geometries for maximum droplet breakup, utilisation of industrial relevant ingredients (*i.e.* high molecular weight biopolymers) and the intrinsic interactions between emulsion formulation and operating conditions (*i.e.* microstructural engineering).

Lastly, it is worth mentioning that although numerous advances have been made in understanding the effects of power ultrasound upon proteins in aqueous solution and for the fabrication of nanoemulsions, this understanding is predominately at lab scale. Although studies are being conducted for both the ultrasound treatment of proteins and emulsion generation at pilot scale, further work is required to fully understand the specific design criteria to allow the effective utilisation of this versatile technology within the food industry.

2.2.7. References

- Abisma I, B., Canselier, J. P., Wilhelm, A. M., Delmas, H., & Gourdon, C. (1999). Emulsification by ultrasound: drop size distribution and stability. *Ultrasonics Sonochemistry*, 6(1–2), 75–83.
- Arzeni, C., Martínez, K., Zema, P., Arias, A., Pérez, O. E., & Pilosof, A. M. R. (2012). Comparative study of high intensity ultrasound effects on food proteins functionality. *Journal of Food Engineering*, 108(3), 463–472.
- Arzeni, C., Pérez, O. E., & Pilosof, A. M. R. (2012). Functionality of egg white proteins as affected by high intensity ultrasound. *Food Hydrocolloids*, 29(2), 308–316.
- Barukčić, I., Lisak Jakopović, K., Herceg, Z., Karlović, S., & Božanić, R. (2014). Influence of high intensity ultrasound on microbial reduction, physico-chemical characteristics and fermentation of sweet whey. *Innovative Food Science & Emerging Technologies*.

- Behrend, O., Ax, K., & Schubert, H. (2000). Influence of continuous phase viscosity on emulsification by ultrasound. *Ultrasonics Sonochemistry*, 7(2), 77–85.
- Behrend, O., & Schubert, H. (2001). Influence of hydrostatic pressure and gas content on continuous ultrasound emulsification. *Ultrasonics Sonochemistry*, 8(3), 271–276.
- Beverung, C. J., Radke, C. J., & Blanch, H. W. (1999). Protein adsorption at the oil/water interface: characterization of adsorption kinetics by dynamic interfacial tension measurements. *Biophysical Chemistry*, 81(1), 59–80.
- Bondy, C., & Söllner, K. (1935). On the mechanism of emulsification by ultrasonic waves. *Transactions of the Faraday Society*, (31), 835–842.
- Chandrapala, J., Martin, G. J. O., Kentish, S. E., & Ashokkumar, M. (2014). Dissolution and reconstitution of casein micelle containing dairy powders by high shear using ultrasonic and physical methods. *Ultrasonics Sonochemistry*, 21(5), 1658–65.
- Chandrapala, J., Zisu, B., Palmer, M., Kentish, S., & Ashokkumar, M. (2011). Effects of ultrasound on the thermal and structural characteristics of proteins in reconstituted whey protein concentrate. *Ultrasonics Sonochemistry*, 18(5), 951–957.
- Charoensuk, D., Wilailuk, C., & Wanlop, C. (2014). Effect of high intensity ultrasound on physicochemical and functional properties of whey protein isolate and mung bean protein isolate. In *The 26th Annual Meeting of the Thai Society for Biotechnology and International Conferenc* (pp. 394–401).
- Chemat, F., Zill-e-Huma, & Khan, M. K. (2011). Applications of ultrasound in food technology: Processing, preservation and extraction. *Ultrasonics Sonochemistry*, 18(4), 813–35
- Chen, L., Chen, J. S., Yu, L., Wu, K. G., Liu, X. L., & Chai, X. H. (2012). Modifications of Soy Protein Isolates Using Ultrasound Treatment for Improved Emulsifying Properties. In *Advanced Materials Research* (Vol. 554–556, pp. 944–948).
- Chivate, M. M., & Pandit, A. B. (1995). Quantification of cavitation intensity in fluid bulk. *Ultrasonics Sonochemistry*, 2(1), S19–S25.
- Crum, L. A. (1975). Bjerknes forces on bubbles in a stationary sound field. *The Journal of the Acoustical Society of America*, 57(6), 1363.
- Cucheval, A., & Chow, R. C. Y. (2008). A study on the emulsification of oil by power ultrasound. *Ultrasonics Sonochemistry*, 15(5), 916–920.
- Damodaran, S. (1997). Food Proteins: An Overview. In S. Damodaran & A. Paraf (Eds.), *Food Proteins and Their Applications* (1st ed., pp. 1–24). New York: Marcel Dekker.
- Delmas, T., Piraux, H., Couffin, A.-C., Texier, I., Vinet, F., Poulin, P., Cates, M., & Bibette, J. (2011). How To Prepare and Stabilize Very Small Nanoemulsions. *Langmuir*, 27(5), 1683–1692.

- Demirdöven, A., & Baysal, T. (2008). The Use of Ultrasound and Combined Technologies in Food Preservation. *Food Reviews International*, 25(1), 1–11.
- Doinikov, A. A., & Dayton, P. A. (2006). Spatio-temporal dynamics of an encapsulated gas bubble in an ultrasound field. *The Journal of the Acoustical Society of America*, 120(2), 661.
- Freitas, S., Hielscher, G., Merkle, H. P., & Gander, B. (2006). Continuous contact- and contamination-free ultrasonic emulsification—a useful tool for pharmaceutical development and production. *Ultrasonics Sonochemistry*, 13(1), 76–85.
- Gogate, P. R., Sutkar, V. S., & Pandit, A. B. (2011). Sonochemical reactors: Important design and scale up considerations with a special emphasis on heterogeneous systems. *Chemical Engineering Journal*, 166(3), 1066–1082.
- Gogate, P. R., Wilhelm, A. M., & Pandit, A. B. (2003). Some aspects of the design of sonochemical reactors. *Ultrasonics Sonochemistry*, 10(6), 325–330.
- Gülseren, İ., Güzey, D., Bruce, B. D., & Weiss, J. (2007). Structural and functional changes in ultrasonicated bovine serum albumin solutions. *Ultrasonics Sonochemistry*, 14(2), 173–183.
- Güzey, D., Gülseren, İ., Bruce, B., & Weiss, J. (2006). Interfacial properties and structural conformation of thermosonicated bovine serum albumin. *Food Hydrocolloids*, 20(5), 669–677.
- Guzey, D., & Weiss, J. (2001). High-intensity ultrasonic processing improves emulsifying properties of proteins. Colloidal and Interfacial Food Science Laboratory, Department of Food Science and Technology, The University of Tennessee.
- Heffernan, S. P., Kelly, A. L., Mulvihill, D. M., Lambrich, U., & Schuchmann, H. P. (2011). Efficiency of a range of homogenisation technologies in the emulsification and stabilization of cream liqueurs. *Innovative Food Science & Emerging Technologies*, 12(4), 628–634.
- Higgins, D. M., & Skauen, D. M. (1972). Influence of power on quality of emulsions prepared by ultrasound. *Journal of Pharmaceutical Sciences*, 61(10), 1567–1570.
- Hu Hu, H., Wu, J., Li-Chan, E. C. Y., Zhu, L., Zhang, F., Xu, X., Gang, F., Lufeng, W., Xingjian, H., & Pan, S. (2013). Effects of ultrasound on structural and physical properties of soy protein isolate (SPI) dispersions. *Food Hydrocolloids*, 30(2), 647–655.
- Jafari, S. M., Assadpoor, E., He, Y., & Bhandari, B. (2008). Re-coalescence of emulsion droplets during high-energy emulsification. *Food Hydrocolloids*, 22(7), 1191–1202.
- Jafari, S. M., He, Y., & Bhandari, B. (2007). Production of sub-micron emulsions by ultrasound and microfluidization techniques. *Journal of Food Engineering*, 82(4), 478–488.

- Jambrak, A. R., Lelas, V., Mason, T. J., Krešić, G., & Badanjak, M. (2009). Physical properties of ultrasound treated soy proteins. *Journal of Food Engineering*, 93(4), 386–393.
- Jambrak, A. R., Mason, T. J., Lelas, V., Herceg, Z., & Herceg, I. L. (2008). Effect of ultrasound treatment on solubility and foaming properties of whey protein suspensions. *Journal of Food Engineering*, 86(2), 281–287.
- Jambrak, A. R., Mason, T. J., Lelas, V., & Krešić, G. (2010). Ultrasonic effect on physicochemical and functional properties of α -lactalbumin. *LWT - Food Science and Technology*, 43(2), 254–262.
- Jambrak, A. R., Mason, T. J., Lelas, V., Paniwnyk, L., & Herceg, Z. (2014). Effect of ultrasound treatment on particle size and molecular weight of whey proteins. *Journal of Food Engineering*, 121(0), 15–23.
- Jena, S., & Das, H. (2006). Modeling of particle size distribution of sonicated coconut milk emulsion: Effect of emulsifiers and sonication time. *Food Research International*, 39(5), 606–611.
- Jiang, L., Wang, J., Li, Y., Wang, Z., Liang, J., Wang, R., Chen, Y., Ma, W., Qi, B., & Zhang, M. (2014). Effects of ultrasound on the structure and physical properties of black bean protein isolates. *Food Research International*, 62, 595–601.
- Jincai, Z., Shaoying, Z., & Rixian, Y. (2013). Ultrasonic Enhanced Walnut Protein Emulsifying Property. *Journal of Food Processing & Technology*, 4(7).
- Kaltsa, O., Michon, C., Yanniotis, S., & Mandala, I. (2013). Ultrasonic energy input influence on the production of sub-micron o/w emulsions containing whey protein and common stabilizers. *Ultrasonics Sonochemistry*, 20(3), 881–91.
- Karki, B., Lamsal, B. P., Jung, S., van Leeuwen, J., Pometto, A. L., Grewell, D., & Khanal, S. K. (2010). Enhancing protein and sugar release from defatted soy flakes using ultrasound technology. *Journal of Food Engineering*, 96(2), 270–278.
- Kato, A., Kobayashi, K., & Chemicals, T. (1993). Improvement of Emulsifying Properties of Egg White Proteins by the Attachment of Polysaccharide through Maillard Reaction in a Dry State, 540–543.
- Kentish, S., Wooster, T. J., Ashokkumar, M., Balachandran, S., Mawson, R., & Simons, L. (2008). The use of ultrasonics for nanoemulsion preparation. *Innovative Food Science & Emerging Technologies*, 9(2), 170–175.
- Kiani, S., & Mousavi, S. M. (2013). Ultrasound assisted preparation of water in oil emulsions and their application in arsenic (V) removal from water in an emulsion liquid membrane process. *Ultrasonics Sonochemistry*, 20(1), 373–7.
- Krise, K. M. (2011). *The effects of microviscosity, bound water and protein mobility on the radiolysis and sonolysis of hen egg white*. PhD Thesis. The Pennsylvania State University.

- Kumar, A., Kumaresan, T., Pandit, A. B., & Joshi, J. B. (2006). Characterization of flow phenomena induced by ultrasonic horn. *Chemical Engineering Science*, 61(22), 7410–7420.
- Kumaresan, T., Kumar, A., Pandit, A. B., & Joshi, J. B. (2006). Modeling Flow Pattern Induced by Ultrasound: The Influence of Modeling Approach and Turbulence Models. *Industrial & Engineering Chemistry Research*, 46(10), 2936–2950.
- Lauterborn, W., Kurz, T., Geisler, R., Schanz, D., & Lindau, O. (2007). Acoustic cavitation, bubble dynamics and sonoluminescence. *Ultrasonics Sonochemistry*, 14(4), 484–91.
- Lee, L., & Norton, I. T. (2013). Comparing droplet breakup for a high-pressure valve homogeniser and a Microfluidizer for the potential production of food-grade nanoemulsions. *Journal of Food Engineering*, 114(2), 158–163.
- Lefebvre, J. (1982). Viscosity of concentrated protein solutions. *Rheologica Acta*, 21(4-5), 620–625.
- Leighton, T. G. (1995). Bubble population phenomena in acoustic cavitation. *Ultrasonics Sonochemistry*, 2(2), S123–S136.
- Leong, T. S. H., Wooster, T. J., Kentish, S. E., & Ashokkumar, M. (2009). Minimising oil droplet size using ultrasonic emulsification. *Ultrasonics Sonochemistry*, 16(6), 721–727.
- Lighthill, S. J. (1978). Acoustic streaming. *Journal of Sound and Vibration*, 61(3), 391–418.
- Lloyd, D. M., Norton, I. T., & Spyropoulos, F. (2014). Processing effects during rotating membrane emulsification. *Journal of Membrane Science*, 466, 8–17.
- Maa, Y. F., & Hsu, C. C. (1999). Performance of sonication and microfluidization for liquid-liquid emulsification. *Pharmaceutical Development and Technology*, 4(2), 233–40.
- Madadlou, A., Mousavi, M. E., Emam-djomeh, Z., Ehsani, M., & Sheehan, D. (2009). Sonodisruption of re-assembled casein micelles at different pH values. *Ultrasonics Sonochemistry*, 16(5), 644–8.
- Malaki Nik, A., Wright, A. J., & Corredig, M. (2010). Interfacial design of protein-stabilized emulsions for optimal delivery of nutrients. *Food & Function*, 1(2), 141–8.
- Mansfield, M., & O’Sullivan, C. (1998). Wave Motion. In *Understanding Physics* (pp. 307–357). Wiley-Blackwell.
- Margulis, M. A., & Margulis, I. M. (2003). Calorimetric method for measurement of acoustic power absorbed in a volume of a liquid. *Ultrasonics Sonochemistry*, 10(6), 343–345.
- Martini, S. (2013). *Sonocrystallization of Fats*. (R. W. Hartel, Ed.) (1st ed.). New York: Springer US.

- Martini, S., Potter, R., & Walsh, M. K. (2010). Optimizing the use of power ultrasound to decrease turbidity in whey protein suspensions. *Food Research International*, 43(10), 2444–2451.
- McCarthy, N. A., Kelly, P. M., Maher, P. G., & Fenelon, M. A. (2014). Dissolution of milk protein concentrate (MPC) powders by ultrasonication. *Journal of Food Engineering*, 126, 142–148.
- McClements, D. J. (1995). Advances in the application of ultrasound in food analysis and processing. *Trends in Food Science & Technology*, 6(9), 293–299.
- McClements, D. J. (2005). *Food Emulsions: Principles, Practices, and Techniques* (2nd ed.). CRC Press.
- McMurry, J. E. (2011). *Organic Chemistry* (8th ed.). Brooks/Cole.
- Mettin, R., Akhatov, I., Parlitz, U., Ohl, C., & Lauterborn, W. (1997). Bjerknes forces between small cavitation bubbles in a strong acoustic field. *Physical Review E*, 56(3), 2924–2931.
- Mine, Y. (2002). Recent advances in egg protein functionality in the food system, *World's Poultry Science Journal*, 58(1), 31-39.
- Morris, E. R., Cutler, A. N., Ross-Murphy, S. B., Rees, D. A., & Price, J. (1981). Concentration and shear rate dependence of viscosity in random coil polysaccharide solutions. *Carbohydrate Polymers*, 1, 5–21.
- Neppiras, E. A. (1980). Acoustic cavitation. *Physics Reports*, 61(3), 159–251.
- Nowicki, A., Kowalewski, T., Secomski, W., & Wójcik, J. (1998). Estimation of acoustical streaming: theoretical model, Doppler measurements and optical visualisation. *European Journal of Ultrasound*, 7(1), 73–81.
- Nowicki, A., Secomski, W., & Wójcik, L. (1997). Acoustic streaming: comparison of low-amplitude linear model with streaming velocities measured by 32-MHz Doppler. *Ultrasound in Medicine & Biology*, 23(5), 783–91.
- Nyborg, W. L. (1953). Acoustic Streaming due to Attenuated Plane Waves. *The Journal of the Acoustical Society of America*, 25(1), 68.
- O'Brien, W. D. (2007). Ultrasound-biophysics mechanisms. *Progress in Biophysics and Molecular Biology*, 93(1-3), 212–55.
- O'Connell, J. E., & Flynn, C. (2007). The Manufacture and Application of Casein-Derived Ingredients. In Y. H. Hui (Ed.), *Handbook of Food Products Manufacturing* (1st ed., pp. 557 – 593). New Jersey: John Wiley & Sons.
- O'Donnell, C. P., Tiwari, B. K., Bourke, P., & Cullen, P. J. (2010). Effect of ultrasonic processing on food enzymes of industrial importance. *Trends in Food Science & Technology*, 21(7), 358–367.

- O'Sullivan, J., Arellano, M., Pichot, R., & Norton, I. (2014). The Effect of Ultrasound Treatment on the Structural, Physical and Emulsifying Properties of Dairy Proteins. *Food Hydrocolloids*, 42(3), 386–396.
- O'Sullivan, J., Murray, B., Flynn, C., & Norton, I. (2015a). Comparison of batch and continuous ultrasonic emulsification processes. *Journal of Food Engineering (In press)*.
- O'Sullivan, J., Murray, B., Flynn, C., & Norton, I. T. (2015b). The Effect of Ultrasound Treatment on the Structural, Physical and Emulsifying Properties of Animal and Vegetable Proteins. *Food Hydrocolloids (In press)*.
- O'Sullivan, J., Pichot, R., & Norton, I. T. (2014). Protein Stabilised Submicron Emulsions. In P. A. Williams & G. O. Phillips (Eds.), *Gums and Stabilisers for the Food Industry 17* (pp. 223–229). Cambridge, UK: The Royal Society of Chemistry.
- Ouzineb, K., Lord, C., Lesauze, N., Graillat, C., Tanguy, P. A., & McKenna, T. (2006). Homogenisation devices for the production of miniemulsions. *Chemical Engineering Science*, 61(9), 2994–3000.
- Ramisetty, K. A., & Shyamsunder, R. (2011). Effect of Ultrasonication on Stability of Oil in Water Emulsions. *International Journal of Drug Delivery*.
- Rayleigh, Lord. (1896). *Theory of Sound*. New York: Dover Publications.
- Servant, G., Laborde, J. L., Hita, A., Caltagirone, J. P., & Gérard, A. (2001). Spatio-temporal dynamics of cavitation bubble clouds in a low frequency reactor: comparison between theoretical and experimental results. *Ultrasonics Sonochemistry*, 8(3), 163–74.
- Shanmugam, A., Chandrapala, J., & Ashokkumar, M. (2012). The effect of ultrasound on the physical and functional properties of skim milk. *Innovative Food Science & Emerging Technologies*, 16, 251–258.
- Soria, A. C., & Villamiel, M. (2010). Effect of ultrasound on the technological properties and bioactivity of food: a review. *Trends in Food Science & Technology*, 21(7), 323–331.
- Stuart, J. . (1963). Unsteady boundary layers. In L. Rosenhead (Ed.), *Laminar Boundary Layers* (1st ed.). London: Oxford University Press.
- Tang, S. Y., Shridharan, P., & Sivakumar, M. (2013). Impact of process parameters in the generation of novel aspirin nanoemulsions – Comparative studies between ultrasound cavitation and microfluidizer. *Ultrasonics Sonochemistry*, 20(1), 485–497.
- Tjøtta, S. (1999). Theoretical Investigation of Heat and Streaming Generated by High Intensity Ultrasound. *Acustica*, 85, 780–787.
- Trujillo, F. J., & Knoerzer, K. (2011a). A computational modeling approach of the jet-like acoustic streaming and heat generation induced by low frequency high power ultrasonic horn reactors. *Ultrasonics Sonochemistry*, 18(6), 1263–73.

- Trujillo, F. J., & Knoerzer, K. (2011b). Modelling the acoustic field and streaming induced by an ultrasonic horn sonoreactor. In K. Knoerzer, P. Juliano, P. Roupas, & C. Versteeg (Eds.), *Innovative Food Processing Technologies* (1st ed.). Indianapolis, USA: Wiley and Sons.
- Uluko, H., Zhang, S., Liu, L., Chen, J., Sun, Y., Su, Y., Li, H., Cui, W., & Lv, J. (2013). Effects of microwave and ultrasound pretreatments on enzymolysis of milk protein concentrate with different enzymes. *International Journal of Food Science & Technology*, n/a–n/a.
- Walstra, P., & van Vliet, T. (2003). Chapter II Functional properties. In R. J. H. W.Y. Aalbersberg P. Jaspere, H.H.J. de Jongh, C.G. de Kruif, P. Walstra and F.A. de Wolf BT - Progress in Biotechnology (Ed.), *Industrial Proteins in Perspective* (Vol. Volume 23, pp. 9–30). Elsevier.
- Westervelt, P. J. (1953). The Theory of Steady Rotational Flow Generated by a Sound Field. *The Journal of the Acoustical Society of America*, 25(1), 60.
- YanJun, S., Jianhang, C., Shuwen, Z., Hongjuan, L., Jing, L., Lu, L., Uloko, H., Yangling, S., Wenming, C., Wupeng, G., & Jiaping, L. (2014). Effect of power ultrasound pretreatment on the physical and functional properties of reconstituted milk protein concentrate. *Journal of Food Engineering*, 124(0), 11–18.
- Zarembo, L. K. (1971). Acoustic Streaming. In L. D. Rozenberg (Ed.), *High Intensity Ultrasonic Fields* (1st ed.). London: Plenum Press.
- Zhang, H., Claver, I. P., Zhu, K.-X., & Zhou, H. (2011). The Effect of Ultrasound on the Functional Properties of Wheat Gluten. *Molecules*, 16(12), 4231–4240.
- Zisu, B., Bhaskaracharya, R., Kentish, S., & Ashokkumar, M. (2010). Ultrasonic processing of dairy systems in large scale reactors. *Ultrasonics Sonochemistry*, 17(6), 1075–81.

***Chapter 3. The Effect of Ultrasound Treatment
on the Structural, Physical and Emulsifying
Properties of Dairy Proteins***

Data and discussions contained within this chapter have been published within:

O'Sullivan, J.J., Arellano, M., Pichot, R. and Norton, I.T. 2014. The effect of ultrasound treatment on the structural, physical and emulsifying properties of dairy proteins. *Food Hydrocolloids*, **42(3)**, 386-396.

Data and discussions contained within this chapter have been in part published within:

O'Sullivan, J.J., Pichot, R. and Norton, I.T. 2014. Protein stabilised submicron emulsions, *Gums and stabilisers for the food industry*, **17**, 223 – 229.

3.1. Abstract

The effect of ultrasound treatment on the structural, physical and emulsifying properties of three dairy proteins: sodium caseinate (NaCas), whey protein isolate (WPI) and milk protein isolate (MPI) was investigated. The pH of untreated NaCas, WPI and MPI solutions was 7.1, 6.8 and 6.7, respectively. Protein solutions were sonicated for 2 min at a frequency of 20 kHz and with a power intensity of $\sim 34 \text{ W cm}^{-2}$. The structural and physical properties of dairy proteins were studied in terms of changes in protein size, molecular structure and hydrodynamic volume using DLS, SDS-PAGE and intrinsic viscosity, respectively. The emulsifying properties of the sonicated proteins were compared to untreated proteins and Tween 80. Ultrasound treatment reduced the size and hydrodynamic volume of the proteins, while there was no measurable reduction in molecular weight. Emulsions prepared with untreated NaCas and WPI had submicron sized droplets ($\sim 120 \text{ nm}$), whilst emulsions produced with untreated MPI and Tween 80 had micron sized droplets ($> 1 \mu\text{m}$) at lower concentrations studied.

Unexpectedly, emulsions produced with ultrasound treated NaCas and WPI had the same droplet sizes as the untreated proteins at all concentrations, despite the reduction in protein size of the sonicated proteins. Emulsions prepared with sonicated MPI at concentrations $\leq 1 \text{ wt. \%}$ had smaller droplet sizes than the emulsions produced with untreated MPI. This effect was consistent with the observed decrease in interfacial tension for ultrasound treated MPI, which will facilitate droplet break-up during emulsification.

3.2. Introduction

Proteins are highly functional molecules that are widely used in the pharmaceutical and food industries, having a wide range of applications. Proteins are of particular interest in food systems in terms of their emulsifying properties, due to their abilities to adsorb at oil-water interfaces and to form interfacial films (Foegeding & Davis, 2011; Lam & Nickerson, 2013). The surface activity of proteins is due to their amphiphilic nature, owing to the presence of both hydrophilic and hydrophobic groups in their molecular structure (Beverung *et al.*, 1999). Due to their bulky structure, proteins diffuse slowly to the interface, in comparison to low molecular weight emulsifiers, such as Tween 80 which diffuse more rapidly (McClements, 2005). Once at the interface, proteins undergo conformational changes (*i.e.* surface denaturation) and with a thermodynamically driven rearrangement tending to align hydrophobic amino acids within the oil phase and hydrophilic amino acids within the aqueous phase (McClements, 2004; Walstra & van Vliet, 2003), the effect of which reduces the interfacial tension and the overall free energy of the system (McClements, 2004). One particular advantage of proteins is that protein-protein interactions at the interface, subsequently leading to the formation of strong viscoelastic films that are more resistant to coalescence and provide both electrostatic or steric stabilisation (Lam & Nickerson, 2013; McClements, 2004). Therefore, it is of great interest for the food industry, to investigate methodologies that are capable of enhancing the emulsifying properties of proteins.

In recent years, low frequency, high energy ultrasound (*i.e.* frequency \leq 100 kHz, power intensity 10 – 100 W cm⁻²) has been used in the food industry to modify the functional properties of proteins. The effect of ultrasound on the physicochemical properties of the treated molecules is related to cavitation (rapid formation and collapse of gas bubbles), which is generated by highly localized changes in pressure (up to 50 MPa) and heat (up to 5000 °C), occurring during very short periods of time (O'Donnell *et al.*, 2010). High shear forces and

turbulence resulting from these cavitations, also contribute to the observed effects of ultrasound (O'Donnell *et al.*, 2010).

The application of ultrasound to proteins has been related to effects on the structural and functional properties of whey protein concentrates (Güzey *et al.*, 2006), soybean proteins (Arzeni *et al.*, 2012; Jambrak *et al.*, 2009; Karki *et al.*, 2010), and egg white proteins (Arzeni *et al.*, 2012; Krise, 2011). Arzeni *et al.*, (2012) studied the influence of ultrasound on the structural properties of whey protein concentrate (WPC), soy protein isolate (SPI) and egg white protein (EWP). They observed a significant reduction of the protein size for WPI and SPI. Guzey & Weiss, (2001) investigated the effect of high-intensity ultrasonic processing on the surface activity of bovine serum albumin (BSA) and WPI. It was reported that ultrasound treatment significantly improved the emulsifying properties of BSA and WPI.

However, there are contradictory reports on the effect of ultrasound on the molecular weight of proteins. For example, ultrasound treatment at 20 and 40 kHz for 30 min resulted in a significant decrease in molecular weight for WPC, WPI (Jambrak *et al.*, 2014) and α -lactalbumin (Jambrak *et al.*, 2010). Whereas, sonication at 20 kHz for 30 min with varying power intensities was reported to have no significant effect on the molecular weight of SPI (Jambrak *et al.*, 2010). In addition, no significant changes in molecular weight were reported for EWP treated with ultrasound at 55 kHz for 12 min (Hu *et al.*, 2013; Karki *et al.*, 2010). Therefore, it is necessary to further investigate the effects of ultrasound on the structural and functional properties of food proteins.

Sodium caseinate (NaCas) is a functional ingredient widely used in the food industry. This protein is used as an emulsifier in a wide range of food applications, including coffee creamers, infant formulas, soups and processed meat (O'Connell & Flynn, 2007). NaCas is a composite mixture of four protein fractions: α_{s1} -, α_{s2} -, β - and κ -caseins (O'Connell *et al.*, 2003). In solution, these caseins are prone to form spherical colloidal associations, or

micelles, due to regions of high hydrophobicity and the charge distribution arising from the amino acid sequence, phosphorylation and glycosylation (Srinivasan *et al.*, 2002). The internal structure of the casein micelle is constituted of the calcium sensitive protein fractions (α_{s1-} , and α_{s2-}), which are held together by cohesive hydrophobic interactions and calcium-phosphoserine crosslinks. The micelle is stabilised by κ -casein which is predominately found at the micelle surface due to its highly hydrophilic C-terminal protruding into the aqueous phase. β -casein exists in a temperature dependant equilibrium between the aqueous phase and the micelle (O'Regan *et al.*, 2009).

Whey protein isolate (WPI) is a nutritional ingredient used in the food industry because of its desirable functional properties, such as emulsification, gelation and foaming (Dalglish, 2011; O'Connell & Flynn, 2007). The main protein fractions in WPI are β -lactoglobulin (β -lg), α -lactalbumin (α -lac) and bovine serum albumin (BSA). Whey proteins have globular conformations. β -lg contains five cysteine residues, four of which occur as intra-molecular disulfide cross-links and one as a free thiol group (-SH). α -lac is a calcium metalloprotein that has four intra-molecular disulphide cross-links. The binding of calcium is essential for proper folding and disulphide bond formation of α -lactalbumin (O'Regan *et al.*, 2009). BSA is stabilised to a great extent by its 17 cysteine disulphide bonds (O'Regan *et al.*, 2009). Milk protein isolate (MPI) is a mixture of micellar casein (~80 %) and whey (~20 %) (Nakamura *et al.*, 1997). The casein in MPI has a micellar structure similar to the native form found in milk, and the whey proteins are present in the globular native form (Fox, 2008).

In the present work, analyses were carried out on commercially available dairy proteins widely used in the food industry, in order to assess the industrial relevance of ultrasound treatment on composite mixtures of food protein systems. The objective of this research was to understand the effects of ultrasound treatment on the structural and physical properties of three dairy proteins: sodium caseinate (NaCas), whey protein isolate (WPI) and

milk protein isolate (MPI). Changes in the structural and physical properties of the proteins were measured in terms of protein size, molecular structure and intrinsic viscosity. Moreover, it was investigated whether the proteins treated by ultrasound have the ability to increase the stability of oil-in-water emulsions against coalescence. Oil-in-water emulsions were prepared with either untreated or ultrasound treated NaCas, WPI and MPI at different concentrations and compared between them and to a low molecular weight emulsifier, Tween 80.

3.3. Materials and methodology

3.3.1. Materials

Acid casein (KerrynorTM A290), whey protein isolate (W994) and milk protein isolate (UltramorTM 9075) were all kindly provided by Kerry Ingredients (Listowel, Ireland). The composition of the three dairy proteins is provided in Table 3.1. Tween 80 and sodium azide were purchased from Sigma Aldrich (UK). The oil used in this study was commercially available rapeseed oil. The water used in all experiments was passed through a double distillation unit (Aquatron A4000D). All materials were used with no further purification or modification of their properties.

Table 3.1. Composition of acid casein, whey protein isolate (WPI) and milk protein isolate (MPI).

	Acid Casein	WPI	MPI
Protein (wt. %)	86	91	86
Moisture (wt. %)	10	4	4
Fat (wt. %)	1	1	1.5
Lactose (wt. %)	0.1	0.5	1
Calcium (wt. %)	0.06	0.5	1.7
Sodium (wt. %)	0.06	0.1	0.08
Potassium (wt. %)	0.13	0.15	0.35
Phosphorus (wt. %)	0.7	0.65	1.1
Magnesium (wt. %)	0.01	0.02	0.08

3.3.2. Methods

3.3.2.1. Preparation of untreated protein solutions

Sodium Caseinate (NaCas) was prepared from acid casein using the method outlined by (O'Connell & Flynn, 2007). NaCas, WPI and MPI were dispersed in water to obtain solutions at concentrations within the range of 0.1 – 5 wt. %. All proteins were completely soluble at this range of concentrations. The pH of untreated NaCas, WPI and MPI at a concentration of 1 wt. % was 7.1, 6.8 and 6.7, respectively. Sodium azide (0.02 wt. %) was added to the solutions as an anti-microbial agent.

3.3.2.2. Ultrasound treatment of protein solutions

An ultrasonic processor (Viber Cell 750, Sonics, USA) with a 12 mm diameter probe in stainless steel was used to sonicate NaCas, WPI and MPI solutions at concentrations of 0.1 - 5 wt. %. 50 ml of protein solution were sonicated in 100 ml glass beakers, which were placed in an ice bath to reduce heat gain. The protein solutions were sonicated for up to 2 min with a frequency of 20 kHz and maximum amplitude of 95 % (ultrasonic wave of 108 μm). This power setting yielded an ultrasonic intensity of $\sim 34 \text{ W cm}^{-2}$, which was determined calorimetrically by measuring the temperature rise of the sample as a function of treatment time, under adiabatic conditions. The acoustic power, P (W), was calculated as follows (Margulis & Margulis, 2003):

$$P = m c_p \left(\frac{dT}{dt} \right) \quad (3.1)$$

where m is the mass of ultrasound treated solution (g), c_p is the specific heat of the material (J/gK) and dT/dt is the rate of temperature change with respect to time, starting at $t = 0$.

The temperature of the protein solutions was measured before and after ultrasound treatment by means of a digital thermometer (TGST3, Sensor-Tech Ltd., Ireland), with an

accuracy of ± 0.1 °C. After sonication treatment, the temperature of all protein solutions was raised to approximately ~ 45 °C.

3.3.2.3. Characterisation of untreated and ultrasound treated proteins

3.3.2.3.1. pH measurements

The pH of the protein solutions was measured before and after ultrasound treatment. pH measurements were made by using a pH meter (SevenEasy, Mettler Toledo, UK). This instrument was calibrated with standard solutions of known pH. The pH values are reported as the mean and the standard deviation of three replicates.

3.3.2.3.2. Microstructure characterisation

The size of untreated and ultrasound treated proteins was measured by dynamic light scattering using a Zetasizer Nano Series (Malvern Instruments, UK), at a protein concentration of 0.1 wt. %. Protein associate size values are reported as Z-average (D_z), that is expressed as the intensity based harmonic mean (2,3) ($D_z = \Sigma S_i / \Sigma (S_i/D_i)$), where S_i is the scattering intensity from a given particle i and D_i is the diameter of the particle i .

The width of the protein size distribution was expressed in terms of span ($Span = D_{v0.9} - D_{v0.1} / D_{v0.5}$), where $D_{v0.9}$, $D_{v0.1}$, and $D_{v0.5}$ are the equivalent volume diameters at 90, 10 and 50 % cumulative volume, respectively. Small span values indicate a narrow protein size distribution. Protein aggregate size and span values are reported as the average and the standard deviation of three replicates.

3.3.2.3.3. Microstructure visualisation

Cryogenic scanning electron microscopy (Cryo-SEM, Philips XL30 FEG ESSEM) was used to visualise the microstructure of untreated and ultrasound treated proteins. One drop of protein solution was frozen to -198 °C in liquid nitrogen. Samples were then fractured at -180

°C and etched for 5 min at -90 °C inside a cryo preparation chamber, the process by which ice is sublimed. Afterwards, samples were coated with gold and scanned at -160 °C.

3.3.2.3.4. Molecular structure characterisation

The molecular structure of untreated and ultrasound treated proteins was determined by sodium dodecyl sulphate polyacrylamide gel electrophoresis (SDS-PAGE), using a Mini-Protean 3 Electrophoresis System (Bio-Rad, UK). 100 µl of protein solution at 1 wt. % concentration were added to 1 ml of native sample buffer (Bio-Rad, UK) in 2 ml micro tubes and sealed. A 10 µl aliquot was taken from each sample and loaded onto a Tris-acrylamide gel (Bio-Rad, UK; 4-20% Mini Protean TGX Gel, 10 wells). A protein standard (Bio-Rad, UK; Precision Plus Protein™ All Blue Standards) was used to determine the molecular weight of the samples. Gel electrophoresis was carried out initially at 55 V (I > 20 mA) for 10 min, then at 155 V (I > 55 mA) for 45 min in a running buffer (Bio-Rad, UK; 10x Tris/Glycine/SDS Buffer). The gels were removed from the gel cassette and stained with Coomassie Bio-safe stain (Bio-Rad, UK) for 1 hr and de-stained with distilled water overnight.

3.3.2.3.5. Intrinsic viscosity measurements

The intrinsic viscosity of untreated and ultrasound treated proteins was determined by a double extrapolation to an infinite dilution method, as described by (Morris *et al.*, 1981), using the models of Huggins and Kraemer, as follows:

$$\text{Huggins (Huggins, 1942): } \eta_{sp}/c = [\eta] + k_H[\eta]^2c \quad (3.2)$$

$$\text{Kraemer (Kraemer, 1938): } \ln \eta_{sp}/c = [\eta] + k_K[\eta]^2c \quad (3.3)$$

where η_{sp} is the specific viscosity (viscosity of the solvent, η_0 / viscosity of the solution, η), c the protein concentration (w/v%), $[\eta]$ the intrinsic viscosity (dL/g), k_H the Huggins constant. η_{rel} is the relative viscosity (viscosity of the solution, η / viscosity of the solvent, η_0) and k_K is the Kraemer constant.

The concentration ranges used for the determination of the intrinsic viscosity of NaCas, WPI and MPI were 0.25 – 0.45 wt. %, 1 – 2.5 wt. % and 0.5 – 2 wt. %, respectively. The validity of the regression procedure is confined within a discrete range of η_{rel} , $1.2 < \eta_{rel} < 2$. The upper limit is due to the hydrodynamic interaction between protein molecules, and the lower limit is due to inaccuracy in the determination of very low viscosity fluids. A value of η_{rel} approaching to 1 indicates the lower limit (Morris *et al.*, 1981).

The viscosity of the protein solutions was measured at 20 °C using a Kinexus rheometer (Malvern Instruments, UK) equipped with a double gap geometry (25 mm diameter, 40 mm height). As reported by (Morris *et al.*, 1981), in order to derive the intrinsic viscosity by extrapolation to infinite dilution, there must be linearity between shear stress and shear rate, which indicates a Newtonian behaviour region on the range of shear rate used in the measurements. The Newtonian plateau region of the NaCas, WPI and MPI solutions at the range of concentrations used, was found within a shear rate range of 25 - 1000 s⁻¹. Thus, the values of viscosity of the protein solutions and that of the solvent (distilled water) were selected from the flow curves data at a constant shear rate of 250 s⁻¹ (within the Newtonian region), which were subsequently used to determine the specific viscosity, η_{sp} , the relative viscosity, η_{rel} , and the intrinsic viscosity, $[\eta]$. At least three replicates of each measurement were made.

3.3.2.4. Preparation of oil-in-water emulsions

10 wt. % of dispersed phase (rapeseed oil) was added to the continuous aqueous phase containing either untreated or sonicated proteins or Tween 80 at different concentrations, ranging from 0.1 to 5 wt. %. This mixture was emulsified first at 8000 rpm for 2 min using a high shear mixer (SL2T, Silverson, UK) to form an oil-in-water pre-emulsion. Afterwards, oil-in-water submicron emulsions were prepared by further emulsifying the pre-emulsion using a high-pressure valve homogeniser (Panda NS 1001L-2K, GEA Niro Soavi, UK) at 125 MPa for 2 passes. The emulsions were prepared at 20 °C in a controlled temperature laboratory.

3.3.2.5. Characterisation of oil-in-water emulsions.

3.3.2.5.1. Droplet size measurements

The droplet size of the emulsions was measured by using laser diffraction (Hydro 2000SM, Mastersizer 2000, Malvern Instruments, UK) immediately after emulsification. Emulsion droplet size values are reported as the volume-surface mean diameter ($d_{3,2} = \Sigma n_i d_i^3 / \Sigma n_i d_i^2$), where n_i is the number of droplets of diameter d_i . The stability of the emulsions was assessed by droplet size measurements over 28 days. The emulsions were stored under refrigerated conditions (4 °C) throughout the duration of the stability study. The droplet size values and the error bars are reported as the mean and the standard deviation, respectively, of three replicates.

3.3.2.5.2. Interfacial tension measurements

The interfacial tension between the aqueous phase (pure water, protein solutions and low molecular weight surfactant solutions) and oil phase (rapeseed oil) was measured using a tensiometer K100 (Krüss, Germany) with the Wilhelmy plate method. The Wilhelmy plate is

made of platinum, of a length, width and thickness of 19.9 mm, 10 mm and 0.2 mm, respectively. The Wilhelmy plate was immersed in 20 g of aqueous phase to a depth of 3 mm with a surface detection speed of 15 mm/min. The surface detection is the speed of the vessel drive used for the detection of the liquid surface. Once the surface has been detected by the microbalance in the tensiometer the vessel moves at the chosen surface detection speed to the position specified by the immersion depth (3 mm). Subsequently, an interface between the aqueous phase and oil phase was created by carefully pipetting 50 g of the oil phase over the aqueous phase. The test was conducted over 3,600 s and the temperature was maintained at 20 °C throughout the duration of the test. The interfacial tension values and the error bars are reported as the mean and the standard deviation, respectively, of three replicates.

3.3.3. Statistical analysis

Student's t-test, a statistical hypothesis test, with a 95 % confidence interval was used to assess the significance of the results obtained. t-test data with $P < 0.05$ were considered statistically significant.

3.4. Results and discussions

3.4.1. Effect of ultrasound treatment on the structural and physical properties of NaCas, WPI and MPI

The effect of time of ultrasound treatment on the size and pH of NaCas, WPI and MPI was initially investigated. Protein solutions at concentration of 0.1 wt. % were sonicated for 15, 30, 60, and 120 s, with a frequency of 20 kHz and maximum amplitude of 95%. Protein size and pH measurements as a function of sonication time, for untreated and sonicated NaCas, WPI and MPI are shown in Table 3.2. As can be seen from results in Table 3.2, there is a significant reduction ($P < 0.05$) in the size of all proteins with the increase in the

sonication time. The results also indicate that after 1 min of ultrasound treatment there is no further reduction in protein size for NaCas, WPI and MPI. This decrease in protein size is suggested to be due to the breakdown of the untreated protein aggregates caused by disruption of associative electrostatic and hydrophobic interactions, induced by the high shear forces originating from ultrasonic cavitations (O'Brien, 2007). It can also be seen (*cf.* Table 3.2), that the pH of all the protein solutions decreased significantly ($P < 0.05$) as the time of ultrasound treatment increased. Furthermore, after 1 min of sonication the pH of all the proteins solutions was not further decreased. The reduction in the pH of the proteins can be due to the exposure of acidic amino acid residues (Sakurai *et al.*, 2009) which were contained within the aggregated structure of the protein micelles prior to sonication. The size of proteins after a 2 min sonication time represents aggregates rather than discrete protein molecules, as, for example, the hydrodynamic radius of sodium caseinate is ~ 8 nm (O'Connell & Flynn, 2007).

Table 3.2. Effect of sonication time on pH and protein size (D_z) of NaCas, WPI and MPI solutions at a concentration of 0.1 wt. %. The standard deviation for all pH measurements was < 0.04 in all cases.

Time (s)	D_z (nm)			pH (-)		
	NaCas	WPI	MPI	NaCas	WPI	MPI
0	245 \pm 12	433 \pm 11	956 \pm 48	7.15	6.82	6.74
15	164 \pm 6	291 \pm 7	338 \pm 5	7.07	6.72	6.66
30	113 \pm 5	152 \pm 15	299 \pm 15	7.03	6.62	6.58
60	60 \pm 5	75 \pm 11	247 \pm 12	6.95	6.57	6.53
120	58 \pm 4	72 \pm 9	256 \pm 6	6.95	6.56	6.51

The stability over time of the protein size and width of the protein size distribution (span) of ultrasound treated NaCas, WPI and MPI were also investigated. Protein solutions at

concentration of 0.1 wt. % were sonicated for 2 min at 20 kHz and $\sim 34 \text{ W cm}^{-2}$, since after 1 minute of sonication there was no further decrease in the size of protein (*cf.* Table 3.2). The aggregate size of the ultrasound treated proteins was measured immediately after sonication and after 1 and 7 days, in order to assess the stability of micelle size. Protein size measurements and span values obtained by dynamic light scattering for untreated and sonicated NaCas, WPI and MPI are shown in Table 3.3.

Table 3.3. Average protein size (D_z) and span of untreated and ultrasound treated NaCas, MPI and WPI at a concentration of 0.1 wt. %.

Protein type	Untreated		Ultrasound treated					
	D_z (nm)	Span (-)	D_z (nm)			Span (-)		
			Day 0	Day 1	Day 7	Day 0	Day 1	Day 7
NaCas	245 ± 12	10.45 ± 0.31	58 ± 4	145 ± 2	166 ± 4	0.33 ± 0.04	0.72 ± 0.06	0.95 ± 0.02
WPI	433 ± 11	1.93 ± 0.24	72 ± 9	189 ± 8	210 ± 2	0.33 ± 0.07	0.66 ± 0.03	0.85 ± 0.08
MPI	956 ± 48	3.84 ± 0.43	256 ± 6	250 ± 14	242 ± 5	1.72 ± 0.09	1.68 ± 0.11	1.34 ± 0.17

As can be seen from Table 3.3, the ultrasound treatment produced a significant reduction ($P < 0.05$) in the size of NaCas and narrowed the protein size distribution. However, on day 7 after ultrasound treatment an increase in size of NaCas can be observed and the width of the size distribution slightly increases. Thus, the ultrasound treatment applied to NaCas induced an effective micelle size reduction of 32 % on day 7. A similar behaviour can be seen for WPI (*cf.* Table 3.3), which results showed a significant size reduction ($P < 0.05$) and narrowing of the protein size distribution after ultrasound treatment, and on day 7 a slight increase in the width of the distribution and an increase in size, representing an effective micelle size reduction of 50 %.

In the case of MPI, results in Table 3.3 showed that ultrasound treatment caused a significant decrease in size ($P < 0.05$) and narrowed the protein size distribution. It can also

be seen that on day 7, the width of the protein size distribution was slightly narrower and the protein aggregate size slightly decreased further, representing an effective size reduction of 75 %. These results are in agreement with those of Jambrak *et al.*, (2014), which showed a significant reduction in WPI associate size after an ultrasound treatment of 15 min at 20 kHz and $\sim 48 \text{ W cm}^{-2}$. Yanjun *et al.*, (2014) also observed a decrease in particle size for MPC treated by ultrasound at 12.5 W and 50 % amplitude for 2 min.

The reason for the observed decrease in size for NaCas and WPI is suggested to relate to a structural disruption in the untreated protein aggregates associated with the cleavage of hydrophobic interactions between the proteins fractions, likely induced by the high shear forces and turbulence resulting from cavitation. The subsequent size increase observed in NaCas and WPI on day 7 after sonication is thought to be due to a reorganisation of the proteins into smaller sub-associates due to non-covalent molecular interactions such as electrostatic and hydrophobic interactions. In the case of MPI, the observed reduction in micelle size is presumably due to ultrasonic cavitation effects, which break up the aggregates of proteins and reduce their size. In order to test these hypotheses, cryo-SEM micrographs were captured of untreated and 7 days after ultrasound treatment of NaCas, MPI and WPI solutions at 1 wt. % for all proteins tested (*cf.* Fig. 3.1).

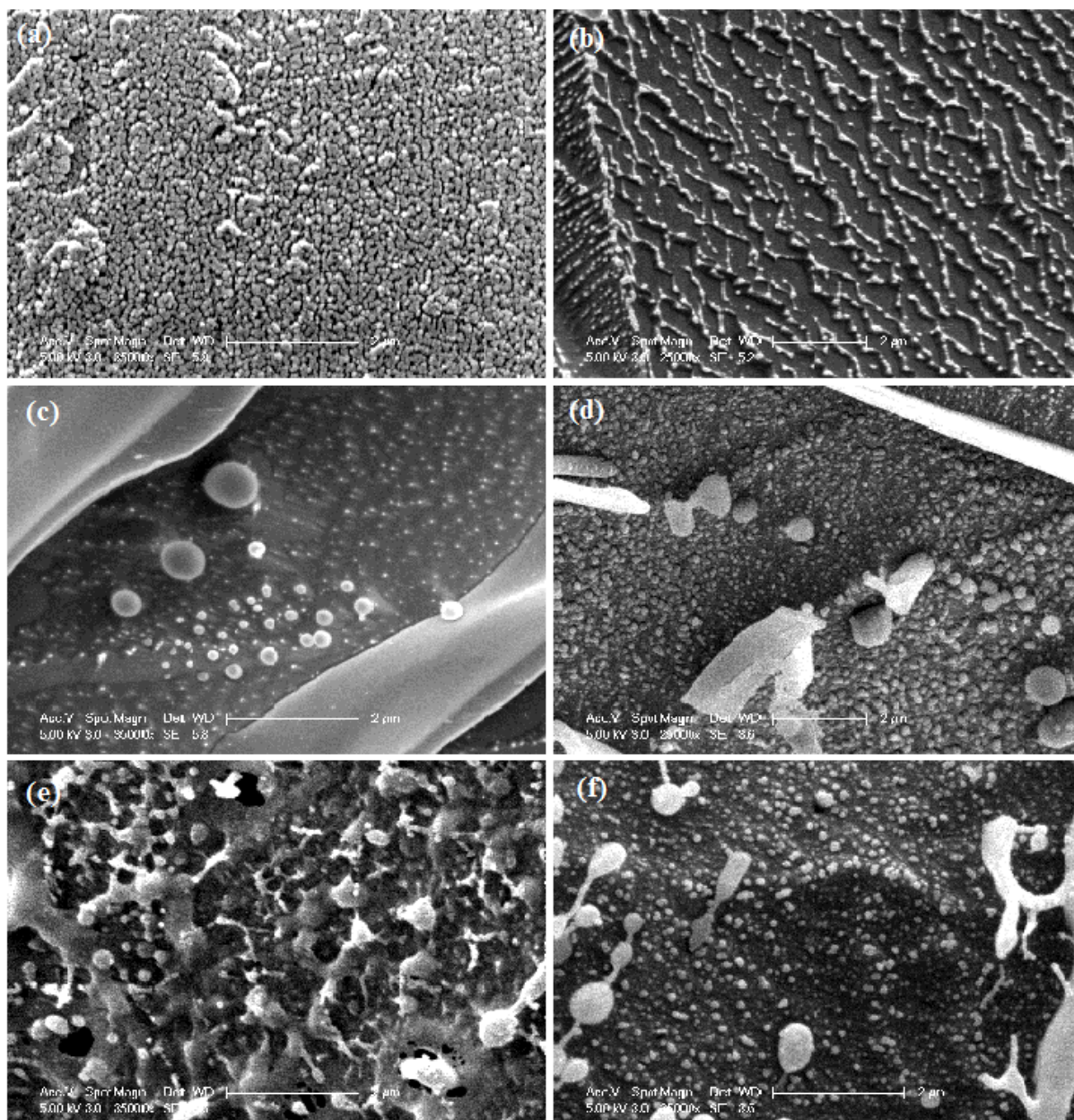


Fig. 3.1. Cryo-SEM micrographs of protein solutions: (a) 1 wt. % Untreated NaCas solution, (b) 1 wt. % Ultrasound treated NaCas solution, (c) 1 wt. % Untreated WPI solution, (d) 1 wt. % Ultrasound treated WPI, (e) 1 wt. % Untreated MPI solution and (f) 1 wt. % Ultrasound treated MPI. Scale bar is 2 µm in all cases.

As can be seen in Fig. 3.1, the untreated aggregates of NaCas in solution (Fig 3.1a) appear to be distributed within a densely packed network and to have a polydisperse protein size; whereas the NaCas treated by ultrasound (*cf.* Fig. 3.1b) appear to be distributed into discrete entities, having a smaller and a slightly more uniform size in comparison to the untreated aggregates of NaCas. The structure of untreated WPI in solution (*cf.* Fig. 3.1c)

appears to have a highly polydisperse size distribution, these micelles also appear to be distributed within a packed network; whilst for the sonicated WPI (*cf.* Fig. 3.1d) a clear reduction in the size can be seen and the size distribution is monodisperse. Additionally, the sonicated WPI micelles appear to be more evenly distributed and separated from each another, in comparison to their untreated counterparts. In the case of untreated MPI in solution (*cf.* Fig. 3.1e), large discrete polydisperse protein micelles can be distinguished; whereas the MPI micelles treated by ultrasound (*cf.* Fig. 3.1f) appear to be smaller and monodisperse. These findings are consistent with the previously observed reduction in aggregate size of sonicated NaCas, WPI and MPI (*cf.* Table 3.3), and validate the hypothesis that ultrasound treatment causes the disruption of the protein micelles, which then reorganise themselves into smaller sub-associates.

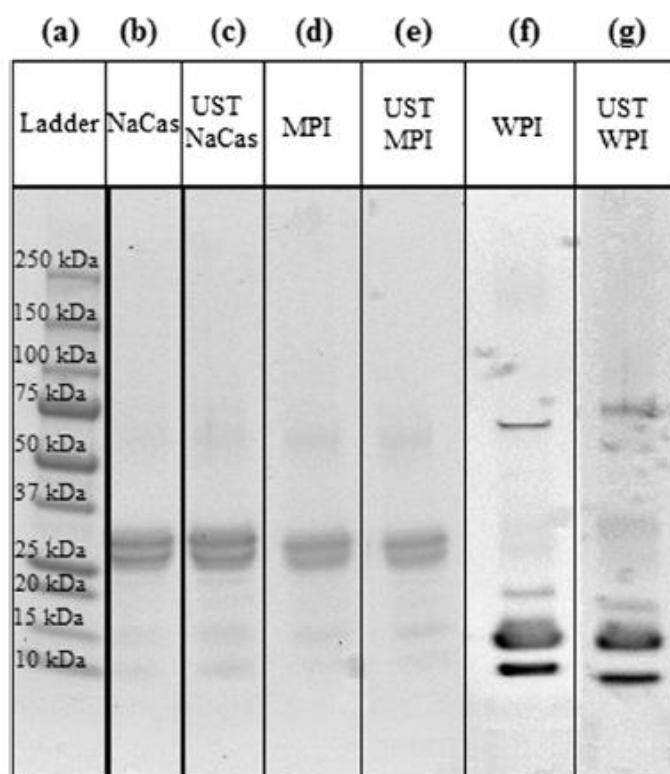


Fig. 3.2. SDS-PAGE electrophoretic profiles of protein solutions: (a) Molecular weight standard (10 kDa – 250 kDa), (b) Untreated NaCas, (c) Ultrasound treated NaCas, (d) Untreated MPI, (e) Ultrasound treated MPI, (f) Untreated WPI and (g) Ultrasound treated WPI.

The molecular structure of untreated and ultrasound treated proteins NaCas, MPI and WPI was subsequently investigated. Proteins solutions at a concentration of 0.1 wt. % were sonicated for 2 min at 20 kHz and $\sim 34 \text{ W cm}^{-2}$, as after 1 minute of sonication there was no further decrease in the size of protein (*cf.* Table 3.2). Electrophoretic profiles obtained by SDS-PAGE for untreated and sonicated NaCas, WPI and MPI are shown in Fig. 3.2. As can be seen from results in Fig. 3.2, no difference in protein fractions between the untreated and ultrasound treated NaCas, WPI and MPI was observed. These results are in agreement with those reported by Gülseren *et al.*, (2007) who showed no differences in molecular weight between untreated and sonicated bovine serum albumin (BSA), treated at 20 kHz, $\sim 20 \text{ W cm}^{-2}$ for 15 min. Yanjun *et al.*, (2014) also observed that ultrasound treatment (12.5 W at 50% amplitude for 2 min) induced no changes in the molecular weight of milk protein concentrate (MPC) solutions. On the other hand, Jambrak *et al.*, (2014) observed a reduction in the molecular weight of WPI and WPC treated by ultrasound (20 kHz, $\sim 48 \text{ W cm}^{-2}$ and 15 min). The difference between these results and those of Jambrak *et al.*, (2014) may have resulted from the different ultrasonic intensity and time of treatment applied to WPI. They used an ultrasound treatment of 15 min and their ultrasound probe provided 35% more ultrasonic intensity to WPI, which may have caused higher shear stress and turbulence effects in their WPI solutions and resulted in the split of the molecular structure of the protein.

The intrinsic viscosity was obtained from the fitting of the Huggins and Kraemer equations to the experimental viscosity data, for the untreated and ultrasound treated NaCas, WPI and MPI in solution at different concentrations, as shown in Fig. 3.3. The values of intrinsic viscosity and Huggins and Kraemer constants for each of the studied proteins are listed in Table 3.4.

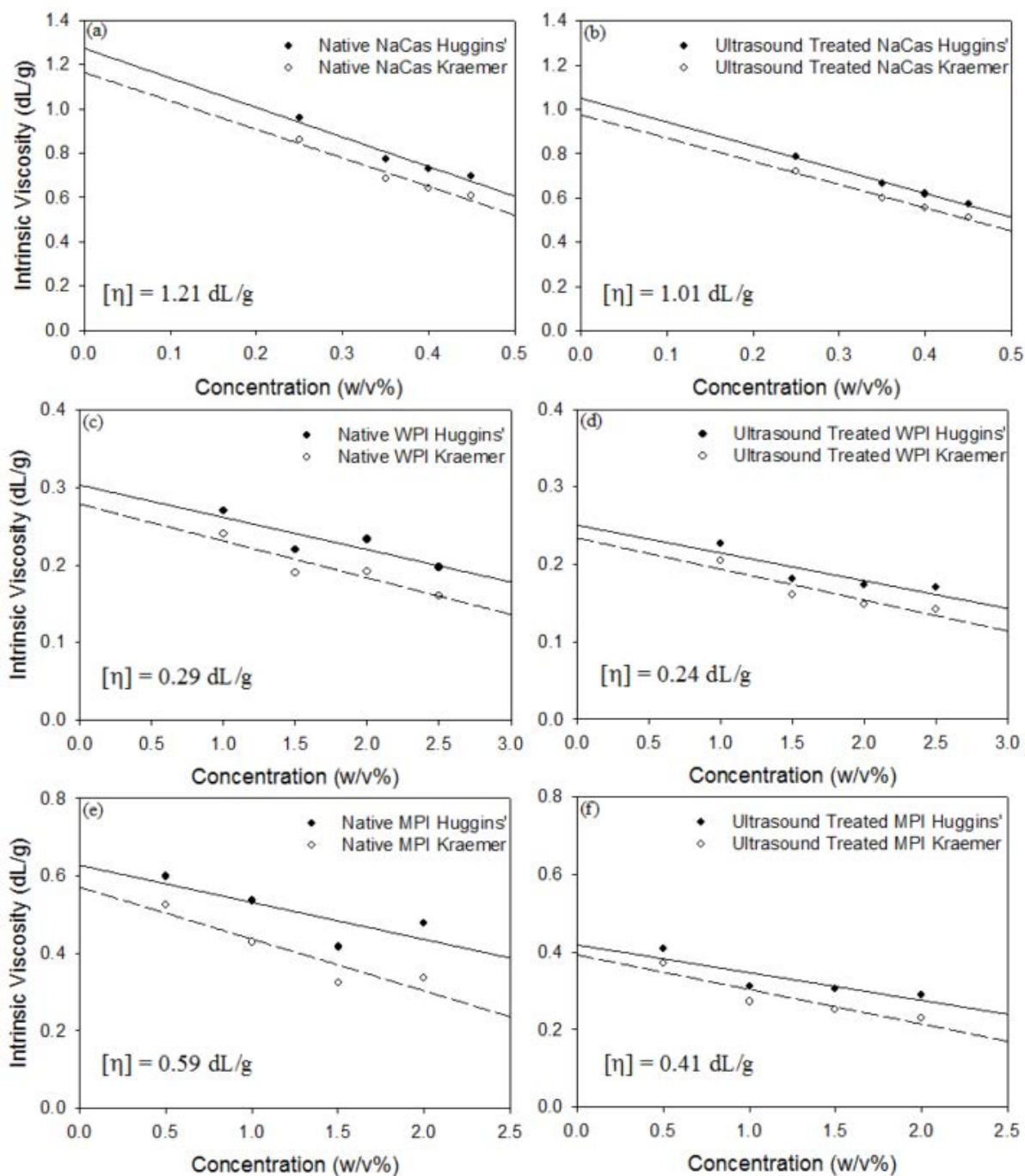


Fig. 3.3. Fitting of the Huggins (●) and Kraemer (○) equations to the viscosity data of the studied protein solutions: (a) Untreated NaCas, (b) Ultrasound treated NaCas, (c) Untreated WPI, (d) Ultrasound treated WPI, (e) Untreated MPI and (f) Ultrasound treated MPI. Average $[\eta]$ values displayed on each plot.

Table 3.4. Intrinsic viscosity ($[\eta]$), Huggins (k_H) and Kraemer (k_K) constants obtained for untreated and ultrasound treated NaCas, WPI and MPI solutions.

Protein in solution	$[\eta]_{\text{Untreated}}$ (dL/g)	$k_{H \text{ Untreated}}$	$k_{K \text{ Untreated}}$	$[\eta]_{\text{Ultrasound}}$ (dL/g)	$k_{H \text{ Ultrasound}}$	$k_{K \text{ Ultrasound}}$
NaCas	1.21 ± 0.02	-1.33	-1.29	1.01 ± 0.03	-1.07	-1.05
WPI	0.29 ± 0.005	-0.042	-0.047	0.24 ± 0.006	-0.036	-0.040
MPI	0.59 ± 0.007	-0.096	-0.134	0.41 ± 0.004	-0.072	-0.089

Intrinsic viscosity, $[\eta]$, measurements provide information about the molecular properties of biopolymers in solution. More specifically, $[\eta]$ reflects the ability of a solvent to hydrate proteins and provides information about the molecular hydrodynamic volume, which is related to the chain conformation of the proteins in solution (Behrouzian *et al.*, 2014). By comparing the obtained values of intrinsic viscosity between the untreated and sonicated dairy proteins (*cf.* Table 3.4), we can see that ultrasound treatment induced a significant reduction ($P < 0.05$) in the intrinsic viscosity of NaCas, WPI and MPI in solution, and thus a significant reduction in the hydrodynamic volume occupied by the proteins and the solvent they entrapped.

These results are also consistent with the reduction in associate size measured by dynamic light scattering (*cf.* Table 3.3) and observed on the cryo-SEM micrographs (*cf.* Fig. 3.1). (Behrouzian *et al.*, 2014) reported intrinsic viscosity values of 0.234 dL/g and 0.514 dL/g for α_{s1} -casein and BSA, respectively. Those values are lower than the results obtained in this work for untreated NaCas, WPI and MPI (*cf.* Table 3.4). These differences may arise due to the complexity of the untreated NaCas, WPI and MPI solutions, which are composed of a mixture of proteins rather than single α_{s1} -casein or BSA used by Lefebvre, (1982). Another possibility is the type of solvent used, which in the work of Lefebvre, (1982) was 6 M guanidine hydrochloride, whilst in the untreated proteins in the present work were dispersed

in serum. High concentrations of guanidine hydrochloride (*i.e.* 6 M) cause protein dissociation, whereby random coil like behaviour is exhibited.

As reported by Tanner & Rha, (1980), the intrinsic viscosity of a protein solution may give a measure of the degree of hydrophobicity of the protein. The intrinsic viscosity of a protein depends on its conformation and thus on its level of hydration, which are a result of the amount of hydrophobic side chains that are buried in the interior of the protein micelles in solution. Khan *et al.*, (2012) also reported that a decrease in intrinsic viscosity can potentially lead to the dehydration of amphiphilic biopolymer micelles, increasing the hydrophobicity of the biopolymer and hence reduced the energy required for the adsorption of amphiphilic biopolymers at the oil-water interface. It can therefore be hypothesised, that the observed reduction in intrinsic viscosity of the proteins induced by the ultrasound treatment (*cf.* Table 3.4), indicates a potential increase in the degree of hydrophobicity of all the investigated proteins, the effect of which is slightly more significant for MPI ($P < 0.041$), followed by NaCas ($P < 0.043$) and WPI ($P < 0.044$).

The Huggins and Kraemer coefficients are adequate to assess the quality of a solvent. Values for the Huggins coefficient (k_H) within a range of 0.25 to 0.5 are attributed to a good solvation, whilst values above 0.5 - 1.0 are related to poor solvents (Delpech & Oliveira, 2005). Similarly, negative values for the Kraemer coefficient (k_K) indicate good solvents and positive values indicate a poor solvation (Delpech & Oliveira, 2005). As can be seen from results in Table 3.4, the values obtained for the Huggins (k_H) and Kraemer (k_K) constants are both negative, which indicate a good solvation considering k_K , but an unusual behaviour in the case of k_H . However, negative values of k_H have also been reported in literature for biopolymers with amphiphilic properties, such as bovine serum albumin dissolved in water (Delpech & Oliveira, 2005), and polydimethylsiloxane–polyurea copolymers dissolved in isopropyl alcohol (Curvale *et al.*, 2008). It is also generally accepted, for hydrocolloids, that

the relation of $k_H + k_K = 0.5$ indicates adequacy of experimental results, given the expected values of k_H and k_K as previously discussed (Yilgor *et al.*, 2006). However, the results presented in Table 3.4 do not yield this value. This effect is thought to be due to the amphiphilic character of the proteins (by comparison to non-amphiphilic polysaccharides) which yields negative values of k_H and k_K . Similar results have been reported in literature for other amphiphilic biopolymers (Curvale *et al.*, 2008; Morris *et al.*, 1981).

3.4.2. Comparison of the emulsifying properties of untreated and ultrasound treated NaCas, WPI and MPI

A series of oil-in-water emulsions were produced with 10 wt. % rapeseed oil and an aqueous continuous phase containing either untreated or ultrasound treated (2 min at 20 kHz, $\sim 34 \text{ W cm}^{-2}$) NaCas, WPI and MPI, or a low molecular weight surfactant, Tween 80 at different concentrations (0.1 - 5 wt. %). The emulsions were passed through a high-pressure valve homogenizer at 125 MPa for 2 passes. Emulsion droplet size measurements obtained by laser diffraction are shown in Fig. 3.4. The emulsion droplet size was measured immediately after emulsification.

Emulsions prepared with untreated and ultrasound treated NaCas and WPI had the same droplet sizes for all the concentrations used, and resulted in similar droplet sizes as those obtained with Tween 80 (*cf.* Fig. 3.4 a & b). This behaviour is unusual, considering the significant aggregate size reduction (increase in surface area-to-volume ratio) observed for sonicated NaCas and WPI (*cf.* Table 3.3), for which it would have been expected to result in a faster adsorption of the proteins at the water-in-oil interface, as reported by (Curvale *et al.*, 2008; Delpech & Oliveira, 2005; Yilgor *et al.*, 2006), and thus lead to a higher reduction in the interfacial tension and to smaller emulsion droplet sizes. Furthermore, the potential increase in the hydrophobicity of the sonicated NaCas and WPI with the decrease in intrinsic viscosity (*cf.* Table 3.4; Khan *et al.*, 2012; Tanner & Rha, 1980) would also be expected to

lead to a faster adsorption of the proteins to the oil-water interface, thus reducing interfacial tension and facilitating droplet break-up. However, it appears that the rate of adsorption to the interface of sonicated NaCas and WPI remains unchanged despite the smaller micelle sizes and higher hydrophobicity obtained, in comparison with untreated NaCas and WPI. Results in Fig. 3.4 a & b also showed that droplet sizes decreased significantly ($P < 0.05$) with the increase in NaCas and WPI concentration, which is in agreement with the results obtained by Srinivasan *et al.*, (2002) for emulsions formed with NaCas, and those measured by Tcholakova *et al.*, (2006) for emulsions containing whey protein concentrate (WPC). The submicron emulsion droplet sizes obtained for both, untreated NaCas and WPI are in agreement with droplet sizes obtained by Dybowska, (2011), in the order of ~120 nm for emulsions containing WPC (3 wt. %), and with those measured by Lee & Norton, (2013), in the order of ~170 nm for emulsions containing NaCas (3 wt. %).

It can also be seen (*cf.* Fig. 3.4) that the obtained emulsion droplet sizes are comparable to the size of untreated proteins (*cf.* Table 3.3). However, it must be considered that the protein size data displayed in Table 3.3 represents aggregates, and not the individual protein fractions composing the micelles. In fact, in solution, proteins form aggregates (micelles) due to electrostatic and hydrophobic interactions (O'Connell *et al.*, 2003). But, in the presence of a hydrophobic dispersed phase (*e.g.* rapeseed oil), the individual protein fractions detach from the bulk micelles and adsorb to the oil-water interface (Beverung *et al.*, 1999; O'Connell & Flynn, 2007). As an example, the size of NaCas discrete molecules has been reported to be ~8 nm (O'Connell & Flynn, 2007; O'Connell *et al.*, 2003), which makes it possible to form the submicron droplets presented in this work.

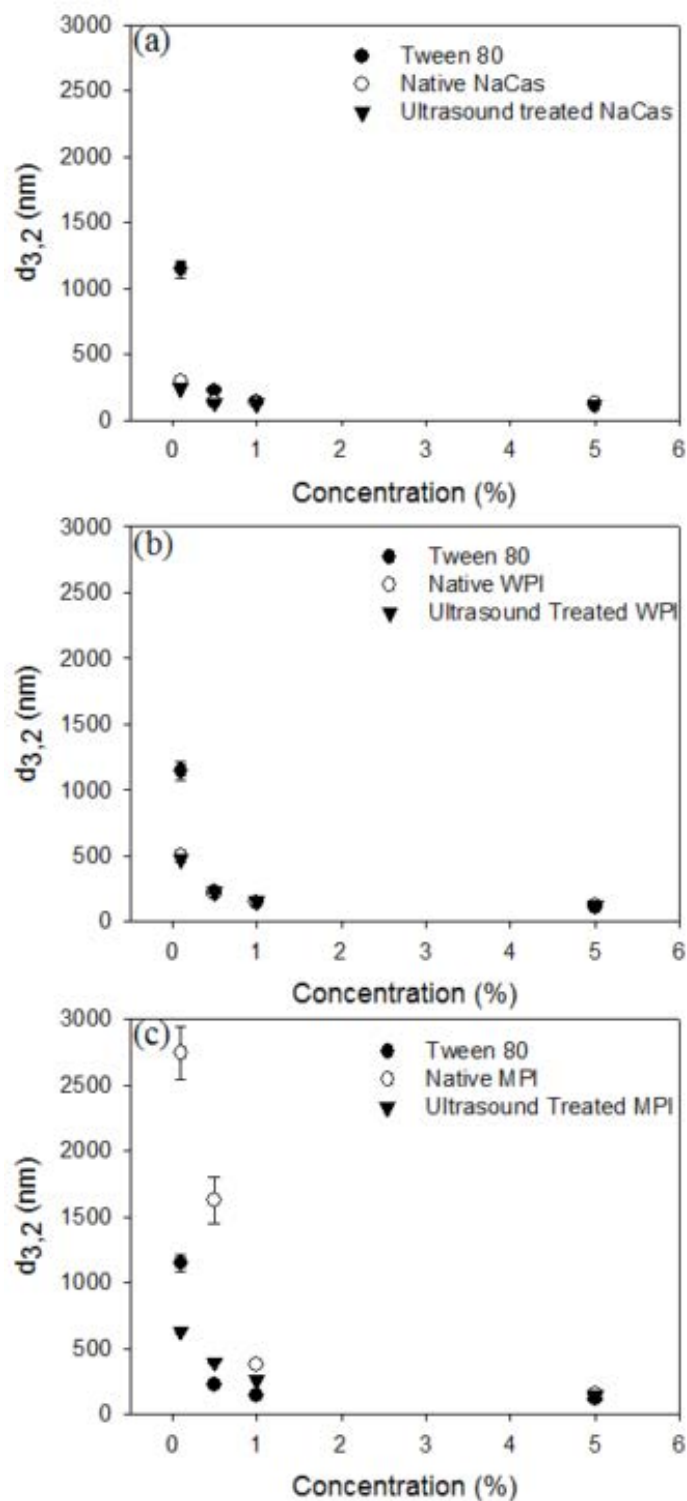


Fig. 3.4. Emulsion droplet size ($d_{3,2}$) as a function of concentrations of: (a) Untreated NaCas, sonicated NaCas and Tween 80, (b) Untreated WPI, sonicated WPI and Tween 80, and (c) Untreated MPI, sonicated MPI and Tween 80.

The results observed in emulsion droplet sizes (*cf.* Fig. 3.4), which were shown to be dependent on the type of emulsifier, can be explained by considering the interfacial tension of the studied systems. Fig. 3.5 presents the interfacial tension between water and oil, obtained for untreated and sonicated NaCas, WPI, MPI, as well as for Tween 80 at 0.1 wt. % concentration. In order to assess the presence of interfacial impurities of the systems, the interfacial tension between pure water and rapeseed oil was measured. As can be seen from Fig. 3.5, the interfacial tension of all systems decreased with time. As a consequence, the decrease in interfacial tension with time is thought to be due to a great extent on the nature of the oil used, and to a lesser extent on the type of emulsifier. As reported by Gaonkar, (1989, 1991), the interfacial tension of commercial vegetable oils against water decreases with time due to the adsorption of surface active impurities, in the oils, at the interface. It was also reported that after purification of the vegetable oils, the time dependency of the interfacial tension is no longer observed (Gaonkar, 1989, 1991).

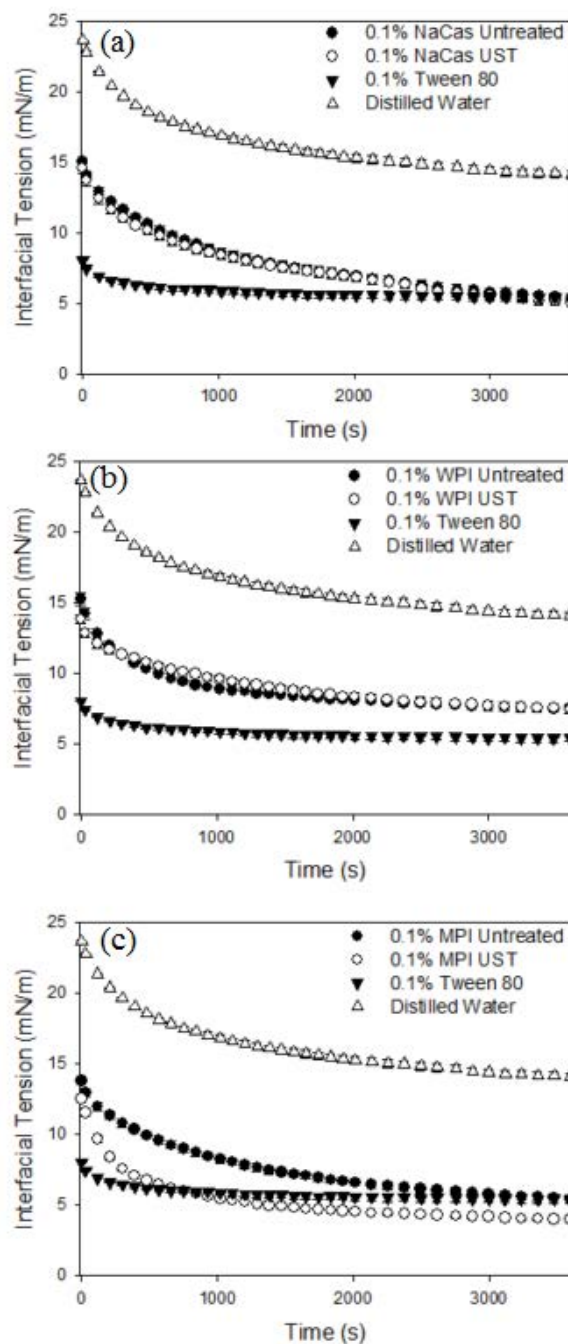


Fig. 3.5. Interfacial tension between water and pure vegetable oil as a function of emulsifier type: (a) Untreated NaCas, sonicated NaCas and Tween 80, (b) Untreated WPI, sonicated WPI and Tween 80 and (c) Untreated MPI, sonicated MPI and Tween 80. The concentration for all emulsifiers was 0.1 wt. %.

As can be seen in Fig. 3.5 a & b, no significant differences ($P > 0.05$) in the obtained values of interfacial tension between the untreated and ultrasound treated NaCas and WPI were observed. These results are consistent with the emulsion droplet sizes seen in Fig. 3.4 a

& b at 0.1 wt. % concentration, and add evidence to the hypothesis that the rate of protein adsorption at the oil-water interface is the same for the untreated and ultrasound treated NaCas and WPI. Results in Fig. 3.5 a & b also showed that lower interfacial values were obtained for Tween 80 than those obtained for untreated and sonicated NaCas and WPI. This effect is likely due to the smaller size and molecular weight of this emulsifier as compared with the bulkier structure of NaCas and WPI. It can also be seen (*cf.* Fig. 3.5 c) that the interfacial tension values obtained for ultrasound treated MPI were significantly lower ($P < 0.05$) than those obtained for untreated MPI, and slightly lower than those obtained with Tween 80. This result is consistent with the obtained emulsion droplet sizes presented in Fig. 3.4 c, and confirms the hypothesis that the micelles of sonicated MPI adsorb faster to the oil-water interface, due to the higher surface area-to volume ratio (*cf.* Table 3.3; smaller protein size) and higher hydrophobicity of these proteins (*cf.* Table 3.4; lower intrinsic viscosity), which significantly reduced the interfacial tension, enhanced oil droplet break-up during emulsification and produced smaller droplet sizes. Furthermore, the compositional differences between MPI and the other investigated dairy proteins, predominately ions, may be a contributing factor to the observed significant reduction ($P < 0.05$) in interfacial tension for ultrasound treated MPI in comparison to untreated MPI.

The stability of the oil-in-water emulsions prepared with untreated and ultrasound treated NaCas, WPI and MPI were investigated during a 28 day period. Emulsions prepared with Tween 80 were also assessed for comparative purposes. Fig. 3.6 shows the evolution of droplet size ($d_{3,2}$) as a function of time for emulsions prepared with untreated and sonicated NaCas, MPI and WPI, as well as with Tween 80 at 1 wt. % concentration.

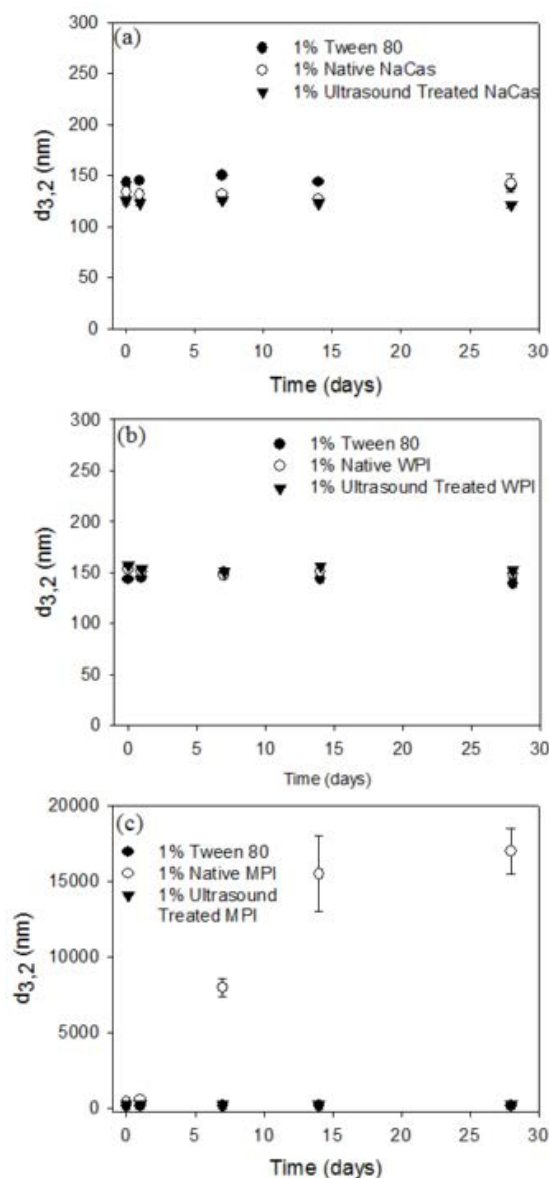


Fig. 3.6. Effect of emulsifier type on droplet size as a function of time for O/W emulsions stabilised by: (a) Untreated NaCas, sonicated NaCas and Tween 80, (b) Untreated WPI, sonicated WPI and Tween 80 and (c) Untreated MPI, sonicated MPI and Tween 80. The concentration for all emulsifiers was 1 wt. %.

Fig. 3.6 a & b show that emulsions prepared with untreated and sonicated NaCas and WPI, as well as with Tween 80 were all stable against coalescence for 28 days. This stability behaviour observed for untreated and ultrasound treated NaCas and WPI was the same for all the concentrations used in this work. In all cases, no oil layer was observed on the upper part of the emulsions over 28 days. In the case of MPI, results in Fig. 3.6 c showed that the emulsions prepared with untreated MPI exhibited coalescence at 1 wt. % concentration, as seen by the

increase in droplet size over time. Coalescence was also observed for emulsions prepared with untreated MPI at 0.1 and 0.5 wt. % concentrations, but the emulsions prepared with untreated MPI at a concentration higher than 1 wt. % were stable for 28 days. A layer of oil was observed at the top of the emulsions which exhibited coalescence. However, it can also be seen (*cf.* Fig. 3.6 c) that the emulsions prepared with ultrasound treated MPI at 1 wt. % concentration were resistant against coalescence over 28 days and had the same stability as the emulsions prepared with Tween 80. This behaviour observed for sonicated MPI was the same for all the concentrations used in this work. This improved stability of the emulsions prepared with sonicated MPI in comparison with untreated MPI is thought to be related to the reduction in micelle size (*i.e.* increase in surface area-to-volume ratio; *cf.* Table 3.3) and to the increase in hydrophobicity (*i.e.* decrease in the intrinsic viscosity; *cf.* Table 3.4) of sonicated MPI as aforementioned. The effect of which results in a faster adsorption of sonicated MPI to the oil-water interface, higher reduction in interfacial tension and thus to smaller droplet sizes.

3.5. Conclusions

This study showed that ultrasound treatment (20 kHz, 34 W cm⁻² for 2 min) of NaCas, WPI and MPI caused a significant ($P < 0.05$) reduction in the protein size and hydrodynamic volume of the proteins. This effect was attributed to the high shear forces resulting from ultrasonic cavitations. However, no differences in molecular weight were observed between untreated and ultrasound treated NaCas, WPI and MPI.

Unexpectedly, the emulsions prepared with ultrasound treated NaCas and WPI had the same submicron droplet sizes as those obtained with their untreated counterparts, and were stable at the same concentrations. These results suggested that ultrasound treatment did not affect significantly the rate at which protein adsorption occurs at the interface, since no significant ($P > 0.05$) changes in interfacial tension were observed between the untreated and

sonicated NaCas and WPI. In contrast, the emulsions prepared with sonicated MPI at concentrations ≤ 1 wt. % had smaller droplet sizes than those obtained with untreated MPI at the same concentrations. This effect was explained by the significant reduction in micelle size (*i.e.* an increase in surface area-to-volume ratio) and increase in hydrophobicity (reflected by the decrease in intrinsic viscosity) of ultrasound treated MPI. These effects led to a faster adsorption of the protein to the oil-water interface, significantly reduced the interfacial tension and thus facilitated droplet break-up during emulsification. In addition, the emulsions prepared with ultrasound treated MPI were stable against coalescence for 28 days at all the concentrations tested, whereas the emulsions produced with untreated MPI showed coalescence 7 days after emulsification at concentrations ≤ 1 wt. %.

3.6. References

- Arzeni, C., Martínez, K., Zema, P., Arias, A., Pérez, O. E., & Pilosof, A. M. R. (2012). Comparative study of high intensity ultrasound effects on food proteins functionality. *Journal of Food Engineering*, *108*(3), 463–472.
- Behrouzian, F., Razavi, S. M. A., & Karazhiyan, H. (2014). Intrinsic viscosity of cress (*Lepidium sativum*) seed gum: Effect of salts and sugars. *Food Hydrocolloids*, *35*(0), 100–105.
- Beverung, C. J., Radke, C. J., & Blanch, H. W. (1999). Protein adsorption at the oil/water interface: characterization of adsorption kinetics by dynamic interfacial tension measurements. *Biophysical Chemistry*, *81*(1), 59–80.
- Chandrapala, J., Zisu, B., Palmer, M., Kentish, S., & Ashokkumar, M. (2011). Effects of ultrasound on the thermal and structural characteristics of proteins in reconstituted whey protein concentrate. *Ultrasonics Sonochemistry*, *18*(5), 951–957.
- Curvale, R., Masuelli, M., & Padilla, A. P. (2008). Intrinsic viscosity of bovine serum albumin conformers. *International Journal of Biological Macromolecules*, *42*(2), 133–7.
- Dalgleish, D. G. (2011). On the structural models of bovine casein micelles-review and possible improvements. *Soft Matter*, *7*(6), 2265–2272.
- Damodaran, S., & Razumovsky, L. (2008). Role of surface area-to-volume ratio in protein adsorption at the air–water interface. *Surface Science*, *602*(1), 307–315.

- Delpech, M. C., & Oliveira, C. M. F. (2005). Viscometric study of poly(methyl methacrylate-g-propylene oxide) and respective homopolymers. *Polymer Testing*, 24(3), 381–386.
- Dybowska, B. E. (2011). Whey protein-stabilized emulsion properties in relation to thermal modification of the continuous phase. *Journal of Food Engineering*, 104(1), 81–88.
- Euston, S. R., & Hirst, R. L. (1999). Comparison of the concentration-dependent emulsifying properties of protein products containing aggregated and non-aggregated milk protein. *International Dairy Journal*, 9(10), 693–701.
- Foegeding, E. A., & Davis, J. P. (2011). Food protein functionality: A comprehensive approach. *Food Hydrocolloids*, 25(8), 1853–1864.
- Fox, P. F. (2008). Chapter 1 - Milk: an overview. In A. Thompson, M. B. Mike Boland and Harjinder SinghA2 - Abby Thompson, & H. S. B. T.-M. Proteins (Eds.), (pp. 1–54). San Diego: Academic Press.
- Gaonkar, A. G. (1989). Interfacial tensions of vegetable oil/water systems: Effect of oil purification. *Journal of the American Oil Chemists' Society*, 66(8), 1090–1092.
- Gaonkar, A. G. (1991). Surface and interfacial activities and emulsion characteristics of some food hydrocolloids. *Food Hydrocolloids*, 5(4), 329–337.
- Gülseren, İ., Güzey, D., Bruce, B. D., & Weiss, J. (2007). Structural and functional changes in ultrasonicated bovine serum albumin solutions. *Ultrasonics Sonochemistry*, 14(2), 173–183.
- Güzey, D., Gülseren, İ., Bruce, B., & Weiss, J. (2006). Interfacial properties and structural conformation of thermosonicated bovine serum albumin. *Food Hydrocolloids*, 20(5), 669–677.
- Guzey, D., & Weiss, J. (2001). High-intensity ultrasonic processing improves emulsifying properties of proteins. Colloidal and Interfacial Food Science Laboratory, Department of Food Science and Technology, The University of Tennessee.
- Hu, H., Wu, J., Li-Chan, E. C. Y., Zhu, L., Zhang, F., Xu, X., Gang, F., Lufeng, W., Xingjian, H., & Pan, S. (2013). Effects of ultrasound on structural and physical properties of soy protein isolate (SPI) dispersions. *Food Hydrocolloids*, 30(2), 647–655.
- Huggins, M. L. (1942). The Viscosity of Dilute Solutions of Long-Chain Molecules. IV. Dependence on Concentration. *Journal of the American Chemical Society*, 64(11), 2716–2718.
- Jambrak, A. R., Lelas, V., Mason, T. J., Krešić, G., & Badanjak, M. (2009). Physical properties of ultrasound treated soy proteins. *Journal of Food Engineering*, 93(4), 386–393.
- Jambrak, A. R., Mason, T. J., Lelas, V., & Krešić, G. (2010). Ultrasonic effect on physicochemical and functional properties of α -lactalbumin. *LWT - Food Science and Technology*, 43(2), 254–262.

- Jambrak, A. R., Mason, T. J., Lelas, V., Paniwnyk, L., & Herceg, Z. (2014). Effect of ultrasound treatment on particle size and molecular weight of whey proteins. *Journal of Food Engineering*, 121(0), 15–23.
- Karki, B., Lamsal, B. P., Jung, S., van Leeuwen, J. (Hans), Pometto III, A. L., Grewell, D., & Khanal, S. K. (2010). Enhancing protein and sugar release from defatted soy flakes using ultrasound technology. *Journal of Food Engineering*, 96(2), 270–278.
- Khan, A., Bibi, I., Pervaiz, S., Mahmood, K., & Siddiq, M. (2012). Surface Tension, Density and Viscosity Studies on the Associative Behaviour of Oxyethylene-Oxybutylene Diblock Copolymers in Water at Different Temperatures. *International Journal of Organic Chemistry*, 02(01), 82–92.
- Kraemer, E. O. (1938). Molecular Weights of Celluloses and Cellulose Derivates. *Industrial & Engineering Chemistry*, 30(10), 1200–1203.
- Krise, K. M. (2011). *The effects of microviscosity, bound water and protein mobility on the radiolysis and sonolysis of hen egg white*. PhD Thesis. The Pennsylvania State University.
- Lam, R. S. H., & Nickerson, M. T. (2013). Food proteins: A review on their emulsifying properties using a structure–function approach. *Food Chemistry*, 141(2), 975–984.
- Lee, L., & Norton, I. T. (2013). Comparing droplet breakup for a high-pressure valve homogeniser and a Microfluidizer for the potential production of food-grade nanoemulsions. *Journal of Food Engineering*, 114(2), 158–163.
- Lefebvre, J. (1982). Viscosity of concentrated protein solutions. *Rheologica Acta*, 21(4-5), 620–625.
- Margulis, M. A., & Margulis, I. M. (2003). Calorimetric method for measurement of acoustic power absorbed in a volume of a liquid. *Ultrasonics Sonochemistry*, 10(6), 343–345.
- McClements, D. J. (2004). Protein-stabilized emulsions. *Current Opinion in Colloid & Interface Science*, 9(5), 305–313.
- McClements, D. J. (2005). *Food Emulsions: Principles, Practices, and Techniques* (2nd ed.). CRC Press.
- Morris, E. R., Cutler, A. N., Ross-Murphy, S. B., Rees, D. A., & Price, J. (1981). Concentration and shear rate dependence of viscosity in random coil polysaccharide solutions. *Carbohydrate Polymers*, 1, 5–21.
- Nakamura, K., Era, S., Ozaki, Y., Sogami, M., Hayashi, T., & Murakami, M. (1997). Conformational changes in seventeen cystine disulfide bridges of bovine serum albumin proved by Raman spectroscopy. *FEBS Letters*, 417(3), 375–378.
- O'Brien, W. D. (2007). Ultrasound-biophysics mechanisms. *Progress in Biophysics and Molecular Biology*, 93(1-3), 212–55.

- O'Connell, J. E., & Flynn, C. (2007). The Manufacture and Application of Casein-Derived Ingredients. In Y. H. Hui (Ed.), *Handbook of Food Products Manufacturing* (1st ed., pp. 557 – 593). New Jersey: John Wiley & Sons.
- O'Connell, J. E., Grinberg, V. Y., & de Kruif, C. G. (2003). Association behavior of β -casein. *Journal of Colloid and Interface Science*, 258(1), 33–39.
- O'Donnell, C. P., Tiwari, B. K., Bourke, P., & Cullen, P. J. (2010). Effect of ultrasonic processing on food enzymes of industrial importance. *Trends in Food Science & Technology*, 21(7), 358–367.
- O'Regan, J., Ennis, M. P., & Mulvihill, D. M. (2009). Milk Proteins. In *Handbook of Hydrocolloids* (pp. 298–358). Elsevier.
- Sakurai, K., Konuma, T., Yagi, M., & Goto, Y. (2009). Structural dynamics and folding of beta-lactoglobulin probed by heteronuclear NMR. *Biochimica et Biophysica Acta*, 1790(6), 527–37.
- Srinivasan, M., Singh, H., & Munro, P. A. (2002). Formation and stability of sodium caseinate emulsions: influence of retorting (121°C for 15 min) before or after emulsification. *Food Hydrocolloids*, 16(2), 153–160.
- Tanner, R., & Rha, C. (1980). Hydrophobic Effect on the Intrinsic Viscosity of Globular Proteins. In G. Astarita, G. Marrucci, & L. Nicolais (Eds.), *In Rheology, Volume 2: Fluids* (pp. 277–283). Boston, MA: Springer US.
- Tcholakova, S., Denkov, N. D., Ivanov, I. B., & Campbell, B. (2006). Coalescence stability of emulsions containing globular milk proteins. *Advances in Colloid and Interface Science*, 123–126(0), 259–293.
- Walstra, P., & van Vliet, T. (2003). Chapter II Functional properties. In R. J. H. W.Y. Aalbersberg P. Jasperse, H.H.J. de Jongh, C.G. de Kruif, P. Walstra and F.A. de Wolf BT - Progress in Biotechnology (Ed.), *Industrial Proteins in Perspective* (Vol. Volume 23, pp. 9–30). Elsevier.
- YanJun, S., Jianhang, C., Shuwen, Z., Hongjuan, L., Jing, L., Lu, L., Uloko, H., Yangling, S., Wenming, C., Wupeng, G., & Jiaping, L. (2014). Effect of power ultrasound pre-treatment on the physical and functional properties of reconstituted milk protein concentrate. *Journal of Food Engineering*, 124(0), 11–18.
- Yilgor, I., Ward, T. C., Yilgor, E., & Atilla, G. E. (2006). Anomalous dilute solution properties of segmented polydimethylsiloxane–polyurea copolymers in isopropyl alcohol. *Polymer*, 47(4), 1179–1186.

Chapter 4. The effect of ultrasound treatment on the structural, physical and emulsifying properties of animal and vegetable proteins

Data and discussions contained within this chapter have been published within:

O'Sullivan, J.J., Murray, B.A., Flynn, C. and Norton, I.T. 2014. The effect of ultrasound treatment on the structural, physical and emulsifying properties of animal and vegetable proteins. *Food Hydrocolloids*.

4.1. Abstract

The ultrasonic effect on the physicochemical and emulsifying properties of three animal proteins; bovine gelatin (BG), fish gelatin (FG) and egg white protein (EWP), and three vegetable proteins; pea protein isolate (PPI), soy protein isolate (SPI) and rice protein isolate (RPI), was investigated. Protein solutions (0.1 – 10 wt. %) were sonicated at an acoustic intensity of $\sim 34 \text{ W cm}^{-2}$ for 2 minutes. The structural and physical properties of the proteins were probed in terms of changes in size, hydrodynamic volume and molecular structure using DLS and laser diffraction, intrinsic viscosity and SDS-PAGE, respectively. The emulsifying performance of ultrasound treated animal and vegetable proteins were compared to their untreated counterparts and Brij 97. Ultrasound treatment reduced the size of all proteins, with the exception of RPI, whilst no reduction in the primary structure molecular weight profile of proteins was observed in all cases. Emulsions prepared with all untreated proteins yielded submicron droplets at concentrations $\leq 1 \text{ wt. } \%$, whilst at concentrations $> 5 \text{ wt. } \%$ emulsions prepared with EWP, SPI and RPI yielded micron sized droplets ($> 10 \mu\text{m}$) due to pressure denaturation of protein from homogenisation. Emulsions produced with sonicated FG, SPI and RPI had the similar droplet sizes as untreated proteins at the same concentrations, whilst sonicated BG, EWP and PPI emulsions at concentrations $\leq 1 \text{ wt. } \%$ had a smaller droplet size compared to emulsions prepared with their untreated counterparts. This effect was consistent with the observed reduction in the interfacial tension between these untreated and ultrasound treated proteins.

4.2. Introduction

Proteins perform a vast array of functions in both the food and pharmaceutical industries, such as emulsification, foaming, encapsulation, viscosity enhancement and gelation. This functionality arises from the complex chemical make-up of these molecules (O'Connell & Flynn, 2007; Walstra & van Vliet, 2003). Proteins are of particular interest in food systems as emulsifiers, due to their ability to adsorb to oil-water interfaces and form interfacial films (Foegeding & Davis, 2011; Lam & Nickerson, 2013). The surface activity of proteins arises from the amphiphilic nature of these molecules, because of the presence of both hydrophobic and hydrophilic amino acid residues in their peptide chains (Damodaran, 1997b). Due to the larger molecular weight of proteins leading to their bulkier structure by comparison to low molecular weight emulsifiers (*e.g.* Brij 97) proteins diffuse more slowly to the oil-water interface through the continuous phase (Beverung *et al.*, 1999; O'Connell & Flynn, 2007). Once at the interface proteins undergo surface denaturation and rearrange themselves in order to position their hydrophobic and hydrophilic amino groups in the oil and aqueous phase respectively, reducing the interfacial tension and overall free energy of the system (Caetano da Silva Lannes & Natali Miquelim, 2013; McClements, 2004). Proteins provide several advantages for emulsion droplet stabilisation, such as protein-protein interactions at interfaces, and electrostatic and steric stabilisation due to the charged and bulky nature of these biopolymers (Lam & Nickerson, 2013; McClements, 2004; O'Connell & Flynn, 2007).

Ultrasound is an acoustic wave with a frequency greater than 20 kHz, the threshold for human auditory detection (Knorr *et al.*, 2004). Ultrasound can be classified in two distinct categories based on the frequency range, high frequency (100 kHz – 1 MHz) low power ($< 1 \text{ W cm}^{-2}$) ultrasound, utilised most commonly for the analytical evaluation of the physicochemical properties of food (Knorr, Zenker, Heinz, & Lee, 2004), and low frequency

(20 – 100 kHz) high power (10 – 1000 W cm⁻²) ultrasound recently employed for the alteration of foods, either physically or chemically (Chemat *et al.*, 2011). The effects of high power ultrasound on food structures is attributed to the ultrasonic cavitations, the rapid formation and collapse of gas bubbles, which is generated by localised pressure differentials occurring over short periods of times (a few microseconds). These ultrasonic cavitations cause hydrodynamic shear forces and a rise in temperature at the site of bubble collapse (up to 5000 °C) contribute to the observed effects of high power ultrasound (Güzey *et al.*, 2006; O'Brien, 2007; O'Donnell *et al.*, 2010).

Ultrasound treatment of food proteins has been related to affects of the physicochemical properties of a number of protein sources including soy protein isolate/concentrate (including soy flakes; (Güzey *et al.*, 2006; O'Brien, 2007; O'Donnell *et al.*, 2010) and egg white protein (Arzeni *et al.*, 2012; Arzeni, Pérez, & Pilosof, 2012; Krise, 2011). Arzeni *et al.*, (2012a, 2012b) studied the effect of ultrasound upon the structural and emulsifying properties of egg white protein (EWP) and observed an increase in the hydrophobicity and emulsion stability of ultrasound treated EWP by comparison to untreated EWP. In addition, Krise, (2011) reported no significant reduction in the primary protein structure molecular weight profile of EWP after sonication at 55 kHz for 12 minutes. Similarly, Karki *et al.*, (2010) and Hu *et al.*, (2013) observed no significant changes in the primary protein structure molecular weight profile of ultrasound treated soy protein. Furthermore, Arzeni *et al.*, (2012) described a significant reduction in protein aggregate size for soy protein isolate (SPI). However, the effect of ultrasound treatment upon gelatin, either mammalian or piscine derived, pea protein isolate or rice protein isolate has yet to be investigated.

Gelatin is a highly versatile biopolymer widely used in a myriad of industries, from the food industry for gelation and viscosity enhancement, and the pharmaceutical industry for

the manufacture of soft and hard capsules (Duconseille *et al.*, 2015; Haug *et al.*, 2004; Schrieber & Gareis, 2007). Gelatin is prepared from the irreversible hydrolysis of collagen (a water insoluble structural protein of connective tissues in animals) under either acidic or alkaline conditions in the presence of heat, yielding a variety of peptide-chain species (Schrieber & Gareis, 2007; Veis, 1964). Gelatin is a composite mixture of three main protein fractions: free α -chains, β -chains, the covalent linkage between two α -chains, and γ -chains, the covalent linkage between three α -chains (Schrieber & Gareis, 2007; Veis, 1964). Gelatin is unique among proteins owing to the lack of appreciable internal structuring, so that in aqueous solutions at sufficiently high temperatures the peptide chains take up random configurations, analogous to the behaviour of synthetic linear-chain polymers (Veis, 1964).

Egg white protein (EWP) is a functional ingredient widely used in the food industry, due to its emulsifying, foaming and gelation capabilities, and utilised within a wide range of food applications, including noodles, mayonnaise, cakes and confectionary (Veis, 1964). EWP is globular in nature with highly defined tertiary and quaternary structures. The main protein fractions of egg white protein include ovalbumin (~55 %), ovotransferrin (~12 %) and ovomucin (~11 %), as well as over 30 other protein fractions (Anton *et al.*, 2009).

Pea protein isolate (PPI) is a nutritional ingredient used in the food industry owing to its emulsifying (Donsi *et al.*, 2010) and gelation properties (Gharsallaoui *et al.*, 2011; Liang & Tang, 2014), and additionally it has hypoallergenic attributes (Sun & Arntfield, 2012). PPI, a pulse legume, is extracted from *Pisum sativum*, and is the main cultivated protein crop in Europe (Boye *et al.*, 2010). The major protein fractions found in PPI are albumins (2S; 5 – 80 kDa) and globulins, the major fractions in pulse legumes are legumin (11S; ~40 kDa), vicilin (7S; ~175 kDa) and convicilin (7-8S; ~290 kDa) (Gonzalez-Perez & Arellano, 2009). Other minor proteins found in pulses include prolamins and glutelins (Boye *et al.*, 2010; Gonzalez-Perez & Arellano, 2009).

Soy protein isolate (SPI) is of particular interest to the food industry, as it is the largest commercially available vegetable protein source owing to its high nutritional value and current low cost, and a highly functional ingredient due to its emulsifying and gelling capabilities, however, this functionality is dependent upon the extraction method utilised for the preparation of the isolate (Saharan & Khetarpaul, 1994). SPI, extracted from *Glycine max*, is an oilseed legume grown primarily in the United States, Brazil, Paraguay and Uruguay (Achouri *et al.*, 2012; Molina *et al.*, 2002; Sorgentini *et al.*, 1995). Similar to pulse legumes, like PPI, the major protein fractions in oilseed legumes are albumins (2S; < 80 kDa) and globulins. The dominant fractions in SPI are glycinin (11S; 300-360 kDa) and β -conglycinin (7S; 150-190 kDa) a trimeric glycoprotein (Gonzalez-Perez & Arellano, 2009).

Rice protein isolate (RPI) is a food ingredient of great importance, reflected by the large annual consumption of rice, 440 million metric tonnes in 2009 (Gonzalez-Perez & Arellano, 2009; Shewry *et al.*, 1995). Up until recently, the protein component of rice (~8 %) was usually discarded, as the starch component (~80 %) yielded greater commercial value (Romero *et al.*, 2012). Despite rice proteins being common ingredients in gels, ice creams and infant formulae (Cao *et al.*, 2009; Gonzalez-Perez & Arellano, 2009), few studies have been conducted on these proteins to ascertain emulsifying, foaming and gelling capabilities (Chrastil, 1992). RPI is extracted from *Oryza sativa*, a cereal grain, and is cultivated primarily in Asia (Agboola *et al.*, 2005; Romero *et al.*, 2012). Similar to PPI and SPI, RPI has four main protein fractions albumin (~5 %), globulin (~12 %), glutelin (~80 %) and prolamin (~3 %), which are water-, salt-, alkali- and alcohol-soluble, respectively (Gonzalez-Perez & Arellano, 2009).

In this work, three animal proteins, bovine gelatin (BG), fish gelatin (FG) and egg white protein (EWP), and three vegetable proteins, pea protein isolate (PPI), soy protein isolate (SPI) and rice protein isolate (RPI), all of which are composite mixtures of a number

of protein fractions, were investigated in order to assess the significance of high power ultrasound treatment on industrially relevant food proteins. The objectives of this research were to discern the effects of ultrasound treatment upon animal and vegetable proteins, in particular changes in physicochemical properties, measured in terms of size, molecular structure and intrinsic viscosity. Furthermore, differences in the performance of proteins as emulsifiers after ultrasound treatment was assessed in terms emulsion droplet size, emulsion stability and interfacial tension. Oil-in-water emulsions were prepared with either untreated or ultrasound treated BG, FG, EWP, PPI, SPI and RPI at different concentrations and compared between them and to a low molecular weight emulsifier, Brij 97.

4.3. Materials and methodology

4.3.1. Materials

Bovine gelatin (BG; 175 Bloom), cold water fish gelatin (FG; 200 Bloom), egg white protein from chickens (EWP), Brij® 97 and sodium azide were purchased from Sigma Aldrich (UK). Pea protein isolate (PPI), soy protein isolate (SPI) and rice protein isolate (RPI) were all kindly provided by Kerry Ingredients (Listowel, Ireland). The composition of the animal and vegetable proteins used in this study is presented in Table 4.1, acquired from the material specification forms from suppliers. The oil used was commercially available rapeseed oil. The water used in all experiments was passed through a double distillation unit (A4000D, Aquatron, UK).

Chapter 4. The effect of ultrasound treatment on the structural, physical and emulsifying properties of animal and vegetable proteins

Table 4.1. Composition and pH (measured at a concentration of 1 wt. % and a temperature of 25 °C) of bovine gelatin (BG), fish gelatin (FG), egg white protein (EWP), pea protein isolate (PPI), soy protein isolate (SPI) and rice protein isolate (RPI).

	BG	FG	EWP	PPI	SPI	RPI
Protein (wt. %)	86	86	85	86	86	84.5
Moisture (wt. %)	10	12	8.4	7.2	6.2	7.7
Fat (wt. %)	0	0	< 0.1	0	3.5	3
Carbohydrate (-)	neg.	neg.	neg.	pos.	pos.	pos.
Ash (wt. %)	0.76	0.09	4.11	4.85	4.96	0.72
pH (-)	5.32	5.02	6.26	7.45	6.95	4.85

4.3.2. Methods

4.3.2.1. Preparation of untreated protein solutions

Bovine gelatin (BG), fish gelatin (FG) and rice protein isolate (RPI) solutions were prepared by dispersion in water and adjusting the pH of the solution to 7.08 ± 0.04 with 1 M NaOH, as the initial pH of the solution is close to the isoelectric point, 5.32, 5.02 and 4.85, for BG, FG and RPI, respectively. The proteins were all dispersed in water to obtain solutions within a protein concentration range of 0.1 – 10 wt. %, where all the animal proteins were soluble at the range of concentrations, whilst the vegetable proteins possessed an insoluble component regardless of hydration time. Sodium azide (0.02 wt. %) was added to the solution to mitigate against microbial activity.

4.3.2.2. Ultrasound treatment of protein solutions

An ultrasonic processor (Viber Cell 750, Sonics, USA) with a 12 mm diameter stainless steel probe was used to ultrasound treat 50 ml aliquots of the protein solutions in

100 ml plastic beakers, which were placed in an ice bath to reduce heat gain. The protein solutions were sonicated with a frequency of 20 kHz and amplitude of 95 % (wave amplitude of 108 μm at 100% amplitude) for up to 2 minutes. This yielded an ultrasonic power intensity of $\sim 34 \text{ W cm}^{-2}$, which was determined calorimetrically by measuring the temperature rise of the sample as a function of treatment time, under adiabatic conditions. The acoustic power intensity, I_a (W cm^{-2}), was calculated as follows (Margulis & Margulis, 2003):

$$I_a = \frac{P_a}{S_A}, \text{ where } P = m \cdot c_p \left(\frac{dT}{dt} \right) \quad (4.1)$$

where P_a (W) is the acoustic power, S_A is the surface area of the ultrasound emitting surface (1.13 cm^2), m is the mass of ultrasound treated solution (g), c_p is the specific heat of the medium (4.18 kJ/gK) and dT/dt is the rate of temperature change with respect to time, starting at $t = 0$ ($^{\circ}\text{C/s}$).

The temperature of the protein solutions was measured before and after sonication by means of a digital thermometer (TGST3, Sensor-Tech Ltd., Ireland), with an accuracy of ± 0.1 $^{\circ}\text{C}$. Prior to ultrasound treatment, the temperature of protein solutions was within the range of $5 - 10$ $^{\circ}\text{C}$, whilst the temperature BG and FG solutions was within a temperature range of $45 - 50$ $^{\circ}\text{C}$, above the helix coil transition temperature. After ultrasonic irradiation, the temperature of all protein solutions was raised to approximately ~ 45 $^{\circ}\text{C}$.

4.3.2.3. Characterisation of untreated and ultrasound treated proteins

4.3.2.3.1. pH measurements

The pH of animal and vegetable protein solutions was measured before and after sonication at a temperature of 20 $^{\circ}\text{C}$. pH measurements were made by using a SevenEasy pH meter (Mettler Toledo, UK). This instrument was calibrated with buffer standard solutions of

known pH. The pH values are reported as the average and the standard deviation of three repeat measurements.

4.3.2.3.2. Microstructure characterisation

The size of untreated and ultrasound treated animal proteins was measured by dynamic light scattering (DLS) using a Zetasizer Nano Series (Malvern Instruments, UK), and the size of untreated and ultrasound treated vegetable proteins was measured by laser diffraction using the Mastersizer 2000 (Malvern Instruments, UK). Protein size values are reported as *Z*-average (D_z). The width of the protein size distribution was expressed in terms of span ($Span = D_{v0.9} - D_{v0.1}/D_{v0.5}$), where $D_{v0.9}$, $D_{v0.1}$, and $D_{v0.5}$ are the equivalent volume diameters at 90, 10 and 50 % cumulative volume, respectively. Low span values indicate a narrow size distribution. The protein size and span values are reported as the average and the standard deviation of three repeat measurements.

4.3.2.3.3. Microstructure visualisation

Cryogenic scanning electron microscopy (Cryo-SEM; Philips XL30 FEG ESSEM) was used to visualise the microstructure of untreated and ultrasound treated proteins. One drop of protein solution was frozen to approximately -180 °C in liquid nitrogen slush. Samples were then fractured and etched for 3 min at a temperature of -90 °C inside a preparation chamber. Afterwards, samples were sputter coated with gold and scanned, during which the temperature was kept below -160 °C by addition of liquid nitrogen to the system.

4.3.2.3.4. Molecular structure characterisation

The molecular structure of untreated and ultrasound treated animal and vegetable proteins was determined by sodium dodecyl sulphate-polyacrylamide gel electrophoresis (SDS-PAGE), using a Mini-Protean 3 Electrophoresis System (Bio-Rad, UK), where proteins

were tested using the reducing method. 100 µl of protein solution at a concentration of 1 wt. % was added to 900 µl of Laemmli buffer (Bio-Rad, UK; 65.8 mM Tris-HCl, 2.1% SDS, 26.3% (w/v) glycerol, 0.01% bromophenol blue) and 100 µl of β-mercaptoethanol (Bio-Rad, UK) in 2 ml micro tubes and sealed. These 2 ml micro tubes were placed in a float in a water bath at a temperature of 90 °C for 30 minutes, to allow the reduction reaction to take place. A 10 µl aliquot was taken from each sample and loaded onto a Tris-acrylamide gel (Bio-Rad, UK; 4-20% Mini Protean TGX Gel, 10 wells). A molecular weight standard (Bio-Rad, UK; Precision Plus Protein™ All Blue Standards) was used to determine the primary protein structure molecular weight profile of the samples. Gel electrophoresis was carried out initially at 55 V (I > 20 mA) for 10 min, then at 155 V (I > 55 mA) for 45 min in a running buffer (10x Tris/Glycine/SDS Buffer, Bio-Rad, UK; 4% Tris, 15% glycine, 0.5% SDS). The gels were removed from the gel cassette and stained with Coomassie Bio-safe stain (Bio-Rad, UK; 4% phosphoric acid, 0.5% methanol, 0.05% ethanol) for 1 hr and de-stained with distilled water overnight.

4.3.2.3.5. Intrinsic viscosity measurements

The intrinsic viscosity of untreated and ultrasound treated animal and vegetable proteins was determined by a double extrapolation to a zero concentration method, as described by (Morris *et al.*, 1981), using the models of Huggins' and Kraemer, as follows:

$$\text{Huggins (Huggins, 1942): } \frac{\eta_{sp}}{c} = [\eta] + k_H[\eta]^2c \quad (4.2)$$

$$\text{Kraemer (Huggins, 1942): } \frac{\ln \eta_{rel}}{c} = [\eta] + k_K[\eta]^2c \quad (4.3)$$

where η_{sp} is the specific viscosity (viscosity of the solvent, η_0 / viscosity of the solution, η), c the protein concentration (w/v%), $[\eta]$ the intrinsic viscosity (dL/g), k_H the Huggins constant.

η_{rel} is the relative viscosity (viscosity of the solution, η / viscosity of the solvent, η_0) and k_K is the Kraemer constant.

The concentration ranges used for the determination of the intrinsic viscosity of BG, FG, EWP, PPI, SPI and RPI were 0.1 – 0.5 wt. %, 0.25 – 1.5 wt. %, 1.5 – 3 wt. %, 0.5 – 0.8 wt. %, 1.5 – 3 wt. % and 0.5 – 2 wt. %, respectively. The validity of the regression procedure is confined within a discrete range of η_{rel} , $1.2 < \eta_{rel} < 2$. The upper limit is due to the hydrodynamic interaction between associates of protein molecules, and the lower limit is due to inaccuracy in the determination of very low viscosity fluids. A value of η_{rel} approaching 1 indicates the lower limit (Morris *et al.*, 1981).

The viscosity of the protein solutions was measured at 20 °C using a Kinexus rheometer (Malvern Instruments, UK) equipped with a double gap geometry (25 mm diameter, 40 mm height). For the determination of intrinsic viscosity by extrapolation to infinite dilution, there must be linearity between shear stress and shear rate, which indicates a Newtonian behaviour region on the range of shear rate used in the measurements. The Newtonian plateau region of the protein solutions at the range of concentrations used was found within a shear rate range of 25 - 1000 s⁻¹. Thus, the values of viscosity of the protein solutions and that of the solvent (distilled water) were selected from the flow curves data at a constant shear rate of 250 s⁻¹ (within the Newtonian region), which were subsequently used to determine the specific viscosity, η_{sp} , the relative viscosity, η_{rel} , and the intrinsic viscosity, $[\eta]$. At least three replicates of each measurement were made.

4.3.2.4. Preparation of oil-in-water emulsions

10 wt. % dispersed phase (rapeseed oil) was added to the continuous aqueous phase containing either untreated or sonicated animal or vegetable proteins or Brij 97 at different concentrations, ranging from 0.1 to 10 wt. %. An oil-in-water pre-emulsion was prepared by

emulsifying this mixture at 8000 rpm for 2 min using a high shear mixer (SL2T, Silverson, UK). Submicron oil-in-water emulsions were then prepared by further emulsifying the pre-emulsion using a high-pressure valve homogeniser (Panda NS 1001L-2K, GEA Niro Soavi, UK) at 125 MPa for 2 passes. The initial temperature of EWP, PPI, SPI and RPI emulsions was a temperature of 5 °C to prevent thermal denaturation of proteins from high pressure homogenisation, whilst denaturation may still occur due the high shear during high pressure processing. The initial temperature of BG and FG emulsions was at a temperature of 50 °C to prevent gelation of gelatin (bovine or fish) during the homogenisation process. High pressure processing increases the temperature of the processed material, and consequently, the final temperatures of emulsions prepared with EWP, PPI, SPI and RPI, and gelatin (BG and FG), after homogenisation were ~45 °C and ~90 °C, respectively.

4.3.2.5. Characterisation of oil-in-water emulsions.

4.3.2.5.1. Droplet size measurements

The droplet size of the emulsions was measured by laser diffraction using a Mastersizer 2000 (Malvern Instruments, UK) immediately after emulsification. Emulsion droplet size values are reported as the volume-surface mean diameter (Sauter diameter; $d_{3,2}$). The stability of the emulsions was assessed by droplet size measurements over 28 days, where emulsions were stored under refrigeration conditions (4 °C) throughout the duration of the stability study. The droplet sizes and error bars are reported as the mean and standard deviation, respectively, of measured emulsions prepared in triplicate.

4.3.2.5.2. Interfacial tension measurements

The interfacial tension between the aqueous phase (pure water, animal or vegetable protein solutions, or surfactant solution) and oil phase (rapeseed oil) was measured using a

tensiometer K100 (Krüss, Germany) with the Wilhelmy plate method. The Wilhelmy plate has a length, width and thickness of 19.9 mm, 10 mm and 0.2 mm, respectively and is made of platinum. The Wilhelmy plate was immersed in 20 g of aqueous phase to a depth of 3 mm. Subsequently, an interface between the aqueous phase and oil phase was created by carefully pipetting 50 g of the oil phase over the aqueous phase. The test was conducted over 3,600 s and the temperature was maintained at 20 °C throughout the duration of the test. The interfacial tension values and the error bars are reported as the mean and standard deviation, respectively, of three repeat measurements.

4.3.2.5.3. Emulsion visualisation

Cryogenic scanning electron microscopy (Cryo-SEM; Philips XL30 FEG ESSEM) was used to visualise the microstructure of pre-emulsions using untreated and sonicated proteins. One drop of pre-emulsion was frozen to approximately -180 °C in liquid nitrogen slush. Samples were then fractured and etched for 3 min at a temperature of -90 °C inside a preparation chamber. Afterwards, samples were sputter coated with gold and scanned, during which the temperature was kept below -160 °C by addition of liquid nitrogen to the system.

4.3.3. Statistical analysis

Student's t-test, a statistical hypothesis test, with a 95 % confidence interval was used to assess the significance of the results obtained. t-test data with $P < 0.05$ were considered statistically significant.

4.4. Results and discussions

4.4.1. Effect of ultrasound treatment on the structural and physical properties of animal and vegetable proteins

The effect of duration of ultrasonic irradiation on the size and pH of animal and vegetable proteins was initially investigated. 0.1 wt. % solutions of BG, FG, EWP, PPI, SPI and RPI were sonicated for 15, 30, 60 and 120 s, with an ultrasonic frequency of 20 kHz and an amplitude of 95 %. Protein size and pH measurements for untreated, and ultrasound treated proteins as a function of time are shown in Fig. 4.1 and Table 4.2. The size of the vegetable protein isolates presented in Fig. 4.1 prior to sonication (*i.e.* $t = 0$) are in a highly aggregated state due to protein denaturation from the processing to obtain these isolates. Fig. 4.1 shows that there is a significant reduction ($P < 0.05$) in protein size with an increase in the sonication time, and the results also highlight that after a sonication of 1 minute there is minimal further reduction in protein size of BG, FG, EWP, PPI and SPI. This decrease in protein size is attributed to disruption of the hydrophobic and electrostatic interactions which maintain untreated protein aggregates from the high hydrodynamic shear forces associated with ultrasonic cavitations.

However, there is no significant reduction ($P > 0.05$) in the size of RPI agglomerates, irrespective of treatment time, due to the highly aggregated structure of the insoluble component of RPI, ascribed to both the presence of carbohydrate within the aggregate structure and the denaturation of protein during the preparation of the protein isolate, restricting size reduction by way of ultrasound treatment (Guraya & James, 2002; Marshall & Wadsworth, 1994; Mujoo, Chandrashekar, & Zakiuddin Ali, 1998).

The pH of all animal and vegetable protein solutions, with the exception of RPI, decreased significantly ($P < 0.05$) with increasing sonication time. Equivalent to the protein

size measurements, after a treatment time of 1 min the pH of protein solutions decreased no further. The decrease in pH of animal and vegetable protein solutions is thought to be associated with the transitional changes resulting in deprotonation of acidic amino acid residues (Sakurai *et al.*, 2009) which were contained within the interior of associated structures of untreated proteins prior to ultrasound treatment. Our results are in agreement with those of O'Sullivan, *et al.*, (2014), who showed that an increased sonication led to a significant reduction of protein size and pH for dairy proteins up to a sonication time of 1 min, as with animal and vegetable proteins, with an ultrasound treatment of 20 kHz and an amplitude of 95%.

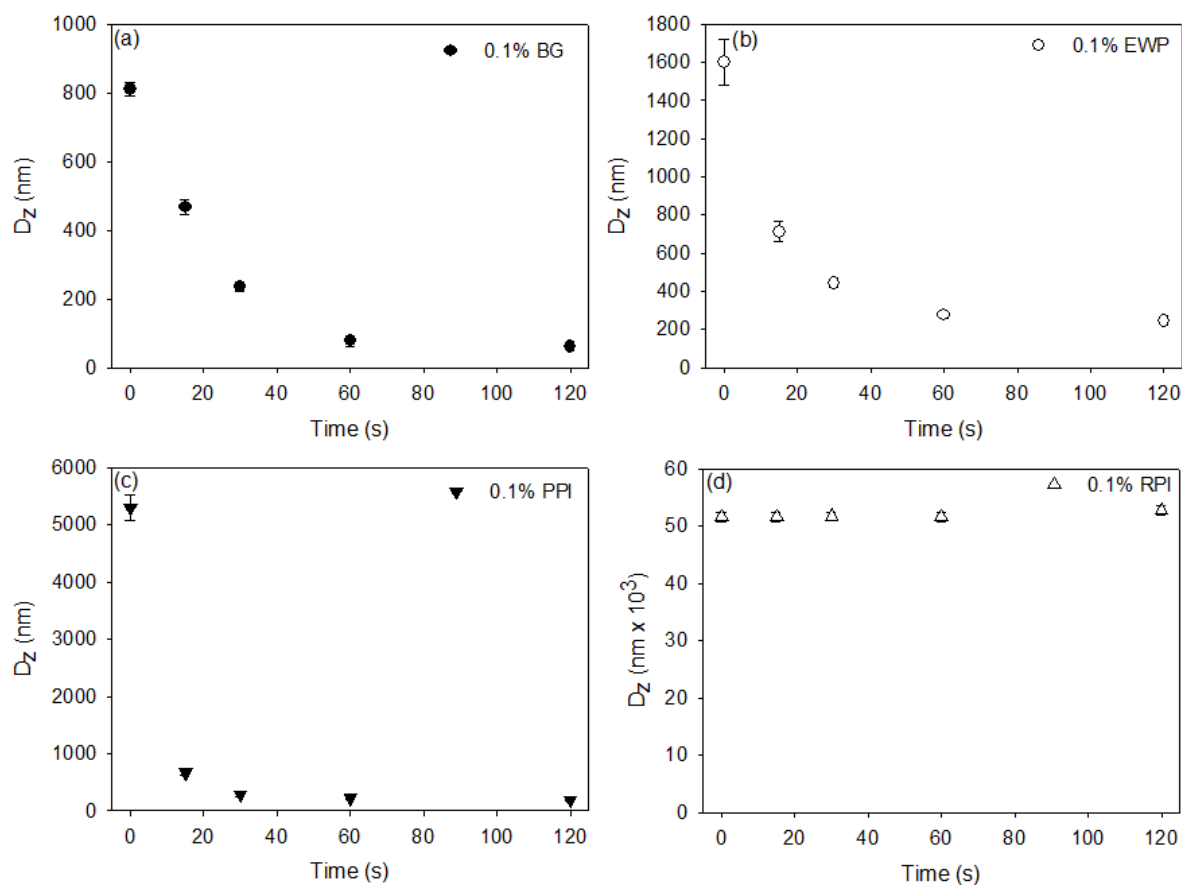


Fig. 4.1. Effect of sonication time on the D_z (nm) of (a) BG, (b) EWP, (c) PPI and (d) RPI.

Chapter 4. The effect of ultrasound treatment on the structural, physical and emulsifying properties of animal and vegetable proteins

Table 4.2. Effect of sonication time on pH of BG, FG, EWP, PPI, SPI and RPI solutions at a concentration of 0.1 wt. %. The standard deviation for all pH measurements was < 0.04 in all cases.

Time (s)	pH (-)				
	0	15	30	60	120
BG	7.09	6.97	6.84	6.71	6.63
FG	7.11	7.02	6.82	6.68	6.77
EWP	6.28	6.19	6.11	6.07	6.04
PPI	7.45	7.36	7.26	7.14	7.12
SPI	6.94	6.8	6.69	6.61	6.59
RPI	7.05	7.04	7.04	7.03	7.02

The stability of sonicated animal and vegetable protein solutions as a function of time was investigated by protein size and protein size distribution (span) of sonicated proteins. Animal and vegetable protein solutions with a concentration of 0.1 wt. % were ultrasound treated at 20 kHz and $\sim 34 \text{ W cm}^{-2}$ for a sonication time of 2 min, as no further decrease in protein size after a sonication time of 1 min was observed (*cf.* Fig. 4.1). The protein size and span values of sonicated animal and vegetable proteins were measured immediately after treatment and after 1 and 7 days, in order to assess the stability of protein size and protein size distribution. Protein size measurements and span values obtained from DLS and laser diffraction for untreated and ultrasound treated animal and vegetable proteins are shown in Table 4.3.

Chapter 4. The effect of ultrasound treatment on the structural, physical and emulsifying properties of animal and vegetable proteins

Table 4.3. Average protein size (D_z) and span of untreated and ultrasound treated animal and vegetable proteins at a concentration of 0.1 wt. %.

D_z (nm)	Ultrasound Treated			
	Untreated	Day 0	Day 1	Day 7
BG	812 ± 19	61 ± 7	112 ± 11	117 ± 8
FG	554 ± 23	52 ± 9	104 ± 13	111 ± 17
EWP	1,600 ± 120	244 ± 5	398 ± 7	412 ± 22
PPI	5,250 ± 230	187 ± 7	198 ± 6	222 ± 4
SPI	1,700 ± 320	265 ± 10	293 ± 9	298 ± 15
RPI	51,600 ± 920	52,800 ± 840	52,400 ± 680	52,500 ± 730
Span (-)	Untreated	Day 0	Day 1	Day 7
BG	1.93 ± 0.54	0.44 ± 0.03	0.67 ± 0.07	0.73 ± 0.06
FG	1.72 ± 0.43	0.35 ± 0.04	0.59 ± 0.06	0.66 ± 0.05
EWP	8.20 ± 0.44	5.80 ± 0.11	6.0 ± 0.11	5.80 ± 0.11
PPI	2.80 ± 0.13	48.1 ± 1.50	47.9 ± 1.70	46.6 ± 2.30
SPI	3.40 ± 0.43	23.5 ± 0.90	24.1 ± 1.20	24.4 ± 1.50
RPI	3.61 ± 0.23	3.57 ± 0.32	3.58 ± 0.43	3.60 ± 0.52

Ultrasound treatment produced a significant reduction ($P < 0.05$) in the size and span of BG, FG and EWP. However, 7 days after sonication an increase in the size and the broadening of the distribution was observed for animal proteins. The effective size reduction of the ultrasound treatment to BG, FG and EWP on day 7 was 85.6 %, 80 % and 74.3 %, respectively. In the case of PPI and SPI, the results in Table 4.3 show that ultrasound treatment significantly ($P < 0.05$) reduced the aggregate size and broadened of the protein size distribution. The size distribution of PPI and SPI after ultrasound treatment is bimodal,

one population having a similar size as the parent untreated protein, and the other population is nano-sized (~120 nm). The span of the distribution and protein size on day 7 for PPI and SPI was quite similar to that after immediate sonication, representing an effective protein size reduction of 95.7 % and 82.3 % for PPI and SPI respectively. This significant reduction in aggregate size of both PPI and SPI from ultrasound treatment allows for improved solubilisation and prolonged stability of these vegetable protein isolates to sedimentation.

These results are in agreement with those of Jambrak *et al.*, (2009), who observed a significant reduction in the size of SPI aggregates. Arzeni *et al.*, (2012) also observed a decrease in the protein size for sonicated SPI, but an increase in size for EWP treated by ultrasound, whereby this increase in size of EWP aggregates is associated with thermal aggregation during the ultrasound treatment. The reason for the observed decrease in the size of the proteins, with the exception of RPI, is due to disruption of non-covalent associative forces, such as hydrophobic and electrostatic interactions, and hydrogen bonding, which maintain protein aggregates in solution (*cf.* section 2.1.1.), induced by high levels hydrodynamic shear and turbulence due to ultrasonic cavitations.

The observed increase in size for BG, FG and EWP after 7 days is thought to be due to reorganisation of proteins into sub-aggregates due to non-covalent interactions (electrostatic and hydrophobic). In the case of PPI and SPI, the static size observed is due to the more defined structure of the PPI and SPI aggregates in comparison to the fully hydrated animal proteins, which allows for greater molecular interactions and mobility (Veis, 1964). In order to validate these hypotheses, cryo-SEM micrographs were captured of untreated and 7 days after sonication of BG and SPI solution at 1 wt. % for all proteins tested (Fig. 4.2).

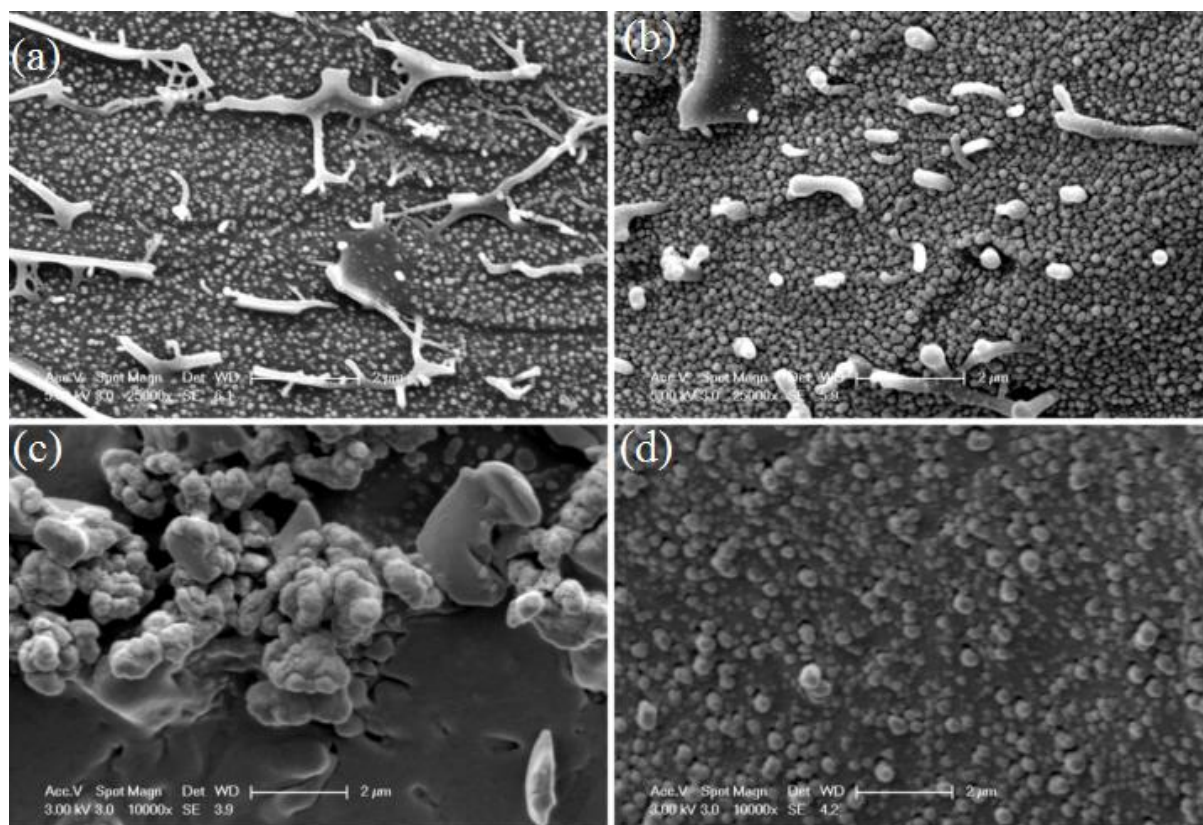


Fig. 4.2. Cryo-SEM micrographs of protein solutions: (a) 1% Untreated BG, (b) 1% Ultrasound treated BG, (c) 1% Untreated SPI and (d) 1% Ultrasound treated SPI. Scale bar is 2 μm in all cases.

Untreated BG in solution (*cf.* Fig. 4.2a) appears to be distributed into discrete fibres, which is consistent with the literature, describing gelatin as a fibrous protein (Veis, 1964), whilst BG treated by ultrasound (*cf.* Fig. 4.2b) appears to be in the form of fibrils of the parent untreated BG fibre, where the width of the fibres and the fibrils is equivalent, yet the length of the fibrils is shorter than the untreated BG fibres. In the case of untreated SPI (*cf.* Fig. 4.2c) large aggregates of protein can be seen, composed of discrete entities, whereas sonicated SPI (*cf.* Fig. 4.2d) has a notably reduced protein size, with a monodisperse size distribution. Similar results were observed for FG, EWP and PPI. These results are in agreement with previously discussed observations (*cf.* Table 4.3), and adds evidence to the hypothesis that ultrasound treatment causes disruption of protein aggregates, that subsequently reorganise themselves into smaller sub-associates.

The molecular structure of untreated and ultrasound treated animal and vegetable proteins was investigated next. Protein solutions at a concentration of 1 wt. % were ultrasound treated for 2 min at 20 kHz, with a power intensity of $\sim 34 \text{ W cm}^{-2}$. Electrophoretic profiles obtained by SDS-PAGE for untreated and ultrasound treated proteins, and the molecular weight standard, are shown in Fig. 4.3.

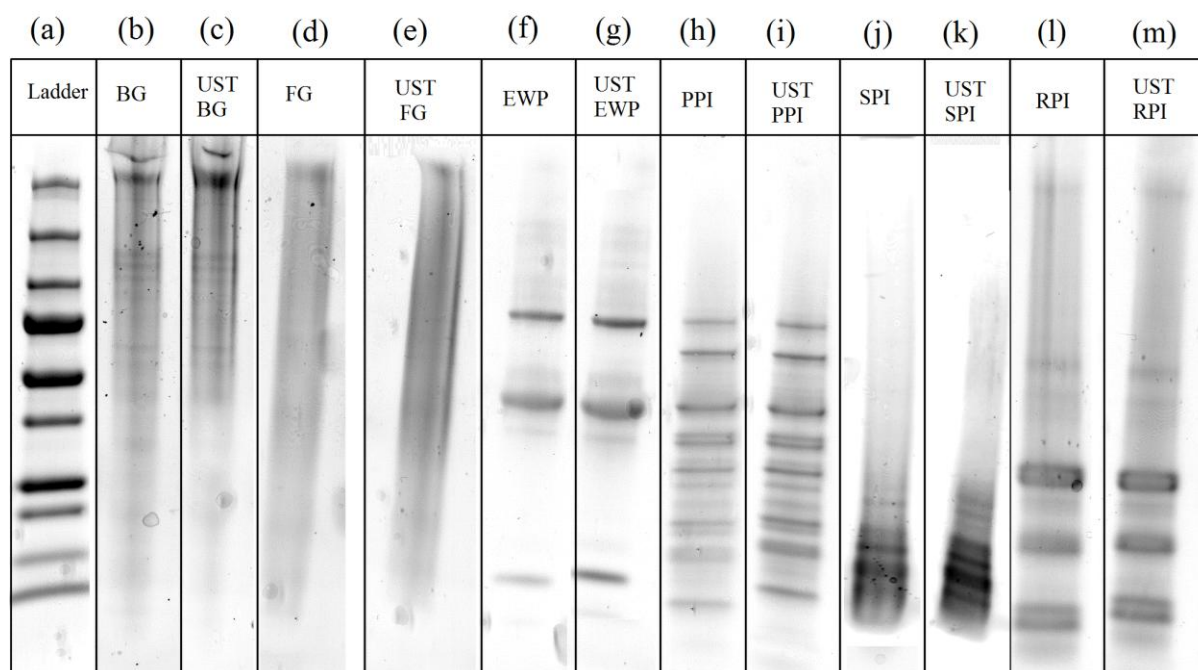


Fig. 4.3. SDS-PAGE electrophoretic profiles of protein solutions: (a) Molecular weight standard (10 kDa – 250 kDa), (b) Untreated BG, (c) Ultrasound treated BG, (d) Untreated FG, (e) Ultrasound treated FG, (f) Untreated EWP, (g) Ultrasound treated EWP, (h) Untreated PPI, (i) Ultrasound treated PPI, (j) Untreated SPI, (k) Ultrasound treated SPI, (l) Untreated RPI and (m) Ultrasound treated RPI.

No difference in the protein fractions was observed between untreated and sonicated BG, FG, EWP, SPI, PPI and RPI (*cf.* Fig. 4.3). These results are in concurrence with those reported by Krise, (2011) who also showed no difference in the primary structure molecular weight profile between untreated and ultrasound treated egg white, with a treatment conducted at 55 kHz, 45.33 W cm^{-2} for 12 min. Moreover, the molecular weight of the obtained protein fractions are in agreement with the literature for gelatin (Gouinlock *et al.*,

1955; Veis, 1964), EWP (Anton *et al.*, 2009), SPI (Gonzalez-Perez & Arellano, 2009), PPI (Sun & Arntfield, 2012) and RPI (Hamaker, 1994; Juliano, 1985).

The intrinsic viscosity, $[\eta]$, was obtained by the fitting of experimental viscosity data to the Huggins' and Kraemer equations, for untreated and ultrasound irradiated animal and vegetable protein solutions, as shown in Fig. 4.4 for EWP and PPI. The other proteins investigated as part of this study (BG, FG, SPI and RPI) display similar behaviour to EWP (*i.e.* negative k_H and k_K values). The values of $[\eta]$ and the Huggins', k_H , and Kraemer, k_K , constants for each of the proteins investigated in this study are listed in Table 4.4.

Table 4.4. Intrinsic viscosity ($[\eta]$), Huggins (k_H) and Kraemer (k_K) constants obtained for untreated and ultrasound treated animal and vegetable protein solutions.

Protein in solution	$[\eta]_{\text{Untreated}}$ (dL/g)	$k_{H \text{ Untreated}}$	$k_{K \text{ Untreated}}$	$[\eta]_{\text{Ultrasound}}$ (dL/g)	$k_{H \text{ Ultrasound}}$	$k_{K \text{ Ultrasound}}$
BG	2.75 ± 0.08	-2.88	-3.09	2.06 ± 0.09	-2.31	-2.39
FG	1.06 ± 0.07	-0.38	-0.41	0.76 ± 0.05	-0.18	-0.24
EWP	0.25 ± 0.001	-0.03	-0.033	0.21 ± 0.001	-0.023	-0.026
PPI	0.8 ± 0.005	0.59	0.034	0.76 ± 0.007	-0.24	-0.29
SPI	0.31 ± 0.002	-0.02	-0.032	0.27 ± 0.001	-0.023	-0.031
RPI	0.55 ± 0.009	-0.15	-0.16	0.56 ± 0.007	-0.13	-0.14

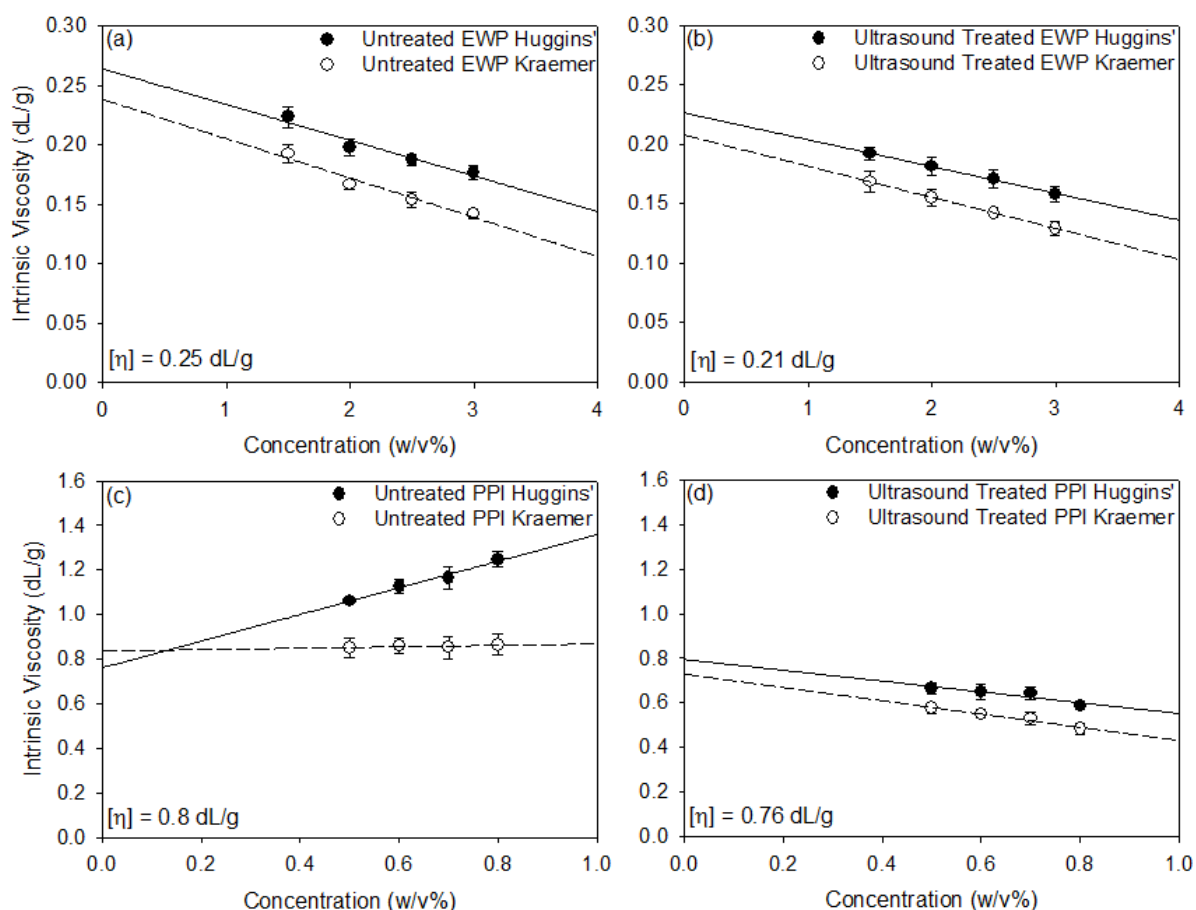


Fig. 4.4. Fitting of the Huggins (●) and Kraemer (○) equations to the viscosity data of the studied protein solutions: (a) Untreated EWP, (b) Ultrasound treated EWP, (c) Untreated PPI and (d) Ultrasound treated PPI.

Intrinsic viscosity, $[\eta]$, demonstrates the volume of water entrained by an aggregate of protein (*i.e.* hydration of proteins) and provides information about the associate hydrodynamic volume, which is related to molecular conformation of proteins in solution (Behrouzian *et al.*, 2014; Harding, 1997; Sousa *et al.*, 1995). A comparison of the $[\eta]$ between untreated and ultrasound treated animal and vegetable proteins (*cf.* Table 4.4) demonstrates that ultrasound treatment induced a significant reduction ($P < 0.05$) in the intrinsic viscosity of five of the protein solution, and consequently a significant reduction in the hydrodynamic volume occupied by the proteins and the solvents entrained within them.

These results are in agreement with the reduction in associate size (*cf.* Table 4.3) and cryo-SEM micrographs (*cf.* Fig. 4.2), however, for the case of RPI, there is no reduction in the intrinsic viscosity, which is consistent with the previous size measurements (*cf.* Table 4.3). Gouinlock *et al.*, (1955), Lefebvre, (1982) and Prakash, (1994) reported intrinsic viscosity values of 6.9 dL/g for gelatin, 0.326 dL/g for ovalbumin and 0.46 dL/g for glycinin (11S; soy globulin), respectively. These values differ to those obtained in this work for untreated BG, EWP and SPI (*cf.* Table 4.4). These differences may be a consequence of the complexity of EWP and SPI solutions, which are composed of a mixture of protein fractions rather than single component ovalbumin and glycinin (Lefebvre, 1982; Prakash, 1994), and in case of gelatin, differences may arise due to variability in preparation of the gelatin from collagen, which determines the molecular weight profile of the resulting gelatin (Veis, 1964). Extrinsic variations in solvent quality greatly affect the determination of intrinsic viscosity and further accounts for the differences between the single fraction proteins and the multi-component proteins investigated in this study. Extrinsic factors affecting intrinsic viscosity include temperature, pH, initial mineral content and composition, co-solvents, additional salts and their concentration (Harding, 1997). Furthermore, the large $[\eta]$ of both BG and FG by comparison to the other proteins investigated as part of this study is due to the random coil conformation of these molecules in solutions, which consequently entrain more water giving a larger overall hydrodynamic volume.

The intrinsic viscosity of a protein solution can be used to indicate the degree of hydrophobicity of the protein (Tanner & Rha, 1980). The intrinsic viscosity of protein associates in solution is dependent on its conformation and degree of hydration, which dictate the amount of hydrophobic residues that are within the interior of protein associates. A decrease in the intrinsic viscosity may lead to dehydration of amphiphilic biopolymers, potentially increasing the hydrophobicity of the biopolymer and thus, reducing the associated

energy required for adsorption of amphiphilic biopolymers to the oil-water interface (Khan *et al.*, 2012). Thus, the significant reduction ($P < 0.05$) of intrinsic viscosity induced by ultrasound treatment (*cf.* Table 4.4), demonstrates the potential for an increase in the degree of hydrophobicity of BG, FG, EWP, PPI and SPI.

The Huggins' and Kraemer coefficients are adequate for the assessment of solvent quality. Positive values of the Huggins' coefficient, k_H , within a range of 0.25 – 0.5 indicate good solvation, whilst k_H values within a range of 0.5 – 1.0 are related to poor solvents (Curvale *et al.*, 2008; Delpech & Oliveira, 2005). Conversely negative values for the Kraemer coefficient, k_K , indicate good solvent, yet positive values express poor solvation (Delpech & Oliveira, 2005; Harding, 1997). The values for the k_H and k_K (*cf.* Table 4.4) are both negative, with the exception of untreated PPI exhibiting a positive k_H value, indicating good solvation when considering k_K , yet unusual behaviour in the case of k_H . Nonetheless, negative values of k_H have been reported in the literature for biopolymers with amphiphilic properties, such as bovine serum albumin (Curvale *et al.*, 2008), sodium caseinate, whey protein isolate and milk protein isolate (O'Sullivan *et al.*, 2014a; O'Sullivan *et al.*, 2014b), all dispersed within serum. Positive k_H values are associated with uniform surface charges of polymers (Sousa *et al.*, 1995), indicating that untreated PPI aggregates have a uniform surface charge, and after ultrasound treatment conformational changes occur yielding an amphiphatic character on the surface of the ultrasound treated PPI, observed by the negative k_H value. It is also important to observe that the relation $k_H + k_K = 0.5$, generally accepted to indicate adequacy of experimental results for hydrocolloids, was not found for any of the proteins investigated in this study (*cf.* Table 4.4). This effect is thought to be associated with the amphiphatic nature of the proteins used in this study (in comparison to non-amphiphilic polysaccharides) yielding negative values of k_H and k_K . Similar results have been reported in the literature for other amphiphilic polymers (Curvale *et al.*, 2008; O'Sullivan, *et al.*, 2014a;

Yilgor *et al.*, 2006). In addition, the values of k_H and k_K tend to decrease after ultrasound treatment indicating improved solvation of proteins (Delpech & Oliveira, 2005).

4.4.2. Comparison of the emulsifying properties of untreated and ultrasound treated animal and vegetable proteins

Oil-in-water emulsions were prepared with 10 wt. % rapeseed oil and an aqueous continuous phase containing either the untreated or ultrasound irradiated (2 min at 20 kHz, $\sim 34 \text{ W cm}^{-2}$) proteins, or a low molecular weight surfactant, Brij 97, at a range of emulsifier concentrations (0.1 – 10 wt. %). Emulsions were prepared using high-pressure valve homogenisation (125 MPa for 2 passes) and droplet sizes as a function of emulsifier type and concentration are shown in Fig. 4.5. The emulsion droplet sizes were measured immediately after emulsification, and all exhibited unimodal droplet size distributions.

Emulsions prepared with sonicated BG (*cf.* Fig 4.5 a), EWP (*cf.* Fig. 4.5 c) and PPI (*cf.* Fig. 4.5 d) at concentrations < 1 wt. % yielded a significant ($P < 0.05$) reduction in emulsion droplet size by comparison to their untreated counterparts. At concentrations ≥ 1 wt. % the emulsions prepared with untreated and ultrasound treated BG, EWP and PPI exhibited similar droplet sizes. The decrease in emulsion droplet size after ultrasound treatment at concentrations < 1 wt. % is consistent with the significant reduction ($P < 0.05$) in protein size (increase in surface area-to-volume ratio) upon ultrasound treatment of BG, EWP and PPI solutions (*cf.* Table 4.3) which allows for more rapid adsorption of protein to the oil-water interface, as reported by Damodaran & Razumovsky (2008). In addition, the significant increase of hydrophobicity of ultrasound treated BG, EWP and PPI and the decrease in intrinsic viscosity (*cf.* Table 4.4; Khan *et al.*, 2012) would lead to an increased rate of protein adsorption to the oil-water interface, reducing interfacial tension allowing for improved facilitation of droplet break-up. The submicron droplets obtained for untreated PPI are in

agreement with droplet sizes obtained by those measured by Donsi *et al.*, (2010), in the order of ~200 nm for emulsions containing pea protein (4 wt. %).

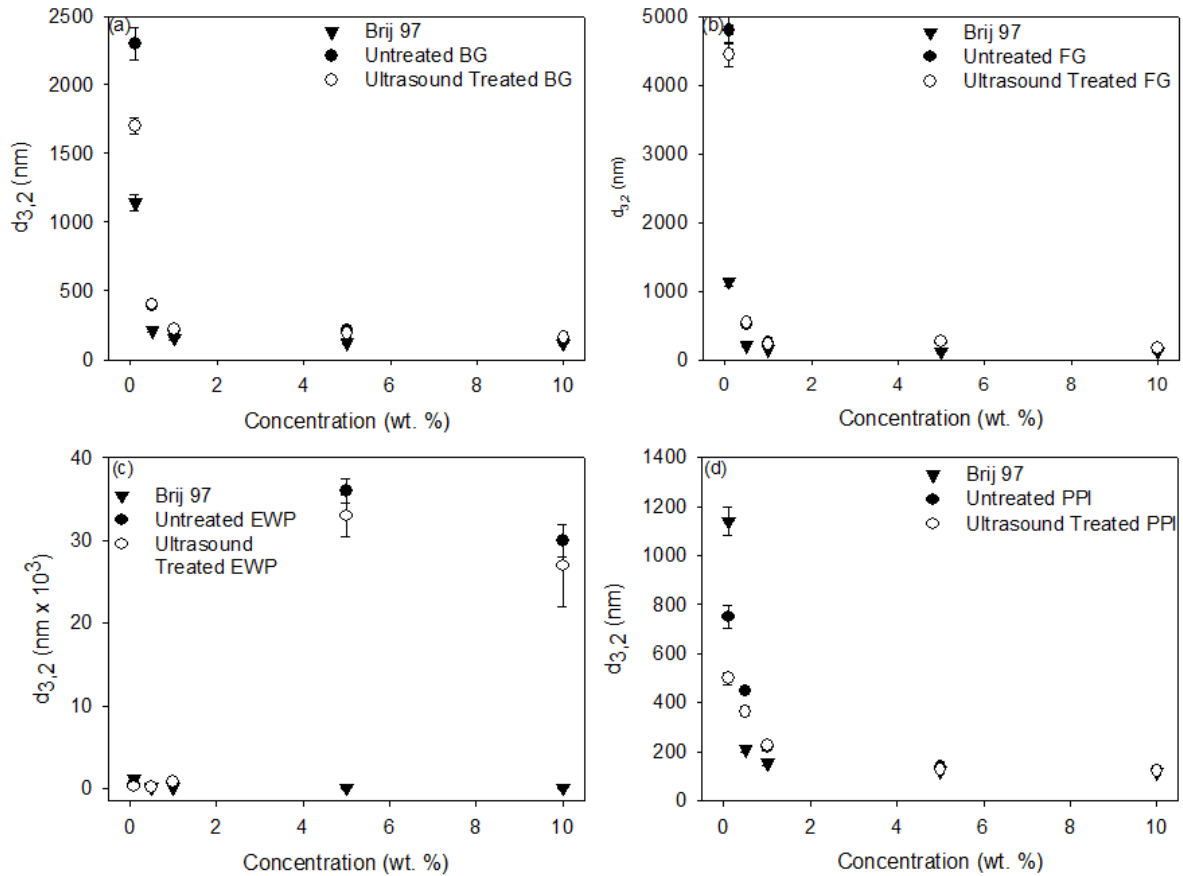


Fig. 4.5. Average droplet size as a function of concentrations of: (a) Untreated BG, sonicated BG and Brij 97, (b) Untreated FG, sonicated FG and Brij 97, (c) Untreated EWP, sonicated EWP and Brij 97 and (d) Untreated PPI, sonicated PPI and Brij 97.

Emulsions prepared with the tested concentrations of untreated and ultrasound treated FG (*cf.* Fig. 4.5 b), SPI and RPI yielded similar droplet sizes, where emulsions prepared with 0.1 wt. % FG yielded emulsion droplets ~5 μm , and both SPI and RPI yielded ~2 μm droplets at the same concentration. Furthermore, at similar concentrations PPI yielded smaller emulsion droplets than those prepared with SPI, making SPI a poorer emulsifier, in agreement with the results of Vose, (1980). This behaviour was anticipated for RPI, where no significant reduction ($P > 0.05$) in protein size was observed (*cf.* Table 4.3), yet unexpected

when considering the significant reduction ($P < 0.05$; increase in surface area-to-volume ratio) of protein size observed for both sonicated FG and SPI (*cf.* Table 4.3). Moreover, the potential increase in hydrophobicity of ultrasound treated FG and SPI expressed by the decrease in intrinsic viscosity (*cf.* Table 4.4; Khan *et al.*, 2012; Tanner & Rha, 1980) would also be expected to result in faster adsorption of protein to the oil-water interface, however it appears that the rate of protein adsorption of ultrasound treated FG and SPI to the oil-water interface remains unchanged regardless of the smaller protein associate sizes and increase in hydrophobicity, when compared with untreated FG and SPI. Even though ultrasound treatment reduces the aggregate size of SPI, proteins possessing an overall low molecular weight, such as EWP (ovalbumin is ~44 kDa), are capable of forming smaller emulsion droplets than larger molecular weight proteins (glycinin is 360 kDa) as lower molecular weight species have greater molecular mobility through the bulk for adsorbing to oil-water interfaces (Beverung *et al.*, 1999; Caetano da Silva Lannes & Natali Miquelim, 2013). The submicron droplets achieved for untreated FG are consistent with droplet sizes obtained by Surh *et al.*, (2006), in the order of ~300 nm for emulsions containing either low molecular weight (~55 kDa) or high molecular weight (~120 kDa) fish gelatin (4 wt. %).

At protein concentrations > 1 wt. % for emulsions prepared with either untreated or ultrasound treated EWP (*cf.* Fig. 4.5 c), SPI and RPI micron sized entities ($> 10 \mu\text{m}$) were formed. Unexpectedly, emulsions prepared with PPI did not exhibit the formation of these entities, even though the structure of PPI is similar to that of SPI. The degree and structure of the denatured component of PPI likely varies to that of SPI and accounts for the non-aggregating behaviour of PPI. Emulsions being processed using high pressure homogenisation experience both increases in temperature and regions of high hydrodynamic shear, both of these mechanisms result in denaturation of proteins. These micron sized entities are attributed to denaturation and aggregation of protein due to the high levels of

hydrodynamic shear present during the homogenisation process, as thermal effects were minimised by ensuring that the emulsions were processed at a temperature of 5 °C, and the outlet temperature was less than 45 °C in all cases, lower than the thermal denaturation temperatures of EWP, SPI and RPI (Ju *et al.*, 2001; Sorgentini *et al.*, 1995; Van der Plancken *et al.*, 2006). Hydrostatic pressure induced gelation of EWP, SPI and RPI has been reported in the literature (Messens *et al.*, 1997; Molina *et al.*, 2002; Tang & Ma, 2009; Zhang-Cun *et al.*, 2013) and the formation of these entities is attributed to the high shear forces exerted upon the proteins while under high shear conditions, whereby the excess of bulk protein allows for greater inter-penetration of protein chains under high shear yielding the formation of discrete entities composed of oil droplets within denatured aggregated protein. Unexpectedly, emulsions prepared with a higher concentration of protein (10 wt. %) yielded a significant ($P < 0.05$) reduction in entity size in comparison to those prepared with the lower concentration (5 wt. %). This behaviour is ascribed to an increased rate of formation and number of aggregates formed at higher concentrations during the short time within the shear field.

Emulsion droplet sizes for all animal and vegetable proteins (treated and untreated) investigated (*cf.* Fig. 4.5) are smaller than that of the size of the untreated proteins (*cf.* Table 4.3). Be that as it may, the reported protein sizes (*cf.* Table 4.3) represent aggregates of protein molecules and not discrete protein fractions. Native ovalbumin and glycinin have hydrodynamic radii (R_h) of approximately 3 nm and 12.5 nm respectively (García De La Torre *et al.*, 2000; Peng *et al.*, 1984), in comparison to size data presented in Table 4.3, whereby the EWP and SPI have D_z values of EWP and SPI of approximately 1.6 and 1.7 μm , respectively. This disparity in size is due to the preparation of these protein isolates whereby shear and temperature result in the formation of insoluble aggregated material, in comparison to the soluble native protein fractions. Proteins in aqueous solutions associate together to

form aggregates due to hydrophobic and electrostatic interactions (O'Connell *et al.*, 2003), however in the presence of a hydrophobic dispersed phase (*i.e.* rapeseed oil) the protein fractions which comprise the aggregate dissociate and adsorb to the oil-water interface (Beverung *et al.*, 1999; O'Connell & Flynn, 2007), which may account for the fabrication of submicron droplets presented in this study.

The emulsion droplet sizes presented in Fig. 4.5, which were shown to be dependent on the emulsifier type, can be interpreted by comparing the interfacial tension of the studied systems. Fig. 4.5 presents the interfacial tension between water and rapeseed oil, for untreated and ultrasound treated BG, FG, PPI and SPI, and Brij 97, all at an emulsifier concentration of 0.1 wt. %. In order to assess the presence of surface active impurities within the dispersed phase, the interfacial tension between distilled water and rapeseed oil was measured. Fig. 4.6 shows that the interfacial tension of all systems decreases continually as a function of time. In light of these results, the decrease of interfacial tension with time is attributed primarily to the nature of the dispersed phase used, and to a lesser degree the type of emulsifier. Gaonkar, (1989, 1991) explained that the time dependent nature of interfacial tension of commercially available vegetable oils against water was due to the adsorption of surface active impurities present within the oils at the oil-water interface. Gaonkar, (1989, 1991) also reported that after purification of the vegetable oils (percolation through a synthetic magnesium silicate bed), the time dependency of interfacial tension was no longer observed.

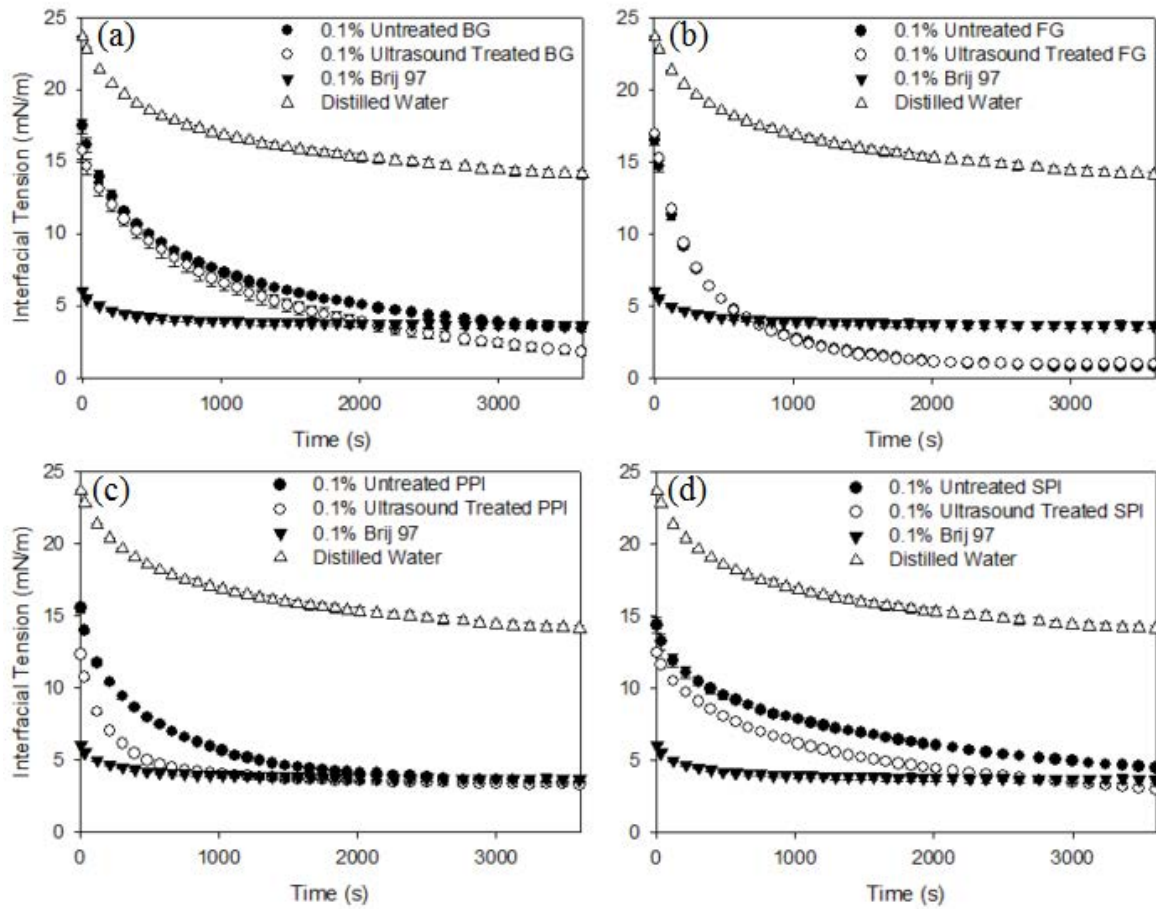


Fig. 4.6. Interfacial tension between water and pure vegetable oil as a function of emulsifier type: (a) Untreated BG, ultrasound treated BG and Brij 97, (b) Untreated FG, ultrasound treated FG and Brij 97, (c) Untreated PPI, ultrasound treated PPI and Brij 97 and (d) Untreated SPI, ultrasound treated SPI and Brij 97.

No significant differences ($P > 0.05$) were observed in the obtained values of interfacial tension between untreated and ultrasound treated FG (*cf.* Fig. 4.6 b) and RPI. These results are consistent with droplet size data, where no significant difference in the droplet size was observed. Significant differences were shown for the initial rate of decrease of interfacial tension when comparing untreated and ultrasound treated PPI (*cf.* Fig. 4.6 c). Ultrasound treated PPI aggregates are smaller than untreated PPI (*cf.* Table 4.3) and have greater hydrophobicity (*i.e.* reduction in $[\eta]$; *cf.* Table 4.4) accounting for the significant reduction of initial interfacial tension, enhancing droplet break-up during emulsification.

Significant differences ($P < 0.05$) in the equilibrium interfacial tension values were observed when comparing untreated and sonicated BG (*cf.* Fig. 4.6 a), EWP and SPI (*cf.* Fig. 4.6 d). These results are consistent with the observed significant reduction ($P < 0.05$) in emulsion droplet size for BG (*cf.* Fig. 4.5 a) and EWP (*cf.* Fig. 4.5 c) and adds evidence to the hypotheses that aggregates of sonicated BG and EWP adsorb faster to the interface due to higher surface area-to-volume ratio (*cf.* Table 4.3; smaller protein size) and increased hydrophobicity (*i.e.* reduction in $[\eta]$; *cf.* Table 4.4), significantly reducing the equilibrium interfacial tension, yielding smaller emulsion droplets. No significant reduction ($P > 0.05$) in emulsion droplet size was noted for SPI, despite the observed reduction in equilibrium interfacial tension of SPI (*cf.* Fig. 4.6 d) which may be a consequence of alternative protein conformations at the oil-water interface. These hypotheses were explored by cryo-SEM of pre-emulsions, to allow for visualisation emulsion droplet interface, prepared with untreated and ultrasound treated BG and SPI at an emulsifier concentration of 1 wt. % for all pre-emulsions tested (*cf.* Fig. 4.7).

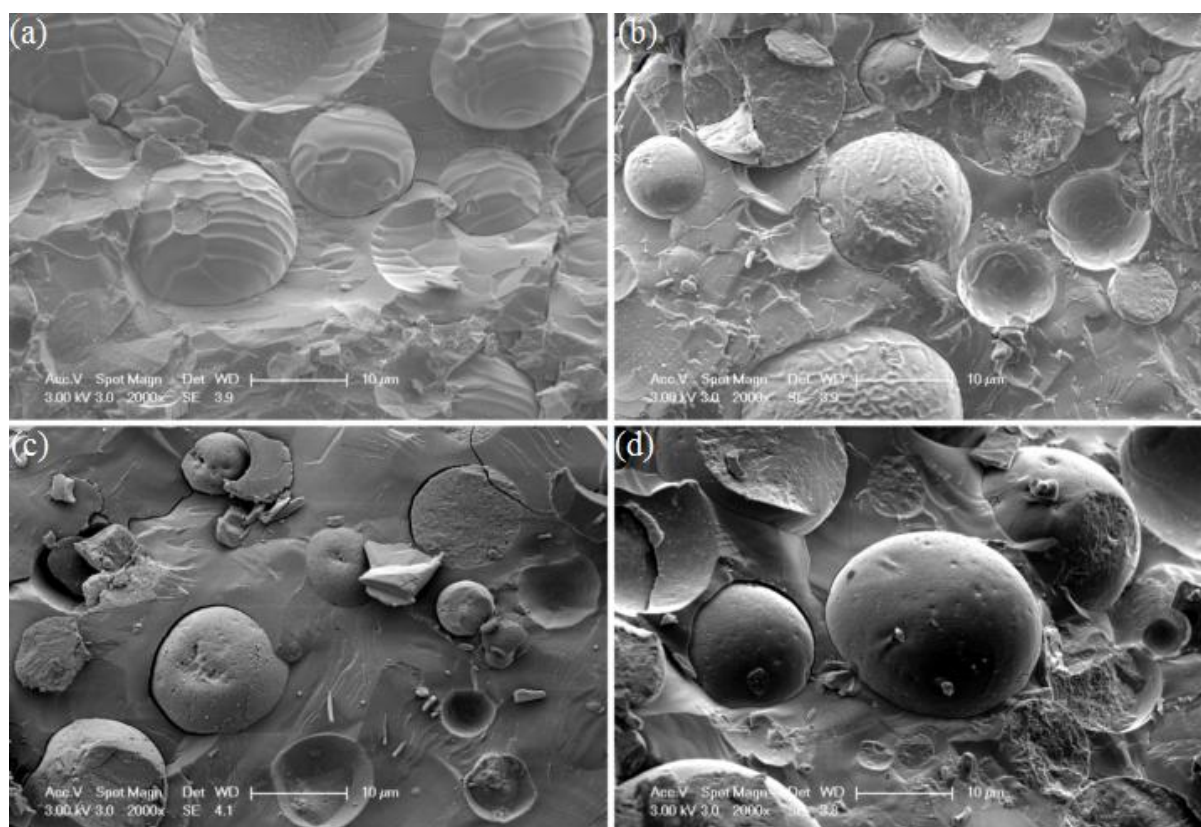


Fig. 4.7. Cryo-SEM micrographs of protein stabilised O/W pre-emulsions: (a) 1% Untreated BG stabilised emulsion, (b) 1% Ultrasound treated BG stabilised emulsion and (c) 1% Untreated SPI stabilised emulsion, (d) 1% Ultrasound treated SPI stabilised emulsion. Scale bar is 10 μm in all cases.

Emulsion droplets of pre-emulsions prepared with untreated BG (*cf.* Fig. 4.7 a) show fibres of gelatin tracking around the surface of the droplets whereas emulsion droplets of pre-emulsions prepared with ultrasound treated BG (*cf.* Fig. 4.7 b) show the smaller fibrils of gelatin at the interface of the droplets, yielding improved interfacial packing of protein, accounting for the lower equilibrium interfacial tension (*cf.* Fig. 4.6 a) and the decrease in droplet size (*cf.* Fig. 4.5 a). The droplet surfaces of pre-emulsions prepared with ultrasound SPI (*cf.* Fig. 4.7 d) appear to be smoother by comparison to the seeming more textured droplet interfaces observed for pre-emulsions prepared with untreated SPI (*cf.* Fig. 4.7 c). These findings are consistent with the interfacial tension data (*cf.* Fig. 4.6), where a significant reduction ($P < 0.05$) of the equilibrium interfacial tension upon sonication of BG

and SPI was observed, and accounted for by visualisation of the improved interfacial packing of protein.

The stability of oil-in-water emulsions prepared with untreated and sonicated proteins, and Brij 97 for comparative purposes, was assessed over a 28 day period. Fig. 4.8 shows the development of droplet size ($d_{3,2}$) as a function of time for emulsions prepared with untreated and ultrasound irradiated BG, FG, PPI and SPI, as well as Brij 97, at an emulsifier concentration of 0.1 wt. %.

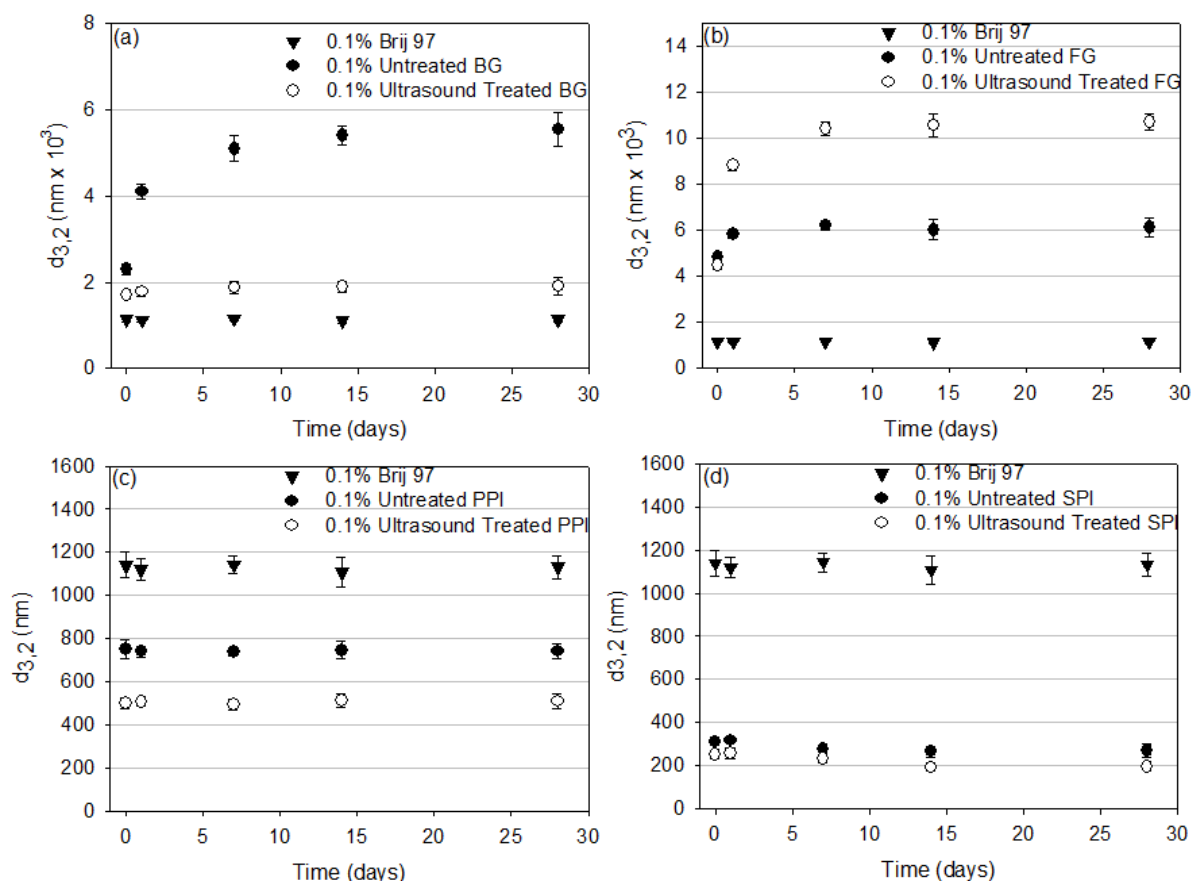


Fig. 4.8. Effect of emulsifier type on droplet size as a function of time for O/W emulsions stabilised by: (a) Untreated BG, ultrasound treated BG and Brij 97, (b) Untreated FG, ultrasound treated FG and Brij 97, (c) Untreated PPI, ultrasound treated PPI and Brij 97, and (d) Untreated SPI, ultrasound treated SPI and Brij 97.

Emulsions prepared with untreated BG (*cf.* Fig. 4.8 a) exhibited a growth in droplet size, and this coalescence was also observed for emulsions prepared with 0.5 wt. % untreated

BG, while emulsions prepared with higher concentrations (≥ 1 wt. %) of untreated BG were stable for the 28 days of the study. However, it can also be seen (*cf.* Fig. 4.8 a) that emulsions prepared with ultrasound treated BG were resistant to coalescence over the 28 days of the study, and had the same stability of Brij 97. The behaviour exhibited by 0.1 wt. % ultrasound treated BG was observed at all concentrations investigated in this study. This improved stability of ultrasound treated BG by comparison to untreated BG is thought to be associated with an increase in the hydrophobicity (*i.e.* decrease in the intrinsic viscosity; *cf.* Table 4.4) and improved interfacial packing of ultrasound treated BG by comparison to untreated BG as observed by a decrease in the equilibrium interfacial tension (*cf.* Fig. 4.6 a) and cryo-SEM visualisation (*cf.* Fig. 4.7 a, b).

In contrast, results in Fig 4.8 b show that emulsions prepared with both untreated and ultrasound treated FG display coalescence, yet ultrasound treated FG displayed a notable decrease in emulsion stability by comparison to untreated FG. The emulsion stability of untreated and ultrasound treated FG is analogous to untreated BG, where coalescence was observed at a concentration of 0.5 wt. %, and stable emulsions were achieved with higher emulsifier concentrations (≥ 1 wt. %). This decrease in emulsion stability after ultrasound treatment of FG is thought to be associated with a weaker interfacial layer of ultrasound treated FG by comparison to untreated FG allowing for a greater degree of coalescence, accounting for the decrease in emulsion stability.

Emulsions prepared with either untreated or sonicated EWP, PPI (*cf.* Fig. 4.8 c), SPI (*cf.* Fig. 4.8 d) and RPI, and Brij 97 (*cf.* Fig 4.8) were all stable against coalescence and bridging flocculation over the 28 days of this study. This stability was observed for all concentrations probed in this study (≥ 0.5 wt. %) of untreated and ultrasound treated EWP, PPI, SPI and RPI investigated, as well as for Brij 97. In all cases no phase separation was observed in the emulsions, whilst emulsions with droplet sizes $> 1 \mu\text{m}$ exhibited gravitational

separation with a cream layer present one day after preparation. Furthermore, the $d_{3,2}$ is lower in all cases at an emulsifier concentration of 0.1wt. % for ultrasound treated proteins by comparison to that of their untreated counterparts, as previously discussed.

4.5. Conclusions

This study showed that ultrasound treatment (20 kHz, $\sim 34 \text{ W cm}^{-2}$ for 2 min) of the three animal and three vegetable proteins significantly ($P < 0.05$) reduced aggregate size and hydrodynamic volume, with the exception of RPI. The reduction in protein size was attributed to the hydrodynamic shear forces associated with ultrasonic cavitations. In spite of the aggregate size reduction, no differences in primary structure molecular weight profile were observed between untreated and ultrasound irradiated BG, FG, EWP, PPI, SPI and RPI.

Emulsions prepared with the ultrasound treated FG, SPI and RPI proteins had the same droplet sizes as those obtained with their untreated counterparts, and were stable at the same concentrations, with the exception of emulsions prepared with ultrasound treated FG where a reduced emulsion stability at lower concentrations ($< 1 \text{ wt. } \%$) was exhibited. These results suggest that sonication did not significantly affect the rate of FG or RPI surface denaturation at the interface, as no significant ($P > 0.05$) reduction in the equilibrium interfacial tension between untreated and ultrasound irradiated FG or RPI was observed.

In comparison, emulsions fabricated with ultrasound treated BG, EWP and PPI at concentrations $< 1 \text{ wt. } \%$ had smaller emulsion sizes than their untreated counterparts at the same concentrations. This behaviour was attributed to a reduction in protein aggregate size (*i.e.* increased mobility through the bulk) and an increase in the hydrophobicity (reflected by a decrease in the intrinsic viscosity) of sonicated BG, EWP and PPI. Furthermore, emulsions prepared with ultrasound treated BG had improved stability against coalescence for 28 days at all concentrations investigated. This enhancement in emulsion stability was attributed to

improved interfacial packing, observed by a lower equilibrium interfacial tension and cryo-SEM micrographs.

Ultrasound treatment can thus improve the solubility of previously poorly soluble untreated vegetable proteins (PPI and SPI) and moreover, is capable of improving the emulsifying performance of other proteins (BG, EWP and PPI).

4.6. References

- Achouri, A., Zamani, Y., & Boye, J. I. (2012). Stability and Physical Properties of Emulsions Prepared with and without Soy Proteins. *Journal of Food Research*, 1(1), 254–267.
- Agboola, S., Ng, D., & Mills, D. (2005). Characterisation and functional properties of Australian rice protein isolates. *Journal of Cereal Science*, 41(3), 283–290.
- Anton, M., Nau, F., & Lechevalier, V. (2009). Egg proteins. In G. O. Philips & P. A. Williams (Eds.), *Handbook of Hydrocolloids* (2nd ed., pp. 359 – 382). Woodhead Publishing Limited.
- Arzeni, C., Martínez, K., Zema, P., Arias, A., Pérez, O. E., & Pilosof, A. M. R. (2012). Comparative study of high intensity ultrasound effects on food proteins functionality. *Journal of Food Engineering*, 108(3), 463–472.
- Arzeni, C., Pérez, O. E., & Pilosof, A. M. R. (2012). Functionality of egg white proteins as affected by high intensity ultrasound. *Food Hydrocolloids*, 29(2), 308–316.
- Behrouzian, F., Razavi, S. M. A., & Karazhiyan, H. (2014). Intrinsic viscosity of cress (*Lepidium sativum*) seed gum: Effect of salts and sugars. *Food Hydrocolloids*, 35(0), 100–105.
- Beverung, C. J., Radke, C. J., & Blanch, H. W. (1999). Protein adsorption at the oil/water interface: characterization of adsorption kinetics by dynamic interfacial tension measurements. *Biophysical Chemistry*, 81(1), 59–80.
- Boye, J., Zare, F., & Pletch, A. (2010). Pulse proteins: Processing, characterization, functional properties and applications in food and feed. *Food Research International*, 43(2), 414–431.
- Caetano da Silva Lannes, S., & Natali Miquelim, J. (2013). Interfacial Behavior of Food Proteins. *Current Nutrition & Food Science*, 9(1), 10–14.
- Cao, X., Wen, H., Li, C., & Gu, Z. (2009). Differences in functional properties and biochemical characteristics of congenetic rice proteins. *Journal of Cereal Science*, 50(2), 184–189.

- Chemat, F., Zill-e-Huma, & Khan, M. K. (2011). Applications of ultrasound in food technology: Processing, preservation and extraction. *Ultrasonics Sonochemistry*, 18(4), 813–35.
- Chrastil, J. (1992). Correlations between the physicochemical and functional properties of rice. *Journal of Agricultural and Food Chemistry*®, 40(9), 1683–1686.
- Curvale, R., Masuelli, M., & Padilla, A. P. (2008). Intrinsic viscosity of bovine serum albumin conformers. *International Journal of Biological Macromolecules*, 42(2), 133–7.
- Damodaran, S. (1997). Protein-stabilized foams and emulsions. In S. Damodaran & A. Paraf (Eds.), *Food Proteins and Their Applications* (1st ed., pp. 57–110). New York: Marcel Dekker.
- Damodaran, S., & Razumovsky, L. (2008). Role of surface area-to-volume ratio in protein adsorption at the air–water interface. *Surface Science*, 602(1), 307–315.
- Delpech, M. C., & Oliveira, C. M. F. (2005). Viscometric study of poly(methyl methacrylate-g-propylene oxide) and respective homopolymers. *Polymer Testing*, 24(3), 381–386.
- Dickinson, E. (1999). Caseins in emulsions: interfacial properties and interactions. *International Dairy Journal*, 9(3-6), 305–312.
- Donsì, F., Senatore, B., Huang, Q., & Ferrari, G. (2010). Development of novel pea protein-based nanoemulsions for delivery of nutraceuticals. *Journal of Agricultural and Food Chemistry*, 58(19), 10653–60.
- Duconseille, A., Astruc, T., Quintana, N., Meersman, F., & Sante-Lhoutellier, V. (2015). Gelatin structure and composition linked to hard capsule dissolution: A review. *Food Hydrocolloids*, 43, 360-376.
- Foegeding, E. A., & Davis, J. P. (2011). Food protein functionality: A comprehensive approach. *Food Hydrocolloids*, 25(8), 1853–1864.
- Gaonkar, A. G. (1989). Interfacial tensions of vegetable oil/water systems: Effect of oil purification. *Journal of the American Oil Chemists' Society*, 66(8), 1090–1092.
- Gaonkar, A. G. (1991). Surface and interfacial activities and emulsion characteristics of some food hydrocolloids. *Food Hydrocolloids*, 5(4), 329–337.
- García De La Torre, J., Huertas, M. L., & Carrasco, B. (2000). Calculation of hydrodynamic properties of globular proteins from their atomic-level structure. *Biophysical Journal*, 78(2), 719–30.

- Gharsallaoui, A., Saurel, R., Chambin, O., & Voilley, A. (2011). Pea (*Pisum sativum*, L.) Protein Isolate Stabilized Emulsions: A Novel System for Microencapsulation of Lipophilic Ingredients by Spray Drying. *Food and Bioprocess Technology*, 5(6), 2211–2221.
- Gonzalez-Perez, S., & Arellano, J. B. (2009). Vegetable protein isolates. In G. O. Philips & P. A. Williams (Eds.), *Handbook of Hydrocolloids* (2nd ed., pp. 383 – 419). Woodhead Publishing Limited.
- Gouinlock, E. V., Flory, P. J., & Scheraga, H. A. (1955). Molecular configuration of gelatin. *Journal of Polymer Science*, 16(82), 383–395.
- Guraya, H. S., & James, C. (2002). Deagglomeration of Rice Starch-Protein Aggregates by High-Pressure Homogenization. *Starch - Stärke*, 54(3-4), 108–116.
- Güzey, D., Gülseren, İ., Bruce, B., & Weiss, J. (2006). Interfacial properties and structural conformation of thermosonicated bovine serum albumin. *Food Hydrocolloids*, 20(5), 669–677.
- Hamaker, B. R. (1994). The Influence of Rice Protein on Rice Quality. In W. E. Marshall & J. I. Wadsworth (Eds.), *Rice Science and Technology* (1st ed., pp. 177–194). New York: Marcel Dekker.
- Harding, S. E. (1997). The intrinsic viscosity of biological macromolecules. Progress in measurement, interpretation and application to structure in dilute solution. *Progress in Biophysics and Molecular Biology*, 68(2–3), 207–262.
- Haug, I. J., & Draget, K. I. (2009). Gelatin. In G. O. Philips & P. A. Williams (Eds.), *Handbook of Hydrocolloids* (2nd ed., pp. 142 – 163). Woodhead Publishing Limited.
- Haug, I. J., Draget, K. I., & Smidsrød, O. (2004). Physical and rheological properties of fish gelatin compared to mammalian gelatin. *Food Hydrocolloids*, 18(2), 203–213.
- Hu, H., Wu, J., Li-Chan, E. C. Y., Zhu, L., Zhang, F., Xu, X., Gang, F., Lufeng, W., Xingjian, H., & Pan, S. (2013). Effects of ultrasound on structural and physical properties of soy protein isolate (SPI) dispersions. *Food Hydrocolloids*, 30(2), 647–655.
- Huggins, M. L. (1942). The Viscosity of Dilute Solutions of Long-Chain Molecules. IV. Dependence on Concentration. *Journal of the American Chemical Society*, 64(11), 2716–2718.
- Jambrak, A. R., Lelas, V., Mason, T. J., Krešić, G., & Badanjak, M. (2009). Physical properties of ultrasound treated soy proteins. *Journal of Food Engineering*, 93(4), 386–393.
- Ju, Z. Y., Hettiarachchy, N. S., & Rath, N. (2001). Extraction, denaturation and hydrophobic Properties of Rice Flour Proteins. *Journal of Food Science*, 66(2), 229–232.
- Juliano, B. O. (1985). *Rice: Chemistry and Technology* (p. 774). American Association of Cereal Chemists. Retrieved from

- Karki, B., Lamsal, B. P., Grewell, D., Pometto, A. L., Leeuwen, J., Khanal, S. K., & Jung, S. (2009). Functional Properties of Soy Protein Isolates Produced from Ultrasonicated Defatted Soy Flakes. *Journal of the American Oil Chemists' Society*, 86(10), 1021–1028.
- Karki, B., Lamsal, B. P., Jung, S., van Leeuwen, J. (Hans), Pometto III, A. L., Grewell, D., & Khanal, S. K. (2010). Enhancing protein and sugar release from defatted soy flakes using ultrasound technology. *Journal of Food Engineering*, 96(2), 270–278.
- Khan, A., Bibi, I., Pervaiz, S., Mahmood, K., & Siddiq, M. (2012). Surface Tension, Density and Viscosity Studies on the Associative Behaviour of Oxyethylene-Oxybutylene Diblock Copolymers in Water at Different Temperatures. *International Journal of Organic Chemistry*, 02(01), 82–92.
- Knorr, D., Zenker, M., Heinz, V., & Lee, D.-U. (2004). Applications and potential of ultrasonics in food processing. *Trends in Food Science & Technology*, 15(5), 261–266.
- Kraemer, E. O. (1938). Molecular Weights of Celluloses and Cellulose Derivates. *Industrial & Engineering Chemistry*, 30(10), 1200–1203.
- Krise, K. M. (2011). *The effects of microviscosity, bound water and protein mobility on the radiolysis and sonolysis of hen egg white. PhD Thesis.*
- Lam, R. S. H., & Nickerson, M. T. (2013). Food proteins: A review on their emulsifying properties using a structure–function approach. *Food Chemistry*, 141(2), 975–984.
- Lefebvre, J. (1982). Viscosity of concentrated protein solutions. *Rheologica Acta*, 21(4-5), 620–625.
- Liang, H.-N., & Tang, C. (2014). Pea protein exhibits a novel Pickering stabilization for oil-in-water emulsions at pH 3.0. *LWT - Food Science and Technology*, 58(2), 463–469.
- Margulis, M. A., & Margulis, I. M. (2003). Calorimetric method for measurement of acoustic power absorbed in a volume of a liquid. *Ultrasonics Sonochemistry*, 10(6), 343–345.
- Marshall, W. E., & Wadsworth, J. . (1994). *Rice Science and Technology*. New York, USA: Marcel Dekker.
- McClements, D. J. (1995). Advances in the application of ultrasound in food analysis and processing. *Trends in Food Science & Technology*, 6(9), 293–299.
- McClements, D. J. (2004). Protein-stabilized emulsions. *Current Opinion in Colloid & Interface Science*, 9(5), 305–313.
- McClements, D. J. (2005). *Food Emulsions: Principles, Practices, and Techniques* (2nd ed.). CRC Press.
- McClements, D. J. (2009). *Biopolymers in Food Emulsions. Modern Biopolymer Science* (First Edit., pp. 129–166). Elsevier Inc.

- Messens, W., Van Camp, J., & Huyghebaert, A. (1997). The use of high pressure to modify the functionality of food proteins. *Trends in Food Science & Technology*, 8(4), 107–112.
- Mine, Y. (2002). Recent advances in egg protein functionality in the food system. *World Poultry Science Journal*, 58(1), 31-39.
- Molina, E., Defaye, A. B., & Ledward, D. A. (2002). Soy protein pressure-induced gels. *Food Hydrocolloids*, 16(6), 625–632.
- Morris, E. R., Cutler, A. N., Ross-Murphy, S. B., Rees, D. A., & Price, J. (1981). Concentration and shear rate dependence of viscosity in random coil polysaccharide solutions. *Carbohydrate Polymers*, 1, 5–21.
- Mujoo, R., Chandrashekar, A., & Zakiuddin Ali, S. (1998). Rice Protein Aggregation During the Flaking Process. *Journal of Cereal Science*, 28(2), 187–195.
- O'Brien, W. D. (2007). Ultrasound-biophysics mechanisms. *Progress in Biophysics and Molecular Biology*, 93(1-3), 212–55. doi
- O'Connell, J. E., & Flynn, C. (2007). The Manufacture and Application of Casein-Derived Ingredients. In Y. H. Hui (Ed.), *Handbook of Food Products Manufacturing* (1st ed., pp. 557 – 593). New Jersey: John Wiley & Sons.
- O'Connell, J. E., Grinberg, V. Y., & de Kruijff, C. G. (2003). Association behavior of β -casein. *Journal of Colloid and Interface Science*, 258(1), 33–39.
- O'Donnell, C. P., Tiwari, B. K., Bourke, P., & Cullen, P. J. (2010). Effect of ultrasonic processing on food enzymes of industrial importance. *Trends in Food Science & Technology*, 21(7), 358–367.
- O'Sullivan, J., Arellano, M., Pichot, R., & Norton, I. (2014). The Effect of Ultrasound Treatment on the Structural, Physical and Emulsifying Properties of Dairy Proteins. *Food Hydrocolloids*, 42(3), 386–396.
- O'Sullivan, J., Pichot, R., & Norton, I. T. (2014). Protein Stabilised Submicron Emulsions. In P. A. Williams & G. O. Phillips (Eds.), *Gums and Stabilisers for the Food Industry 17* (pp. 223–229). Cambridge, UK: The Royal Society of Chemistry.
- Pamies, R., Hernández Cifre, J. G., del Carmen López Martínez, M., & García de la Torre, J. (2008). Determination of intrinsic viscosities of macromolecules and nanoparticles. Comparison of single-point and dilution procedures. *Colloid and Polymer Science*, 286(11), 1223–1231.
- Peng, I. C., Quass, D. W., Dayto, W. R., & Allen, C. E. (1984). The Physicochemical and Functional Properties of Soybean 11S Globulin---A Review. *Cereal Chemistry*, 61, 480–490.
- Prakash, V. (1994). Structural similarity among proteins from oil seeds: An overview. *Journal of Scientific and Industrial Research*, 53(9), 684–691.

- Romero, A., Beaumal, V., David-Briand, E., Cordobes, F., Guerrero, A., & Anton, M. (2012). Interfacial and emulsifying behaviour of rice protein concentrate. *Food Hydrocolloids*, 29(1), 1–8.
- Saharan, K., & Khetarpaul, N. (1994). Protein quality traits of vegetable and field peas: varietal differences. *Plant Foods for Human Nutrition (Dordrecht, Netherlands)*, 45(1), 11–22.
- Sakurai, K., Konuma, T., Yagi, M., & Goto, Y. (2009). Structural dynamics and folding of beta-lactoglobulin probed by heteronuclear NMR. *Biochimica et Biophysica Acta*, 1790(6), 527–37.
- Schrieber, R., & Gareis, H. (2007). *Gelatine Handbook - Theory and Industrial Practice* (1st ed., pp. 1 – 348). Wiley-Blackwell.
- Shewry, P. R., Napier, J. A., & Tatham, A. S. (1995). Seed storage proteins: structures and biosynthesis. *The Plant Cell*, 7(7), 945–56.
- Sorgentini, D. A., Wagner, J. R., & Aiudin, M. C. (1995). Effects of Thermal Treatment of Soy Protein Isolate on the Characteristics and Structure-Function Relationship of Soluble and Insoluble Fractions, 2471–2479.
- Sousa, I. M. N., Mitchell, J. R., Hill, S. E., & Harding, S. E. (1995). Intrinsic Viscosity and Mark-Houwink Parameters of Lupin Proteins in Aqueous Solutions. *Les Cahiers de Rhéologie*, 14, 139–148.
- Sun, X. D., & Arntfield, S. D. (2012). Molecular forces involved in heat-induced pea protein gelation: Effects of various reagents on the rheological properties of salt-extracted pea protein gels. *Food Hydrocolloids*, 28(2), 325–332.
- Surh, J., Decker, E., & McClements, D. (2006). Properties and stability of oil-in-water emulsions stabilized by fish gelatin. *Food Hydrocolloids*, 20(5), 596–606.
- Tang, C.-H., & Ma, C.-Y. (2009). Effect of high pressure treatment on aggregation and structural properties of soy protein isolate. *LWT - Food Science and Technology*, 42(2), 606–611.
- Tanner, R., & Rha, C. (1980). Hydrophobic Effect on the Intrinsic Viscosity of Globular Proteins. In G. Astarita, G. Marrucci, & L. Nicolais (Eds.), *In Rheology, Volume 2: Fluids* (pp. 277–283). Boston, MA: Springer US.
- Van der Plancken, I., Van Loey, A., & Hendrickx, M. E. (2006). Effect of heat-treatment on the physico-chemical properties of egg white proteins: A kinetic study. *Journal of Food Engineering*, 75(3), 316–326.
- Veis, A. (1964). *Macromolecular Chemistry of Gelatin* (1st ed.). New York: Academic Press.
- Vose, J. R. (1980). Production and functionality of starches and protein isolates from legume seeds. *Cereal Chemistry*, 57, 406–410.

- Walstra, P., & van Vliet, T. (2003). Chapter II Functional properties. In R. J. H. W.Y. Aalbersberg P. Jasperse, H.H.J. de Jongh, C.G. de Kruif, P. Walstra and F.A. de Wolf BT - Progress in Biotechnology (Ed.), *Industrial Proteins in Perspective* (Vol. Volume 23, pp. 9–30). Elsevier.
- Yilgor, I., Ward, T. C., Yilgor, E., & Atilla, G. E. (2006). Anomalous dilute solution properties of segmented polydimethylsiloxane–polyurea copolymers in isopropyl alcohol. *Polymer*, 47(4), 1179–1186.
- Zhang-Cun, W., Wei-Huan, T., Sheng-Wen, C., Xue-Wei, Z., Jian-Qiang, Z., Chang-Wen, L., & Dao-Qiang, Y. (2013). Effects of High Hydrostatic Pressure on the Solubility and Molecular Structure of Rice Protein. *Chinese Journal of High Pressure Physics*.

Chapter 5. Comparison of batch and continuous ultrasonic emulsification processes

Data and discussions contained within this chapter have been submitted for publication within:

O'Sullivan, J.J., Murray, B.A., Flynn, C. and Norton, I.T. 2015. Comparison of batch and continuous ultrasonic emulsification processes. *Journal of Food Engineering*.

Data and discussions contained within this chapter have been in part submitted for publication within:

O'Sullivan, J.J. and Norton, I.T. 2016. Novel ultrasonic emulsification technologies, *Gums and stabilisers for the food industry*, 18.

5.1. Abstract

Batch and continuous ultrasonic emulsification processes on both lab and pilot scales were investigated using Tween 80, milk protein isolate (MPI) or pea protein isolate (PPI) as emulsifiers. The process parameters of processing volume, residence time and ultrasonic amplitude, as well as emulsion formulations, emulsifier type and concentration, were studied for the effect on emulsion droplet size. Emulsions prepared with ultrasound yielded submicron droplets, ~150 nm, with Tween 80, MPI and PPI, utilising all processing methodologies. Inverse power laws were obtained correlating emulsion droplet size with respect to energy density, highlighting the efficiency of the continuous over batch processing. This efficiency is ascribed to the smaller processing volumes, associated with continuous ultrasonic emulsification. Longer processing times were required for MPI and PPI to achieve submicron droplets (< 200 nm) in comparison to Tween 80 as greater times are necessary for interfacial adsorption and surface stabilisation, shown by interfacial tension measurements.

5.2. Introduction

Low frequency (≤ 100 kHz), high power (> 10 W cm⁻²) ultrasound is a versatile technology widely utilised within the food industry for the alteration and generation of microstructures (McClements, 1995). It is a long established technique for the preparation of emulsions (Bondy & Söllner, 1935). Sonication readily produces submicron droplets when using low molecular weight surfactants (Abisma l *et al.*, 1999). Submicron dispersed phase droplets confer several advantages over larger droplets, including an increase in the bioavailability of lipophilic components and a surface area for controlled release. Increased emulsion stability due to reduced creaming or sedimentation which limits aggregation and coalescence enhances the commercial shelf life (McClements, 2011; O'Sullivan *et al.*, 2014).

Ultrasound treatment of liquid media operates through the generation of cavitation bubbles due to pressure differentials during acoustic wave propagation (Servant *et al.*, 2001). Cavitation bubbles disperse and attenuate ultrasonic waves due to the acoustic impedance differential between the liquid and gaseous phases, resulting in either partial or complete scattering of the acoustic waves (McClements, 1995). Systems containing many bubbles exhibit multiple scattering as the bubbles behave like mirrors, causing reflection of the acoustic wave and an effective increase in the absorption of acoustic energy (Juliano *et al.*, 2011; McClements & Povey, 1989). Cavitations are concentrated in the volume at the tip of the sonotrode, this localisation results in high levels of energy input (Martini, 2013; Trujillo & Knoerzer, 2011a). Given the high number of cavitations within the vicinity of the tip of the sonotrode, higher attenuation (*i.e.* gradual loss of intensity) levels are observed and are dominated by acoustic scattering. The acoustic intensity decays exponentially with increasing distance from the sonotrode tip, effectively dissipated at distances as low as 1 cm from the tip (Chivate & Pandit, 1995). Ultrasonic cavitations are highly unstable entities prone to rapid collapse creating highly localised regions of hydrodynamic shear (O'Donnell *et al.*, 2010).

These acoustically induced cavitations result in the disruption of micron sized dispersed phase droplets and facilitate the formation of submicron emulsion droplets (Gogate *et al.*, 2011).

Emulsification utilising ultrasonic technologies has been a field of growing interest over the past decade, with extensive investigations conducted upon the process parameters (*i.e.* contact time with the acoustic field, ultrasonic power, volume processed, etc.), in addition to emulsion formulations (Jafari *et al.*, 2007; Kentish *et al.*, 2008). Low molecular weight emulsifiers (*i.e.* surfactants) have predominantly been utilised as part of these studies. To date, there is a lack of literature on the use of industrially relevant high molecular weight emulsifiers (*i.e.* proteins). The work of Kaltsa *et al.* (2013) on whey protein and Heffernan *et al.* (2011) on sodium caseinate show that the formation of submicron emulsions via batch ultrasonic emulsification is possible. No systematic investigations of process parameters or continuous methods using proteins as emulsifiers with ultrasound are currently available.

The objective of this research was to understand the influence of ultrasonic process parameters and emulsion formulation, emulsifier type and concentration, on the microstructure of oil-in-water emulsions (*i.e.* Sauter mean diameter, $d_{3,2}$). The efficacy of batch and continuous process configurations for the production of submicron emulsions with industrially relevant ingredients using low frequency, high power ultrasound was assessed. Comparisons between batch and continuous processing were explored in terms of processing time within the acoustic field, acoustic power and processing volume. The effect of emulsifier type, was investigated with a low molecular weight surfactant (Tween 80) and high molecular weight biopolymer (milk protein isolate and pea protein isolate), over a range of concentrations to assess the performance of these ingredients as emulsifiers during the sonication process.

5.3. Materials and methodology

5.3.1. Materials

Milk protein isolate (MPI), a composite mixture of ~80% micellar casein and ~20% whey protein (Fox, 2008), and pea protein isolate (PPI) were both kindly provided by Kerry Ingredients and Flavours (Listowel, Ireland). The composition of these proteins is provided in Table 5.1. Tween 80 and sodium azide were purchased from Sigma Aldrich (UK). The oil used in this study was commercially available rapeseed oil. The water used in all experiments was passed through a double distillation unit (A4000D, Aquatron, UK).

Table 5.1. Composition and pH of milk protein isolate (MPI) and pea protein isolate (PPI)

	MPI	PPI
Protein (wt. %)	86	86
Moisture (wt. %)	4	7.2
Fat (wt. %)	1.5	0
Carbohydrate (-)	1	pos.
Ash (wt. %)	6	4.85
pH at a concentration of 1 wt. % (-)	6.74	7.45

5.3.2. Methods

5.3.2.1. Preparation of emulsifier solutions

Tween 80, MPI and PPI were dispersed in water at 40 °C for a minimum of three hours to obtain solutions at concentrations in the range of 0.1 – 3 wt. %. Tween 80 and MPI are completely soluble at these concentrations, whilst PPI exhibited a sedimenting component

irrespective of hydration time. Sodium azide (0.02 wt. %) was added to the solutions to diminish the microbial activity.

5.3.2.2. Ultrasonic processing and acoustic intensity determination

A lab scale ultrasonic processor (Viber Cell 750, Sonics, USA) with a stainless steel microtip ($d = 3$ mm; $S_A = 0.07$ cm²) was used for the preparation of emulsions using batch and continuous configurations, operating at 20 kHz. Continuous emulsification was further investigated with scale up trials utilising a pilot scale ultrasonic processor (UIP1000hd, Hielscher Ultrasonics GmbH, Germany) with a titanium tip ($d = 20$ mm; $S_A = 3.8$ cm²).

Emulsions were sonicated at different amplitudes to vary the acoustic power transmitted, whereby the lab and pilot scale ultrasonic processors operated within amplitude ranges of 20 – 40 % (maximum amplitude of 108 μ m) and 50 – 100 % (maximum amplitude of 57 μ m), respectively. The acoustic intensity (I_a) was determined calorimetrically by measuring the temperature rise of the sample as a function of time, under adiabatic conditions. The acoustic intensity, I_a (W cm⁻²), was calculated using Eq. 5.1 from Margulis & Margulis, (2003):

$$I_a = \frac{P_a}{S_A}, \text{ where } P_a = m c_p \left(\frac{dT}{dt} \right) \quad (5.1)$$

Where, P_a is the acoustic power (W), S_A is the surface area of the tip of the sonotrode (cm²), m is the mass of ultrasound treated medium (g), c_p is the specific heat of the medium (J g⁻¹ K⁻¹) and dT/dt is the rate of temperature change with respect to time of the medium (K s⁻¹), starting at $t = 0$. The temperature was measured by means of a digital thermometer (TGST3, Sensor-Tech Ltd., Ireland), with an accuracy of ± 0.1 K. The acoustic power (P_a) and acoustic intensity (I_a) for the lab scale and pilot scale ultrasonic processors are provided in Table 5.2, for the ultrasonic amplitudes employed during emulsification.

Table 5.2. Acoustic power (P_a) and acoustic intensity (I_a) for lab (Viber Cell 750) and pilot (UIP1000hd) scale ultrasonic processors.

Ultrasonic Processor	Amplitude (%)	Acoustic Power (W)	Acoustic Intensity (W cm^{-2})
Viber Cell 750	20	8.5	120.3
	30	19	269.1
	40	32	453.3
UIP1000hd	50	78	20.5
	60	98	25.7
	70	131	34.4
	80	164	43.2
	90	208	54.7
	100	234	61.6

5.3.2.3. Emulsion preparation and characterisation

10 wt. % of dispersed phase (rapeseed oil) was to added to the continuous phase containing either Tween 80 or MPI at concentrations, ranging from 0.1 - 3 wt. %. A coarse pre-emulsion was prepared via high shear mixing at 8,000 rpm for 2 minutes for lab and pilot scale trials, utilising SL2T and AXR Silverson mixers, respectively (Silverson, UK).

5.3.2.3.1. Batch configuration for ultrasonic emulsification

Lab scale batch ultrasonic processing (Viber Cell 750, Sonics, USA) was undertaken with the ultrasonic probe centrally located with an immersion depth of 3 mm in the pre-emulsion, with volumes ranging from 3 – 100 mL, sonication times from 1 – 300 s and ultrasonic amplitudes of 20 – 40 %.

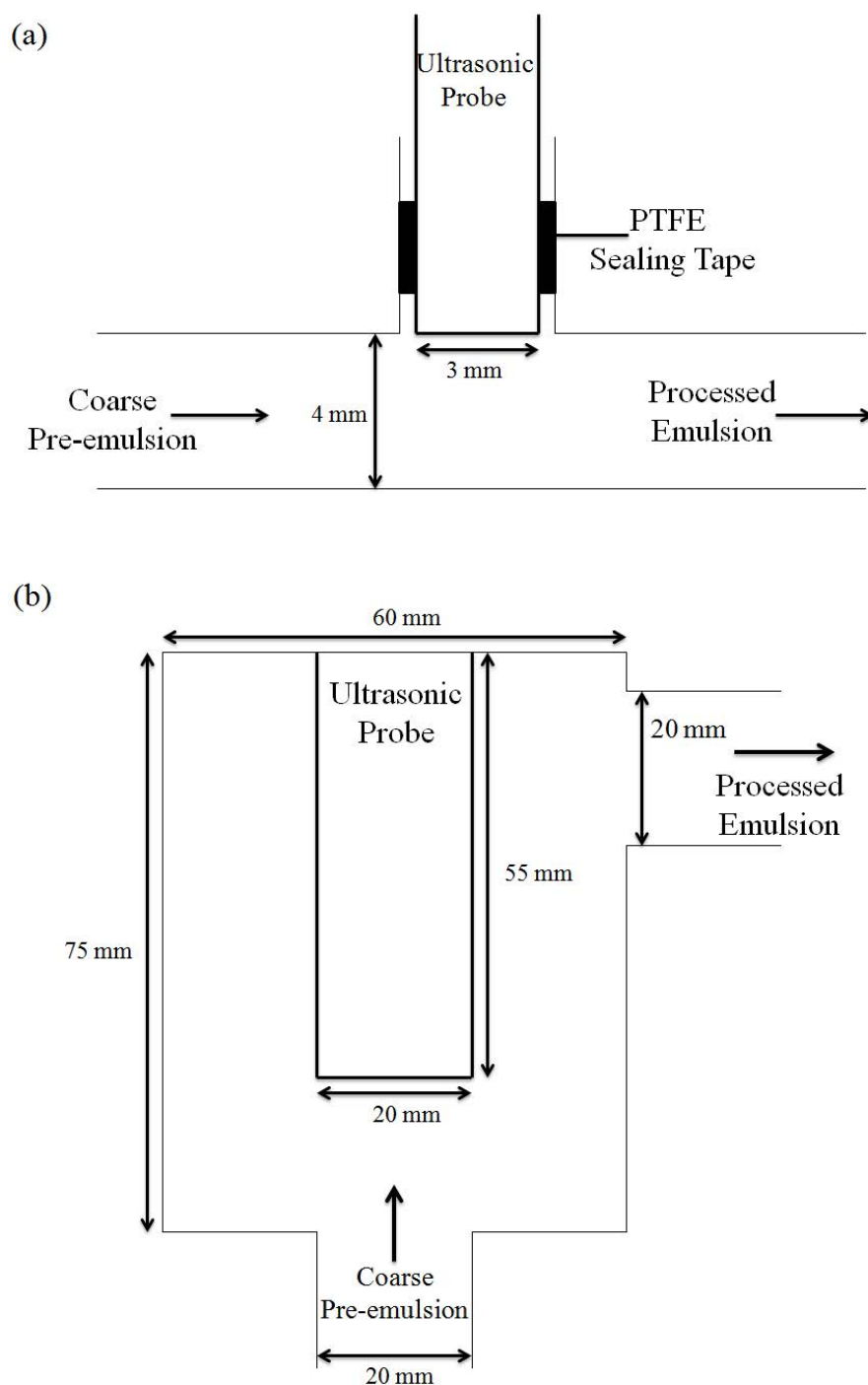


Fig. 5.1. Schematic of continuous ultrasonic emulsification setups for (a) lab scale and (b) pilot scale trials.

5.3.2.3.2. Continuous configuration for ultrasonic emulsification

Lab scale continuous processing (Viber Cell 750, Sonics, USA) was carried out by positioning the ultrasonic probe orthogonal to the path of flow of the pre-emulsion, using a brass tee junction with an internal diameter of 4 mm. The ultrasonic probe was positioned 4

mm from the base of the tee junction (*cf.* Fig. 5.1 a) and surrounded by ice to mitigate against heat gain. The pre-emulsion was pumped peristaltically (Masterflex L/S Digital Pump System with Easy-Load II Pump Head, Cole-Parmer, UK) with volumetric flow rates of 25 – 250 mL/min and an ultrasonic amplitude range of 20 – 40%.

Pilot scale continuous processing (UIP1000hd, Hielscher Ultrasonics GmbH, Germany) had the flow path of pre-emulsion in the same plane as the ultrasonic probe. The ultrasonic probe was positioned 20 mm from the inlet of the coarse emulsion and the outlet was positioned perpendicular to the sonotrode (*cf.* Fig. 5.1 b). The pre-emulsion was pumped centrifugally (Millipore, UK) with volumetric flow rates ranging from 2,700 – 5,700 mL/min (163 – 343 L/hr) with ultrasonic amplitudes of 50 – 100 %.

The residence time, t , which the pre-emulsion is within the acoustic field for both continuous processing methodologies is controlled by variation of the volumetric flowrate (Q), and is determined from *Eq. 5.2*:

$$t = V/Q \quad (5.2)$$

Where t is the residence time (s), V is the volume under the influence of the acoustic field (m^3) and Q is the volumetric flowrate ($\text{m}^3 \text{ s}^{-1}$). The volumes under the influence of the acoustic field for the lab and pilot scale continuous processes are $5 \times 10^{-8} \text{ m}^3$ and $6.3 \times 10^{-6} \text{ m}^3$, respectively. The residence times for pre-emulsions within the acoustic field for continuous processing in both lab and pilot scale ultrasonic processors are provided in Table 5.3.

5.3.2.3.3. Droplet size measurements

The droplet size of the emulsions was measured by laser diffraction using a Mastersizer 2000 (Malvern Instruments, UK) immediately after emulsification. Emulsion

droplet size values are reported as the surface mean diameter (Sauter mean diameter; $d_{3,2} = \Sigma n_i d_i^3 / \Sigma n_i d_i^2$), where n_i is the number of droplets of diameter d_i .

Table 5.3. Residence times (t) of pre-emulsion within acoustic field for lab (Viber Cell 750) and pilot (UIP1000hd) scale ultrasonic processors with respect to volumetric flowrate (Q).

Ultrasonic processor	Volumetric flowrate (mL/min)	Residence time (ms)
Viber Cell 750	25	120
	50	60
	100	30
	150	20
	200	15
	250	12
UIP1000hd	2,700	140
	4,500	84
	5,700	66.3

5.3.2.3.4. Interfacial tension measurements

The interfacial tension between the aqueous phases (pure water, low molecular weight surfactant, or high molecular weight biopolymer solutions) and the oil phase (rapeseed oil) was measured using a tensiometer K100 (Krüss, Germany) with the Wilhelmy plate method, as detailed by O’Sullivan *et al.*, (2015). The interfacial tension values and the error bars are reported as the mean and standard deviation, respectively, of three repeat measurements.

5.3.3. Statistical analysis

Student's t-test, a statistical hypothesis test, with a 95% confidence interval was used to assess the significance of the results obtained. t-test data with $P < 0.05$ were considered statistically significant.

5.4. Results and discussions

5.4.1. Comparison of lab scale batch and continuous configurations for effect of processing time and ultrasonic power

The effect of processing size for lab batch configuration for a fixed ultrasonic amplitude and emulsifier concentration upon emulsion droplet size was initially investigated. Fig. 5.2 shows pre-emulsions prepared with 1.5 wt. % Tween 80 which were sonicated with an ultrasonic amplitude of 40 % (*i.e.* 453.3 W cm⁻²). Droplet size measurements as a function of processing time, from 0 to 300 s, and batch sizes from 3 to 150 g.

Increasing the processing time of batch ultrasonic homogenisation results in a decrease in the resultant emulsion droplet size regardless of batch size, this has also been reported by Abisma I *et al.*, (1999) and Jafari *et al.*, (2007). The time required to achieve the minimum droplet size is a function of the processing volume, larger batch sizes require prolonged processing times to achieve the minimum droplet size which has been shown by Maa & Hsu (1999). Ultrasonic processing of smaller volumes is more efficient as the acoustic energy emanated from the tip of the sonotrode is absorbed more intensely resulting in more rapid size reduction. This volume effect arises from the complete dissipation of acoustic intensity at distances as low as 1 cm from the tip (Chivate & Pandit, 1995) highlighting the importance of ultrasonic tip location for effective processing (Gogate *et al.*, 2011).

The effect of residence time of pre-emulsion within the acoustic field at the lab scale with respect to continuous processing is presented in Fig. 5.3, this was achieved by variation of the volumetric flow rate to alter the acoustic residence time. Pre-emulsions with 1.5 wt. % Tween 80 were sonicated with an ultrasonic amplitude of 40 % (*i.e.* 453.3 W cm⁻²). Droplet size changes as a function of residence time for lab scale continuous ultrasonic processing is shown in Fig. 5.3.

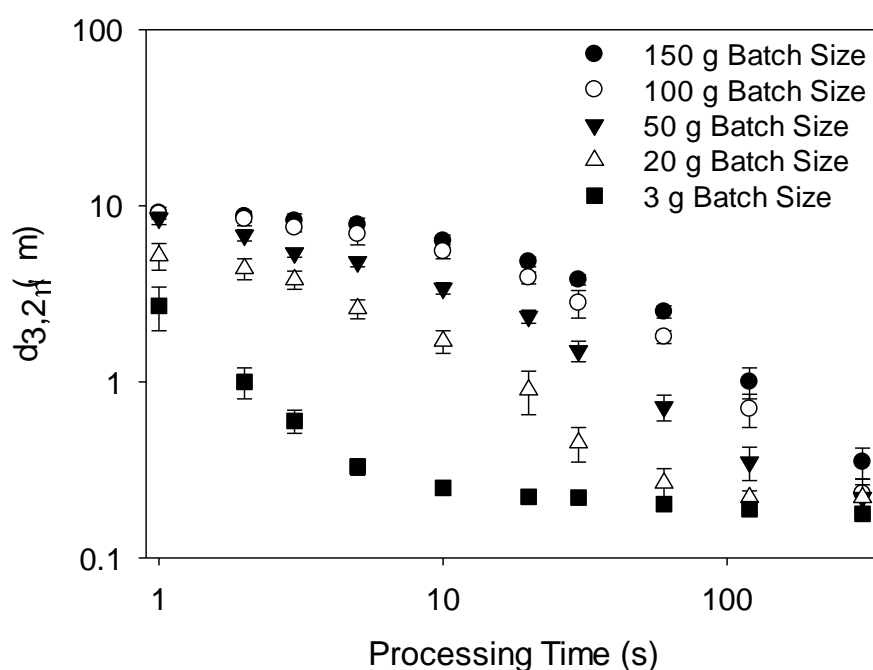


Fig. 5.2. Effect of batch size and ultrasonic processing time on droplet size ($d_{3,2}$) of emulsions stabilised with 1.5 wt. % Tween 80 prepared employing lab scale batch ultrasonic homogenisation.

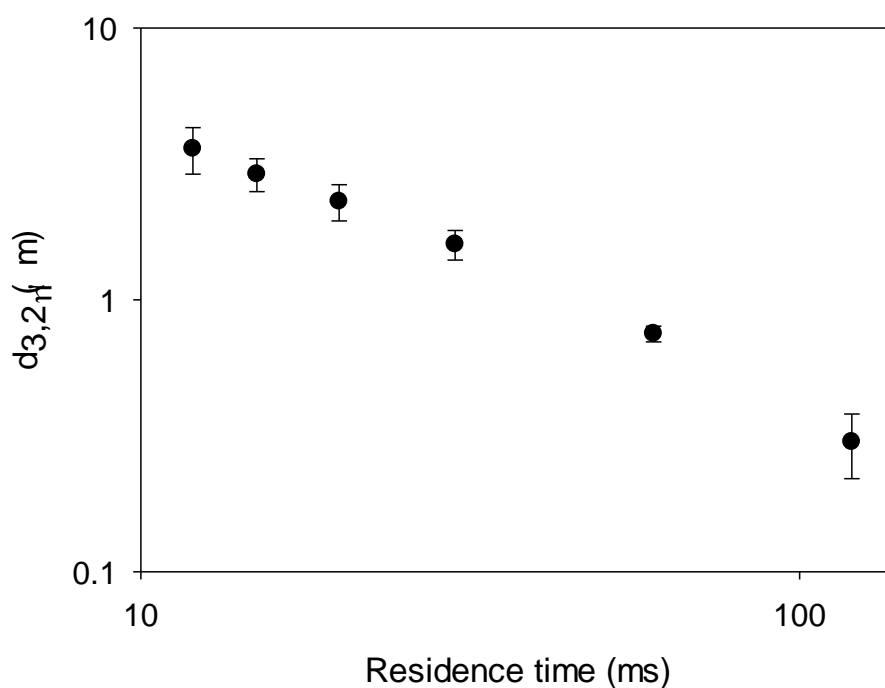


Fig. 5.3. Effect of acoustic processing time on droplet size ($d_{3,2}$) of emulsions stabilised with 1.5 wt. % Tween 80 prepared employing continuous lab scale ultrasonic processor (40% amplitude).

Similar to the behaviour shown in Fig. 5.2 for batch processing, increasing the residence time of pre-emulsions within the acoustic field for continuous processing increases energy transmission to the pre-emulsion, enhancing droplet size reduction (Kentish *et al.*, 2008). However, the timescale for emulsification utilising continuous ultrasonic processing is milliseconds in comparison to seconds for batch processing, this is due to the flow rates of pre-emulsion through the system. Submicron emulsion droplet sizes are achieved with the continuous configuration in milliseconds owing to the smaller processing volume (5×10^{-2} mL) by comparison to those of batch processing (≥ 3 mL). The smaller volumes considered for residence times with continuous processing allow for a greater increase in the volume effect seen with batch systems. This allows the entire flow path to be subject to acoustic energy which improves transmission of acoustic energy to generate smaller emulsion droplets and increases the efficacy of this process.

The effect of energy transmission to the pre-emulsion (*i.e.* different acoustic amplitudes) upon resultant emulsion droplet size was also investigated. 1.5 wt. % Tween 80 pre-emulsions were sonicated with ultrasonic amplitudes of 20 – 40 % for both lab scale batch and continuous configurations, with a 50 g mass of pre-emulsion for lab scale batch processing. Fig. 5.4 shows droplet size measurements as a function of processing time and ultrasonic amplitude for both batch and continuous processing.

Increasing the acoustic amplitude yields greater ultrasonic energy transmission to the pre-emulsion (*cf.* Table 5.2), decreasing the time required to achieve the minimum emulsion droplet size which is determined by the emulsion formulation, ~200 nm (*cf.* Fig. 5.4 a). The acoustic power imparted to a liquid system controls the number of bubbles, with a higher power (*i.e.* amplitude) generating more bubbles (Trujillo & Knoerzer, 2011a). The unstable nature of ultrasonically generated bubbles results in the number of cavitation events being related to the number of bubbles present. The cavitation events result in high levels of hydrodynamic shear which acts upon the pre-emulsion reducing droplet size, so more power more rapidly reduces droplet size.

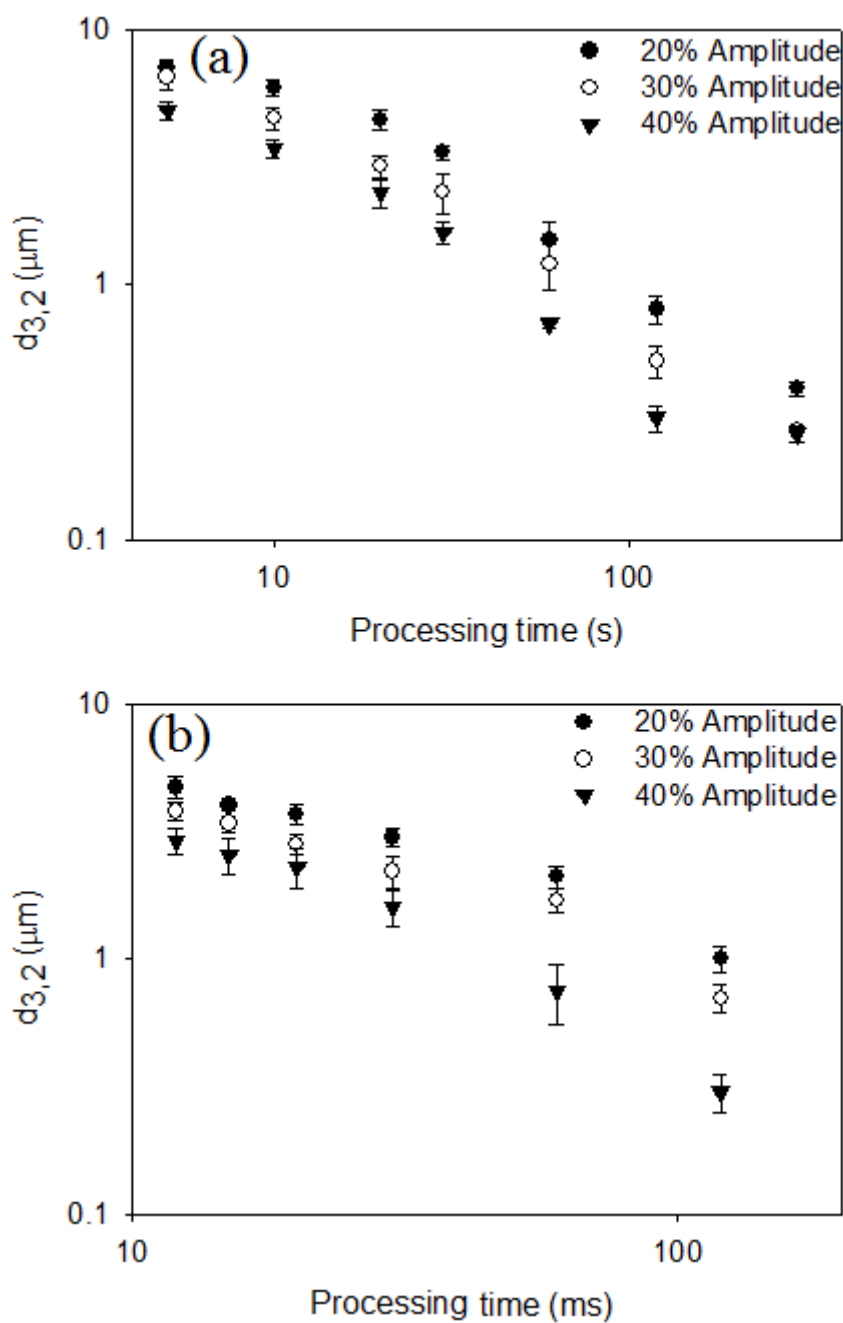


Fig. 5.4. Effect of ultrasonic amplitude and processing time (t) with the acoustic field upon droplet size ($d_{3,2}$) of emulsions fabricated with 1.5 wt. % Tween 80 prepared utilising (a) lab scale batch (50 g) and (b) lab scale continuous configurations.

Similar trends were exhibited with the lab scale continuous configurations (*cf.* Fig. 5.4b), whereby increasing the ultrasonic amplitude reduced the processing time required to decrease emulsion droplet size, for comparable reasons as previously discussed. Given the

lower residence times associated with the continuous processing methodology, it appears emulsions with smaller droplet sizes can be achieved more effectively due to more efficient utilisation of acoustic energy with this configuration. Furthermore, operating at higher acoustic energies (*i.e.* greater ultrasonic amplitudes) predominately decreases the timescale by which smaller emulsion droplets are formed. In order to test these hypotheses, the effect of energy with respect to volume processed, energy density (E_v ; MJ m⁻³), was subsequently determined for the assessment of the efficiency of energy utilisation of each of the configurations investigated.

Emulsion droplet size data for all configurations (*cf.* Fig. 5.4) was normalised with respect to energy, whereby residence time (t ; s), acoustic intensity (I_a ; W cm⁻²), tip surface area (S_A ; cm²) and processing volume (V ; m³) were used to obtain energy density (E_v ; MJ m⁻³) of the systems, determined with Eq. 5.3:

$$E_v = \frac{I_a S_A t}{V} \quad (5.3)$$

Droplet size measurements ($d_{3,2}$) as a function of energy density (E_v) are shown in Fig. 5.5 for both lab scale configurations.

Normalisation of the emulsion droplet size data yielded a linear trend, with logarithmic plot axes this can be fitted by Eq. 5.4, an inverse power law:

$$f(x) = \frac{a}{x^b} \quad (5.4)$$

Where, $f(x)$ is emulsion droplet size ($d_{3,2}$; μm), x is energy density (E_v ; MJ m⁻³), a is the value of $f(x)$ when $x = 1$ and b is the gradient of the fit.

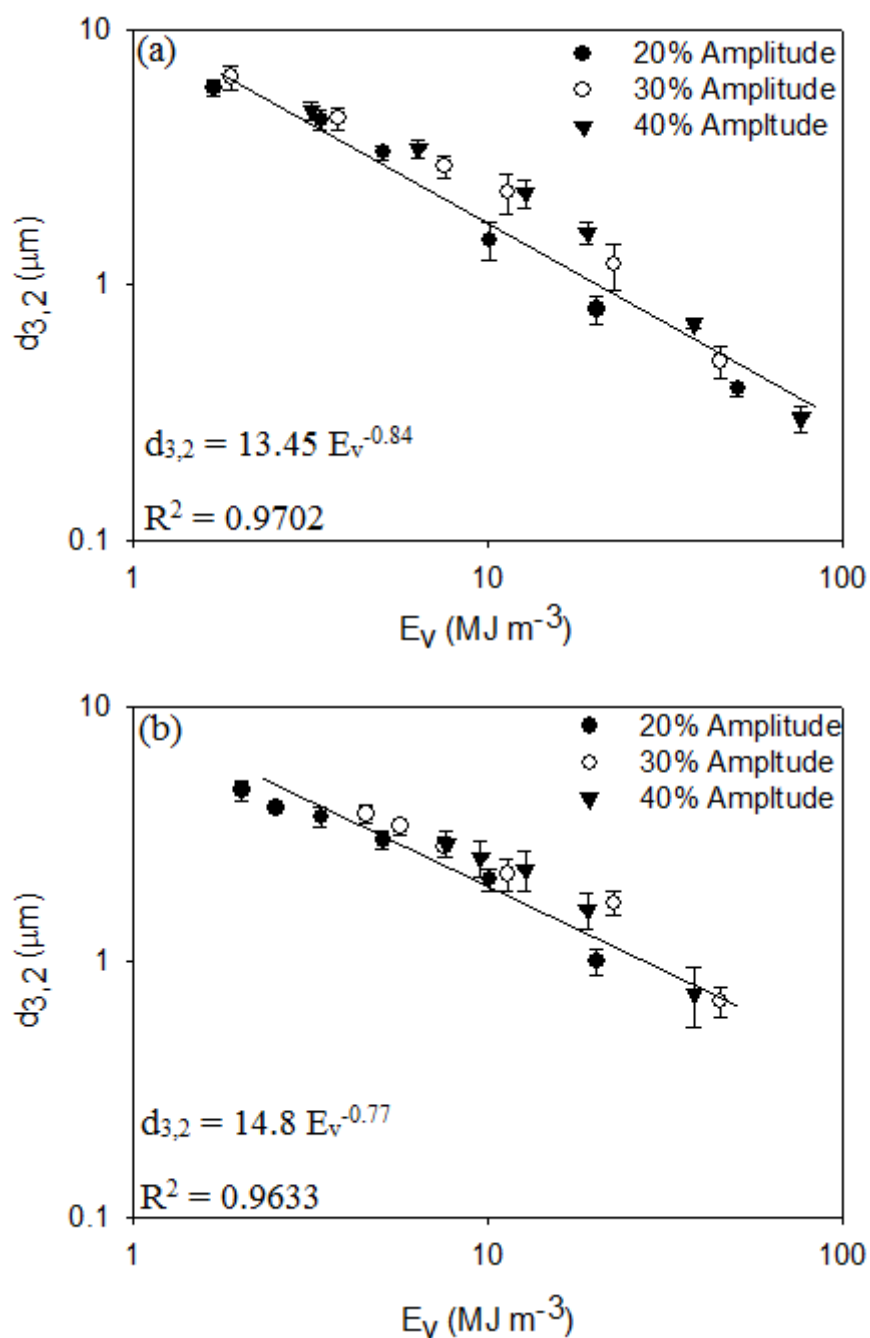


Fig. 5.5. Effect of energy density (E_v) upon emulsion droplet size ($d_{3,2}$) utilising (a) lab scale batch ultrasonic processing (20 - 40% amplitudes) and (b) lab scale continuous ultrasonic processing (20 - 40% amplitudes) for 1.5 wt. % Tween 80 stabilised emulsions.

For both lab scale configurations, master curves were obtained which predict emulsion droplet size with respect to energy density for all ultrasonic amplitudes

investigated. Similar coefficient values (a and b) were obtained for the batch and continuous process configurations (*cf.* Eq. 5.5 and 5.6), but significant differences ($P < 0.05$) in energy density between batch and continuous process were observed, whereby the energy density for the continuous configuration is lower than the batch configuration by approximately 50%. The energy density differential between configurations is predominately attributed to the difference in processing volume, for which continuous processing has a chamber volume 1,000 times less than that of the batch configuration, allowing for more effective transmission of acoustic energy to the pre-emulsion. Additionally, the effect of acoustic amplitude yields no difference on the obtained predictive curves for the determination of emulsion droplet size at a given energy input, highlighting that the energy provided, a combination of acoustic power and processing time, are the determining factors of emulsion droplet size for lab scale ultrasonic emulsification processes.

$$\text{Lab scale batch configuration: } d_{3,2} = \frac{13.45}{E_v^{0.84}} \quad (5.5)$$

$$\text{Lab scale continuous configuration: } d_{3,2} = \frac{14.8}{E_v^{0.77}} \quad (5.6)$$

5.4.2. Effect of emulsifier concentration and type on emulsion formation

Oil-in-water emulsions were prepared as described in section 5.3 using batch and continuous processes via the previously described ultrasonic emulsification configurations, in the presence of both a low molecular weight surfactant (*i.e.* Tween 80) and high molecular weight biopolymers (*i.e.* MPI and PPI), at a range of emulsifier concentrations (0.1 – 3 wt. %). Emulsions were fabricated utilising lab scale batch (50 g) and continuous configurations (ultrasonic amplitude of 40 %). Emulsion droplet size ($d_{3,2}$) as a function of emulsifier type and concentration is shown in Fig. 5.6. Emulsion droplet sizes were measured immediately after emulsification.

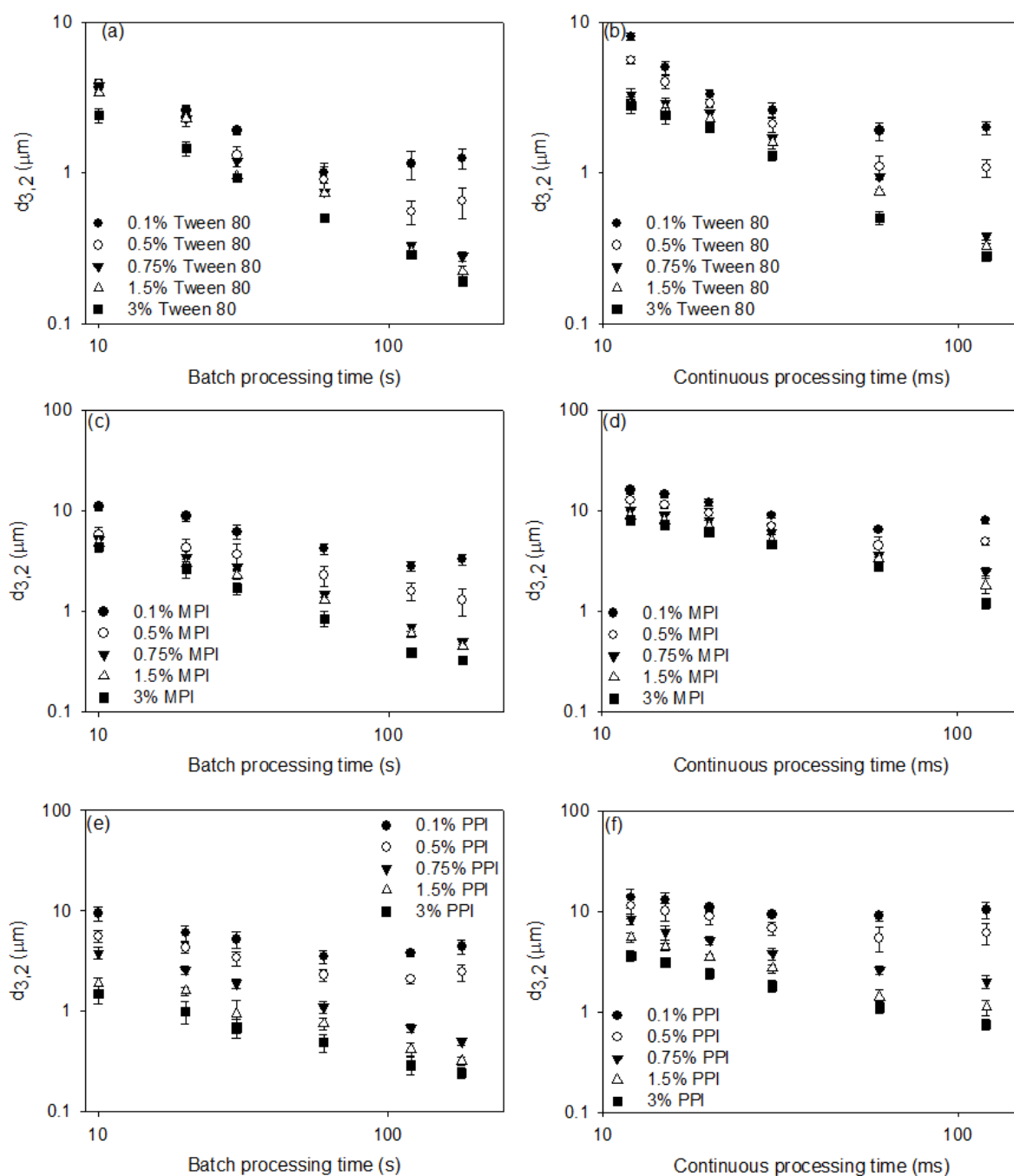


Fig. 5.6. Effect of emulsifier type and concentration (0.1 – 3 wt. %) upon emulsion droplet size ($d_{3,2}$) of: (a) Tween 80 for batch ultrasonic processing, (b) Tween 80 for continuous ultrasonic processing, (c) MPI for batch ultrasonic processing, (d) MPI for continuous ultrasonic processing, (e) PPI for batch ultrasonic processing and (f) PPI for continuous ultrasonic processing. All data is for lab scale methodologies (ultrasonic amplitude of 40%) and the batch size is 50 g.

Regardless of emulsifier type or the processing methodology employed, increasing the emulsifier concentration allows for the formation of smaller emulsion droplets with slower processing times. This is due to increased emulsifier concentration, whereby more emulsifier molecules are present within the continuous phase allowing reduced times for adsorption to the newly formed interface. This allows for more rapid formation of submicron emulsion droplets (Beverung *et al.*, 1999). A minimum surfactant concentration is required to stabilise the emulsion interface, if this is reached submicron emulsion droplets can be produced. At emulsifier concentrations > 0.5 wt. %, for both emulsifier types and processing methodologies, the difference in the emulsion droplet size is not statistically significant ($P > 0.05$). This shows that once sufficient emulsifier is present to stabilise the interfaces an excess of emulsifier is present within the continuous phase. This is in agreement with those results of O'Sullivan *et al.*, (2014) for Tween 80 and MPI, and O'Sullivan *et al.*, (2015) for PPI, whereby emulsions were prepared utilising high pressure valve homogenisation at concentrations > 0.5 wt. %.

At lower emulsifier concentrations (≤ 0.5 wt. %) rapid emulsion coalescence was exhibited for batch and continuous processes, for all investigated emulsifiers. This re-coalescence of emulsion droplets is attributed to a combination of insufficiency of emulsifier to stabilise the interface within the respective formulations and over processing of the emulsions. Back coalescence of emulsion droplets is commonly exhibited in systems where insufficient emulsifier is present, and over processing occurs. Jafari *et al.*, (2008) detail the factors involved in the re-coalescence behaviour of emulsions prepared utilising ultrasonic equipment. The predominant rationale ascribed to the observed re-coalescence phenomena is a combination of the low adsorption rate of emulsifier, due to the low concentrations present, and the high energy density associated with ultrasonic processing, whereby the likelihood of

droplet collision is increased within the area of emulsification (*i.e.* proximity to the tip of the sonotrode).

As previously discussed for emulsion formulations prepared with Tween 80, the residence time during which the pre-emulsion in the acoustic field is of the order of milliseconds for continuous processing in comparison to batch processing, where the timescale is an order of magnitude greater, that of seconds. Emulsions prepared with Tween 80 form smaller emulsion droplets in shorter residence times in the acoustic field in comparison to the high molecular weight emulsifiers, MPI and PPI, for all emulsifier concentrations and processing configurations. This behaviour is ascribed to a combination of lower diffusion rates for the higher molecular weight species, and longer surface denaturation times required for surface stabilisation of emulsion droplets with proteins (Beverung *et al.*, 1999).

The rate of diffusion of an emulsifier to an interface and the time required for conformational changes upon adsorption was probed with studies of interfacial tension. Fig. 5.7 presents the interfacial tension between rapeseed oil and water, 0.1 wt. % Tween 80, MPI and PPI solutions. The presence of naturally present surface active surface impurities within the dispersed phase was assessed by measuring the interfacial tension of distilled water and rapeseed oil. The interfacial tension decreases continually with respect to time (*cf.* Fig. 5.7), and this behaviour is attributed to the nature of the dispersed phase and to a lesser extent the type of emulsifier utilised. Gaonkar, (1989, 1991) described how the time dependant nature of interfacial tension of commercially available rapeseed oils with pure water was due to the presence of surface active impurities present within the oils. Furthermore, after purification of these oils the time dependant nature of the interfacial tension was no longer exhibited demonstrating that the time dependant nature of interfacial tension is due to surface active impurities within the commercially available rapeseed oil.

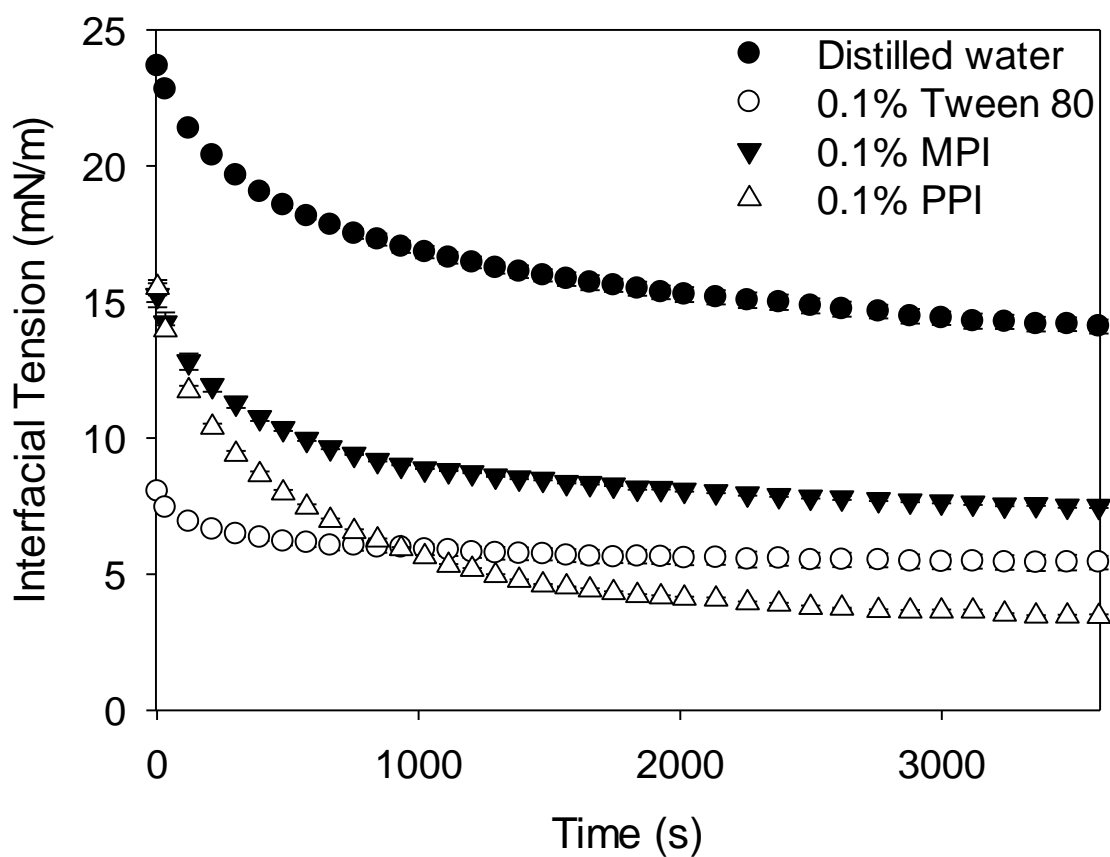


Fig. 5.7. Comparison of interfacial tension between distilled water (●), Tween 80 (○), MPI (▼) and PPI (△) with rapeseed oil. The concentration for all emulsifiers was 0.1 wt. %.

The initial interfacial tension value for 0.1 wt. % Tween 80 is significantly ($P < 0.05$) lower than that of 0.1 wt. % MPI or PPI (*cf.* Fig. 5.7), demonstrating how the lower molecular weight emulsifier is capable of adsorbing to the oil-water interface more rapidly, accounting for the increased rate of droplet breakup for Tween 80 in comparison to that of MPI or PPI. The equilibrium value of interfacial tension differs significantly between Tween 80, MPI and PPI due to a combination of molecular weight differences, the average molecular weight of Tween 80 and, the tested proteins are 1.3 and > 24 kDa, respectively (O'Sullivan, *et al.*, 2014; O'Sullivan *et al.*, 2015) and required surface denaturation for interfacial stabilisation. This demonstrates that lower molecular weight emulsifiers (*i.e.*

Tween 80) have a better interfacial packing and enhanced facilitation of droplet breakup by comparison to higher molecular weight entities (*i.e.* MPI and PPI). Furthermore, these results are consistent with the emulsion droplet size data (*cf.* Fig. 5.6), whereby the equilibrium value of interfacial tension of PPI is significantly lower ($P < 0.05$) than that of MPI, allowing for the improved facilitation of emulsion droplet breakup for emulsion fabricated with PPI, allowing for the formation of smaller emulsion droplets more rapidly for emulsions prepared, in comparison to MPI, at the same concentrations.

The effect of emulsifier concentration above the 0.5 wt. % limiting concentration upon the previously discussed correlative models relating emulsion droplet size ($d_{3,2}$) with respect to energy density (E_v) was consequently assessed. Fig. 5.8 shows emulsion droplet size as a function of energy density for emulsions prepared with a range of Tween 80, MPI and PPI concentrations utilising lab scale batch and continuous ultrasonic processing (50 g), with an ultrasonic amplitude of 40 %.

Increasing the emulsifier concentration above the 0.5 wt. % limiting concentration yields a marginal reduction in emulsion droplet size with respect to energy density, indicating that increased emulsifier concentrations allows for a marginally more efficient utilisation of acoustic energy, with the exception of PPI, for which significant ($P < 0.05$) differences were observed in emulsion droplet size with increased emulsifier concentrations. This behaviour with PPI is attributed to the highly aggregated state of PPI and its extensive disruption via ultrasound treatment (O'Sullivan, Murray, et al., 2015b). Regardless of emulsifier type or processing configuration (batch or continuous), no significant differences were observed between the power law fittings for Tween 80 or MPI, whilst significant differences were observed for the power law fittings of PPI. The inverse power law model for $d_{3,2}$ and E_v did not accurately predict the behaviour of sonicated emulsions with deficiency of emulsifier (< 0.5 wt. %).

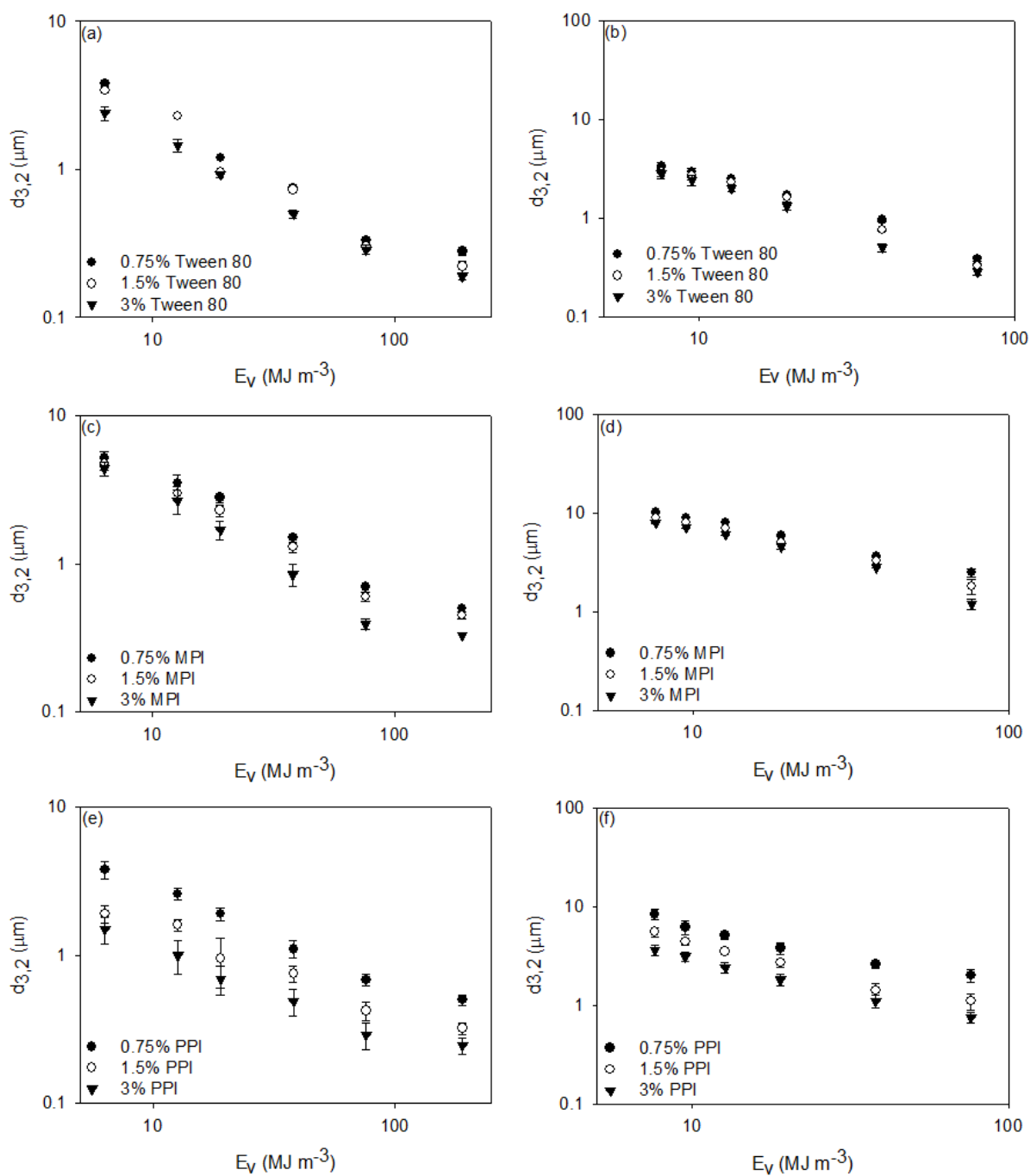


Fig. 5.8. Effect of energy density (E_v) upon emulsion droplet size ($d_{3,2}$) for emulsions prepared with (a) Tween 80 for batch ultrasonic processing, (b) Tween 80 for continuous ultrasonic processing, (c) MPI for batch ultrasonic processing, (d) MPI for continuous ultrasonic processing, (e) PPI for batch ultrasonic processing and (f) PPI for continuous ultrasonic processing, at emulsifier concentrations ranging from 0.75 – 3 wt. % (40% amplitude and 50 g for batch processing).

5.4.3. Effect of energy density on pilot scale continuous ultrasonic emulsification

The effect of energy density on pilot scale continuous ultrasonic homogenisation and the emulsion droplet size ($d_{3,2}$) produced was assessed. Pre-emulsions prepared with 1.5 wt. % Tween 80, MPI and PPI were processed at ultrasonic amplitudes of 50 % and 90 %. Droplet size measurements as a function of energy density are shown in Fig. 5.9.

Pilot scale processing yields two distinct fits for emulsion droplet size with respect to energy density, unlike lab scale they are dependent on the ultrasonic amplitude. The significant difference in gradient (*i.e.* b) between the fits demonstrates that processing of emulsions at higher ultrasonic energies yields more efficient utilisation of energy for emulsion droplet breakup.

There is a disparity between the results obtained for the lab scale (*cf.* Fig. 5.5) and that of the pilot scale predictive models (*cf.* Fig. 5.9), whereby for the lab scale configurations all fall onto one master curve independent of ultrasonic amplitude, whilst the pilot scale processing exhibits two distinct slopes based on ultrasonic amplitude. This is attributed to the configuration of the pilot scale in comparison to the lab scale setups, whereby the tip of the sonotrode is located 2 cm from the entrance to the chamber (*cf.* Fig. 5.1). It is therefore possible that the ultrasonic cavitations which instigate emulsification are sufficiently distanced from the entrance to the chamber allowing some elements of pre-emulsion to bypass the acoustic field either partially or completely. Increasing the ultrasonic amplitude results in the ultrasonic cavitations occurring closer to the entrance of the chamber, allowing for improved emulsification efficiency. Thus, operating at higher acoustic intensities provides more efficient use of acoustic energy for the fabrication of submicron droplets, as is exhibited by the difference in gradients between processing at 50 % and 90 % amplitudes (*cf.* Fig. 5.9).

The lab scale continuous configuration is more efficient in size reduction at all amplitudes investigated due to the narrow distance between the tip of the sonotrode and the base of the tee-junction (3 mm) inhibiting the bypassing effect exhibited in the pilot scale configuration, highlighting the importance of adequate ultrasonic processor design for efficient emulsification (Gogate *et al.*, 2011).

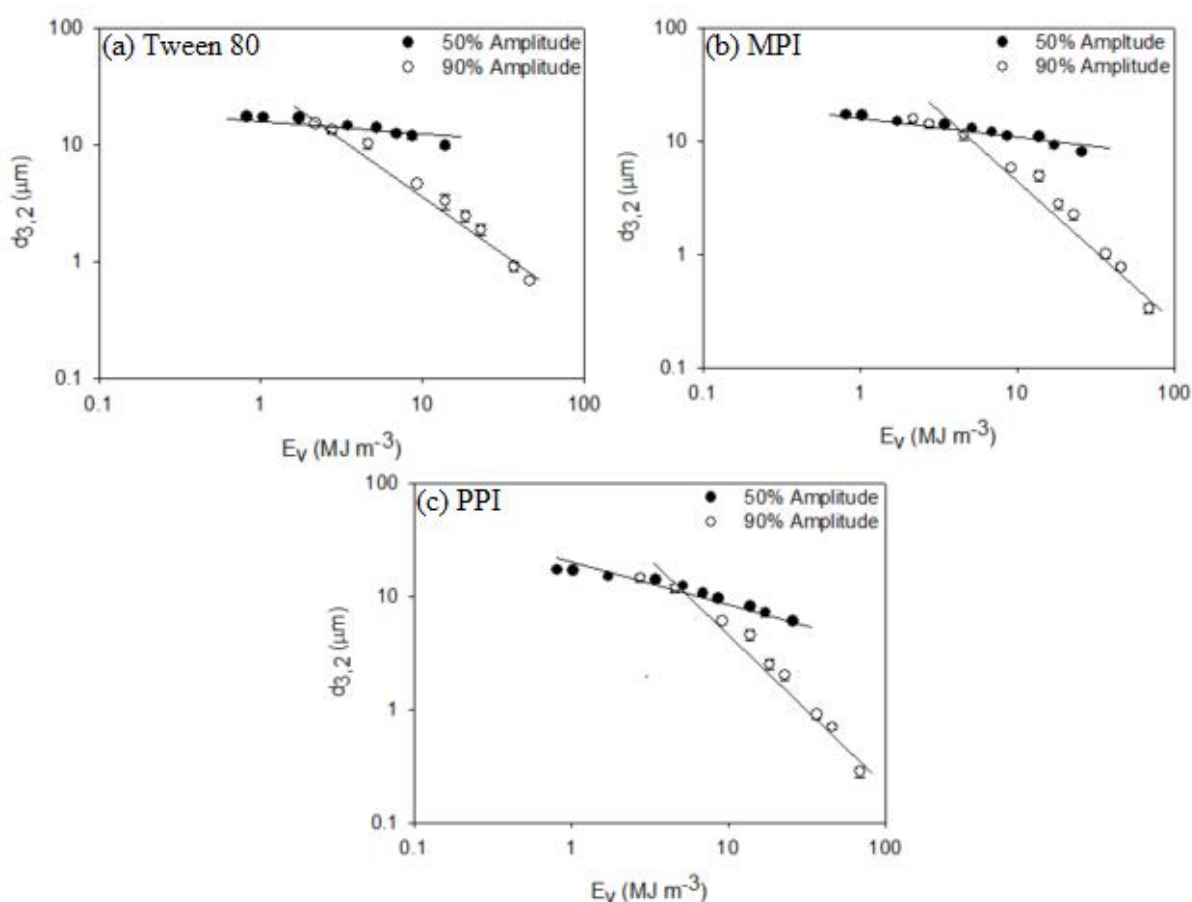


Fig. 5.9. Effect of energy density (E_v) upon emulsion droplet size ($d_{3,2}$) utilising pilot scale continuous ultrasonic processing (ultrasonic amplitudes of 50% and 90%) for (a) 1.5 wt. % Tween 80 , (b) 1.5 wt. % MPI and (c) 1.5 wt. % PPI stabilised emulsions.

The acoustic energy provided by ultrasound is used more effectively in the instance of the continuous methodology, whereby more than 90% of the energy provided is employed for emulsification, in comparison to traditional methods of emulsification, such as valve homogenisation, whereby in certain scenarios it is thought that less than 30% of the provided

energy is utilised in the fabrication of emulsion droplets, the remainder of the energy is dissipated as a combination of thermal and acoustic losses (Lee *et al.*, 2013; McClements, 2005; O'Sullivan *et al.*, 2015).

5.5. Conclusions

This study showed the capacity of low frequency, high power ultrasound for the formation of submicron emulsion droplets at both lab scale (batch and continuous) and pilot scale (continuous). From the process parameters investigated, the efficient formation of submicron droplets is achieved with higher ultrasonic amplitudes and lower processing volumes, as acoustic energy is utilised more efficiently in lower processing volumes. Prolonged contact times of pre-emulsion with an acoustic field allow for greater droplet breakup. The timescale of emulsification for both continuous processing methodologies is milliseconds in comparison to seconds for batch processing, yet submicron emulsions are achieved in both due to the intense utilisation of acoustic energy.

The investigated process parameters were combined to relate emulsion droplet size ($d_{3,2}$) with respect to energy density (E_v), where an inverse power law model relation was obtained. These fits were dependent predominantly upon the emulsifier type, whilst independent of emulsifier concentration (> 0.5 wt. %) for Tween 80 and MPI, yet dependent for PPI, and independent of ultrasonic amplitude for the lab scale methodologies. The pilot scale continuous configuration is dependent upon the ultrasonic amplitude, unlike the lab scale, due to bypassing of elements of pre-emulsion from the acoustic field at lower ultrasonic amplitudes. Additionally, the fittings were unable to predict the re-coalescence behaviour exhibited for both emulsifiers at low emulsifier concentrations (*i.e.* ≤ 0.5 wt. %).

The high molecular weight biopolymers (*i.e.* MPI and PPI) achieved submicron droplets at a slower rate than that of the low molecular weight surfactant (*i.e.* Tween 80).

This is due to the lower rates of diffusion through the bulk and greater time required for surface stabilisation by proteins in comparison to that of small molecule surfactants, as reported from interfacial tension measurements.

5.6. References

- Abisma I, B., Canselier, J. P., Wilhelm, A. M., Delmas, H., & Gourdon, C. (1999). Emulsification by ultrasound: drop size distribution and stability. *Ultrasonics Sonochemistry*, 6(1–2), 75–83.
- Beverung, C. J., Radke, C. J., & Blanch, H. W. (1999). Protein adsorption at the oil/water interface: characterization of adsorption kinetics by dynamic interfacial tension measurements. *Biophysical Chemistry*, 81(1), 59–80.
- Bondy, C., & Söllner, K. (1935). On the mechanism of emulsification by ultrasonic waves. *Transactions of the Faraday Society*, (31), 835–842.
- Chivate, M. M., & Pandit, A. B. (1995). Quantification of cavitation intensity in fluid bulk. *Ultrasonics Sonochemistry*, 2(1), S19–S25.
- Fox, P. F. (2008). Chapter 1 - Milk: an overview. In A. Thompson, M. B. Mike Boland and Harjinder SinghA2 - Abby Thompson, & H. S. B. T.-M. Proteins (Eds.), (pp. 1–54). San Diego: Academic Press.
- Freitas, S., Hielscher, G., Merkle, H. P., & Gander, B. (2006). Continuous contact- and contamination-free ultrasonic emulsification—a useful tool for pharmaceutical development and production. *Ultrasonics Sonochemistry*, 13(1), 76–85.
- Gaonkar, A. G. (1989). Interfacial tensions of vegetable oil/water systems: Effect of oil purification. *Journal of the American Oil Chemists' Society*, 66(8), 1090–1092.
- Gaonkar, A. G. (1991). Surface and interfacial activities and emulsion characteristics of some food hydrocolloids. *Food Hydrocolloids*, 5(4), 329–337.
- Gogate, P. R., Sutkar, V. S., & Pandit, A. B. (2011). Sonochemical reactors: Important design and scale up considerations with a special emphasis on heterogeneous systems. *Chemical Engineering Journal*, 166(3), 1066–1082.
- Heffernan, S. P., Kelly, A. L., Mulvihill, D. M., Lambrich, U., & Schuchmann, H. P. (2011). Efficiency of a range of homogenisation technologies in the emulsification and stabilization of cream liqueurs. *Innovative Food Science & Emerging Technologies*, 12(4), 628–634.
- Jafari, S. M., Assadpoor, E., He, Y., & Bhandari, B. (2008). Re-coalescence of emulsion droplets during high-energy emulsification. *Food Hydrocolloids*, 22(7), 1191–1202.

- Jafari, S. M., He, Y., & Bhandari, B. (2007). Production of sub-micron emulsions by ultrasound and microfluidization techniques. *Journal of Food Engineering*, 82(4), 478–488.
- Juliano, P., Trujillo, F. J., Barbosa-Canovas, G. V., & Knoerzer, K. (2011). The need for thermophysical properties in simulating emerging food processing technologies. In K. Knoerzer, P. Roupas, & C. Versteeg (Eds.), *Innovative Food Processing Technologies: Advances in Multiphysics Simulation* (1st ed.). Indianapolis, USA: Wiley and Sons.
- Kaltsa, O., Michon, C., Yanniotis, S., & Mandala, I. (2013). Ultrasonic energy input influence on the production of sub-micron o/w emulsions containing whey protein and common stabilizers. *Ultrasonics Sonochemistry*, 20(3), 881–91.
- Kentish, S., Wooster, T. J., Ashokkumar, M., Balachandran, S., Mawson, R., & Simons, L. (2008). The use of ultrasonics for nanoemulsion preparation. *Innovative Food Science & Emerging Technologies*, 9(2), 170–175.
- Lee, L. L., Niknafs, N., Hancock, R. D., & Norton, I. T. (2013). Emulsification: Mechanistic understanding. *Trends in Food Science & Technology*, 31(1), 72–78.
- Maa, Y. F., & Hsu, C. C. (1999). Performance of sonication and microfluidization for liquid-liquid emulsification. *Pharmaceutical Development and Technology*, 4(2), 233–40.
- Margulis, M. A., & Margulis, I. M. (2003). Calorimetric method for measurement of acoustic power absorbed in a volume of a liquid. *Ultrasonics Sonochemistry*, 10(6), 343–345.
- Martini, S. (2013). *Sonocrystallization of Fats*. (R. W. Hartel, Ed.) (1st ed.). New York: Springer US.
- McClements, D. J. (1995). Advances in the application of ultrasound in food analysis and processing. *Trends in Food Science & Technology*, 6(9), 293–299.
- McClements, D. J. (2005). *Food Emulsions: Principles, Practices, and Techniques* (2nd ed.). CRC Press.
- McClements, D. J. (2011). Edible nanoemulsions: fabrication, properties, and functional performance. *Soft Matter*, 7(6), 2297.
- McClements, D. J., & Povey, M. J. W. (1989). Scattering of ultrasound by emulsions. *Journal of Physics D: Applied Physics*, 22(1), 38–47.
- O'Donnell, C. P., Tiwari, B. K., Bourke, P., & Cullen, P. J. (2010). Effect of ultrasonic processing on food enzymes of industrial importance. *Trends in Food Science & Technology*, 21(7), 358–367.
- O'Sullivan, J., Arellano, M., Pichot, R., & Norton, I. (2014). The Effect of Ultrasound Treatment on the Structural, Physical and Emulsifying Properties of Dairy Proteins. *Food Hydrocolloids*, 42(3), 386–396.

- O'Sullivan, J., Greenwood, R., & Norton, I. (2015). Applications of ultrasound for the functional modification of proteins and nanoemulsion formation: A review. *Trends in Food Science and Technology*.
- O'Sullivan, J., Murray, B., Flynn, C., & Norton, I. T. (2015). The Effect of Ultrasound Treatment on the Structural, Physical and Emulsifying Properties of Animal and Vegetable Proteins. *Food Hydrocolloids*, (In Press).
- O'Sullivan, J., Pichot, R., & Norton, I. T. (2014). Protein Stabilised Submicron Emulsions. In P. A. Williams & G. O. Phillips (Eds.), *Gums and Stabilisers for the Food Industry 17* (pp. 223–229). Cambridge, UK: The Royal Society of Chemistry.
- Servant, G., Laborde, J. L., Hita, A., Caltagirone, J. P., & Gérard, A. (2001). Spatio-temporal dynamics of cavitation bubble clouds in a low frequency reactor: comparison between theoretical and experimental results. *Ultrasonics Sonochemistry*, 8(3), 163–74.
- Trujillo, F. J., & Knoerzer, K. (2011). A computational modeling approach of the jet-like acoustic streaming and heat generation induced by low frequency, high power ultrasonic horn reactors. *Ultrasonics Sonochemistry*, 18(6), 1263–73.

***Chapter 6. Conclusions and future
recommendations***

The objective of this thesis was to advance the understanding of low frequency, high power ultrasound upon the structure of proteins in aqueous solution and submicron emulsion fabrication. Ultrasound treatment has shown potential for the generation, alteration and modification of food microstructures, yet the underlying principles are to be fully elucidated. Proteins are essential for human nutrition, and are commonly utilised as functional ingredients within food formulations. Thus, understanding the effect of ultrasound upon protein structure will assist the development of ingredients with improved functionality. This study is of particular relevance to Kerry Group who manufactures and distributes both protein derived ingredients and emulsion systems for food and pharmaceutical industries globally. Therefore, a technology that offers the potential for the functional modification of proteins and the fabrication of submicron emulsions is of considerable relevance.

To conduct this study, proteins derived from dairy, animal and vegetable sources were treated with ultrasound and physicochemical differences between untreated and ultrasound treated were characterised using a myriad of techniques. Subsequently, emulsions prepared with ultrasound treated proteins were assessed by comparison to those fabricated with their untreated counterparts, and low molecular weight surfactants, at a range of emulsifier concentrations. Emulsion formation and stability was examined in terms of emulsion droplet size, interfacial tension and long-term stability tests.

Furthermore, power ultrasound is known to be capable for the fabrication of submicron emulsion droplets, however, the interactions between emulsion formulation and process parameters upon emulsion formation are not well understood. To address this, a fundamental study was conducted to assess the effect of process configuration (*i.e.* batch or continuous), processing parameters (*i.e.* acoustic power and residence time) and emulsion formulation (*i.e.* emulsifier type and concentration) on emulsion droplet size ($d_{3,2}$).

The main conclusions from this thesis are summarised in the following three sections.

6.1. Understanding the ultrasonic effect upon the physicochemical properties of proteins

- **Ultrasound treatment reduces the aggregate size of dairy, animal and legume proteins in aqueous solution**

Ultrasound treatment significantly reduced the aggregate size of dairy (*i.e.* NaCas, MPI and WPI), animal (*i.e.* BG, FG and EWP) and legume (*i.e.* PPI and SPI) proteins due to disruption of associative non-covalent interactions (*i.e.* hydrogen bonding, hydrophobic and electrostatic interactions) attributed to the high levels of hydrodynamic shear associated with ultrasonic cavitations.

- **Ultrasound treatment of cereal proteins unable to reduce aggregate size in aqueous solution**

No aggregate size reduction was observed for RPI from ultrasound treatment, irrespective of treatment time. This behaviour is attributed to insufficient energy provided from the ultrasound treatment to disrupt the disulphide bonds (*cf.* Table 2.2) maintaining the aggregated structure of these proteins, whereby this disulphide bonding occurs due to protein denaturation from the preparation of these protein isolates.

- **Ultrasound treatment provides insufficient energy to reduce the primary amino acid sequence**

SDS-PAGE demonstrated that there was no reduction in the primary structure of proteins, thus no scission of the peptide bond. Ultrasound treatment provides insufficient energy to hydrolyse the peptide bond, especially given the partial double character it exhibits, giving it

significantly greater associated bond energy (*cf.* Table 2.2). Ultrasound treatment supplies sufficient energy to disrupt the non-covalent interaction maintaining protein aggregates in aqueous solution.

- **Ultrasound treatment increases the hydrophobicity of proteins, with the exception of cereal proteins, in aqueous solution**

The size reduction of proteins via ultrasound treatment was measured both using light scattering techniques (*i.e.* DLS and laser diffraction), and rheology (*i.e.* intrinsic viscosity). A reduction in the value of intrinsic viscosity of proteins in solution demonstrates a decrease in the hydration of protein associates, and a potential increase in the hydrophobicity of proteins, exhibited by intrinsic viscosity reduction by ultrasound treatment (Tanner & Rha, 1980).

6.2. Understanding the ultrasonic effect of the emulsifying performance of proteins

- **Ultrasound treated proteins yield smaller emulsion droplets in comparison to untreated counterparts at low emulsifier concentrations**

Emulsions prepared with ultrasound treated MPI, BG, EWP and PPI yielded smaller emulsion droplets in comparison to emulsions prepared with untreated counterparts, at low emulsifier concentrations (< 1 wt. %). This behaviour is attributed to reduction in protein size and increase in the hydrophobicity from ultrasound treatment. Whilst, emulsions prepared with ultrasound treated NaCas, WPI, FG, SPI and RPI yielded no significant reduction in emulsion droplet size, ascribed to limited improvement in adsorption behaviour as measured by interfacial tension.

- **Ultrasound treated dairy, animal and vegetable proteins yield more stable or comparable emulsion stability in comparison to untreated counterparts, with the exception of emulsions prepared with ultrasound treated FG**

Emulsions prepared with ultrasound treated MPI and BG yielded stable emulsions resistant to coalescence over the 28 day stability study, whilst emulsions prepared with FG displayed a decrease in emulsion stability. The improved stability for ultrasound treated MPI and BG emulsions is ascribed to an improvement in interfacial packing and a more viscoelastic interface, as measured by interfacial tension and observed from cryogenic scanning electron micrographs, whilst the reduction in stability for ultrasound treated FG emulsions is attributed to a weaker interfacial layer, by comparison to their untreated counterparts. Emulsions prepared with ultrasound treated NaCas, WPI, EWP, PPI, SPI and RPI exhibit comparable emulsion stability to emulsions prepared with their untreated counterparts.

- **Ultrasound treated MPI, BG, EWP, PPI and SPI possess greater molecular mobility and improved interfacial packing behaviour, whilst NaCas, WPI, FG and RPI exhibit comparable interfacial behaviour**

Ultrasound treatment of proteins improves the interfacial behaviour through increased molecular mobility through the bulk to the interface, observed by a decrease in the initial value of interfacial tension, and improved interfacial packing, observed from lower equilibrium values of interfacial tension, for MPI, BG, EWP, PPI and SPI. These improvements in the interfacial properties account for the reduction in emulsion droplet size and increased emulsion stability, and are attributed to the measured reduction in protein aggregate size. The interfacial tension for NaCas, WPI, FG and RPI is comparable to that of

their untreated counterparts, ascribed to less significant reduction in protein aggregate size in comparison to the other investigated proteins.

6.3. Understanding acoustic emulsification

- **Increased processing times and ultrasonic energy allows for the generation of submicron emulsions**

Increasing the processing time of pre-emulsions allow for the generation of submicron emulsion droplets, as the pre-emulsion is within the shear field for prolonged times. In addition, increased levels of ultrasonic energy allow for the more rapid formation of submicron emulsion droplets, given the increased number of ultrasonic cavitations due to the increased ultrasonic amplitudes.

- **Continuous ultrasonic emulsification yields submicron emulsion droplets more efficiently in comparison to batch ultrasonic emulsification**

Continuous ultrasonic emulsification yields submicron emulsion droplets twice as efficiently as batch configuration for lab scale processing as shown from energy density comparisons. The smaller processing volume of the continuous configuration allows for the more intense dissipation of acoustic energy in comparison to batch processing, a volume effect, yielding more rapid generation of submicron emulsion droplets.

- **Emulsions with deficient emulsifier demonstrate re-coalescence behaviour**

Emulsions with low emulsifier concentrations (*i.e.* < 0.75 wt. %) demonstrate re-coalescence behaviour for both batch and continuous processing due to a combination of insufficiency of emulsifier and the high energy density of ultrasonic processing. The high energy density results in droplet collisions leading to coalescence of emulsion droplets, due to the incomplete interfacial coverage of emulsion droplet surfaces.

- **Low molecular weight emulsifiers form submicron emulsions more rapidly than higher molecular weight emulsifiers**

Lower molecular emulsifiers (*i.e.* Tween 80) form submicron emulsion droplets more rapidly than higher molecular weight emulsifiers (*i.e.* MPI and PPI) when sufficient emulsifier is present, as lower molecular weight emulsifiers have greater molecular mobility through the continuous phase to the oil-water interface, as shown by interfacial tension measurements.

- **Higher acoustic energies necessary for pilot scale continuous emulsification for effective emulsification**

Higher acoustic energies are required while utilising pilot scale ultrasonic emulsification processes, as a bypassing behaviour of pre-emulsion is exhibited at lower amplitudes, due to the minimal reduction in emulsion droplet size by comparison to higher amplitudes (*i.e.* greater acoustic energy). Increased acoustic energies display a pronounced region of ultrasonic cavitations (*i.e.* region of hydrodynamic shear) up to the entrance of the ultrasonic chamber, whilst a reduced region is exhibited for lower amplitudes, allowing for bypassing of pre-emulsions.

6.4. Future recommendations

This sections aims to highlight areas of which justify further potential research based on the contemplations and conclusions developed from this study.

- **Investigate the hydrolysis of proteins from ultrasound treatment**

Ultrasound treatment has been shown to reduce the molecular weight profile of cellulose ethers (*i.e.* polysaccharides) as measured by intrinsic viscosity and steric exclusion chromatography (Goodwin *et al.*, 2011), whilst there is debate within the literature as to

whether low frequency, high power ultrasound is capable of reducing the primary amino acid sequence of proteins by scission of the peptide bond (Jambrak *et al.*, 2014; Yanjun *et al.*, 2014).

In the present study, the ultrasonic treatment times employed provide insufficient energy to achieve hydrolysis of the peptide bond, given the bond energies of the peptide bond (*i.e.* C-N) and its dimeric form (*i.e.* C=N bonds) due to the adjacent carboxylic group (*cf.* Table 2.1). However, a combination of either prolonged treatment times or more intense treatment (*i.e.* greater acoustic intensity) offer the potential for the reduction of molecular weight with low degrees of hydrolysis, reducing the allergenic attributes of certain proteins (*i.e.* dairy or soy proteins), and maintaining sufficient tertiary structure for the formation and stabilisation of emulsion droplets.

- **Investigate the rate and degree of enzymatic proteolysis in the presence of ultrasound**

Protein hydrolysates are commonly utilised ingredients within infant and clinical nutrition formulations, as they exhibit improved digestibility with lower allergenicity attributes in comparison to the parent protein. The food industry is moving toward utilisation of newer protein sources derived from vegetable, which, due to the processing of these ingredients, possess a large denatured insoluble component. Thus, the rate of hydrolysis reaction and yield (*i.e.* soluble component) from these reactions is often prolonged and low, respectively, by comparison to the hydrolysis of conventional protein sources which are readily hydrolysed (*i.e.* dairy proteins).

It is expected that ultrasound treatment of protein hydrolysis reactions offer potential of both disruption of insoluble protein aggregates and expansion of quaternary/tertiary structure allowing for increased rates of hydrolysis and improved yields. Based on the work conducted in this study, ultrasound treatment has been shown to alter the quaternary and/or tertiary

structure of proteins, potentially reducing the proteolytic activity of enzymes. Therefore, optimisation of pulsed ultrasonic treatment offers potential to disrupt the insoluble aggregates of proteins, whilst minimising detrimental effects to enzymes allowing for increased rates and yields of enzymatic hydrolysis reactions.

- **Extend the understanding of the effect of ultrasound treatment on protein structure in solution to those adsorbed at interfaces**

In the present study the effect of ultrasound treatment was extensively probed for a wide range of proteins in aqueous solutions, and predominately improved the emulsifying performance of proteins. Be that as it may, this work also indicated that the improved emulsifying performance from ultrasound treatment does not extend to proteins adsorbed at emulsion droplet interfaces prior to ultrasound treatment. The emulsions prepared with MPI and PPI utilising batch and continuous ultrasonic processes as the method of emulsification at concentrations < 0.75 wt. % yielded larger emulsion droplets (*cf.* Fig. 5.6) than those of emulsions prepared with MPI and PPI ultrasound treated prior to emulsification (*cf.* Fig. 3.4 and 4.5).

This disparity could be addressed by the fabrication of emulsions with untreated and ultrasound treated proteins, and subsequently ultrasonically treating the untreated emulsions, and further processing these emulsions utilising the same emulsification technology, which is capable of achieving smaller emulsion droplets with a more uniform (*i.e.* low span) droplet size distribution than ultrasonic technologies (*i.e.* microfluidics).

- **Investigating the effect of ultrasound treatment on the physicochemical properties and emulsifying performance of additional non-conventional protein sources**

Extensive research is being conducted on the extraction and implementation of proteins isolates from non-conventional sources for utilisation within the food industry, such as potato protein isolate, lentil protein isolate, wheat protein isolate and blue sweet lupine protein isolate to mention but a few. The majority of these upcoming isolates are derived from vegetable sources and their extraction methods result in the denaturation of protein yielding an insoluble component, often with a particle size $> 1 \mu\text{m}$, resulting in an unstable isolate which is prone to rapid phase separation (*i.e.* sedimentation).

This study has shown that ultrasound treatment can improve the solubilisation and interfacial behaviour of legume derived protein isolates (*i.e.* pea and soy) by size reduction. However, no size reduction was observed for the tested cereal protein (*i.e.* rice), and consequently no change in the physicochemical properties and emulsifying performance of this protein. It is expected that other proteins derived from cereals (*e.g.* wheat or bran) would be resistant to size reduction from ultrasound treatment, whilst proteins derived from other vegetable sources (*e.g.* blue sweet lupine or lentil) would be susceptible to size reduction because of structural similarities between the different vegetable proteins. However, the effect of ultrasound on tuberous proteins (*i.e.* potato), have yet to be explored.

- **Development of a continuous ultrasonic process for the functional modification of proteins**

The first two results chapter of this thesis focused on the effect of sonication of protein solutions employing batch processing methodologies, for the functional modification of these ingredients. To increase the industrial applicability of this work development and optimisation of continuous processing methodologies should be investigated, whereby, the

processing power (*i.e.* acoustic energy) and flow rate (*i.e.* residence time) would be optimised in order to achieve the functional improvements observed from batch processing.

6.5. References

- Goodwin, D. J., Picout, D. R., Ross-Murphy, S. B., Holland, S. J., Martini, L. G., & Lawrence, M. J. (2011). Ultrasonic degradation for molecular weight reduction of pharmaceutical cellulose ethers. *Carbohydrate Polymers*, 83(2), 843–851.
- Jambrak, A. R., Mason, T. J., Lelas, V., Paniwnyk, L., & Herceg, Z. (2014). Effect of ultrasound treatment on particle size and molecular weight of whey proteins. *Journal of Food Engineering*, 121(0), 15–23.
- Tanner, R., & Rha, C. (1980). Hydrophobic Effect on the Intrinsic Viscosity of Globular Proteins. In G. Astarita, G. Marrucci, & L. Nicolais (Eds.), *In Rheology, Volume 2: Fluids* (pp. 277–283). Boston, MA: Springer US.
- YanJun, S., Jianhang, C., Shuwen, Z., Hongjuan, L., Jing, L., Lu, L., Uloko, H., Yangling, S., Wenming, C., Wupeng, G., & Jiaping, L. (2014). Effect of power ultrasound pre-treatment on the physical and functional properties of reconstituted milk protein concentrate. *Journal of Food Engineering*, 124(0), 11–18.

***Appendix A. Mathematical models for acoustic
streaming***

Ultrasonic emanation from the tip of the sonotrode is referred to as acoustic streaming (Nyborg, 1953; Tjøtta, 1999). There are two main acoustic streaming theories which describe this phenomena mathematically, that developed by Rayleigh (Rayleigh, 1896), Nyborg (Nyborg, 1953) and Westervelt (Westervelt, 1953), referred to as the RNW theory, and that proposed by Lighthill, the Stuart streaming theory (Lighthill, 1978). The RNW theory is applied to systems where the Reynolds number (*i.e.* the ratio of inertial to viscous forces) is very low, and the Stuart streaming theory is applicable to systems whereby the acoustic jets take the form of an inertially dominated turbulent jet (*i.e.* high Reynolds number) with powers in excess of 4×10^{-4} W (Trujillo & Knoerzer, 2011a).

A.1. Rayleigh, Nyborg and Westervelt (RNW) streaming theory

Acoustic streaming is calculated from the RNW theory by combining the continuity equation (*cf.* Eq. A.1) and the Navier-Stokes equations (*cf.* Eq. A.2).

$$\frac{\partial \rho}{\partial t} = -\nabla \cdot (\rho \vec{v}) \quad (\text{A.1})$$

$$\rho \left(\frac{\partial \vec{v}}{\partial t} + \vec{v} \cdot \nabla \vec{v} \right) = -\nabla p + \mu \nabla^2 \vec{v} + \vec{F} \quad (\text{A.2})$$

Where ρ is density (kg m^{-3}), \vec{v} is velocity (m s^{-1}), t is time (s), p is pressure (Pa), μ is viscosity (Pa s) and \vec{F} represents the force per unit volume that causes streaming (N m^{-3}). The convective acceleration term ($\vec{v} \cdot \nabla \vec{v}$), also known as the inertia term, is neglected and subsequently \vec{F} can be calculated as a spatial variation of the Reynolds number (Lighthill, 1978), implementing the Einstein notation, force, F , can be written in terms of the j component:

$$F_j = -\frac{\partial(\rho v_i v_j)}{\partial x_i} \quad (\text{A.3})$$

The spatial variations of the Reynolds stress are dictated by sound attenuation (*i.e.* absorption of sound; Trujillo & Knoerzer, 2011b). In particular for acoustic waves whereby plane wave attributes are observed (*i.e.* constant compression-to-compression amplitude with respect to velocity in a given vector), the force associated with the attenuation of a sound field is obtained from the following expression (Tjøtta, 1999):

$$\vec{F} = -\frac{1}{c}\nabla\vec{I}_a \quad (\text{A.4})$$

Where c is the speed of sound (m s^{-1}) and \vec{I}_a is the acoustic power intensity (W cm^{-2}). The solution to Eq. A.1 and A.2 was obtained by successive approximations, whereby each value was expanded as a series of terms, representing the excess pressure, $p^1 = (p - p_0)$, the excess velocity, $v^1 = (v - v_0)$, and the excess density, $\rho^1 = (\rho - \rho_0)$, at any given location in the acoustic field (Nyborg, 1953; Zarembo, 1971):

$$p^1 = p_1 + p_2 + \dots \quad (\text{A.5})$$

$$v^1 = v_1 + v_2 + \dots \quad (\text{A.6})$$

$$\rho^1 = \rho_1 + \rho_2 + \dots \quad (\text{A.7})$$

Terms with a subscript 0 represent the system under placid fluid conditions. The first order terms of the equations (*i.e.* a subscript of 1) are usually the solution to the wave equation. These values vary in a sinusoidal manner with respect to the frequency, ω , of the acoustic wave, and hence represent the sound field (Nyborg, 1953). The second order approximation terms (*i.e.* a subscript of 2) are time-averaged terms, also known as time-independent terms, correction terms to be added to the first order values. The first order velocity term, v_l , represents the velocity of compressions and rarefactions of particles during the transmission of acoustic waves through a medium, thus the velocity through the medium is of the same magnitude as the speed of sound. The speed of sound through water is

approximately 1,500 m s⁻¹. The time-independent streaming velocity (*i.e.* v_2) is within the order of a few meters per second.

Even though solutions have been derived to describe acoustic streaming based on the RNW theory (Nowicki, Secomski, & Wójcik, 1997; Nowicki, Kowalewski, Secomski, & Wójcik, 1998), it was demonstrated that neglecting the inertia term from the Navier-Stokes equation is applicable to systems with very low flows exhibiting low Reynolds numbers ($Re < 1$) and low sources of acoustic power (Lighthill, 1978; Zarembo, 1971). Therefore, the RNW theory is not applicable to the jet streaming exhibited by low frequency, high power transducers (Trujillo & Knoerzer, 2011a).

A.2. Stuart streaming theory

Stuart, (1963) developed the concept that for systems which exhibited higher Reynolds numbers, such as systems utilising high acoustic powers, the Navier-Stokes equation of motion (*cf.* Eq. A.8) must be used with the inclusion of the inertia term ($\bar{v} \cdot \nabla \bar{v}$):

$$\rho(\bar{v} \cdot \nabla \bar{v}) = -\nabla \bar{p} + \mu \nabla^2 \bar{v} + \vec{F} \quad (\text{A.8})$$

Eq. A.8 is the time-independent version of the Navier-Stokes equation, where the transient term is removed and \bar{v} and \bar{p} represent the time average variations of velocity and pressure, respectively, equivalent to the second order terms from the successive approximations devised by Nyborg, (1953) (*cf.* Eq. A.5 and A.6) as they also represent time-averaged values. The term ‘Stuart streaming’ was introduced to describe the acoustic streaming at higher Reynolds numbers resulting from high power acoustic beams from transducers. This type of acoustic streaming is the most commonly utilised within the food industry for the functional modification of ingredients and the development of microstructures. Lighthill, (1978) described that “it is hardly an exaggeration to say that all

really noticeable acoustic streaming motions are Stuart streaming,” and furthermore proved that acoustic streaming takes the form of an inertially dominated turbulent jet upon exceeding an acoustic power of 4×10^{-4} W.

High power acoustic streaming manifests in the form of a jet showing a narrower beam of sound emanating from the source with an acoustic power of $P_0 = I_0 S_A$, where P_0 is the acoustic power at the tip of the sonotrode (W), I_0 is the acoustic power intensity at the tip of the sonotrode (W cm^{-2}) and S_A is the cross sectional area of the sonotrode tip (cm^2) (Lighthill, 1978). In the absence of attenuation (*cf.* section 2.3.1.2.) the principles of conservation of energy are applicable, whereby the energy entering the beam from the transducer tip is equal to that leaving the beam. Thus this conservation of energy can be expressed as follows:

$$IA = \text{constant} \tag{A.9}$$

Attenuation of the sound beam reduces the power of the sound beam according to:

$$P = P_0 e^{-\beta x} \tag{A.10}$$

Where x is the distance from the source emanating the sound beam (m) and $e^{-\beta x}$ is the damping term which accounts for spatial attenuation of the acoustic beam, primarily due to ultrasonic cavitations. β is the attenuation coefficient proposed by Lighthill, (1978) defined as the proportional loss of ultrasonic energy per unit displacement travelled by a acoustic wave.

In addition, attenuation of sound beams can be expressed in terms of dampening of the pressure amplitude, p , whereby the absorption coefficient is α (Nyborg, 1953; Tjøtta, 1999). For plane waves the relationship between the attenuation coefficient, β , and the absorption coefficient, α , is $\beta = 2\alpha$.

$$p = P_0 e^{-\alpha x} e^{j(\omega t - I\alpha)} \tag{A.11}$$

Lighthill, (1978) proposed that the sonotrode emanates the ultrasonic power as a sound beam where the net force at a given distance, x , is determined by applying the law of conservation of momentum, yielding the acoustic momentum flow rate after attenuation. Application of the law of conservation of momentum allows for the conclusion that a reduction in the ‘acoustic momentum,’ F_a (*cf. Eq. A.12*), increases the ‘hydrodynamic momentum,’ F_h (*cf. Eq. A.13*), in the path of the sound beam, also referred to as streaming.

$$F_a = \frac{P}{c} = \frac{P_0}{c} e^{-\beta x} \quad (\text{A.12})$$

$$F_h = \frac{P_0}{c} - \frac{P_0}{c} e^{-\beta x} = \frac{P_0}{c} (1 - e^{-\beta x}) \quad (\text{A.13})$$

The spatial rate of decay of the hydrodynamic momentum flow rate, F_L , acts as a net force per unit displacement in a given direction, x , generating motion of the medium (*cf. Eq. A.14*). If there was no impedance present within the path of the sound beam as a consequence of cavitations, the attenuation coefficient, β , would have a value of zero, and the net force would thus become neglected. Therefore, streaming is a result of acoustic attenuation caused by ultrasonic cavitations in the locus of the sound beam (*cf. section 2.3.1.2.*).

$$F_L = -\frac{dF_a}{dx} = \frac{\beta}{c} P_0 e^{-\beta x} = \frac{\beta}{c} P \quad (\text{A.14})$$

For high values of the attenuation coefficient, β , the streaming motion of the acoustic beam is comparable to that of a turbulent jet, whereby the damping term, $e^{-\beta x}$, approaches zero at short distances by which over short distances within the locus of the sonotrode tip the momentum delivered to the medium is equal to P_0/c (*cf. Eq. A.14*; Trujillo & Knoerzer, 2011a).

The average flow of a turbulent jet has a comparable solution to that of a laminar jet for a constant eddy viscosity, μ_t (*cf. Eq. A.15*), where K_m represents the mechanical momentum ($K_m = \rho_0 F_h$) (Schlichting, 1979).

$$\mu_t = 0.016 \sqrt{K_m} \quad (\text{A.15})$$

When the attenuation coefficient, β , is low the eddy viscosity along the path of the acoustic beam increases as the hydrodynamic momentum flow rate, F_h , increases as per *Eq. A.13*.

The velocity profile of the acoustic beam emanating from the sonotrode tip, v , is equivalent to a jet and can be described by a Gaussian distribution:

$$v = \sqrt{\frac{2K_m}{\rho^2 \pi S^2}} e^{[-(r/S)]} \quad (\text{A.16})$$

Where r is the radius of the acoustic beam (m) and S is the width of the jet as a function of distance from the sonotrode tip (m), $S = S(x)$. The velocity profile (*cf. Eq. A.16*) can be justified if the acoustic intensity (I_a) additionally exhibits a Gaussian tendency (Lighthill, 1978).

Ultrasonic processing utilised within the food industry for the development of microstructures and functional modification of food ingredients is usually high power ultrasound processing which is most adequately modelled and explained by the Stuart streaming theory (McClements, 1995; Trujillo & Knoerzer, 2011a).

A.3. References

- Lighthill, S. J. (1978). Acoustic streaming. *Journal of Sound and Vibration*, 61(3), 391–418.
- McClements, D. J. (1995). Advances in the application of ultrasound in food analysis and processing. *Trends in Food Science & Technology*, 6(9), 293–299.
- Nowicki, A., Kowalewski, T., Secomski, W., & Wójcik, J. (1998). Estimation of acoustical streaming: theoretical model, Doppler measurements and optical visualisation. *European Journal of Ultrasound*, 7(1), 73–81.
- Nowicki, A., Secomski, W., & Wójcik, L. (1997). Acoustic streaming: comparison of low-amplitude linear model with streaming velocities measured by 32-MHz Doppler. *Ultrasound in Medicine & Biology*, 23(5), 783–91.
- Nyborg, W. L. (1953). Acoustic Streaming due to Attenuated Plane Waves. *The Journal of the Acoustical Society of America*, 25(1), 68.
- Rayleigh, Lord. (1896). *Theory of Sound*. New York: Dover Publications.
- Schlichting, H. (1979). *Boundary Layer Theory*. McGraw-Hill.
- Stuart, J. . (1963). Unsteady boundary layers. In L. Rosenhead (Ed.), *Laminar Boundary Layers* (1st ed.). London: Oxford University Press.
- Tjøtta, S. (1999). Theoretical Investigation of Heat and Streaming Generated by High Intensity Ultrasound. *Acustica*, 85, 780–787.
- Trujillo, F. J., & Knoerzer, K. (2011a). A computational modeling approach of the jet-like acoustic streaming and heat generation induced by low frequency, high power ultrasonic horn reactors. *Ultrasonics Sonochemistry*, 18(6), 1263–73.
- Trujillo, F. J., & Knoerzer, K. (2011b). Modelling the acoustic field and streaming induced by an ultrasonic horn sonoreactor. In K. Knoerzer, P. Juliano, P. Roupas, & C. Versteeg (Eds.), *Innovative Food Processing Technologies* (1st ed.). Indianapolis, USA: Wiley and Sons.
- Westervelt, P. J. (1953). The Theory of Steady Rotational Flow Generated by a Sound Field. *The Journal of the Acoustical Society of America*, 25(1), 60.
- Zaremba, L. K. (1971). Acoustic Streaming. In L. D. Rozenberg (Ed.), *High Intensity Ultrasonic Fields* (1st ed.). London: Plenum Press

***Appendix B. Selected droplet size distribution
data from results presented in chapters 3, 4 and
5***

The following droplet size distribution (DSD) data is provided for selected examples of emulsions prepared in the experimental chapters (*i.e.* chapters 3, 4 and 5) of this thesis. The presented data can be broadly categorised as those comparing emulsions prepared with untreated and ultrasound treated proteins, and a comparison of emulsions prepared using ultrasound as the emulsification methodology.

Fig. B.1 compares the DSD of untreated sodium caseinate (NaCas), ultrasound treated sodium caseinate (NaCas) and Tween 80, all at an emulsifier concentration of 0.1 wt. %. The droplet size distributions of NaCas emulsions were comparable whether untreated or ultrasound treated, as detailed in chapter 3.

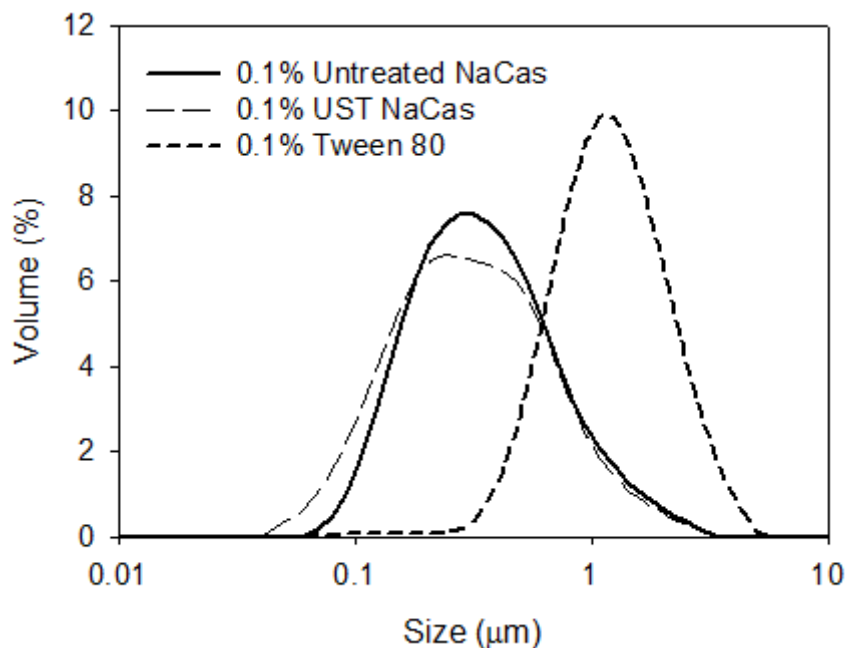


Fig. B.1. Comparison of DSD of untreated NaCas, UST NaCas and Tween 80, all at an emulsifier concentration of 0.1 wt. %

Fig. B.2 compares the DSD of untreated whey protein isolate (WPI), ultrasound treated whey protein isolate (WPI) and Tween 80, all at an emulsifier concentration of 0.1 wt. %. The droplet size distributions of WPI emulsions were comparable whether untreated or ultrasound treated, as detailed in chapter 3.

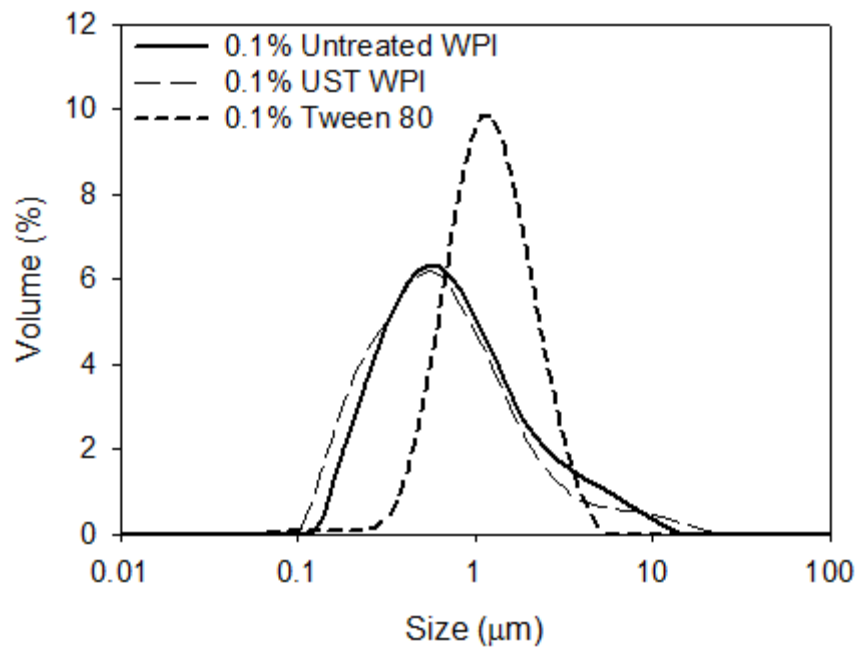


Fig. B.2. Comparison of DSD of untreated WPI, UST WPI and Tween 80, all at an emulsifier concentration of 0.1 wt. %

Fig. B.3 compares the DSD of untreated bovine gelatin (BG), ultrasound treated bovine gelatin (BG) and Brij 97, all at an emulsifier concentration of 0.1 wt. %. The droplet size distributions of ultrasound treated BG emulsions were smaller than untreated BG stabilised emulsions, as detailed in chapter 4.

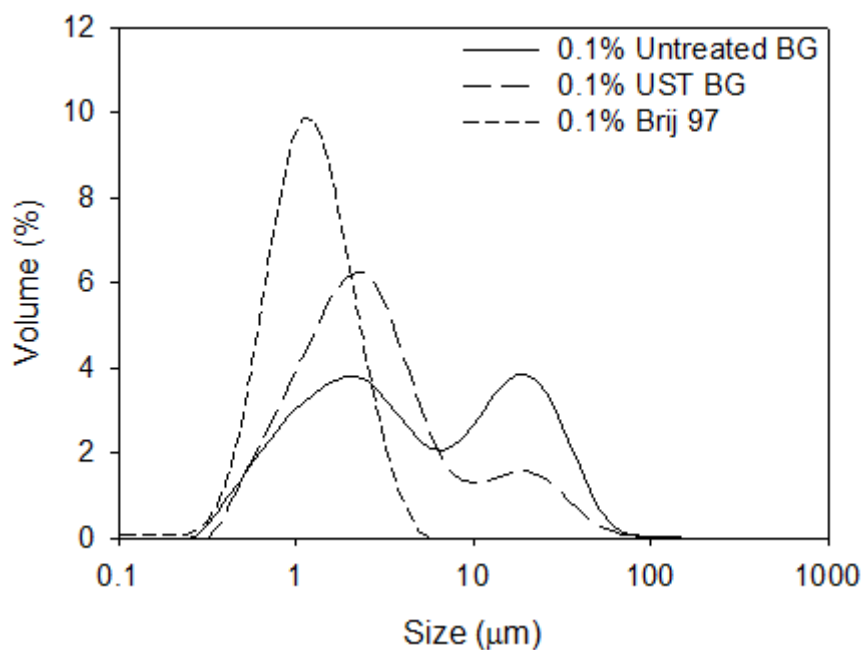


Fig. B.3. Comparison of DSD of untreated BG, UST BG and Brij 97, all at an emulsifier concentration of 0.1 wt. %

Fig. B.4 compares the DSD of untreated fish gelatin (FG), ultrasound treated fish gelatin (FG) and Brij 97, all at an emulsifier concentration of 0.1 wt. %. The droplet size distributions of FG emulsions were comparable whether untreated or ultrasound treated, as detailed in chapter 4.

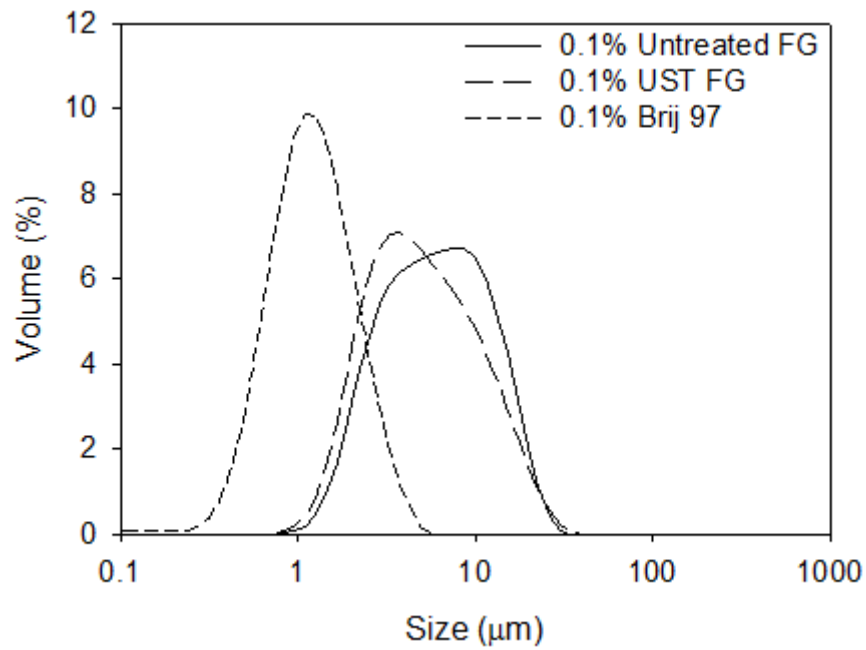


Fig. B.4. Comparison of DSD of untreated FG, UST FG and Brij 97, all at an emulsifier concentration of 0.1 wt.

%

Fig. B.5 compares the DSD of untreated egg white protein (EWP), ultrasound treated egg white protein (EWP) and Brij 97, all at an emulsifier concentration of 0.1 wt. %. The droplet size distributions of ultrasound treated EWP emulsions were smaller than untreated EWP stabilised emulsions, as detailed in chapter 4.

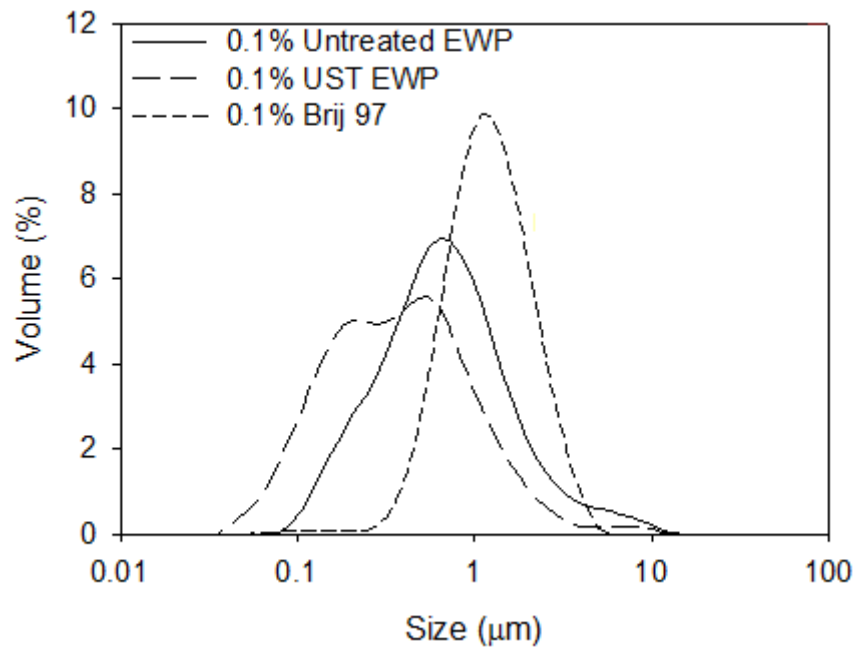


Fig. B.5. Comparison of DSD of untreated EWP, UST EWP and Brij 97, all at an emulsifier concentration of 0.1 wt. %

Fig. B.6 compares the DSD of untreated soy protein isolate (SPI), ultrasound treated soy protein isolate (SPI) and Brij 97, all at an emulsifier concentration of 0.1 wt. %. The droplet size distributions of ultrasound treated SPI emulsions were smaller than untreated SPI stabilised emulsions, as detailed in chapter 4.

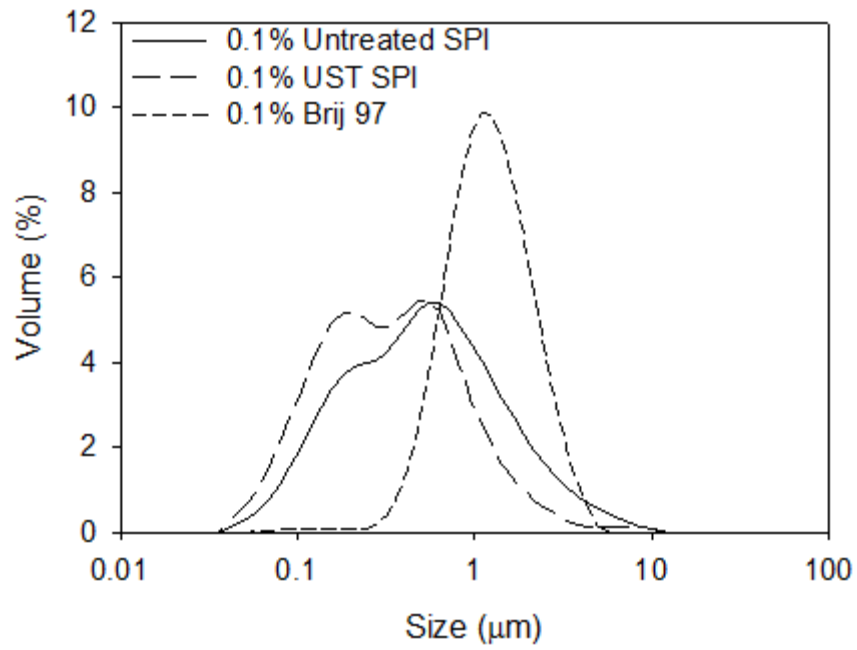


Fig. B.6. Comparison of DSD of untreated SPI, UST SPI and Brij 97, all at an emulsifier concentration of 0.1 wt. %

Fig. B.7 compares the effect of processing time for emulsions prepared with 1,5 wt. % Tween 80 via ultrasound using batch processing (150 g) and an ultrasonic amplitude of 40%.

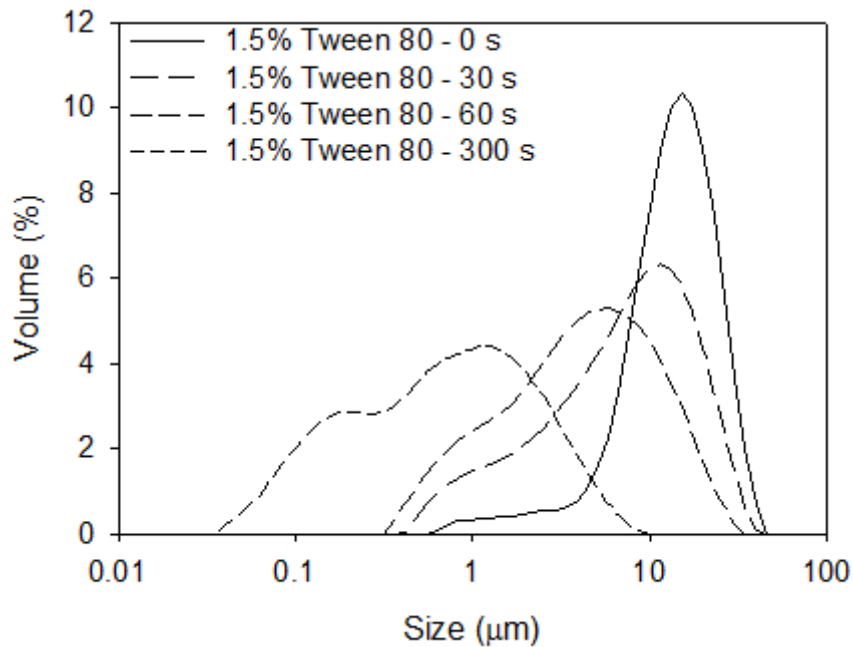


Fig. B.7. Comparison of processing times (0, 30, 60 and 300 s) for the fabrication of emulsions via batch ultrasonic emulsification with an acoustic amplitude of 40% and a batch size of 150 g

Fig. B.8 compares the effect of processing time for emulsions prepared with 1,5 wt. % Tween 80 via ultrasound using batch processing (50 g) and an ultrasonic amplitude of 40%.

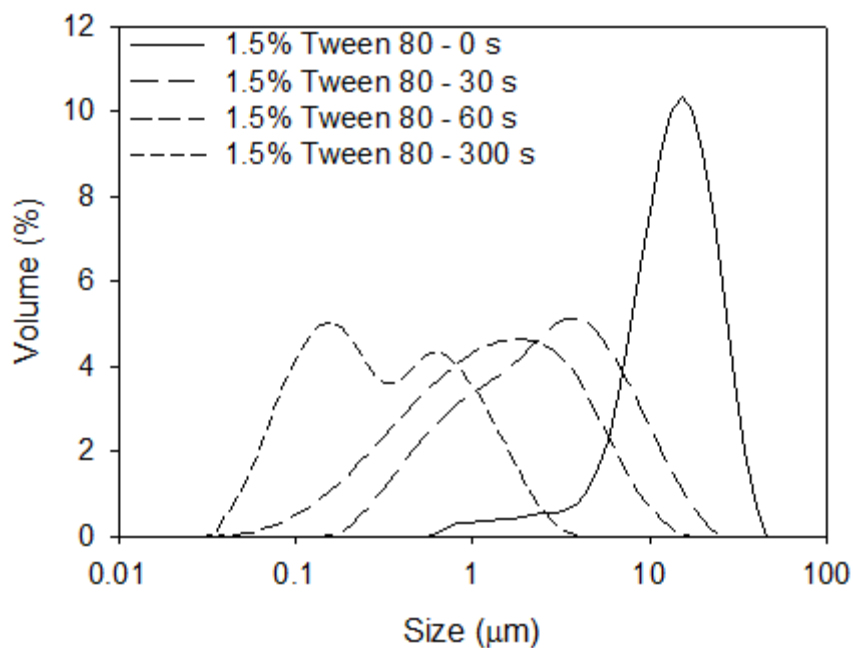


Fig. B.8. Comparison of processing times (0, 30, 60 and 300 s) for the fabrication of emulsions via batch ultrasonic emulsification with an acoustic amplitude of 40% and a batch size of 50 g

Fig. B.9 compares the effect of processing time for emulsions prepared with 1,5 wt. % Tween 80 via ultrasound using batch processing (3 g) and an ultrasonic amplitude of 40%.

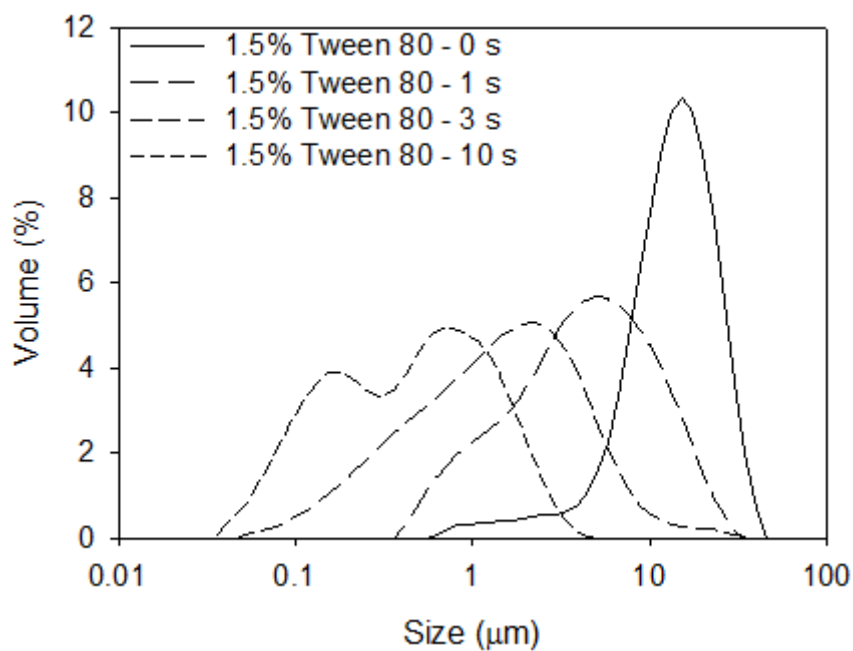


Fig. B.9. Comparison of processing times (0, 1, 3 and 10 s) for the fabrication of emulsions via batch ultrasonic emulsification with an acoustic amplitude of 40% and a batch size of 3 g

Fig. B.10 compares the effect of ultrasonic amplitude for emulsions prepared with 1,5 wt. % Tween 80 via ultrasound using batch processing (50 g) and a processing time of 50 g.

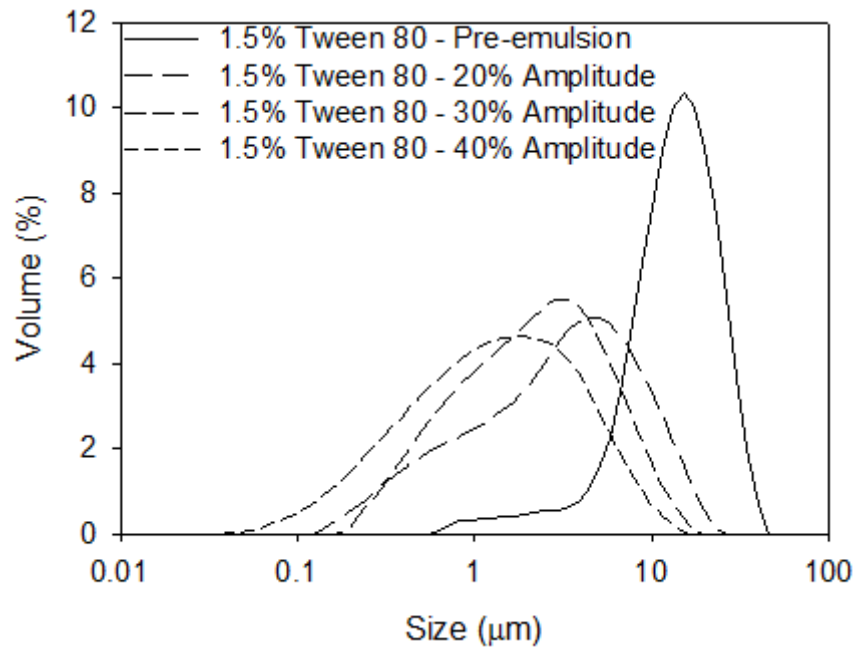


Fig. B.10. Comparison of ultrasonic amplitude (20, 30 and 40 %) for the fabrication of emulsions via batch ultrasonic emulsification with a processing time of 60 s and a batch size of 50 g

***Appendix C. Selected rheology flow profile data
from results presented in chapters 3 and 4***

The following rheology flow profile data is provided for selected examples of protein solutions prepared in the experimental chapters 3 and 4 of this thesis, used for the determination of intrinsic viscosity as described in sections 3.3.2.3.5. and 4.3.2.3.5. of this thesis. The flow curves follow the expected behaviour, whereby untreated proteins have higher viscosities than their untreated counterparts.

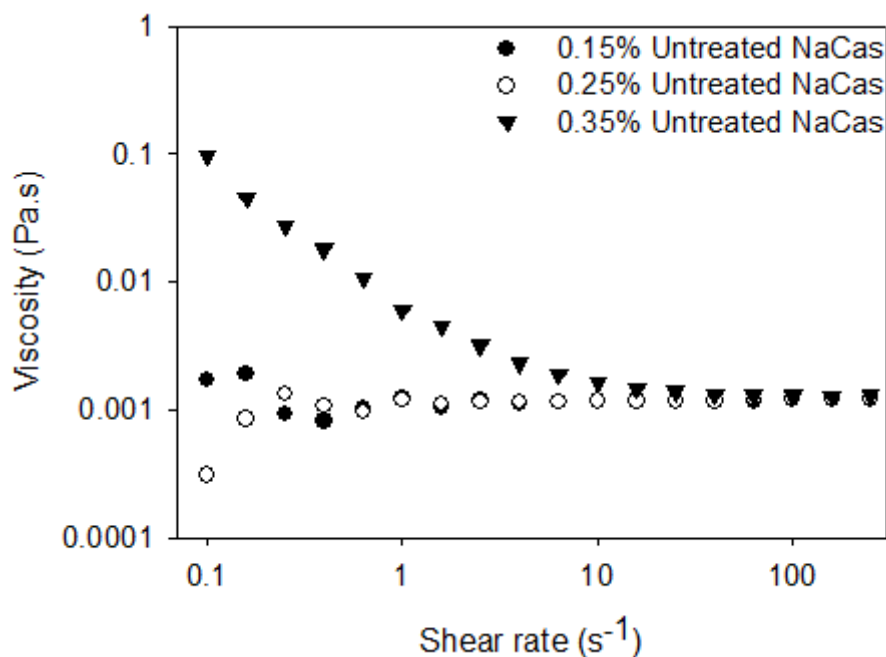


Fig. C.1. Comparison of the flow curves of untreated sodium caseinate (NaCas) solutions as a function of concentration (0.15 – 0.35 wt . %), used for the determination of intrinsic viscosity

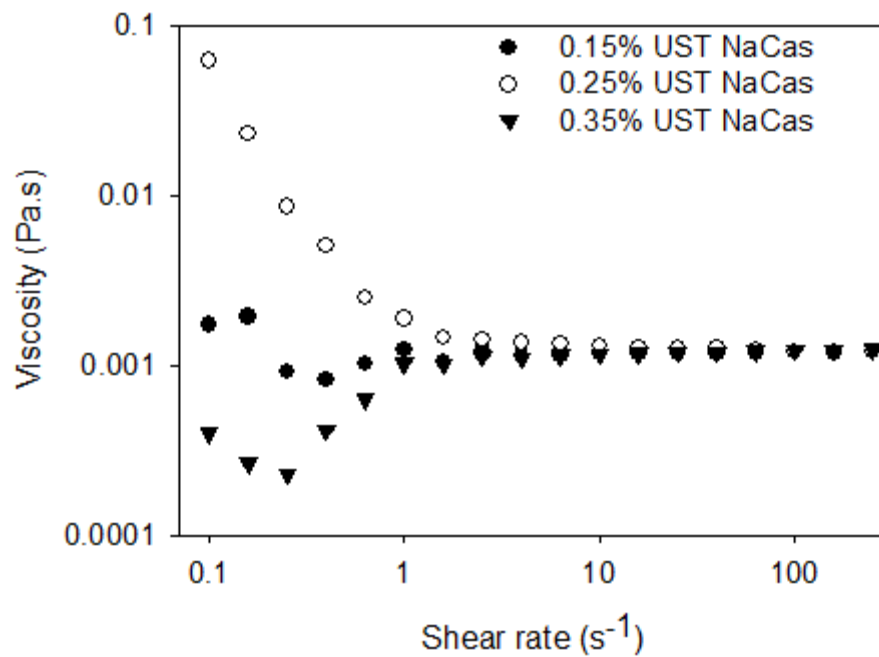


Fig. C.2. Comparison of the flow curves of UST NaCas solutions as a function of concentration (0.15 – 0.35 wt . %), used for the determination of intrinsic viscosity

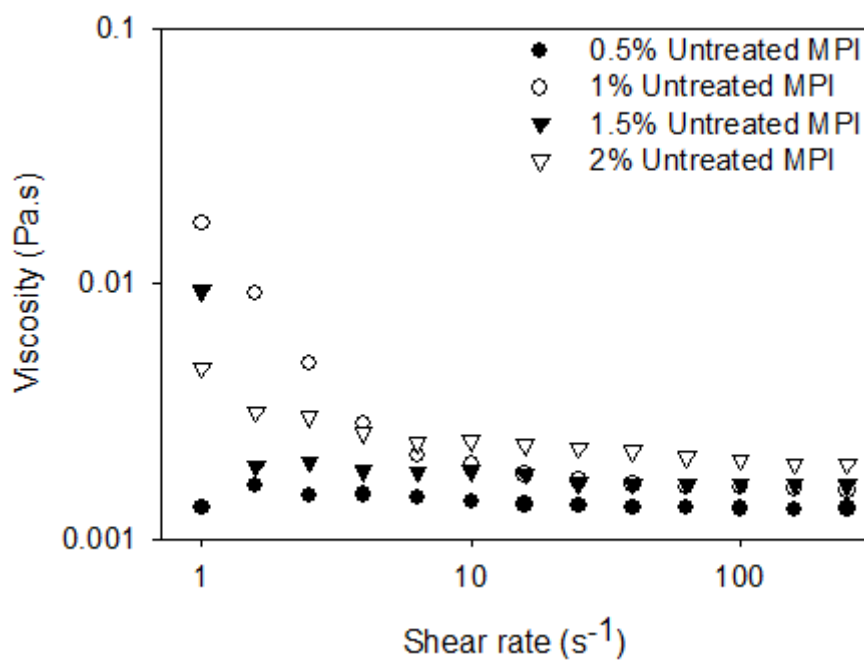


Fig. C.3. Comparison of the flow curves of untreated milk protein isolate (MPI) solutions as a function of concentration (0.5 – 2 wt . %), used for the determination of intrinsic viscosity

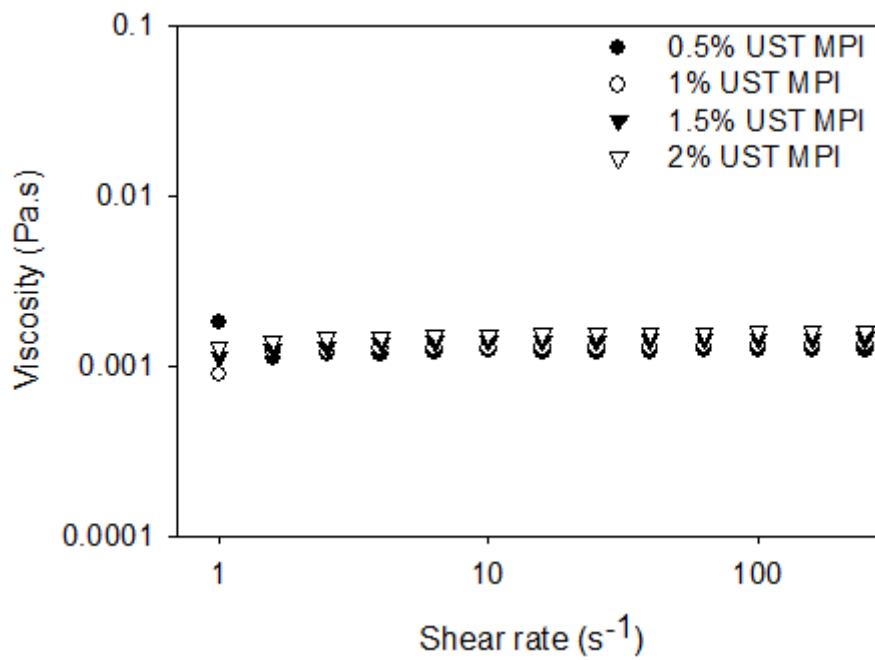


Fig. C.4. Comparison of the flow curves of UST MPI solutions as a function of concentration (0.5 – 2 wt . %), used for the determination of intrinsic viscosity

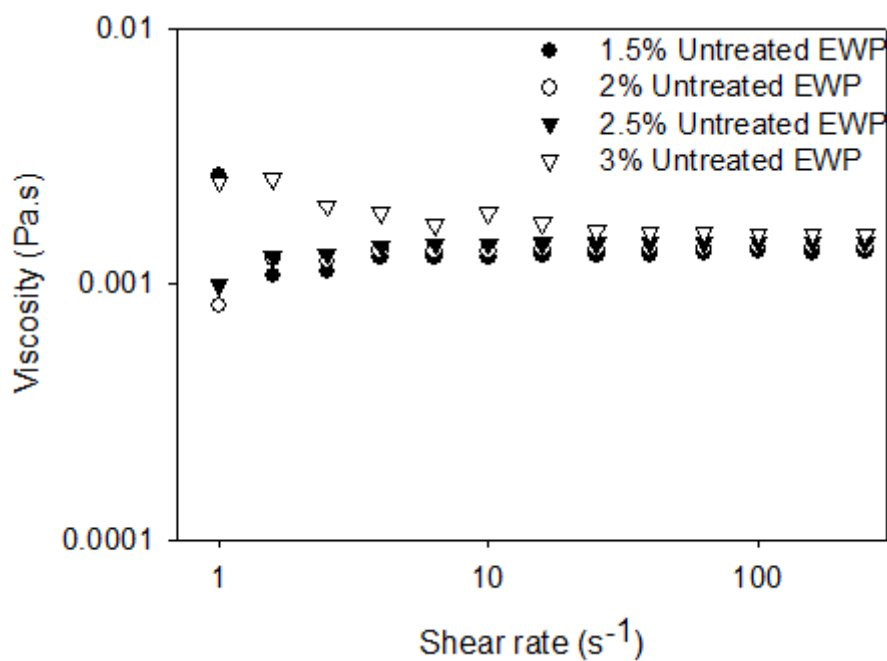


Fig. C.5. Comparison of the flow curves of untreated egg white protein (EWP) solutions as a function of concentration (1.5 – 3 wt . %), used for the determination of intrinsic viscosity

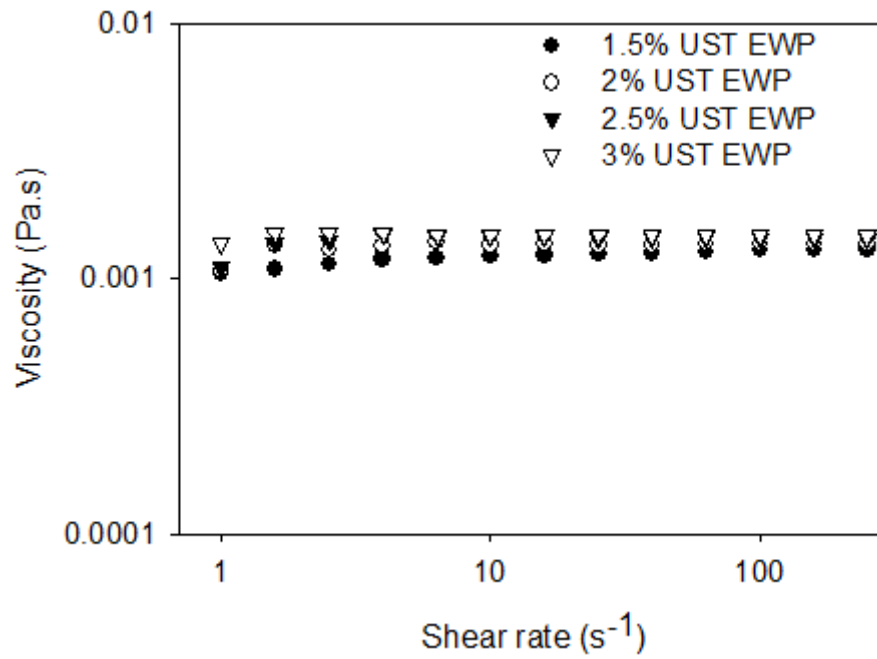


Fig. C.6. Comparison of the flow curves of UST EWP solutions as a function of concentration (1.5 – 3 wt . %), used for the determination of intrinsic viscosity

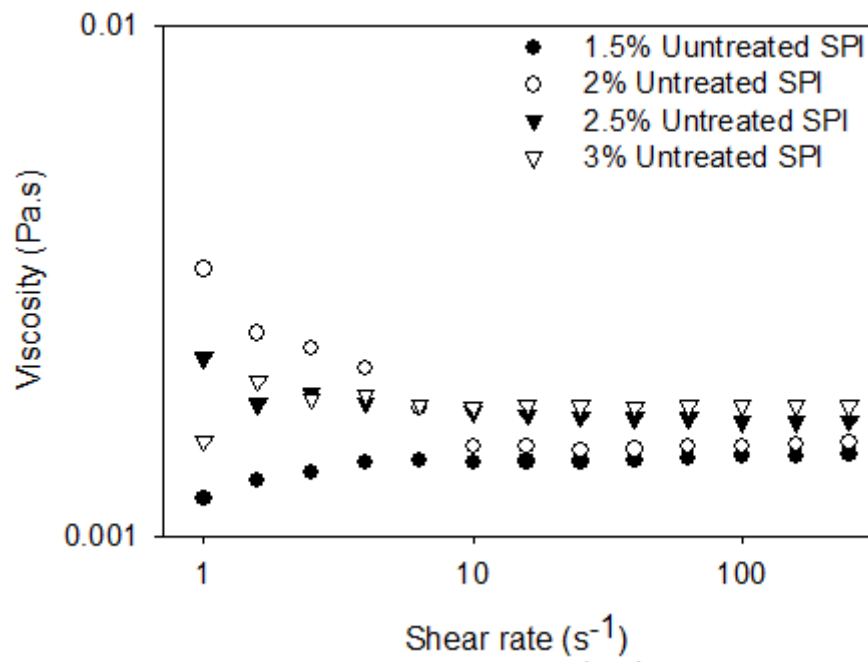


Fig. C.7. Comparison of the flow curves of untreated soy protein isolate (SPI) solutions as a function of concentration (1.5 – 3 wt . %), used for the determination of intrinsic viscosity

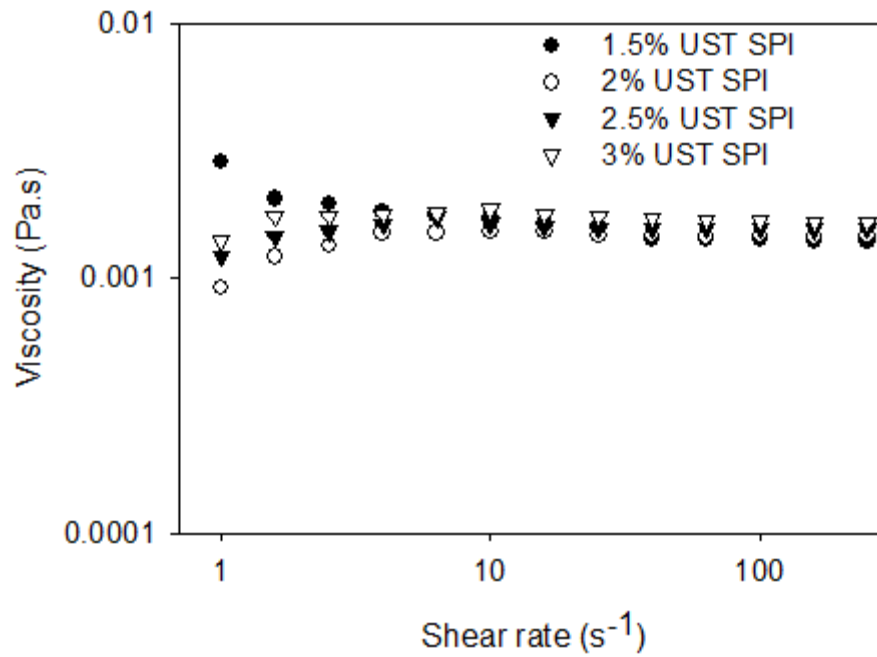


Fig. C.8. Comparison of the flow curves of UST SPI solutions as a function of concentration (1.5 – 3 wt . %), used for the determination of intrinsic viscosity